

Catalytic Asymmetric Reactions between Alkenes and Aldehydes

Inaugural-Dissertation

zur

Erlangung der Doktorwürde

der Mathematisch-Naturwissenschaftlichen Fakultät

der Universität zu Köln

vorgelegt von

Luping Liu

aus Hebei (VR China)

Köln 2017

Berichterstatter: Prof. Dr. Benjamin List
Prof. Dr. Hans-Günther Schmalz
Tag der mündlichen Prüfung: 11.10.2017

TABLE OF CONTENTS

TABLE OF CONTENTS

ABSTRACT	III
LIST OF ABBREVIATIONS	V
1 INTRODUCTION	1
2 BACKGROUND	3
2.1 ASYMMETRIC ORGANOCATALYSIS	3
2.1.1 <i>Introduction</i>	3
2.1.2 <i>Asymmetric Brønsted Acid Catalysis</i>	7
2.2 ASYMMETRIC REACTIONS BETWEEN ALDEHYDES AND OLEFINS	16
2.2.1 <i>Asymmetric Carbonyl–Ene Cyclization</i>	16
2.2.2 <i>Asymmetric Hetero-Diels–Alder Reaction of Dienes and Aldehydes</i>	21
3 OBJECTIVES OF THIS THESIS	26
3.1 CATALYTIC ASYMMETRIC REACTIONS OF SIMPLE ALKENES WITH ALDEHYDES	26
3.2 HIGHLY ACIDIC AND CONFINED BRØNSTED ACIDS	29
4 RESULTS AND DISCUSSION	31
4.1 ORGANOCATALYTIC ASYMMETRIC CARBONYL–ENE CYCLIZATION	31
4.1.1 <i>Reaction Design and Initial Study</i>	31
4.1.2 <i>Substrate Scope</i>	33
4.1.3 <i>Mechanistic Studies and Discussion</i>	36
4.2 ORGANOLCATALYTIC ASYMMETRIC TRANSFORMATIONS VIA OXOCARBENIUM IONS	44
4.2.1 <i>Catalytic Asymmetric Prins Cyclization</i>	44
4.2.2 <i>Catalytic Asymmetric Oxa-Pictet–Spengler Reaction</i>	53
4.3 ASYMMETRIC [4+2]-CYCLOADDITION REACTION OF DIENES WITH ALDEHYDES	60
4.3.1 <i>Reaction Design and Initial Study</i>	60
4.3.2 <i>Catalyst Design and Synthesis</i>	63
4.3.3 <i>Utilization of New Catalysts</i>	65
4.3.4 <i>Substrate Scope of Aromatic Aldehydes</i>	67
4.3.5 <i>Substrate Scope of Aliphatic Aldehydes</i>	69
4.3.6 <i>Diene Scope</i>	71
4.3.7 <i>Gram-Scale Synthesis and Derivatization</i>	73
4.3.8 <i>Discussion</i>	74
5 SUMMARY	78
5.1 ORGANOLCATALYTIC ASYMMETRIC CARBONYL–ENE CYCLIZATION	78
5.2 ORGANOLCATALYTIC ASYMMETRIC TRANSFORMATIONS VIA OXOCARBENIUM IONS	79

TABLE OF CONTENTS

5.2.1 A General Organocatalytic Asymmetric Prins Cyclization	79
5.2.2 Organocatalytic Asymmetric Oxa-Pictet–Spengler Reaction	80
5.3 CATALYTIC ASYMMETRIC [4+2]-CYCLOADDITION OF DIENES WITH ALDEHYDES	81
5.4 HIGHLY ACIDIC AND CONFINED BRØNSTED ACIDS	82
6 OUTLOOK	84
6.1 A HIGHLY ENANTIOSELECTIVE SYNTHESIS OF MENTHOL	84
6.2 AN ORGANOLCATALYTIC ASYMMETRIC ALLYLATION OF ALDEHYDES	85
7 EXPERIMENTAL PART	86
7.1 GENERAL EXPERIMENTAL CONDITIONS	86
7.2 ORGANOLCATALYTIC ASYMMETRIC CARBONYL–ENE CYCLIZATION	89
7.2.1 Substrates Synthesis	89
7.2.2 Products	94
7.2.3 Mechansitic Studies	102
7.2.4 X-Ray Data	125
7.3 ORGANOLCATALYTIC ASYMMETRIC TRANSFORMATIONS VIA OXOCARBENIUM IONS	131
7.3.1 Prins Cyclization	131
7.3.2 Oxa-Pictet–Spengler Reaction	149
7.4 CATALYTIC ASYMMETRIC [4+2]-CYCLOADDITION REACTION OF DIENES WITH ALDEHYDES	168
7.4.1 Products	168
7.4.2 Catalyst Synthesis	185
7.4.3 X-Ray Data	192
7.4.4 Mechanistic Studies	218
8 BIBLIOGRAPHY	221
9 ACKNOWLEDGEMENTS	228
10 APPENDIX	229
10.1 ERKLÄRUNG	229
10.2 TEILPUBLIKATIONEN	230

ABSTRACT

This doctoral work describes catalytic asymmetric reactions between alkenes and aldehydes, enabled by the development of chiral Brønsted acids. Valuable and functionalized enantiomerically enriched cyclic compounds were efficiently furnished from inexpensive and commercially available reagents with high degrees of atom economy.

In the first part of this thesis, the first highly enantioselective organocatalytic intramolecular carbonyl–ene cyclization of olefinic aldehydes is presented. In the second part, asymmetric cyclizations via oxocarbenium ions are described. One is a general asymmetric catalytic Prins cyclization of aldehydes with homoallylic alcohols, in which the oxocarbenium ion is attacked intramolecularly by a pendent alkene. The other one is an asymmetric *oxa*-Pictet–Spengler reaction between aldehydes and homobenzyl alcohols, in which the oxocarbenium ion is trapped by an intramolecular arene. The first general asymmetric [4+2]-cycloaddition of simple and unactivated dienes with aldehydes is developed in the last part of this thesis. This methodology is extremely robust and scalable. Valuable enantiomerically enriched dihydropyran compounds could be readily obtained from inexpensive and abundant dienes and aldehydes.

New types of confined Brønsted acids were rationally designed and synthesized, including imino-imidodiphosphates (*i*IDPs), nitrated imidodiphosphates (*n*IDPs), and imidodiphosphorimidates (IDPis). Beyond the application of these catalysts in various asymmetric reactions between simple alkenes and aldehydes, mechanistic investigations are also disclosed in this doctoral work.

ABSTRACT

Diese Doktorarbeit beschreibt hochenantioselektive Reaktionen zwischen einfachen Alkenen und Aldehyden, welche durch chirale Brønsted-Säuren als Katalysatoren ermöglicht wurden. Wertvolle, hochfunktionalisierte und enantiomerenangereicherte zyklische sowie heterozyklische Verbindungen wurden effizient und hochgradig atomökonomisch, ausgehend von kommerziell erhältlichen und günstigen Startmaterialien, hergestellt.

Im ersten Teil der Arbeit wird eine hochenantioselektive und organokatalytische intramolekulare Carbonyl–En-Zyklisierung von olefinischen Aldehyden vorgestellt. Im zweiten Teil werden zwei verschiedene asymmetrische Zyklisierungsreaktionen über Oxocarbenium-Ionen beschrieben. Eine dieser Reaktionen stellt die katalytische Prins-Zyklisierung von gängigen Aldehyden und homoallylischen Alkoholen dar, in welcher das Oxocarbeniumion intramolekular mit einem nukleophilen Alkenrest reagiert. Die andere Transformation beschreibt eine asymmetrische *Oxa*-Pictet–Spengler-Reaktion von Aldehyden mit homobenzylischen Alkoholen, wobei das Oxocarbeniumion mit dem aromatischen Ringsystem reagiert. Im letzten Teil der Arbeit wird die erste generelle asymmetrische [4+2]-Cycloaddition zwischen einfachen und nichtaktivierten Dienen und Aldehyden entwickelt. Diese Methode ist extrem robust und skalierbar. Wertvolle enantiomerenangereicherte Dihydropyran-Verbindungen konnten ausgehend von kommerziell erwerbbaaren Dienen und Aldehyden hergestellt werden.

Neue Klassen sterisch anspruchsvoller Brønsted-Säuren wurden konzipiert und synthetisiert. Hierbei standen Imino-Imidophosphate (IDPs), nitrierte Imidodiphosphate (*n*IDP) und Imidodiphosphoimide (IDPi) im Fokus. Neben der Anwendung dieser Katalysatoren in verschiedenen asymmetrischen Reaktionen, werden die erarbeiteten mechanistischen Studien am Ende dieser Doktorarbeit beschrieben und erläutert.

LIST OF ABBREVIATIONS

Ac	acyl
ACDC	asymmetric counteranion-directed catalysis
ad	adamantyl
AIBN	2,2'-azo <i>bisisobutyronitrile</i>
Alk	alkyl
An	<i>p</i> -anisyl
aq.	Aqueous
Ar	aryl
9-BBN	9-borabicyclo[3.3.1]nonane
BHT	2,6- <i>di-t</i> -butyl- <i>p</i> -cresol
BINAP	2,2'- <i>bis</i> (diphenylphosphino)-1,1'-binaphthyl
BINOL	1,1'-bi-2-naphthol
BLA	Brønsted acid assisted chiral Lewis acid
Bn	benzyl
Boc	<i>tert</i> -butyloxycarbonyl
BOM	benzyloxymethyl
Bz	benzoyl
Bu	butyl
caclcd	calculated
cat.	catalyst
Cbz	benzyloxycarbonyl
conv.	conversion
Cy	cyclohexyl
d	day
DCE	1,1-dichloroethane
DCM	dichloromethane
DFT	density functional theory

LIST OF ABBREVIATIONS

DIBAL	diisobutylaluminum hydride
DIPEA	diisopropylethylamine
DMAP	<i>N,N</i> -4-dimethylaminopyridine
DMF	dimethylformamide
DMP	Dess-Martin periodinane
DMS	dimethylsulfide
DMSO	dimethylsulfoxide
dr	diastereomeric ratio
DSI	disulfonimide
EDG	electron donating group
ee	enantiomeric excess
EI	electron impact
er	enantiomeric ratio
equiv	equivalents
Et	ethyl
ESI	electrospray ionization
EWG	electron withdrawing group
FMO	frontier molecular orbital
Fmoc	9-fluorenylmethoxycarbonyl
GC	gas chromatography
h	hour
HMDS	1,1,1,3,3,3-hexamethyldisilazane
HOMO	highest occupied molecular orbital
HPLC	high performance liquid chromatography
HRMS	high resolution mass spectrometry
<i>i</i>	iso
IDP	imidodiphosphate
IDPi	imidodiphosphorimidate
<i>i</i> IDP	imino-imidodiphosphate
IR	infrared spectroscopy

LIST OF ABBREVIATIONS

L	ligand
LA	Lewis acid
LAH	lithium aluminum hydride
LB	Lewis base
LDA	lithium diisopropylamide
<i>m</i>	meta
m	multiplet
M	molar
<i>m</i> CPBA	<i>meta</i> -chloroperbenzoic acid
Me	methyl
MeCy	methylcyclohexane
Mes	mesityl
Ms	mesyl (methanesulfonyl)
MS	mass spectrometry or molecular sieves
MTBE	methyl <i>t</i> -butyl ether
nd	not determine
<i>n</i> IDP	nitrated imidodiphosphate
nr	no reaction
NMR	nuclear magnetic resonance spectroscopy
Nu	nucleophile
Ns	2-nitrobenzenesulfonyl
<i>o</i>	ortho
P	product
<i>p</i>	<i>para</i>
piv	pivaloyl
Ph	phenyl
Pr	propyl
PTC	Phase transfer catalyst
Py	pyridine
quant.	quantitative

LIST OF ABBREVIATIONS

quint	quintet
rac	racemic
rt	room temperature
R _f	retention factor in chromatography
S	substrate
Salen	<i>bis</i> (salicylidene)ethylenediamine
<i>t</i>	tert, tertiary
t	triplet
TADDOL	$\alpha,\alpha,\alpha',\alpha'$ -tetraaryl-1,3-dioxolan-4,5-dimethanol
TBAF	tetra- <i>n</i> -butylammonium fluoride
TBS	<i>tert</i> -butyl(dimethyl)silyl
TEA	triethylamine
Tf	trifluoromethylsulfonyl
TFA	trifluoroacetic acid
THF	tetrahydrofuran
THP	tetrahydropyran
TLC	thin layer chromatography
TMEDA	<i>N,N,N',N'</i> -tetramethyl ethylenediamine
TMS	trimethylsilyl
TOF	turnover frequency
Tol	<i>p</i> -tolyl
TON	turnover number
TRIP	3,3'-bis(2,4,6-triisopropylphenyl)-1,1'-binaphthyl-2,2'-diyl-hydrogen phosphate
TsOH	<i>para</i> -toluene sulfonic acid
k_B	Boltzmann constant: $1.3806488 \times 10^{-23}$ J/K,
h	Planck constant: $6.62606957 \times 10^{-34}$ J·s.

1 INTRODUCTION

Chirality is a geometric property of three-dimensional objects,^{1,2} and it was recognized by the chemists Le Bel and van't Hoff in the 1870s.^{3,4} Later, Mislow provided a definition of chirality: "An object is chiral if and only if it is not superposable on its mirror image; otherwise it is achiral."⁵

The inherent chirality in nature creates a unique world. The 20 life-sustaining proteinogenic α -amino acids found in eukaryotes are exclusively in levo-forms. The three-dimensional receptors in a living body, such as proteins built from chiral α -amino acids, are able to differentiate between enantiomers. For example, the levo-asparagine is tasteless, while the dextro-form is sweet. Chirality becomes more important in pharmacological research due to a three-dimensional specific recognition between a drug and its action target.^{6,7} According to the U.S. Food & Drug Administration in 2006, 75% of small-molecule drugs were single enantiomers.⁸ Therefore, the synthesis of enantiopure drugs is highly demanded in modern pharmaceutical research.

Enantiopure compounds can be prepared via three main approaches: 1. resolution of racemates, which is not economical with a maximum yield of 50%;⁹ 2. chiral pool synthesis, in which a stoichiometric enantiopure starting material is required;¹⁰ 3. asymmetric synthesis, in which the stereogenic centers are created from achiral starting materials.¹¹ Among all, asymmetric catalysis provides an optimal access to enantiopure products using catalytic amounts of chiral catalysts for enantioselective induction.

Complementary to enzymatic catalysis and chiral transition metal catalysis, organocatalysis has emerged as the third pillar of asymmetric catalysis, which was triggered by the discovery of aminocatalysis in 2000.^{12,13} Different from the catalysts generated from chiral organic ligands and metal species in transition metal catalysis, the low-molecular-weight organic molecules themselves function as catalysts for chemical transformations in organocatalysis.¹⁴ In fact, many challenging asymmetric transformations, which could not be solved by either enzymatic catalysis or transition metal catalysis, have been realized using organocatalysis. Continually excellent work coming from the Denmark, Jacobsen, Yamamoto, MacMillan, List, and other groups, has demonstrated that the creation of robust catalyst motifs is the key to successful asymmetric catalysis.

1 INTRODUCTION

“One challenge that is likely to be addressed includes the Brønsted acid-catalyzed activation of new substrate classes such as unactivated carbonyl compounds or simple olefins, which will presumably require the design of even stronger chiral acids.”¹⁴

Benjamin List, 2010

Despite tremendous progress and glorious moments in asymmetric synthesis, the lack of broad substrate scopes, especially unactivated and/or small substrates, is a common problem in this field. This doctoral work focuses on general catalytic asymmetric reactions between simple, unactivated alkenes and aldehydes, many of which are inexpensive and abundant chemical feedstocks.

In the following chapters, an overview of organocatalysis, especially Brønsted acid catalysis, is given. This is succeeded by the development of the carbonyl–ene cyclization and the hetero-Diels–Alder reaction. Subsequently, my own work on chiral Brønsted acid-catalyzed asymmetric reactions between alkenes and aldehydes is presented.

2 BACKGROUND

2.1 Asymmetric Organocatalysis

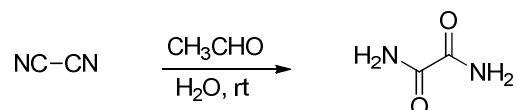
2.1.1 Introduction

As the demand for enantiopure compounds in pharmaceuticals, fragrances, flavors, and materials increases, the development of asymmetric catalysis has correspondingly escalated in modern synthetic chemistry research. Chiral catalysts accelerate a chemical reaction by lowering the energy barrier and provide chiral environments for stereoselective inductions, affording enantiomerically enriched products. Utilizing and/or inspired by catalytic processes with extraordinary activity and selectivity in nature, enzyme catalysis and chiral metal catalysis have been regarded as two main methodologies in asymmetric synthesis. In recognition of the importance and the achievement of this field, the 2001 Nobel Prize in Chemistry has been awarded to Knowles and Noyori for their work on transition metal-catalyzed enantioselective hydrogenations¹⁵ and to Sharpless for his work on transition metal-catalyzed asymmetric oxidations¹⁶.

“New synthetic methods are most likely to be encountered in the fields of biological and organometallic chemistry.”¹⁷

Dieter Seebach, 1990

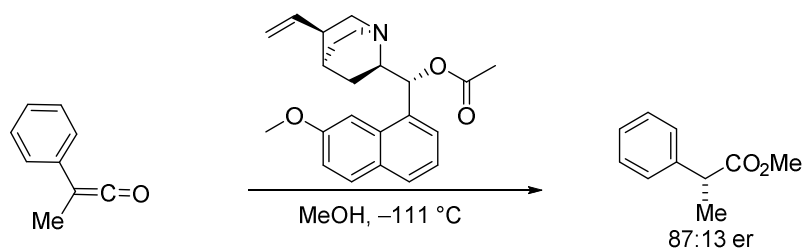
Complementary to transition metal catalysis and enzyme catalysis, simple organic molecules have rapidly emerged as powerful catalysts at the beginning of the 21st century. There are several advantages in organocatalysis. For example, most organocatalysts are quite practical without the requirement of a glove box or ultra-dried solvents. In fact, as early as in 1860, von Liebig demonstrated that a small organic molecular acetaldehyde could catalyze the hydrolysis of cyanogen.¹⁸



Scheme 2.1 Acetaldehyde-catalyzed hydrolysis of cyanogen.

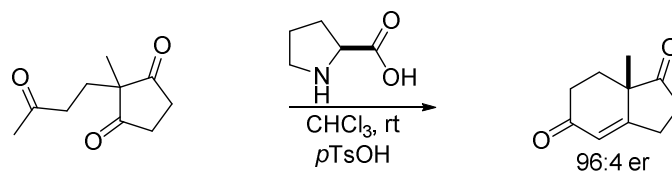
After one century, in 1960 Precejus reported an alkaloid-catalyzed enantioselective addition of methanol to ketenes with moderate enantioselectivity. This is the first significantly enantioselective organocatalytic reaction.¹⁹

2 BACKGROUND



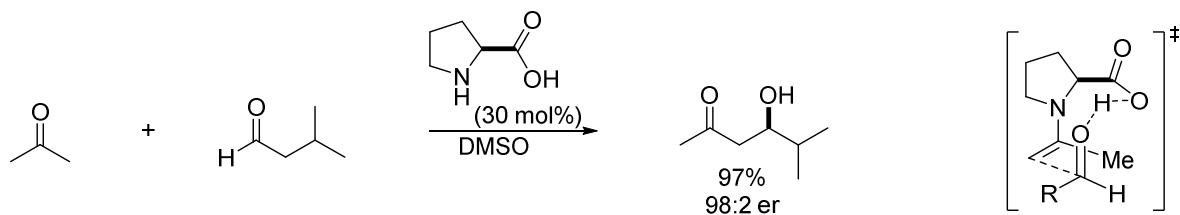
Scheme 2.2 Organocatalytic asymmetric esterification of ketene.

Subsequently, two different groups simultaneously discovered the Hajos-Parrish-Eder-Sauer-Wiechert reaction in the early 1970s.^{20,21} In this reaction, a proline-catalyzed intramolecular aldol reaction occurred, and important progesterone intermediates were furnished following dehydration. This discovery demonstrated the potential of organocatalysis in asymmetric synthesis.



Scheme 2.3 Hajos-Parrish-Eder-Sauer-Wiechert reaction.

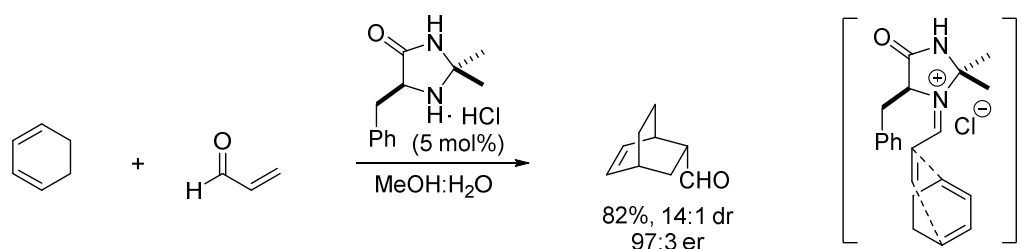
Nevertheless, it was not until the beginning of the 21st century, that the design and development of enamine catalysis by List and coworkers triggered a gold rush in organocatalysis. Inspired by the active core of the enzyme aldolase, the authors reported a (*S*)-proline-catalyzed aldol reaction of acetone with aldehydes.¹² Excellent enantioselectivity and yield were achieved. To elucidate the reaction mechanism, a computational study was conducted.²² The condensation of the chiral (*S*)-proline with the ketone forms a more nucleophilic enamine species. Meanwhile, the hydrogen bond was formed between the acid group in the catalyst and the aldehyde, lowering the LUMO of the aldehyde. Therefore, the Proline-catalyzed aldol reaction of the ketone with aldehydes was accelerated via both a HOMO raising as well as a LUMO lowering process.



Scheme 2.4 (*S*)-proline-catalyzed aldol reaction.

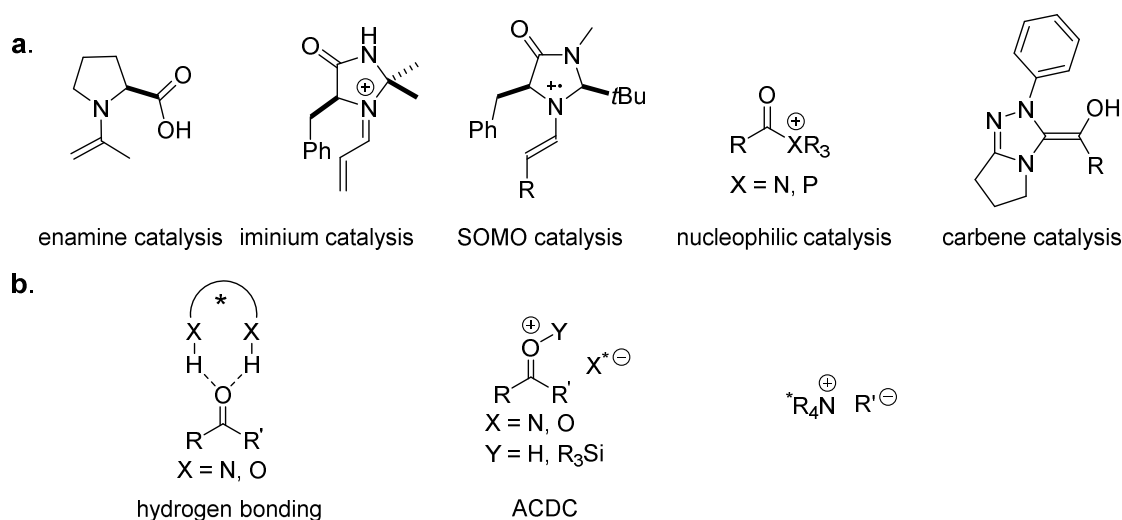
2 BACKGROUND

Subsequently, another breakthrough in organocatalysis was made by the MacMillan group.¹³ They demonstrated the first highly enantioselective organocatalytic Diels–Alder reaction of enals with dienes, which was catalyzed by a chiral imidazolidinone through iminium catalysis. The authors proposed that the LUMO of the dienophile was lowered due to the formation of iminium species, resulting from the condensation between the secondary amine catalyst and an enal.



Scheme 2.5 Imidazolidinone-catalyzed Diels–Alder reaction.

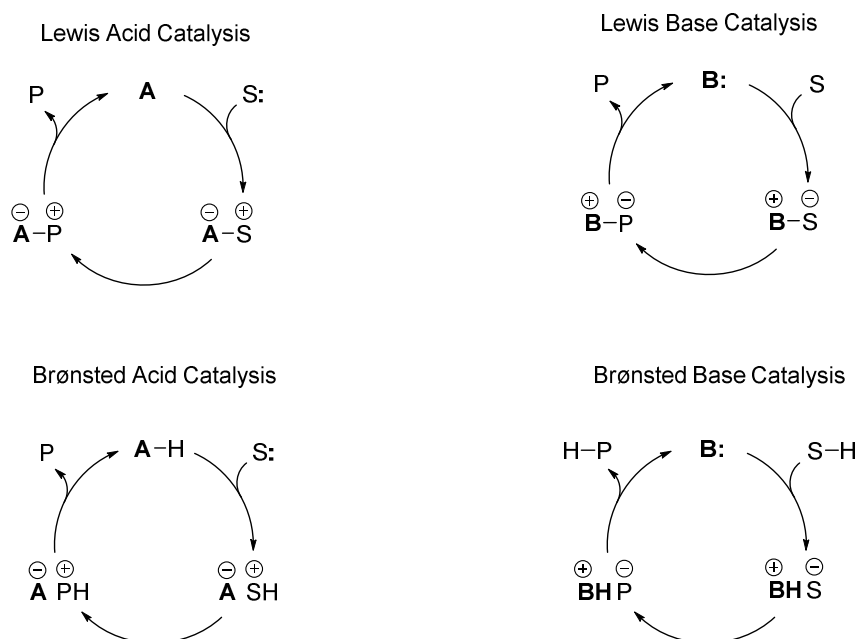
Triggered by the developed enamine catalysis and iminium catalysis, organocatalysis quickly emerged as a powerful tool in synthetic chemistry. The success of this rapid growth of organocatalysis highly relies on a deep understanding of the reaction mechanism and the creation of different activation modes. Several activation modes in organocatalysis have been established according to the interactions between catalysts and substrates. These activation modes are generally classified into two categories: covalent catalysis (Scheme 2.6a) and non-covalent catalysis (Scheme 2.6b).²³ Covalent catalysis includes enamine catalysis, iminium catalysis, SOMO catalysis, nucleophilic catalysis, and carbene catalysis, while non-covalent catalysis includes hydrogen bonding catalysis, asymmetric counteranion-directed catalysis (ACDC), and phase transfer catalysis.^{24,25}



Scheme 2.6 (a) Covalent catalysis. (b) Non-covalent catalysis.

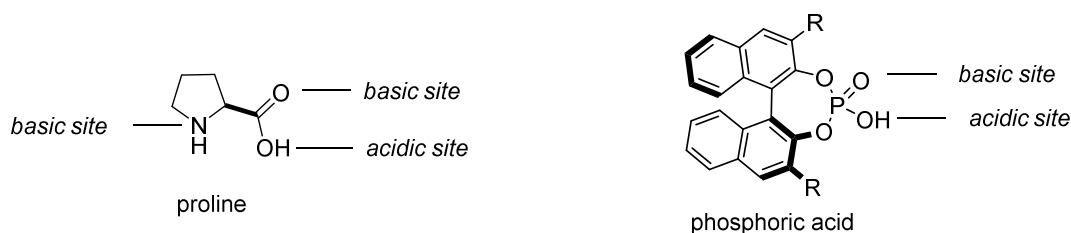
2 BACKGROUND

On the other hand, catalysts could be generally categorized into four distinct types on the basis of their interactions with substrates: Brønsted acid, Lewis acid, Brønsted base, and Lewis base. Accordingly, the List group introduced the following systematical classification of reaction modes based on the organocatalysts: Brønsted acid catalysis, Lewis acid catalysis, Brønsted base catalysis, and Lewis base catalysis (Scheme 2.7).²⁶ In Lewis acid and Lewis base catalysis, catalysts activate the substrates by accepting or donating electrons, while Brønsted acid and base catalysis are initiated by a protonation or deprotonation of the substrates.



Scheme 2.7 Classification of reaction modes based on catalysts. S, substrate; P, product; A, Acid; and B, Base.

However, many popular organocatalysts, for example proline, chiral phosphoric acids, and some chiral thiourea catalysts, are bifunctional and possess both acidic and basic sites. The nucleophiles in the reactions are activated by the basic sites, while the electrophiles are activated by the acidic sites (Scheme 2.8).

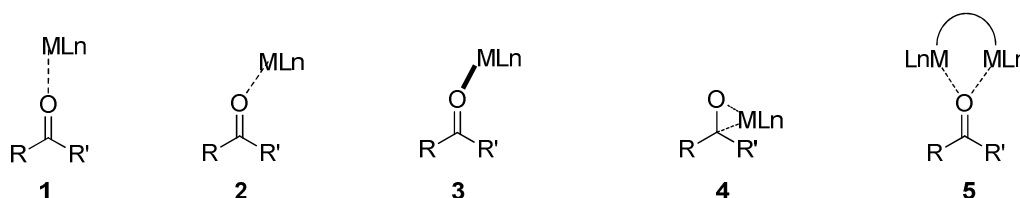


Scheme 2.8 Bifunctional organocatalysts.

2 BACKGROUND

2.1.2 Asymmetric Brønsted Acid Catalysis

Lewis acid catalysis plays a crucial role in chemical synthesis and has been extensively investigated. For example, several coordination modes have already been established to activate a carbonyl group in Lewis acid catalysis (Scheme 2.9): 1. electrostatic interaction between a metal and a carbonyl; 2. coordination between a metal and the lone pair of a carbonyl, in which the metal is in the nodal plane of the carbonyl group; 3. coordination between a metal and the lone pair of a carbonyl, in which the metal is bent out of the nodal plane of the carbonyl group; 4. η^2 coordination of the metal to a carbonyl; 5. bidentate coordination between a carbonyl and two metals.²⁷



Scheme 2.9 Activation modes of carbonyl in Lewis acid catalysis.

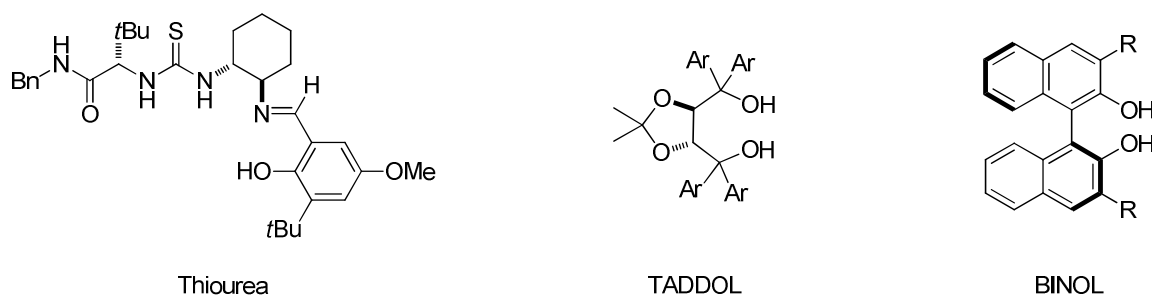
Compared to diverse metal species in Lewis acid catalysis, the active site in Brønsted acid catalysis is a single acidic proton. Two distinct activation modes have been established on the basis of the interaction between Brønsted catalysts and electrophiles: general Brønsted acid catalysis and specific Brønsted acid catalysis (Scheme 2.10).²⁸



Scheme 2.10 Activation modes in Brønsted acid catalysis.

Weak chiral Brønsted acids, such as chiral thioureas,²⁹ squaramides,³⁰ TADDOLs³¹ and BINOLs,³² are classified as general Brønsted acid catalysts. Hydrogen bonds are formed between electrophiles and the weak Brønsted acids, leading to the lowering of the LUMOs of the electrophiles. These hydrogen bonding catalysts have been widely used in asymmetric transformations, such as the Strecker reactions, Michael additions, hetero-Diels–Alder reactions, and many others.

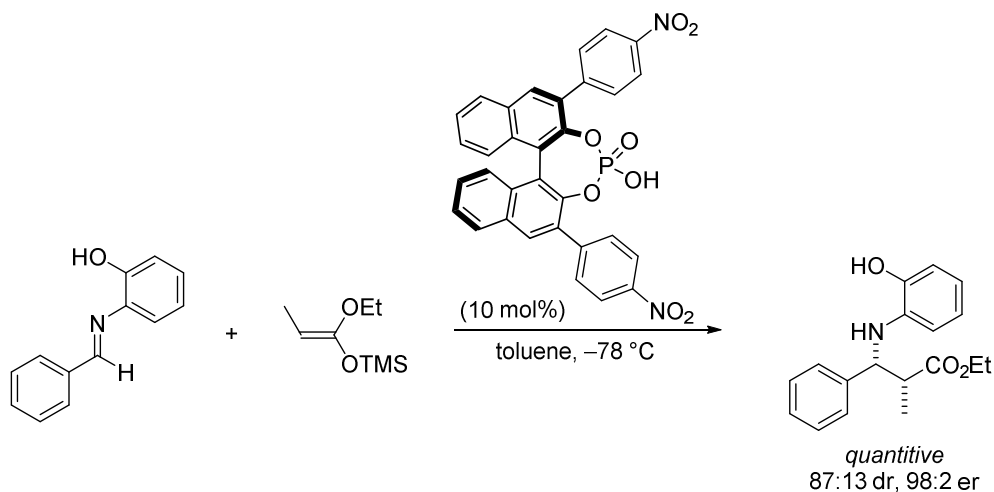
2 BACKGROUND



Scheme 2.11 Selected catalysts in general Brønsted acid catalysis.

Strong achiral Brønsted acids have been used to catalyze chemical reactions.³³ Frequently-used ones include $\text{CF}_3\text{SO}_3\text{H}$, HNTf_2 , HCl , HBF_4 , and benzenesulfonic acids, which have been utilized to catalyze a variety of transformations such as allylation reactions, Aldol reactions, Mannich reactions, Michael additions, Diels–Alder reactions, and hydrations or hydroaminations of alkenes.

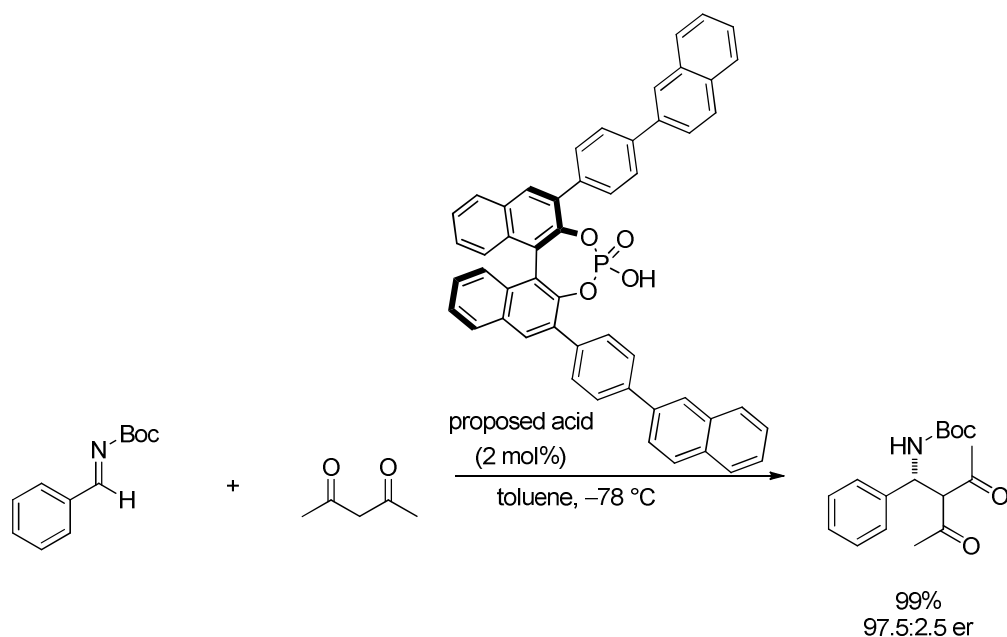
In contrast, asymmetric Brønsted acid catalysis is still in its infancy. It was not until 2004 that the Akiyama group reported a chiral BINOL-derived phosphoric acid-catalyzed highly enantioselective Mannich reaction between aromatic imines and silyl ketene acetals (Scheme 2.12).³⁴



Scheme 2.12 Chiral Brønsted acid-catalyzed Mannich reaction.

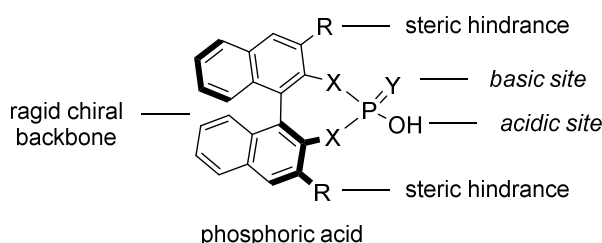
Independently, the Terada group reported a proposed phosphoric acid-catalyzed asymmetric Mannich reaction between *N*-Boc protected aromatic imines and diketones in the same year (Scheme 2.13).³⁵ However, it was revealed six years later that the real catalyst was not the phosphoric acid, but in this case rather the corresponding calcium salt.³⁶ These two reports are regarded as milestones in chiral Brønsted acid catalysis and initiated the rapid development of stronger chiral Brønsted acids.

2 BACKGROUND



Scheme 2.13 Proposed Phosphoric acid-catalyzed Mannich reaction.

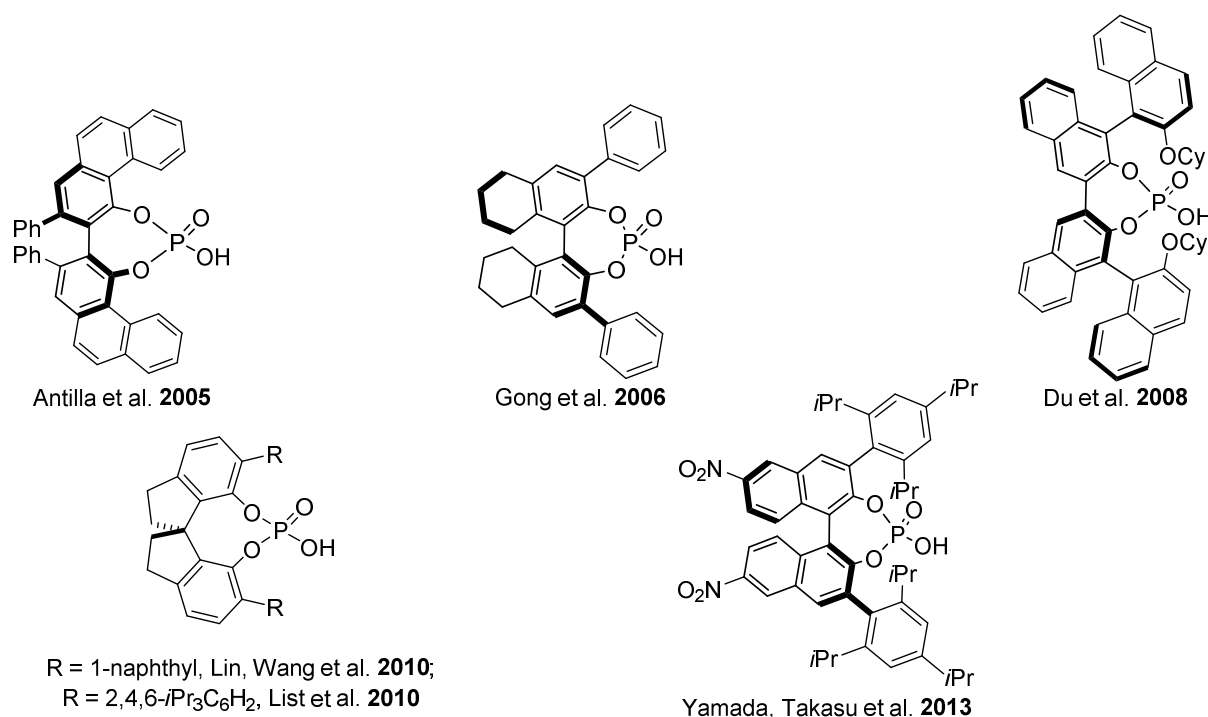
Chiral phosphoric acids have emerged as powerful catalysts since their discovery.^{33,37} We ascribe the success of these chiral BINOL-derived phosphoric acids in asymmetric catalysis to their following features: 1. bifunctionality; 2. tunability; 3. rigid and chiral backbone. The bifunctional property of chiral Brønsted acids plays a crucial role in the cooperative activations of both nucleophiles and electrophiles in the reactions. The modulation of the 3,3'-substituents leads to a class of diverse phosphoric acids since the substituents at the 3,3'-positions of phosphoric acids are highly related to the steric hindrance and the acidity of the catalysts. The List group introduced a bulky 2,4,6-*i*Pr₃C₆H₂ group to this position and obtained one of the most popular chiral phosphoric acids, TRIP,³⁸ which has been successfully applied to asymmetric-counteranion directed catalysis (ACDC) and other asymmetric reactions.^{39,40}



Scheme 2.14 Features of chiral phosphoric acids.

2 BACKGROUND

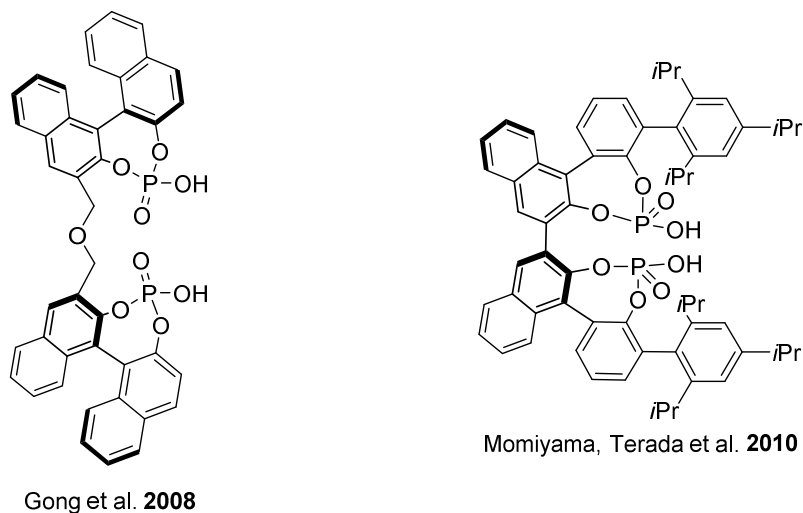
The rigid BINOL core can also be modulated and several strategies have been successfully implemented (Scheme 2.15). The Antilla group reported a VAPOL-derived phosphoric acid-catalyzed imine amidation.⁴¹ The Gong group introduced a H₈-BINOL-derived phosphoric acid, which showed its privilege in a highly enantioselective Biginelli reaction.⁴² Du and coworkers developed a doubly axial chiral phosphoric acid and applied this new catalyst to an asymmetric reduction of quinolines.⁴³ Two groups independently introduced SPINOL backbones to the phosphoric acid catalysis in 2010. Lin, Wang, and coworkers reported a highly enantioselective Friedel-Crafts reaction between indoles and imines, which was catalyzed by a 1-naphthyl-substituted SPINOL-derived phosphoric acid.⁴⁴ Simultaneously, the List group developed a bulky SPINOL-derived phosphoric acid: STRIP, which was used for an enantioselective kinetic resolution of alcohols via transacetalization.⁴⁵ SPINOL-derived phosphoric acids proved superior over the corresponding BINOL counterparts in some transformations, however the lack of practical approaches to synthesize SPINOL hindered the development of this novel catalyst motif. Gratifyingly, Tan and coworker recently reported an efficient and catalytic approach to synthesize enantiomerically enriched SPINOL derivatives.⁴⁶ Yamada, Takasu, and coworkers reported another novel catalyst, nitrated-TRIP, which had been utilized to catalyze a kinetic resolution of secondary alcohols. High stereoselectivities were generally achieved at ambient temperatures.⁴⁷



Scheme 2.15 Selected diverse backbones of chiral phosphoric acid catalysts.

2 BACKGROUND

Different chiral bis-phosphoric acids have been developed. In 2008 Gong and coworkers reported an organocatalytic asymmetric three-component 1,3-dipolar addition reaction of aldehydes, amino esters, with dipolarophiles, which was enabled by an ether-linked BINOL-derived bisphosphoric acid.⁴⁸ Momiyama, Terada and coworkers designed another chiral and axial bis-phosphoric acid and applied this new catalyst motif to an highly enantioselective Diels–Alder reaction between α,β -unsaturated aldehydes and amidodienes.⁴⁹

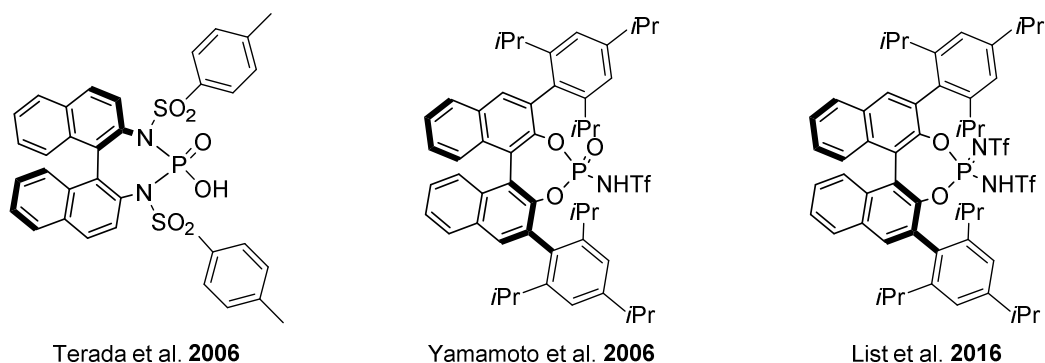


Scheme 2.16 Selected chiral bis-phosphoric acid catalysts.

However, the initial progress of chiral phosphoric acids has mainly relied on using reactive and basic electrophiles, such as imines. The development of highly acidic chiral Brønsted acids (Scheme 2.17 and 2.18) enables chemists to tackle more challenging reactions, facilitating the diversity of asymmetric synthesis.

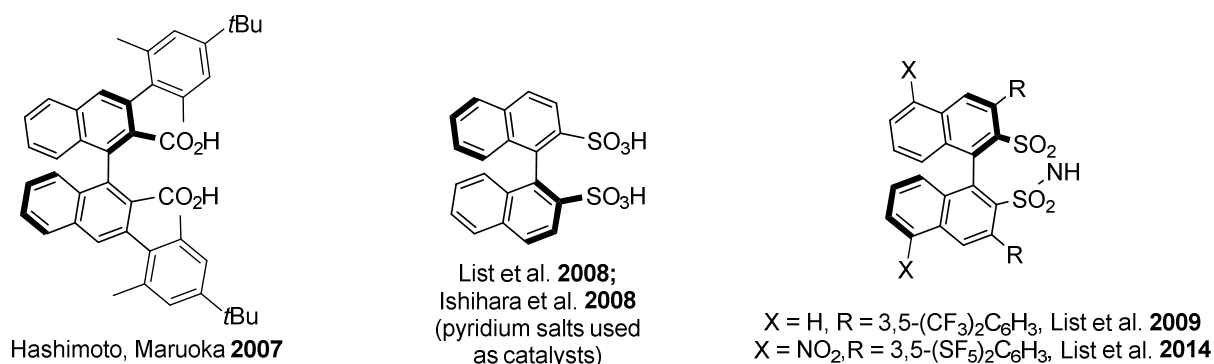
In 2006, the Terada group developed a novel chiral phosphordiamidic acid, which was applied to an asymmetric Mannich reaction between *N*-acyl imines and 1,3-dicarbonyl compounds (Scheme 2.17).⁵⁰ Simultaneously, the Yamamoto group developed a highly acidic chiral *N*-triflyl phosphoramidate, which was used in an asymmetric Diels–Alder reaction of α,β -unsaturated ketone with silyloxydiene with excellent stereoselectivity.⁵¹ Recently, List and Kaib developed an extremely acidic chiral phosphoramidimidate, which was applied to the synthesis of α -tocopherol.⁵² A dramatic improvement of conversion was obtained, compared to other previously reported stronger chiral Brønsted acids.

2 BACKGROUND



Scheme 2.17 Selected phosphoric acid derivatives.

In 2007, Hashimoto and Maruoka developed a new chiral BINOL-derived dicarboxylic acid and applied this catalyst to a highly enantioselective Mannich reaction of arylaldehyde *N*-Boc imines with diazo compounds.⁵³ One year later, the List group reported another even stronger chiral BINOL-derived disulfonic acid-catalyzed three-component Hosomi–Sakurai reaction, although the enantioselectivity was not achieved.^{54a} However, Ishihara and coworkers reported a highly enantioselective Mannich reaction, which was catalyzed by the corresponding pyridium-disulfonates.^{54b} The List group also developed other highly acidic chiral disulfonimides which have been used as precatalysts for Lewis acids in several highly enantioselective transformations, such as Mukaiyama–Aldol reactions, Mukaiyama–Mannich reactions, and the cyanosilylation of aldehydes.^{55–57} Recently, List and coworkers introduced a chiral nitrated-disulfonimide, which was applied to an enantioselective Torgov cyclization. This methodology was further utilized in the shortest enantioselective synthesis of (+)-estrone.⁵⁸

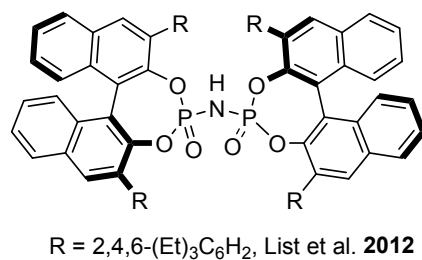


Scheme 2.18 Selected stronger BINOL-derived chiral Brønsted acids.

Due to their relatively open active site, scarce progress has been made in the asymmetric reactions of small substrates in phosphoric acid catalysis. To address this issue, the List group developed a chiral imidodiphosphate (IDP) with 2,4,6-Et₃C₆H₂ substituents, which possesses an extremely confined chiral microenvironment (Scheme 2.19). This Brønsted

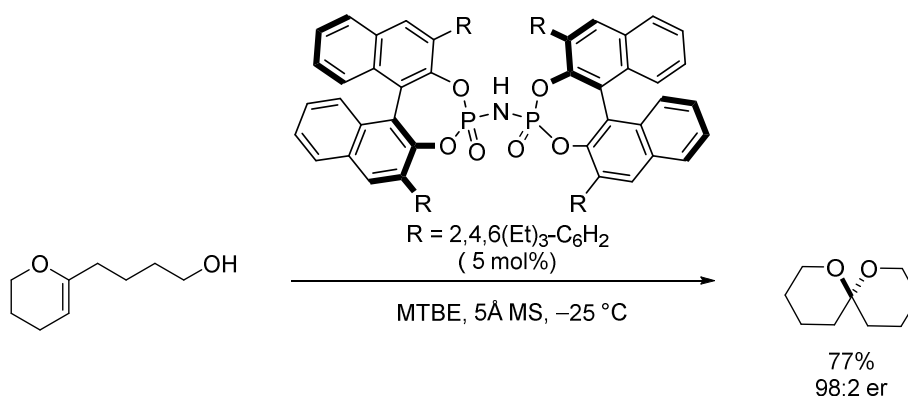
2 BACKGROUND

acidic catalyst was successfully used for asymmetric reactions of small substrates (Scheme 2.20 and 2.21).^{59,60}



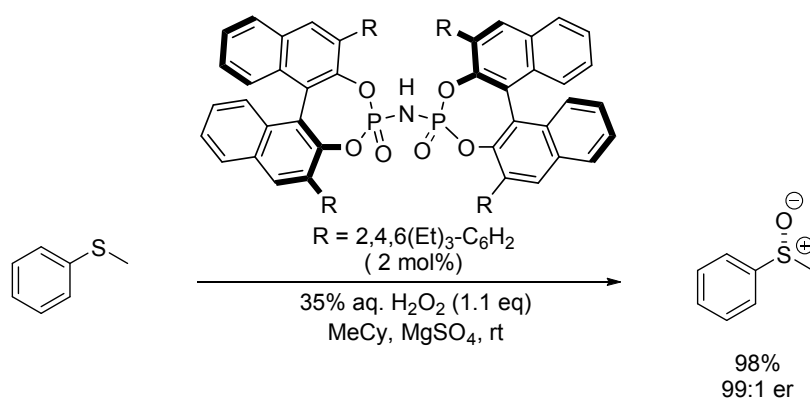
Scheme 2.19 Chiral confined Brønsted acids.

List and Čorić utilized this IDP to catalyze the spiroacetalization of hydroxyenol ethers and various enantiomerically enriched spiroacetals, including some natural products that were obtained with excellent stereoselectivities (Scheme 2.20).⁵⁹



Scheme 2.20 IDP-catalyzed spiroacetalization.

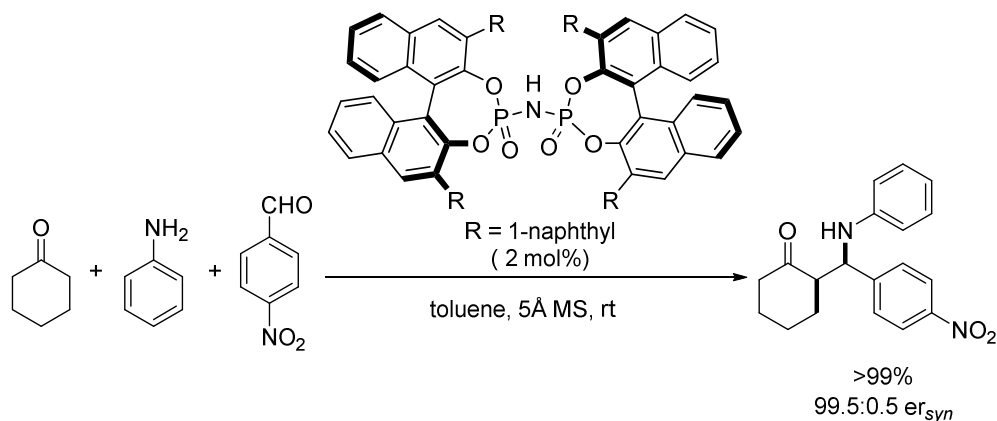
This confined Brønsted acid imidodiphosphate (IDP) with 2,4,6-Et₃C₆H₂ substituents was also applied to an asymmetric oxidation of sulfides by the same group. A variety of chiral sulfoxides were furnished with excellent yields and enantioselectivities (Scheme 2.21).⁶⁰



Scheme 2.21 IDP-catalyzed sulfoxidation.

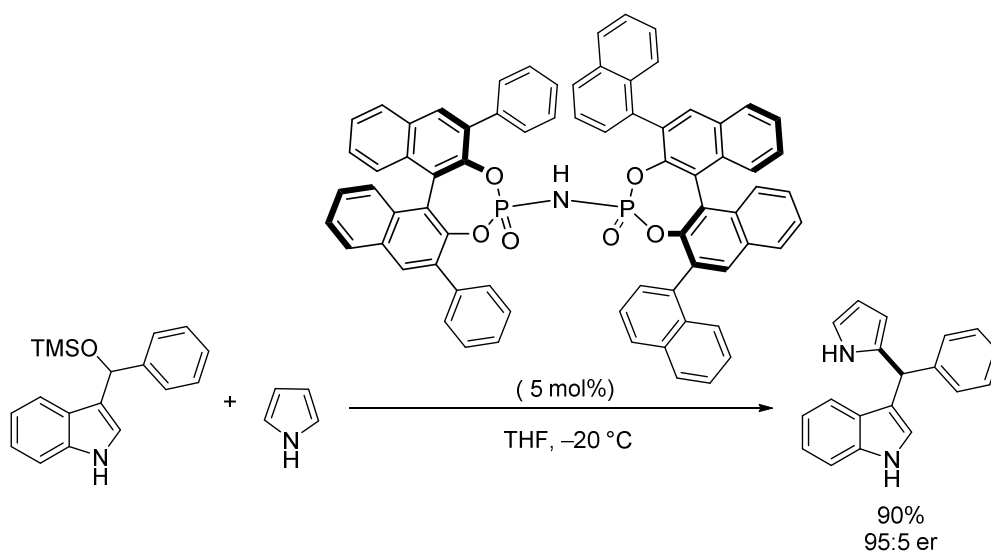
2 BACKGROUND

Subsequently, this type of confined imidodiphosphate has been successfully utilized in other asymmetric reactions. Zheng, Zhang, and coworkers reported a 1-naphthyl substituted imidodiphosphate-catalyzed asymmetric three-component Mannich reaction. Syn- β -amino ketones were obtained with generally high enantioselectivities (Scheme 2.22).⁶¹



Scheme 2.22 IDP-catalyzed Mannich reaction.

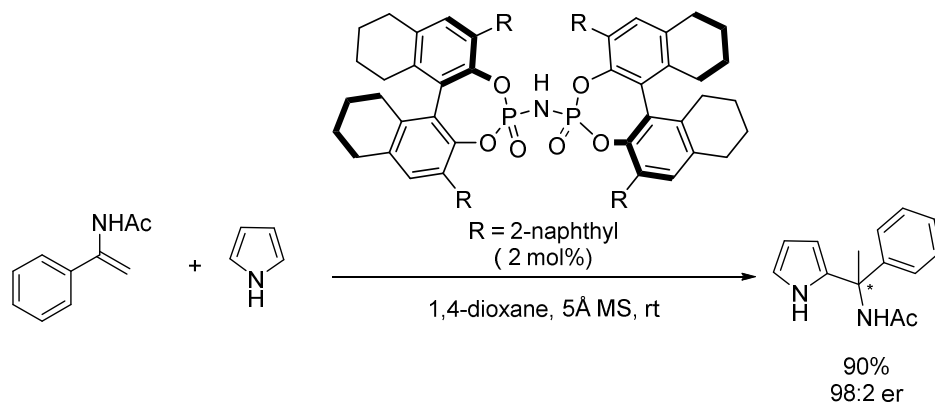
The modulation of imidodiphosphate has been implemented, even though the efforts have mainly been put in modifying the BINOL backbones. Jiang, Zhang and coworkers developed a novel hybrid imidodiphosphate which was derived from two BINOL frameworks with different 3,3'-substituents. This new chiral acid was applied to an asymmetric Friedel–Crafts reaction and functionalized pyrrolylsubstituted triarylmethanes were obtained with good yields and high enantioselectivities (Scheme 2.23).⁶²



Scheme 2.23 IDP-catalyzed Friedel–Crafts reaction.

2 BACKGROUND

The same group reported H₈-BINOL-derived chiral imidodiphosphate-catalyzed highly chemo-, regio- and enantioselective aza-Friedel-Crafts reactions between pyrroles and enamides or imines to afford enantiopure bioactive aryl-(2-pyrrolyl)methanamine products with high yields and enantioselectivities (Scheme 2.24).⁶³



Scheme 2.24 H₈-IDP-catalyzed aza-Friedel-Craft reaction.

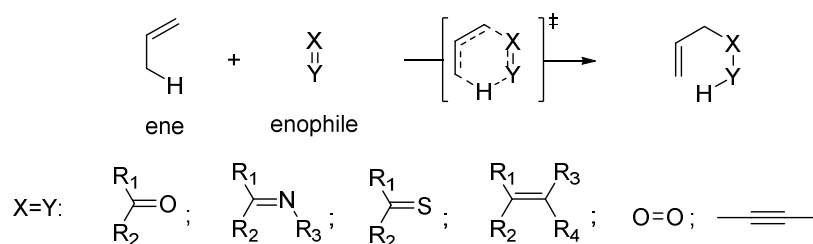
2 BACKGROUND

2.2 Asymmetric Reactions between Aldehydes and Olefins

Despite tremendous progress in asymmetric synthesis, broad substrate scopes, especially unactivated and/or small substrates have remained challenging. This doctoral work aims at general asymmetric reactions between unactivated carbonyl compounds and simple olefins, such as the carbonyl–ene reaction and the hetero-Diels–Alder reaction of simple dienes with aldehydes.

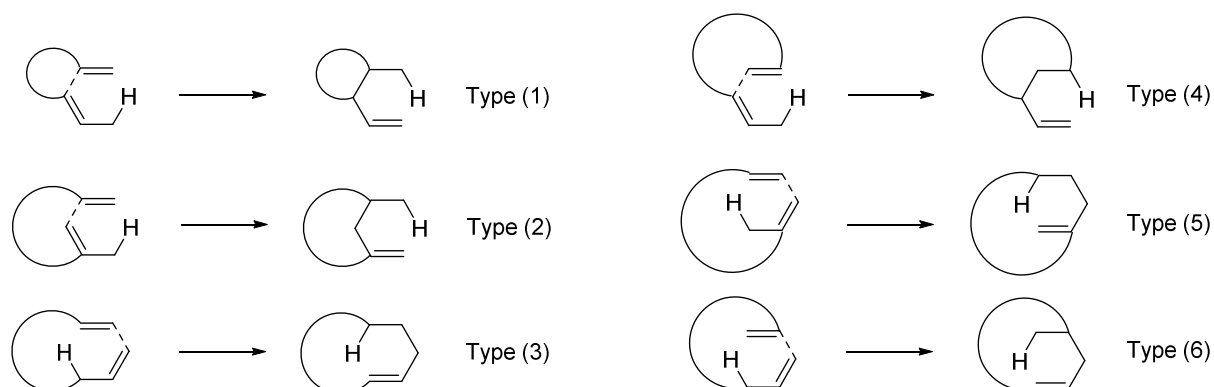
2.2.1 Asymmetric Carbonyl–Ene Cyclization

The ene reaction is a chemical transformation between an olefin containing an allylic C–H (ene) and a multiple bond (enophile), discovered by Prof. Alder in 1943.⁶⁴ A concerted pathway is always envisioned, and a new C–C σ bond is formed along with a migration of a π bond and 1,5-hydrogen shift (Scheme 2.25).



Scheme 2.25 The ene reaction.

The corresponding intramolecular carbonyl–ene reaction is one of the most efficient and atom economical approaches to form C–C bonds and to construct functionalized cyclic compounds.^{65–67} As shown in Scheme 2.26, the intramolecular ene reaction is generally categorized into six distinct types depending on the connectivity between the alkene and the electrophile, on the basis of the work by Mikami, Oppolzer, and Snider.⁶⁵

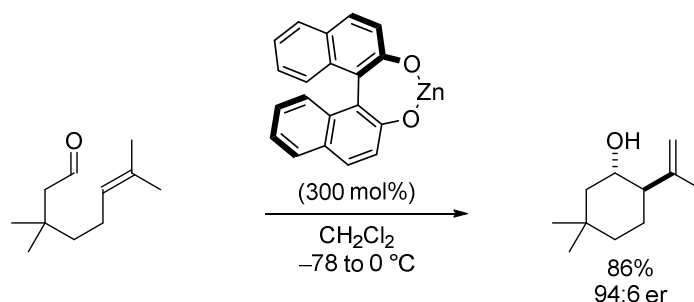


Scheme 2.26 Classification of intramolecular ene reaction.

2 BACKGROUND

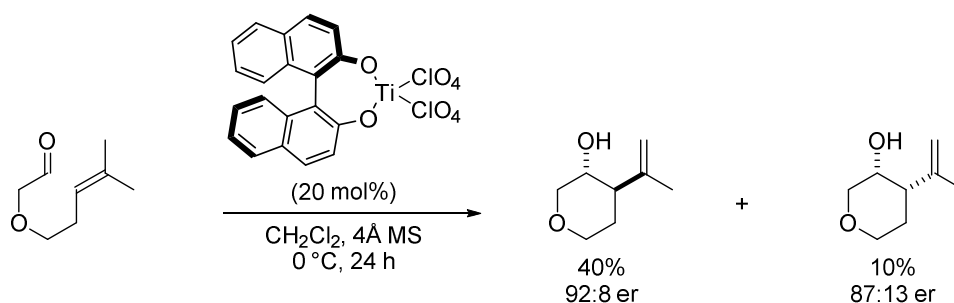
Intramolecular carbonyl–ene reactions, in which carbonyl groups act as the enophiles, normally require temperatures higher than 140 °C.⁶⁸ Several strategies have been implemented to accelerate the carbonyl–ene cyclization: 1. introduction of Lewis acid catalysts, which significantly lower the LUMO of the carbonyl; 2. application of electron-biased substrates, such as an electron-deficient carbonyl and/or an electron-rich alkene^{69,70}; 3. use of steric acceleration.

BINOL-derived chiral Lewis acids with different metal species have been extensively explored in asymmetric carbonyl–ene cyclization reaction in the last 30 years. In 1986, Yamamoto and coworkers reported the first Lewis acid-catalyzed asymmetric carbonyl–ene cyclization reaction (Scheme 2.27).⁷¹ Even though a good yield and enantioselectivity of the *trans*-diastereoisomer were achieved, 3 equiv. of the Lewis acidic zinc-BINOL complex were required. This work is regarded as a milestone for asymmetric carbonyl–ene cyclizations and 3,3,7-trimethyloct-6-enal has been continually used as a standard substrate in carbonyl–ene cyclization reactions since then.



Scheme 2.27 The first Lewis acid-promoted asymmetric carbonyl–ene cyclization.

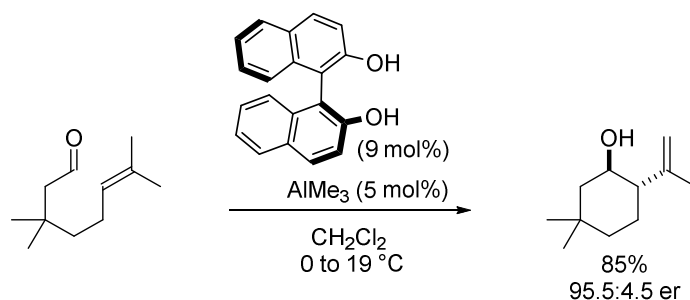
Later, the Mikami group reported the first catalytic asymmetric intramolecular carbonyl–ene cyclization reaction using a chiral titanium-BINOL complex as the catalyst. Six- and seven-membered cyclic products were obtained with moderate diastereoselectivities and moderate to good enantioselectivities.⁷²



Scheme 2.28 The first catalytic asymmetric carbonyl–ene cyclization.

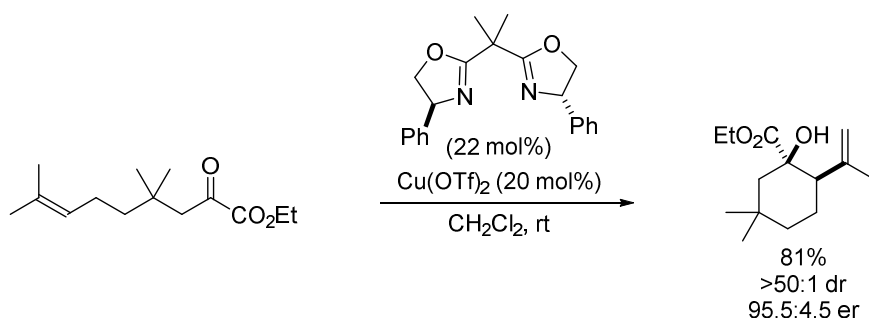
2 BACKGROUND

Recently, Hori, Mino, and coworkers reported a chiral aluminum-BINOL complex-catalyzed asymmetric carbonyl–ene cyclization (Scheme 2.29).⁷³ Compared to previous results, the cycloadduct of 3,3,7-trimethyloct-6-enal was obtained with an improved yield and stereoselectivity using a reduced amount of the catalyst. Toste, Bergman, Raymond, and coworkers designed and synthesized a chiral amide-directed supramolecule and employed this supramolecule to the carbonyl–ene cyclization of 3,3,7-trimethyloct-6-enal with competitive results.⁷⁴



Scheme 2.29 Chiral Al-BINOL complex-catalyzed asymmetric carbonyl–ene cyclization.

Lewis acids with other chiral ligands, e.g. BOX ligand and Pybox ligand, were also employed in asymmetric carbonyl–ene cyclizations.^{75–78} In 2003, the Yang group reported a highly enantioselective intramolecular carbonyl–ene reaction of olefinic keto esters, which was catalyzed by the chiral Lewis acid $[\text{Cu}((\text{S,S})\text{-Ph-BOX})](\text{OTf})_2$.⁷⁵ Functionalized cycloadducts were obtained in good yields and excellent stereoselectivities, even though activated substrates bearing an electron deficient carbonyl were required.

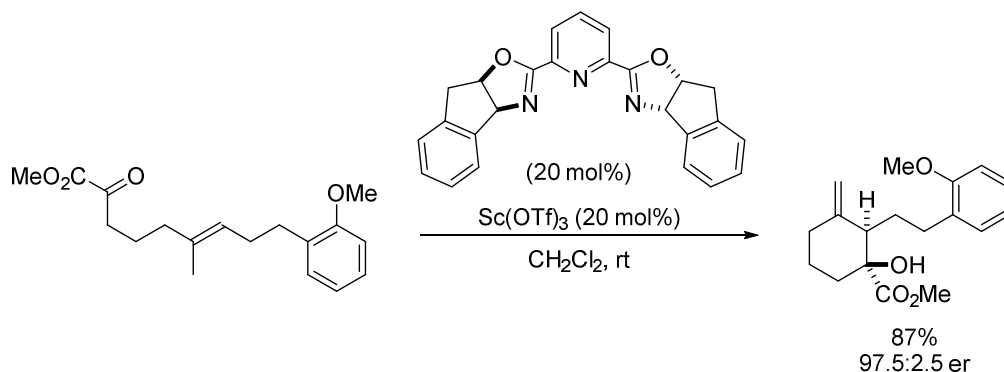


Scheme 2.30 Asymmetric carbonyl–ene cyclization of olefinic keto esters.

Recently, Loh and coworkers reported a chiral Lewis acid $[\text{Sc-Pybox}](\text{OTf})_3$, which catalyzed a highly enantioselective intramolecular carbonyl–ene reaction.⁷⁶ This

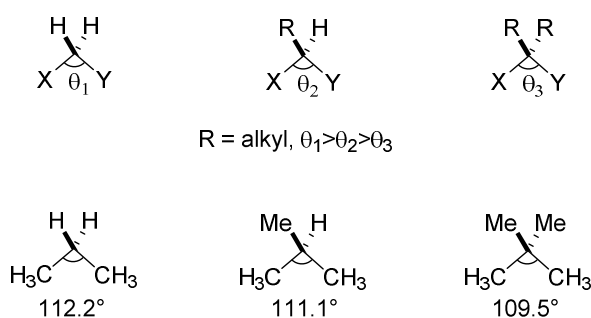
2 BACKGROUND

methodology was applied to an enantioselective total synthesis of a natural terpenoid product (+)-tripthenolide.



Scheme 2.31 Enantioselective carbonyl-ene cyclization.

Steric acceleration has been exploited in intramolecular cyclization reactions for more than one century.^{79–81} One of the typical strategies to accelerate a reaction through steric accelerations is the *gem*-dialkyl effect, which is also known as Thorpe–Ingold effect. In the Thorpe–Ingold effect, hydrogen atoms are replaced with alkyl groups on the tethering carbon, which decreases the angle between the reacting ends and increases the interaction between each other.^{82,83} As shown in scheme 2.32, the C–C–C angle in propane is 112.2°, however, C–C–C angle in isobutane is reduced to 111.1°, while the angle is further reduced to 109.5° in neopentane, which is due to the replacement of hydrogens by methyl groups on the tethering carbon. This strategy has also been used in asymmetric intramolecular carbonyl-ene reactions. For example, the frequently used substrate 3,3,7-trimethyloct-6-enal is an activated substrate due to the *gem*-dialkyl effect.

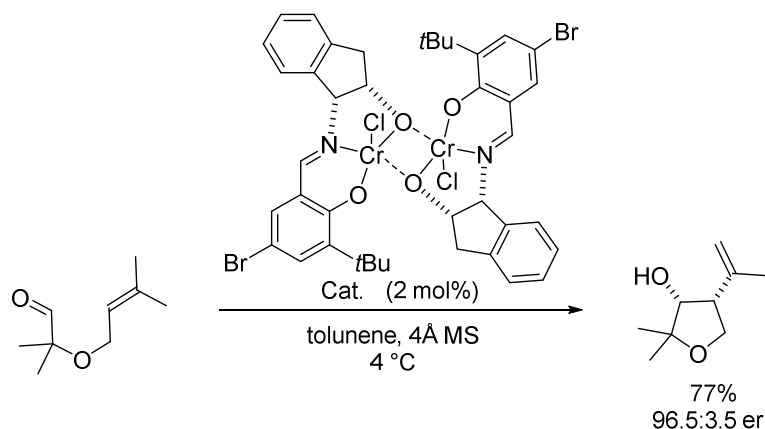


Scheme 2.32 Thorpe–Ingold effect.

Recently, Jacobsen and coworkers reported a highly enantioselective chiral dimeric chromium complex-catalyzed carbonyl-ene cyclization reaction.⁷⁸ *Cis*-diastereoselective products were exclusively afforded in good yields with high stereoselectivities in this

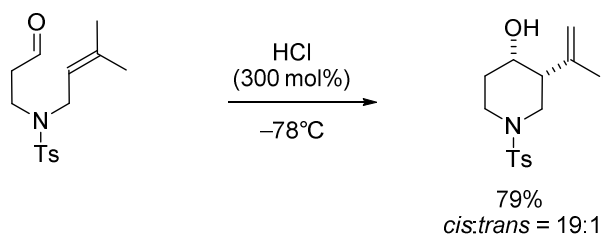
2 BACKGROUND

case. However, reactive substrates with Thorpe–Ingold-type substitutions were used in this work.



Scheme 2.33 Thorpe–Ingold effect in asymmetric carbonyl–ene cyclization.

Even though it is very fruitful in Lewis acid-catalyzed enantioselective intramolecular carbonyl–ene reactions, chiral Brønsted acid catalysis has rarely been utilized in this field. There were several achiral Brønsted acid-catalyzed non-enantioselective carbonyl–ene cyclizations reported by Snaith and coworkers.^{84,85} Different diastereoselectivity was obtained using achiral Brønsted acids compared to previously reported Lewis acid-catalyzed variants. This inspired us to investigate the relatively unexplored field of chiral Brønsted acid-catalyzed carbonyl–ene cyclization reactions.

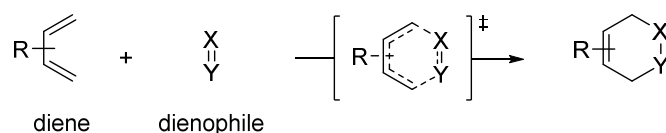


Scheme 2.34 Achiral acid-catalyzed carbonyl–ene cyclization

2 BACKGROUND

2.2.2 Asymmetric Hetero-Diels–Alder Reaction of Dienes and Aldehydes

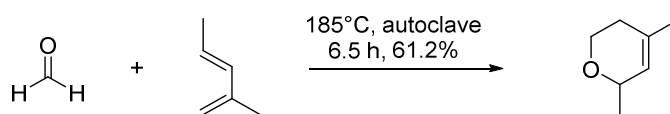
The Diels–Alder (DA) reaction between dienes and olefins (dienophiles) serves to construct functionalized cyclohexene compounds (Scheme 2.35). The DA reaction is mechanistically considered to proceed through a concerted and six-membered aromatic transition state.^{86–90}



Scheme 2.35 Diels–Alder reaction.

This reaction was named after the German chemists Otto Diels and Kurt Alder. They pioneeringly investigated a cycloaddition reaction between benzoquinone and cyclopentadiene in 1928.⁹¹ After this milestone discovery, the Diels–Alder reaction immediately drew the attention of synthetic chemists.^{92,93} Tremendous progress has been made in this field, such as: 1. well-established reaction mechanisms and theories on the basis of both experiments and computational studies, including the Alder endo rule, molecular orbital theory, and frontier orbital theory;^{94,95} 2. exploration and extension of the reaction scope, which has been widely used in academic and/or industrial area; 3. the recent development of DA reactions on exploration of asymmetric variants. In 1950, the Noble Prize in chemistry was awarded to Prof. Diels and Prof. Alder for their work on the Diels–Alder reaction.

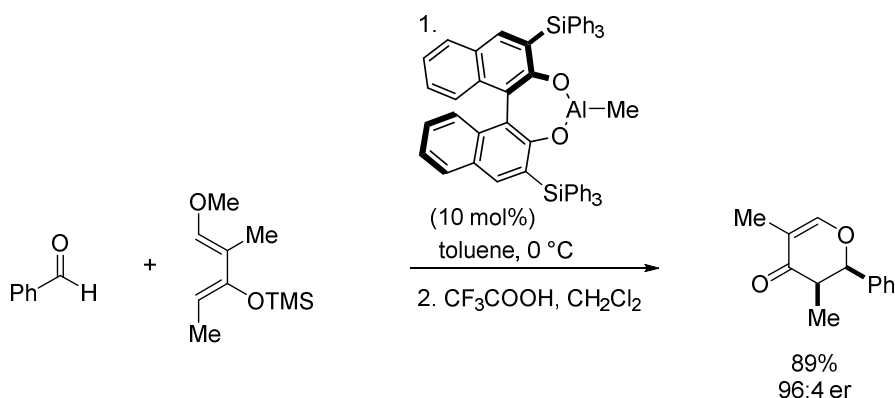
Likewise, the hetero-Diels–Alder (HDA) reaction between dienes and aldehydes is arguably the most efficient and atom economical approach to oxygen heterocycles.⁹⁶ Six-membered oxygen heterocycles are frequently found within carbohydrates, pharmaceuticals, agrochemicals, and fragrances. However, it was not until 1949 that Gresham and Steadman reported the first HDA reaction between formaldehyde and methylpentadiene (Scheme 2.36). Valuable functionalized dihydropyran compounds were obtained from abundant feedstocks, such as formaldehyde and simple dienes.⁹⁷



Scheme 2.36 Pioneering HDA reaction of a diene with an aldehyde.

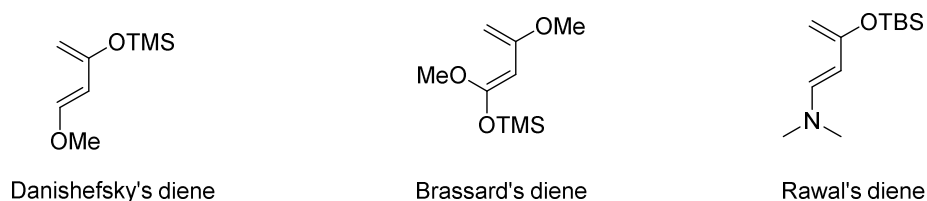
2 BACKGROUND

As mentioned above, the recent progress of HDA reactions between dienes and aldehydes has mainly focused on the development of asymmetric methodologies. In the past three decades, a variety of chiral Lewis acid complexes have been applied to asymmetric HDA reaction between dienes and aldehydes, including chiral boron, aluminum, indium, chromium, zinc and titanium complexes.⁹⁸ Yamamoto and his coworkers reported the first highly enantioselective HDA reaction between dienes and aldehydes, which was catalyzed by a chiral BINOL-Al complex (Scheme 2.37).⁹⁹ Good yields and excellent stereoselectivities were achieved using a highly reactive Danishefsky-type diene.



Scheme 2.37 The first highly enantioselective HDA reaction of dienes with aldehydes.

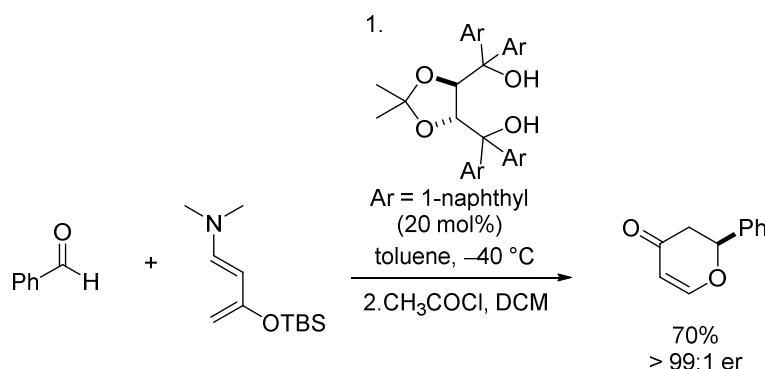
The discovery of Danishefsky's diene boosted the applications of HDA reactions in organic synthesis.^{93,96} The introduction of this activated reagent, narrowing the energy gap between HOMO_{diene} and LUMO_{dienophile}, enabled the performance of asymmetric HDA reactions under mild reaction conditions.¹⁰⁰ Moreover, this reagent also contributed to the high regioselectivity. Several other activated dienes were developed subsequently, for example, Brassard's diene, and Rawal's diene (Scheme 2.38).¹⁰¹⁻¹⁰³



Scheme 2.38 Activated diens.

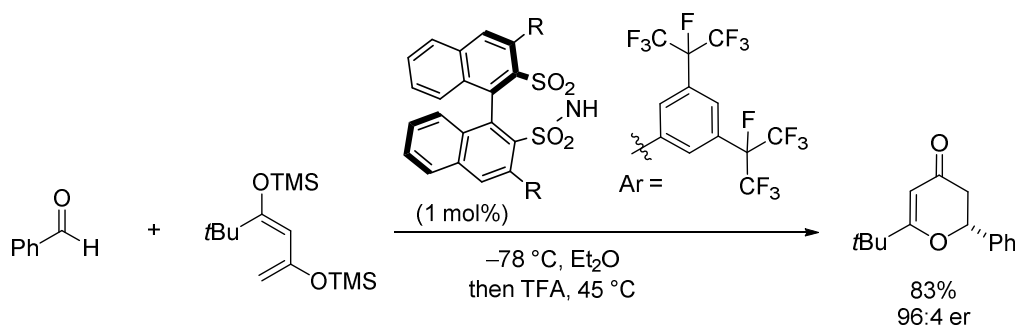
2 BACKGROUND

Complementary to Lewis acid catalysis, Brønsted acid-catalyzed HDA reactions between dienes and aldehydes have also been investigated recently. In 2003, Rawal and coworkers reported a TADDOL-catalyzed asymmetric HDA reaction between Rawal's diene and aldehydes.¹⁰² They proposed a novel hydrogen bonding activation between the chiral alcohol catalyst and the carbonyl group. Functionalized dihydropyrones were obtained in generally good yields and enantioselectivities.



Scheme 2.39 Organocatalytic cycloaddition of an activated diene with aldehydes.

List and coworkers reported a highly enantioselective HDA reaction of substituted 1,3-bis(silyloxy)-1,3-dienes with aldehydes in 2012, which was catalyzed by a highly acidic disulfonimide (DSI). High yields and enantioselectivities were generally achieved. The authors proposed a stepwise mechanism involving a Mukaiyama aldol reaction.

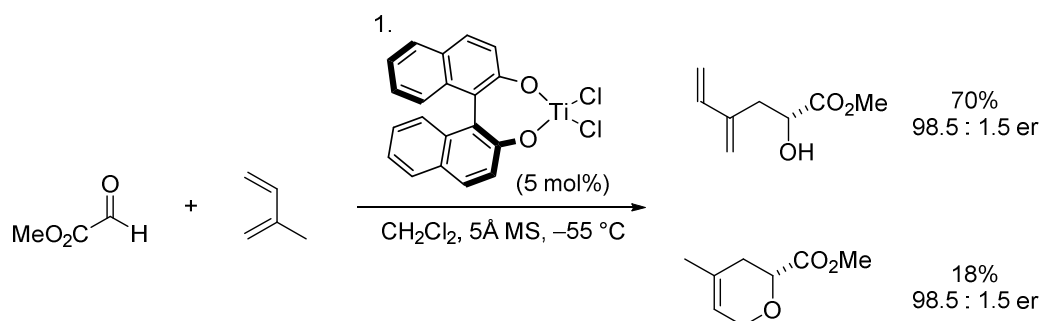


Scheme 2.40 DSI-catalyzed cycloaddition of activated dienes with aldehydes.

However, the successful enantioselective, catalytic variants of these asymmetric HDA reactions have been limited to activated and electronically engineered dienes. Unactivated and simple dienes, such as isoprene, were also explored in asymmetric Lewis acid catalyzed hetero-Diels–Alder reactions, although activated dienophiles, such as glyoxylate, were required.^{104,105}

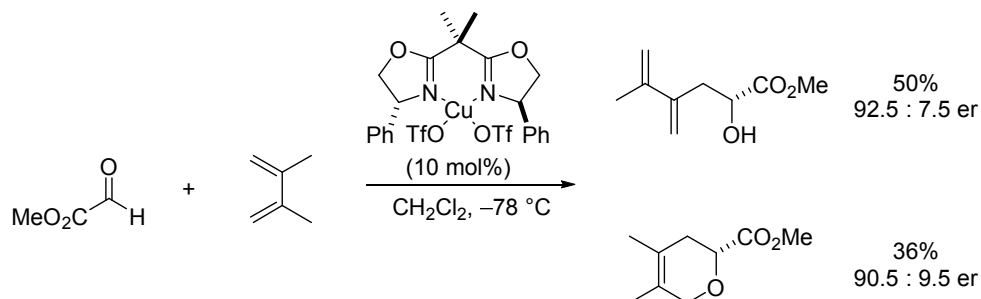
2 BACKGROUND

In 1991, Mikami and coworkers reported a chiral BINOL-Ti complex-catalyzed reaction between methyl glyoxylate and isoprene.¹⁰⁴ As shown in Scheme 2.39, the carbonyl-ene adduct was obtained as the main product compared to the [4+2]-cycloadduct.



Scheme 2.41 Asymmetric HDA reaction of glyoxylate with isoprene.

Similar results were observed in a chiral Cu-BOX complex-catalyzed reaction between methyl glyoxylate and 2,3-dimethylbuta-1,3-diene reported in 1995 by Jørgensen and coworkers.¹⁰⁵ Compared to the report above, the amount of [4+2]-cycloadduct was increased, even though the enantioselectivity was moderate. So far, an efficient chiral Lewis acid-catalyzed HDA reaction of simple and unactivated dienes with aldehydes has remained unmet.



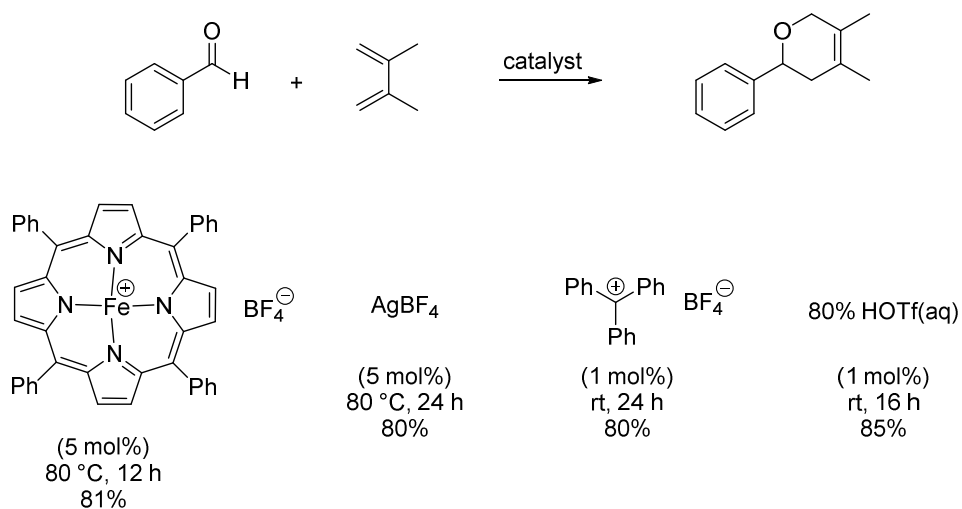
Scheme 2.42 Chiral Cu-BOX complex-catalyzed asymmetric HDA reaction.

Compared to the progress in chiral Lewis acid catalysis, there are no reports on chiral Brønsted acid-catalyzed HDA reactions of simple and unactivated dienes with activated aldehydes due to several known side reactions, including Prins reactions^{106,107} and cationic oligomerization reactions.¹⁰⁸

The development of asymmetric HDA reactions of simple and unactivated dienes with activated aldehydes is still in its infancy. Unsurprisingly, asymmetric HDA reactions between simple and unactivated dienes and unactivated aldehydes are still unknown so far. In principle, this virgin field continuously attracts chemists' interests. Encouraged by

2 BACKGROUND

the achiral acid-catalyzed [4+2]-cycloaddition between simple and unactivated dienes and aldehydes (Scheme 2.43),^{107,109-111} we were determined to develop a general asymmetric variant in this doctoral thesis.



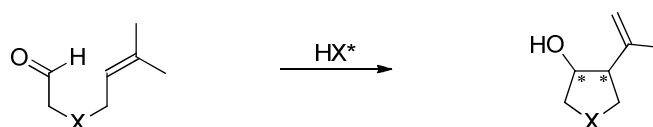
Scheme 2.43 Achiral acid-catalyzed HDA reaction.

3 OBJECTIVES OF THIS THESIS

3.1 Catalytic Asymmetric Reactions of Simple Alkenes with Aldehydes

The goal of this doctoral work is to develop Brønsted acid-catalyzed asymmetric reactions between simple, unactivated alkenes and aldehydes. Highly fundamental, yet challenging enantioselective transformations including a carbonyl–ene cyclization, a Prins cyclization, an *oxa*-Pictet–Spengler reaction, and a hetero-Diels–Alder reaction were explored.

This PhD work began with the intramolecular carbonyl–ene cyclization, which has been frequently used in natural product synthesis. Chiral Lewis acid-catalyzed asymmetric versions of the carbonyl–ene cyclization have been investigated since the 1980s. The first highly stereoselective version was reported by the Jacobsen group in 2008, and highly *cis*-diastereoselective cycloadducts were exclusively afforded. However, reactive substrates with Thorpe–Ingold-type substitutions were required in this work. Alternatively, an organocatalytic asymmetric intramolecular carbonyl–ene cyclization was rarely investigated. We envisioned that an appropriate Brønsted acid would be able to activate the aldehyde group through mono activation, thereby accelerating the intramolecular carbonyl–ene cyclization. The confined chiral microenvironment of the Brønsted acid could minimize alternative transition states to guarantee high stereoselectivities (Scheme 3.1). A general Brønsted acid-catalyzed asymmetric carbonyl–ene cyclization of unactivated olefinic aldehydes without Thorpe–Ingold-type substitutions was targeted in this doctoral work.



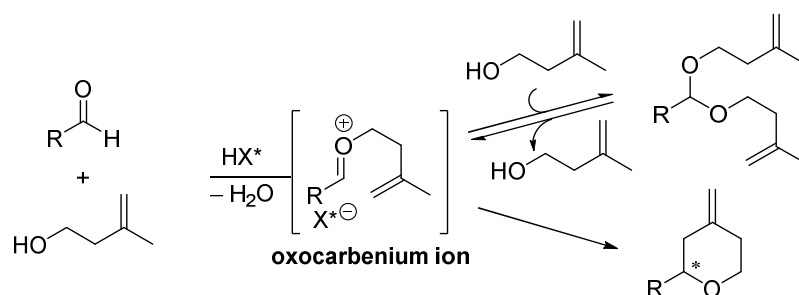
Challenges:

1. Asymmetric addition of less nucleophilic alkenes to aldehydes.
2. Unactivated substrates without Thorpe–Ingold-type substitutions.
3. Enantio- and diastereoselectivity.

Scheme 3.1 Brønsted acid-catalyzed asymmetric carbonyl–ene cyclization.

3 OBJECTIVES OF THIS THESIS

Enantioselective intermolecular cyclizations between aldehydes and alkenes were also explored in this thesis. The Prins cyclization between an aldehyde and a homoallylic alcohol is an efficient approach to deliver tetrahydropyrans, via an *in situ* generated oxocarbenium ion. Surprisingly, only a few asymmetric Prins cyclizations have been reported thus far, probably due to the high reactivity of the intermediate oxocarbenium ion. In addition, the relatively low nucleophilicity of alkenes leads to undesirable side reactions, such as the formation of an acetal (Scheme 3.2). Our group realized the first highly enantioselective Prins cyclization in 2015, though highly activated salicylaldehydes were required to achieve reasonable reactivity. When benzaldehyde was used, the corresponding acetal was formed as the major product under the optimized reaction conditions. Herein, the first general asymmetric Prins cyclization of diverse aromatic and aliphatic aldehydes is presented.



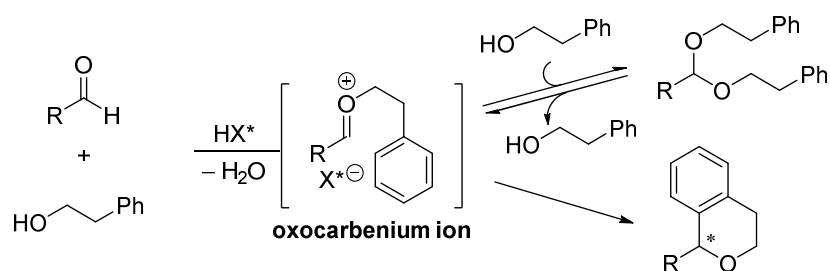
Challenges:

1. Asymmetric addition of less nucleophilic alkenes to oxocarbenium ion intermediates.
2. Avoid side products such as acetals.
3. Unactivated aldehydes.
4. Enantio- and regioselectivity.

Scheme 3.2 Brønsted acid-catalyzed asymmetric Prins cyclization.

In continuation of our studies on the asymmetric Prins cyclization, we hypothesized that the oxocarbenium ion intermediate could, in principle, be trapped by an even less nucleophilic group, such as an arene, effecting the so-called *oxa*-Pictet–Spengler reaction. A broad range of substrates such as diverse aromatic and aliphatic aldehydes were envisaged. In addition to the challenge of stereo- and regioselective control, the possibility of the formation of the side product acetal should be precluded. The rational design and synthesis of a new type of chiral Brønsted acid might enable a general asymmetric *oxa*-Pictet–Spengler reaction (Scheme 3.3). Potentially bioactive isochroman products would be obtained in this envisioned asymmetric *oxa*-Pictet–Spengler reaction between aldehydes and homobenzyl alcohols.

3 OBJECTIVES OF THIS THESIS

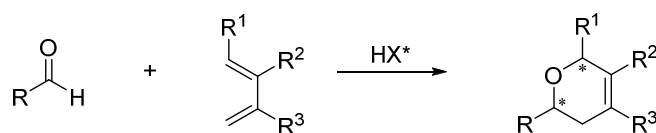


Challenges:

1. Asymmetric addition of weak arenes to oxocarbenium ion intermediates.
2. Avoid side products such as acetals.
3. Enantio- and regioselectivity.

Scheme 3.3 Brønsted acid-catalyzed *oxa*-Pictet–Spengler Reaction.

Following the fruitful success of asymmetric intramolecular carbonyl–ene cyclization and Prins cyclization, a direct intermolecular transformation was next explored as part of the overarching goal towards Brønsted acid-catalyzed asymmetric cycloaddition between simple alkenes and aldehydes. A general asymmetric [4+2]-cycloaddition of simple dienes with aldehydes was envisioned, providing an efficient approach to valuable dihydropyran compounds. A highly acidic and chiral acid would be required to lower the LUMO of aldehydes, due to the lower nucleophilicity of simple dienes. Moreover, several side reactions might occur, since acid-catalyzed Alder–Ene reactions, Aldol reactions and the cationic polymerization reactions were observed in the previously reported hetero-Diels–Alder reaction of aldehydes with dienes.



Challenges:

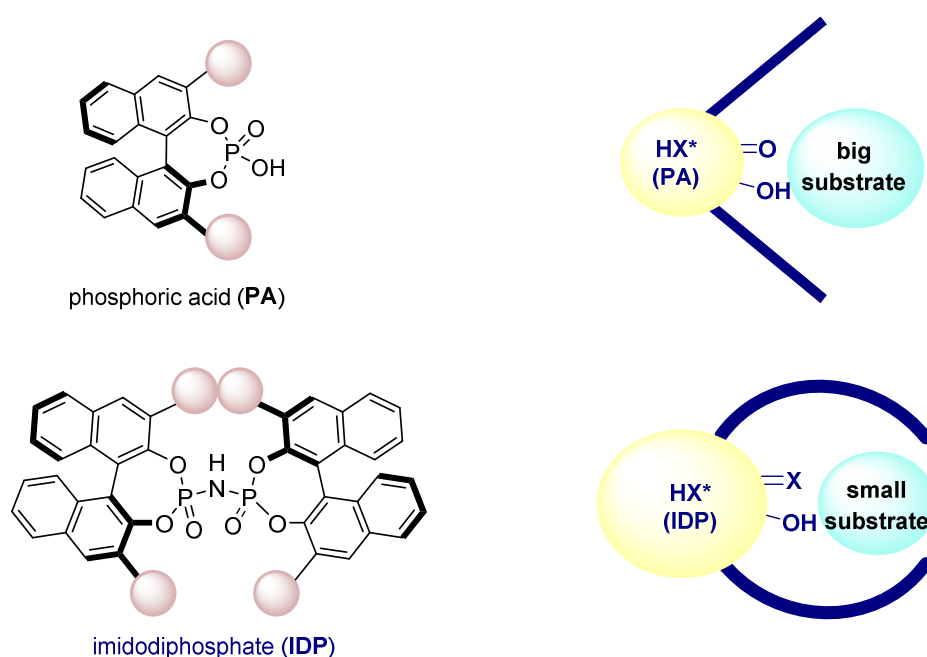
1. Unactivated substrates.
2. Avoid side reactions.
3. Enantio-, diastereo- and regioselectivity.

Scheme 3.4 A general asymmetric [4+2]-cycloaddition of dienes with aldehydes.

3 OBJECTIVES OF THIS THESIS

3.2 Highly Acidic and Confined Brønsted Acids

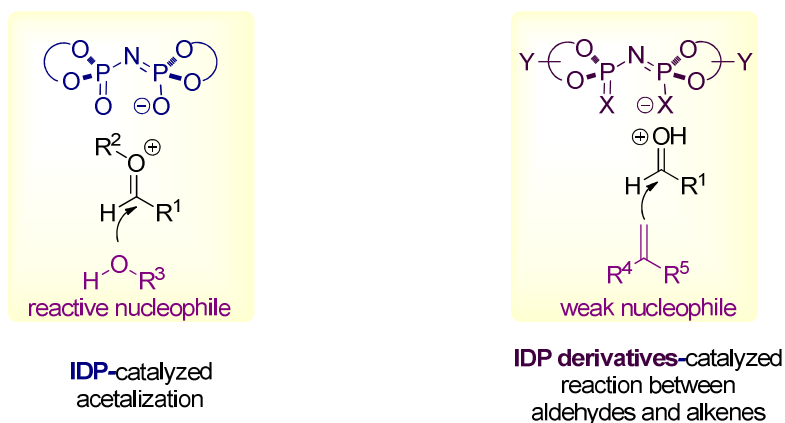
In the last decade, phosphoric acids had enabled a variety of highly enantioselective transformations and thereby effected a tremendous development in organic synthesis.³³ However, since the active site is relatively open, scarce progress has been made in the asymmetric reactions of small substrates in phosphoric acid catalysis. In 2012, the List group developed a new type of Brønsted acid, C_2 -symmetric imidodiphosphate (IDP), which provided a highly compact chiral pocket for the asymmetric acetalization of small substrates (Scheme 3.5).⁵⁹



Scheme 3.5 Confined chiral Brønsted acid.

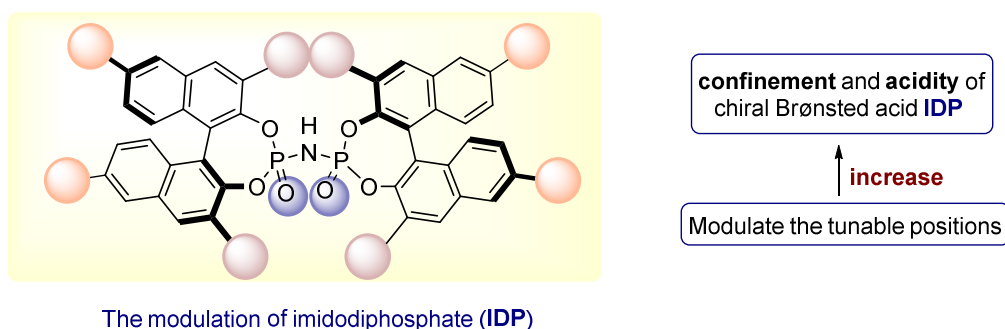
Complementary to highly nucleophilic hydroxyl groups in well-studied IDP-catalyzed enantioselective acetalization reactions,^{112–113} less nucleophilic alkenes were explored in this doctoral work (Scheme 3.6). We envisioned that highly acidic and confined Brønsted acids were required to achieve high yields and stereoselectivities in the asymmetric reactions between simple aldehydes and unactivated alkenes.

3 OBJECTIVES OF THIS THESIS



Scheme 3.6 Utilization of highly acidic and confined Brønsted acids.

To enhance the acidity and steric hindrance of the confined imidodiphosphate (IDP) catalyst, three positions were mainly modulated in this thesis: (1) the active site, (2) the 3,3'-positions, and (3) the 6,6'-positions of the BINOL backbones (Scheme 3.7). The development of the chiral Brønsted acid imidodiphosphate (IDP) and its derivatives made it possible to tackle extremely challenging asymmetric transformations in synthetic chemistry.



Scheme 3.7 Highly acidic and confined chiral Brønsted acids.

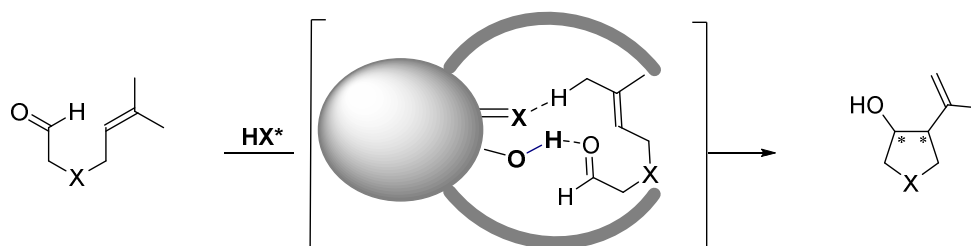
4 RESULTS AND DISCUSSION

4.1 Organocatalytic Asymmetric Carbonyl–Ene Cyclization

4.1.1 Reaction Design and Initial Study

The intramolecular carbonyl–ene cyclization provides an efficient and atom economic approach to diverse cyclic compounds.^{64,114} Activated substrates such as olefinic α -keto esters^{75,76} or olefinic aldehydes⁷⁸ with Thorpe–Ingold-type substitutions were frequently in previously reported asymmetric carbonyl–ene cyclizations, due to the weak nucleophilicity of the alkene. As discussed in the background part, organocatalysis has been rarely developed in this field, compared to the fruitful Lewis acid-catalyzed asymmetric intramolecular carbonyl–ene cyclizations.

We envisioned that confined chiral Brønsted acids would enable a general highly enantioselective carbonyl–ene cyclization (Scheme 4.1). Presumably, the hydrogen bond between the chiral bifunctional Brønsted acid and the carbonyl would accelerate the cyclization step. The compact microenvironment surrounding the active site of the chiral acid would be amenable to distinguish different conformations of the cyclic ring in the transition state.



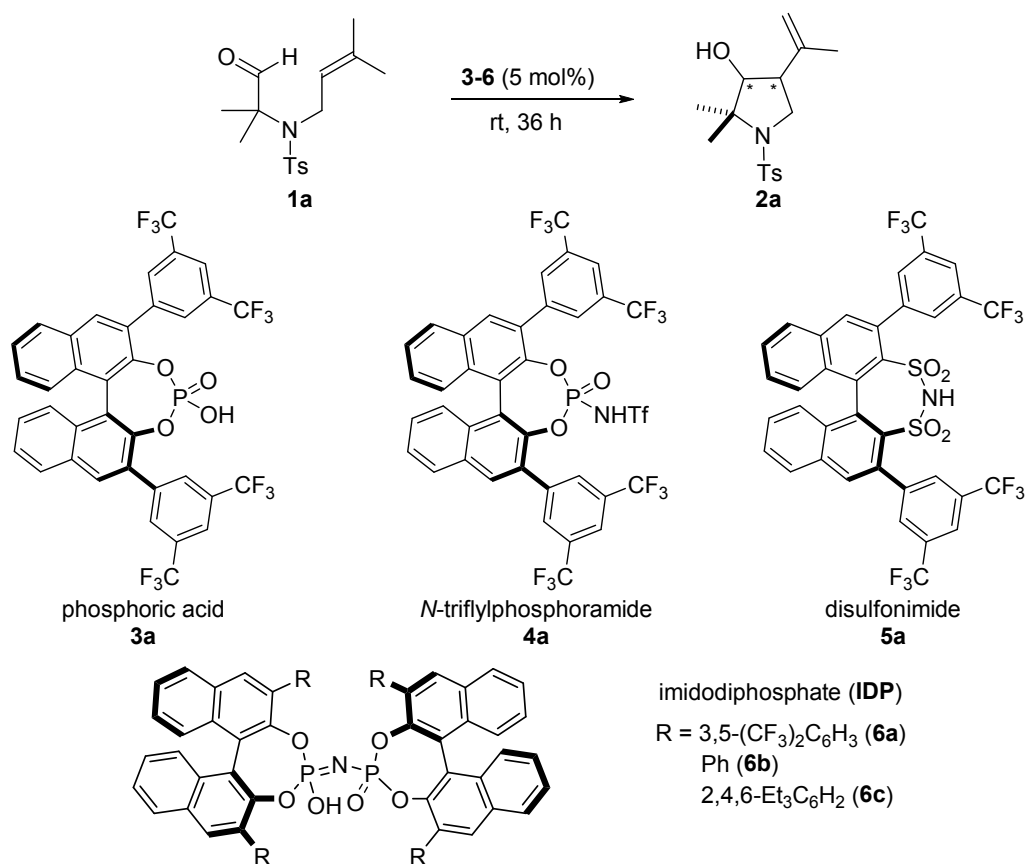
Scheme 4.1 Brønsted acid-catalyzed carbonyl–ene cyclization reaction.

We began our investigation with the chiral acid-catalyzed cyclization of olefinic aldehyde **1a** to obtain pyrrolidine **2a**. Different types of BINOL-derived Brønsted acids including phosphoric acid **3a**,^{33,115,116} *N*-triflylphosphoramidate **4a**,^{51,117,118} and disulfonimide **5a**,^{55,119} were explored. Gratifyingly, all these catalysts were able to afford the desired product with high *trans*-diastereoselectivities, but with low enantioselectivities (Table 4.1, entries 1–3). We reasoned that the active sites in chiral

4 RESULTS AND DISCUSSION

acids **3a–5a** were relatively open and might therefore not be amenable for high enantiocontrol of the small substrate **1a**. Subsequently, a more confined Brønsted acid imidodiphosphate **6a**¹²⁰ was tested, giving a promising enantiomeric ratio (er) of 74.5:24.5. After modulating the substituents at the 3,3'-positions of the imidodiphosphates, catalyst **6c** with 2,4,6- Et₃C₆H₂ substituents fully converted **1a** to **2a** with an excellent diastereomeric ratio (dr) of 43:1 and a 97.5:2.5 er. The dr of **2a** could reach 50:1 after optimizing the solvent.

Table 4.1 Optimization of reaction conditions.^a



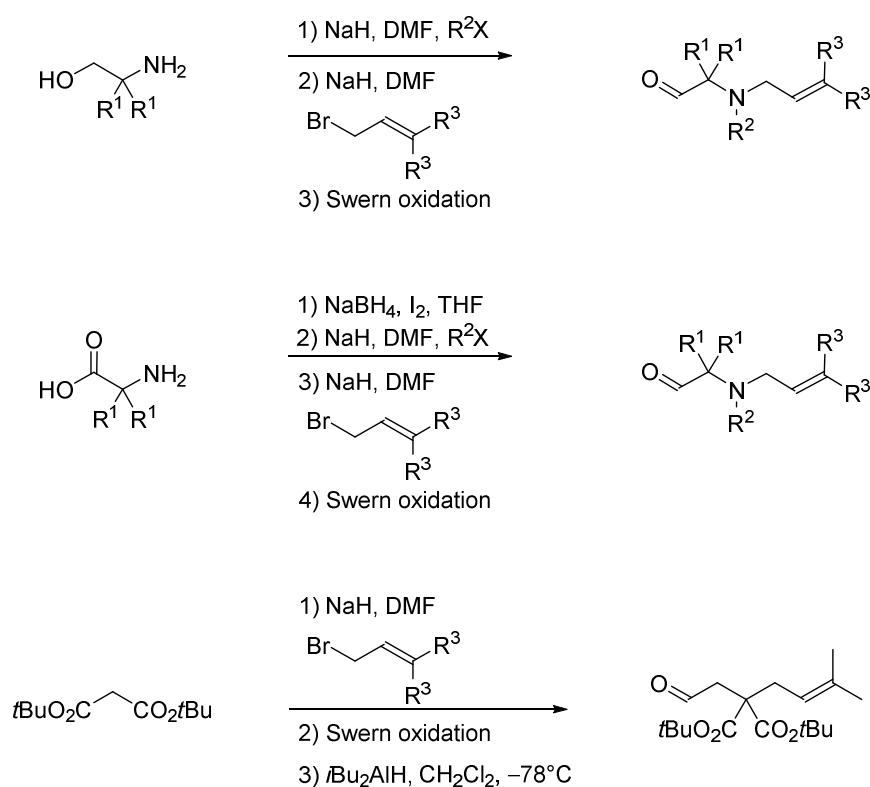
entry	catalyst	solvent	conv.(%)	<i>trans</i> : <i>cis</i> ^b	er _{<i>trans</i>} ^b
1	3a	CH ₂ Cl ₂	>95	16:1	58:42
2	4a	CH ₂ Cl ₂	>95	12:1	64:36
3	5a	CH ₂ Cl ₂	>95	24:1	58.5:41.5
4	6a	CH ₂ Cl ₂	>95	18:1	75.5:24.5
5	6b	CH ₂ Cl ₂	56	19:1	53.5:46.5
6	6c	CH ₂ Cl ₂	>95	43:1	97.5:2.5
7	6c	MeCy	>95	50:1	97.5:2.5

4 RESULTS AND DISCUSSION

^aUnless otherwise indicated, reactions were performed with **1a** (0.1 mmol) and catalyst (5 mol%) in 1.0 mL of solvent for 36 h at room temperature. ^bDetermined by HPLC.

4.1.2 Substrate Scope

With optimized reaction conditions at hand, the scope of this reaction was explored next. Different olefinic aldehydes could be obtained in two to four steps from commercially available amino acids, amino alcohols, or di-*tert*-butyl-malonate (Scheme 4.2).^{78,121}



Scheme 4.2 Syntheses of substrates.

Under optimized reaction conditions, functionalized pyrrolidines were obtained from α,α -disubstituted α -amino olefinic aldehydes in generally high yields with excellent diastereoselectivities and good to excellent enantioselectivities (entries 1–4). Substrates with cyclic olefins were also explored (entries 5–6). Substrate **1f** performed smoothly to product **2f** with a >20:1 dr and a 95.5:4.5 er, but the enantioselectivity of **2e** was slightly declined (92:8 er). Gratifyingly, products **2g** and **2h** could both be obtained with good diastereoselectivities, excellent enantioselectivities, and in good yields by slightly increased catalyst loadings and reaction temperatures, and by extending the reaction times (Table 4.2, entries 7–8). Moreover, 3,4-disubstituted tetrahydrofurans could be

4 RESULTS AND DISCUSSION

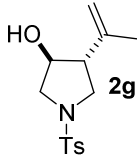
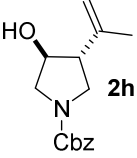
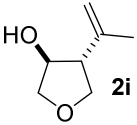
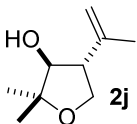
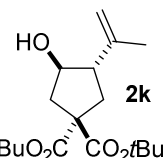
obtained in moderate to good yields and high enantiopurities (entries 9–10). The reaction of non-Thorpe-Ingold-substrate **1i** proceeded well under the neat conditions. A carbocyclic five-membered ring was also obtained smoothly when using di-*tert*-butyl-malonate-derived substrate **1k** (Table 4.2, entry 11).

Table 4.2 Reaction scope.^a

entry	t (d)	product 2	yield (%) ^b	<i>trans</i> : <i>cis</i> ^c	<i>e</i> _{<i>trans</i>} ^c
1	1.5		97	> 20:1	97.5:2.5
2	1.5		97	> 20:1	97.5:2.5
3	1.5		83	> 20:1	95.5:4.5
4 ^d	5		77	4:1	95:5
5	2		80	> 20:1	92:8
6	2		96	> 20:1	95.5:4.5

4 RESULTS AND DISCUSSION

Continuing **Table 4.2** Reaction scope.^a

entry	t (d)	product 2	yield (%) ^b	<i>trans:cis</i> ^c	<i>e</i> r _{<i>trans</i>} ^c
7 ^{e,f}	5		85	10:1	98:2
8 ^{e,f}	11		73	8:1	98:2
9 ^{h,g}	4		78	> 20:1	97:3
10	4		90	> 20:1	98:2
11 ^{e,f}	5		81	> 20:1	98:2

^aSubstrate **1** (0.1 mmol), catalyst **6c** (5 mol%) in cyclohexane (1 mL) at rt. ^bDetermined by ¹H-NMR. ^cDetermined by HPLC or GC analysis. ^dReaction at 10 °C. ^e**6c** (7.5 mol%). ^fReaction at rt, then at 50 °C. ^gNeat conditions. ^hNMR yield using an internal standard. ⁱ**6c** (10 mol%)

4 RESULTS AND DISCUSSION

The absolute configuration of **2a** was determined as *3S,4R* using single-crystal X-ray diffraction analysis (Figure 4.1). The corresponding *cis-3R,4R* diastereomer was obtained using Jacobsen's chiral Cr-dimer as the catalyst.

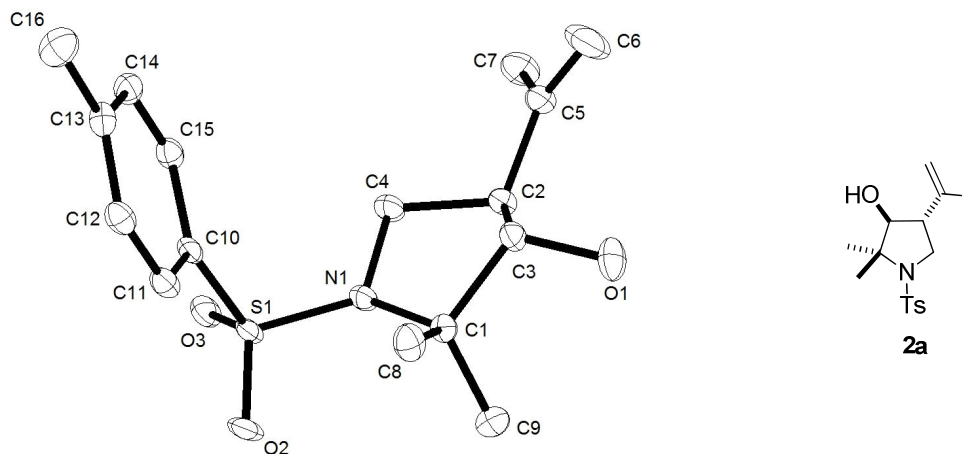


Figure 4.1 X-ray crystal structure of **2a**.

4.1.3 Mechanistic Studies and Discussion

Mechanistic Studies

During our investigation, an interesting observation triggered us to uncover the mechanism of this Brønsted acid-catalyzed asymmetric carbonyl–ene cyclization of **1a**. During the monitoring of the reaction process a weak new spot above the catalyst was observed on the thin layer chromatography (TLC) when irradiated with UV-light ($\lambda = 254$ nm). However this newly generated weak spot disappeared along with the completion of the reaction. Presumably, the new species could be a reversible isomer of substrate **1a** or a reversible side product, since the desired product **2a** could be fully afforded. However, it was also possible that the new species was an intermediate in the catalytic cycle.

4 RESULTS AND DISCUSSION

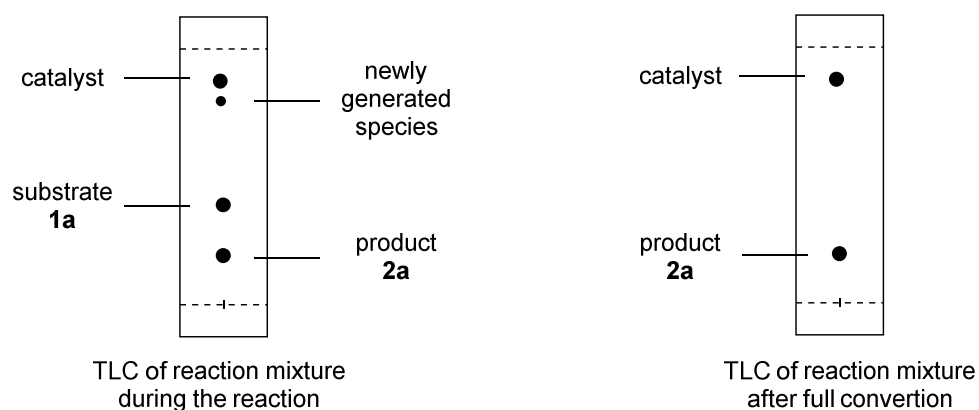
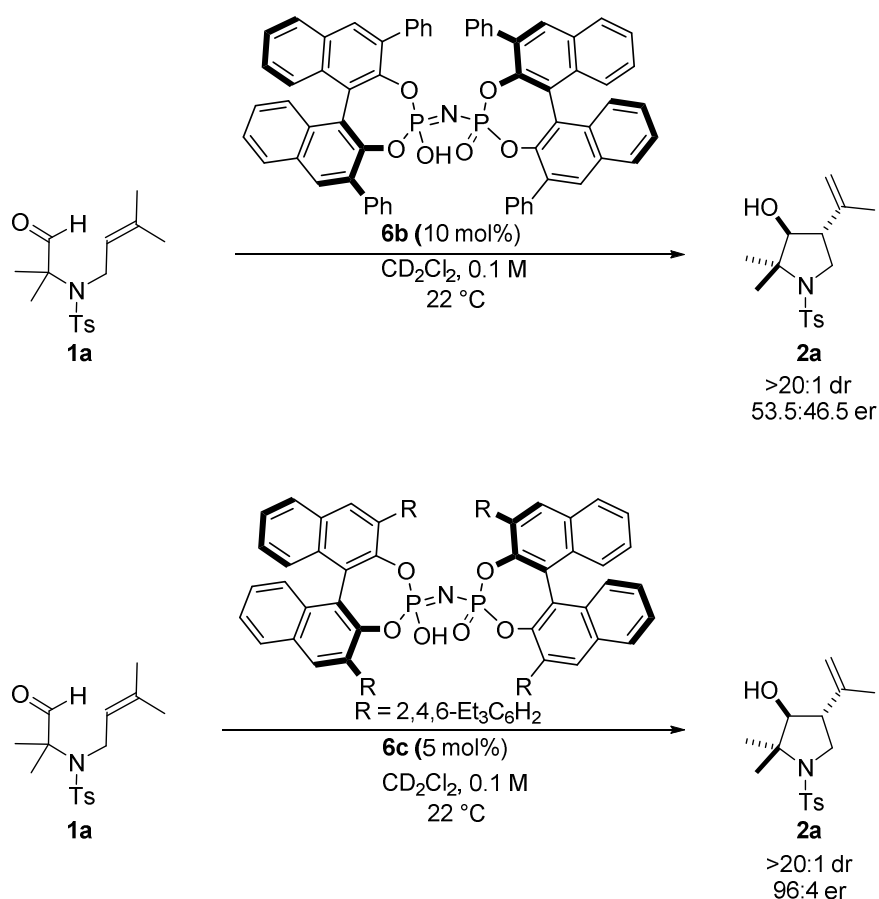


Figure 4.2 TLCs of reaction mixture.

To figure out this interesting species and to elucidate the mechanism of this asymmetric intramolecular carbonyl–ene cyclization, we carefully investigated the cyclization of **1a** catalyzed by **6b** and **6c**, respectively. ESI-MS and NMR studies of both reactions were carried out next.



4 RESULTS AND DISCUSSION

ESI-MS Study

As shown in Figure 4.3, in the initial electrospray ionization mass spectrometry (ESI-MS) study a new peak at m/z 1291 appeared within minutes (Figure 4.3b) matching the mass of the catalyst **6b-1a** (or **2a**) adduct in the cyclization of **1a** catalyzed by catalyst **6b**. Similarly, the new peak at m/z 1627 in the cyclization of **1a** catalyzed by **6c** matched the mass of catalyst **6c-1a** (or **2a**) adduct (Figure 4.3c). Presumably, a covalent intermediate was generated from the catalyst and substrate during the reaction. This exciting but unexpected result motivated us to determine the structure of the covalent adduct.

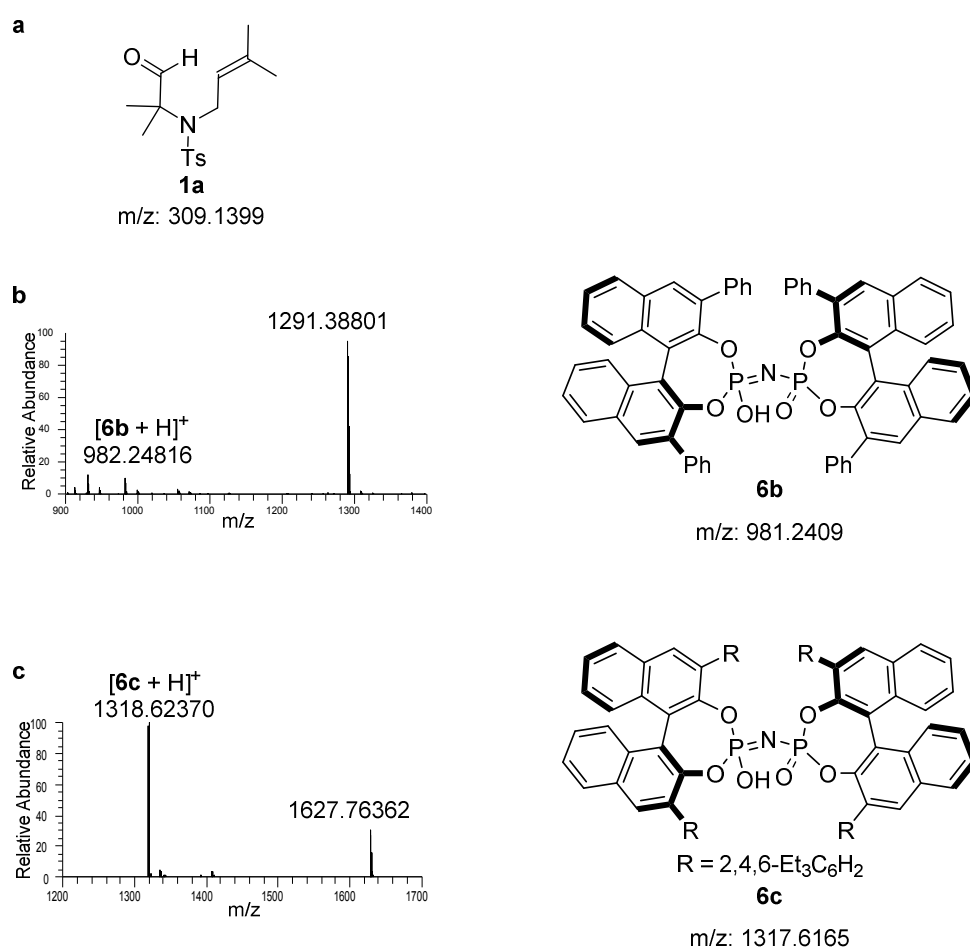


Figure 4.3 ESI-MS study of cyclization of **1a**: (a) The MS of **1a**. (b) Using catalyst **6b**. (c) Using catalyst **6c**.

4 RESULTS AND DISCUSSION

NMR Kinetic Study

NMR studies of the **6b**-catalyzed cyclization of **1a** were performed (Figure 4.4).¹²² According to the NMR data analysis, the covalent adduct **7b** was rapidly formed as soon as substrate **1a** and catalyst **6b** were dissolved in CD₂Cl₂ (Figure 4.4a). Interestingly, eight peaks were detected in the ³¹P NMR spectrum of **7b** (Figure 4.4b). These peaks reflected two different diastereomeric intermediates containing two chemically non-equivalent phosphorus atoms, that were coupling with each other, in line with the observed poor enantioselectivity and high *trans*-diastereoselectivity of **2a** (53.5:46.5 er and >20:1 dr). Moreover, free catalyst **6b** remained below the detection limit during the reaction. Presumably, the reaction proceeded via a covalent intermediate **7b** and the release of catalyst **6b** from **7b** could be the rate-determining step.

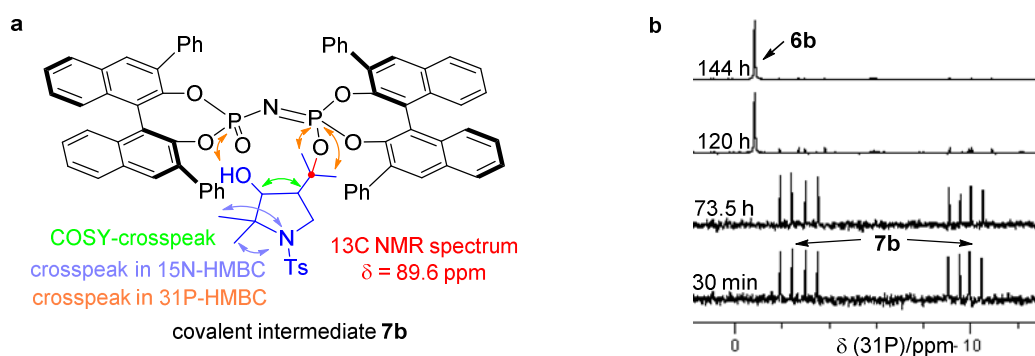


Figure 4.4 (a) Intermediate **7b**. (b) ³¹P NMR spectra of reaction mixtures.

NMR kinetic studies of the **6b**-catalyzed cyclization of **1a** were performed (Figure 4.5). As shown in Figure 4.5, the quasi-steady-state kinetic could be reached during the reaction. The reaction was zero-order with **1a**, but first-order with intermediate **7b**. Apparently, the continual transformation of **7b** accomplished the regeneration of catalyst **6b** and afforded product **2a**. As we speculated, the reaction indeed proceeded via a covalent intermediate **7b** and the release of catalyst **6b** from **7b** turned out to be the rate-determining step.

4 RESULTS AND DISCUSSION

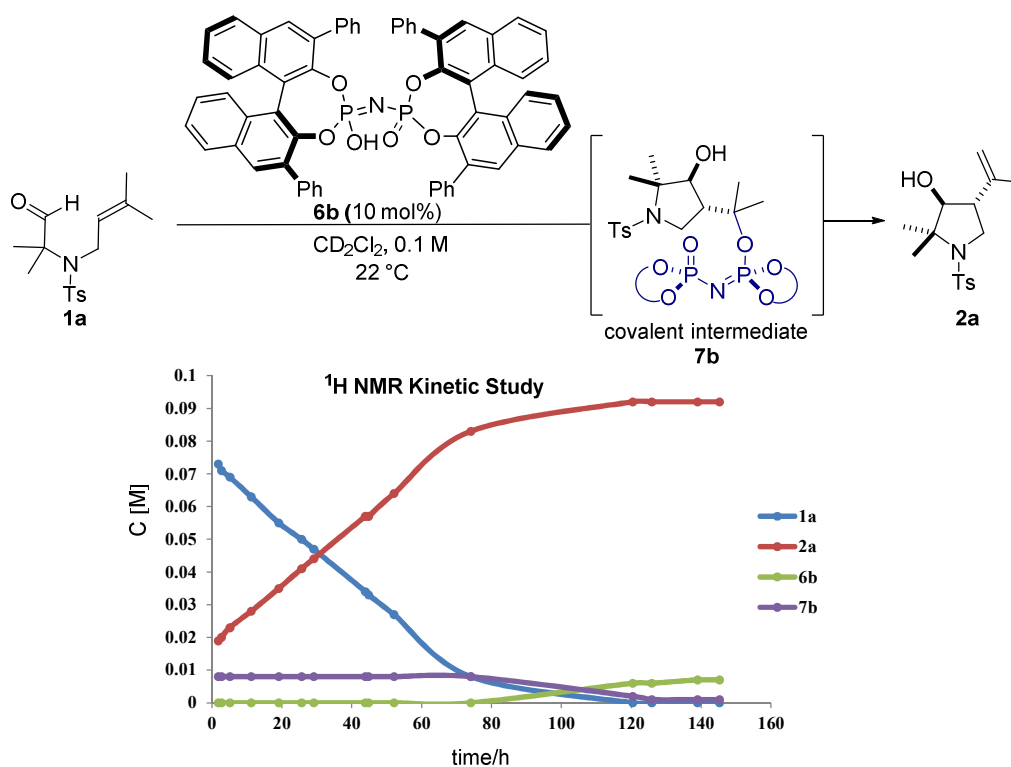


Figure 4.5 ^1H NMR kinetics of the cyclization of **1a** to **2a** using catalyst **6b**.

Similarly, **7c** was observed as soon as substrate **1a** and catalyst **6c** were dissolved in CD_2Cl_2 (Figure 4.6a). Four peaks were observed in the ^{31}P NMR spectrum of **7c** (Figure 4.6b), which were different from the eight peaks in the ^{31}P NMR spectrum of **7b** (Figure 4.4b). This was due to the high enantioselectivity and diastereoselectivity of **2a** when using **6c** as the catalyst (97.5:2.5 er and >20:1 dr). The observed AB spin system of two chemically non-equivalent ^{31}P nuclei of one single diastereomer of **7c** (Figure 4.6b) was also consistent with the high stereoselectivity.

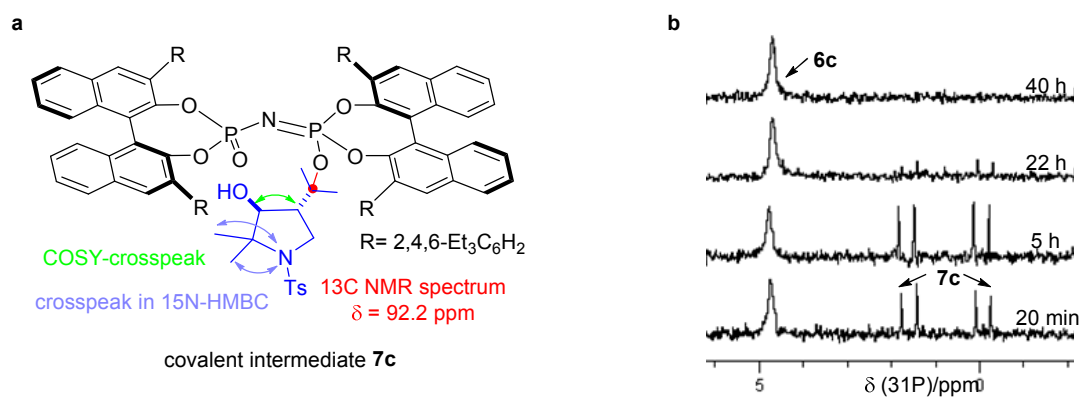
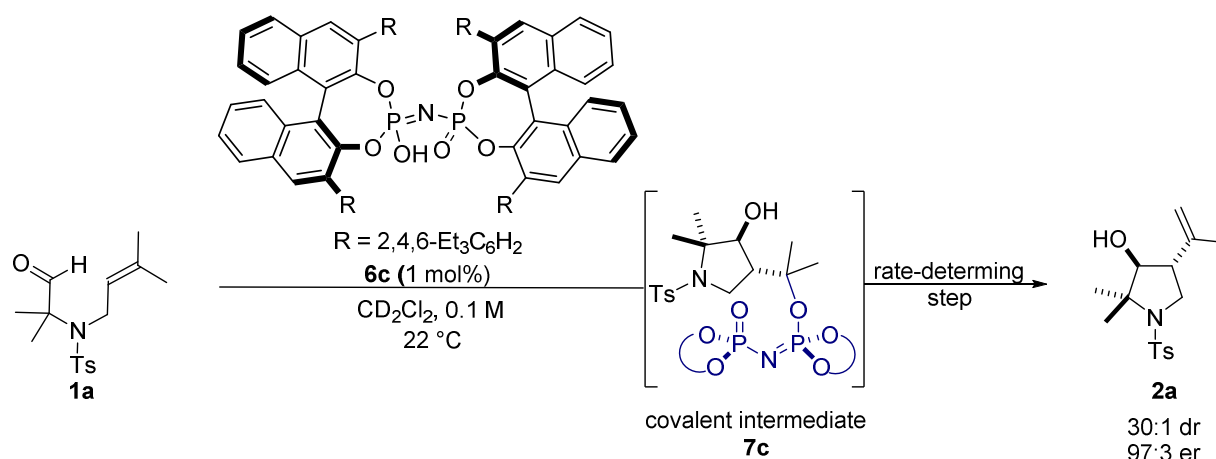


Figure 4.6 (a) Intermediate **7c**. (b) ^{31}P NMR spectra of reaction mixtures.

4 RESULTS AND DISCUSSION

Presumably, the quasi-steady-state kinetic could also be reached in the **6c**-catalyzed cyclization of **1a**. We assumed that a sufficient amount of **6c** was likely to be fully converted into adduct **7c** at the beginning of the reaction. With this assumption, we carried out a cyclization reaction of **1a** with only 1 mol% of catalyst **6c** at 294.2 K. An excellent 97:3 er and 30:1 dr of **2a** were observed. According to the ^1H NMR spectra (Figure 4.7) and ^{31}P NMR spectra (Figure 4.8) of the reaction, catalyst **6c** remained below the detection limit at the beginning of the reaction, while the concentration of adduct **7c** kept essentially constant. The continual transformation of compound **7c** accomplished the regeneration of catalyst **6c** and afforded product **2a**. The quasi-steady-state kinetic of **6c** was indeed reached and we could figure out that the release of catalyst **6c** from compound **7c** was the rate-determining step of this transformation (Scheme 4.3).



Scheme 4.3 Rate-determining step.

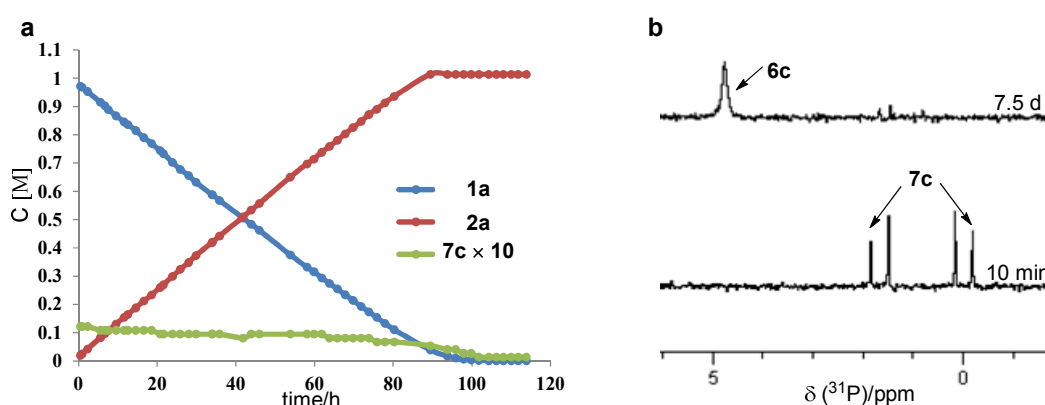


Figure 4.7 (a) ^1H NMR kinetics of the cyclization of **1a** to **2a** using catalyst **6c**.

(b) ^{31}P NMR spectra of reaction mixtures taken at different time.

4 RESULTS AND DISCUSSION

Thermodynamic Kinetic Study

The Eyring equation was generally used in NMR kinetic studies to determine the thermodynamic parameters in the **6c**-catalyzed cyclization of **1a** (equation 4.1).¹²⁴

$$\ln(kh/k_B T) = -\Delta H/RT + \Delta S/R \quad (4.1) \quad \begin{array}{l} k_B : \text{Boltzmann constant} \\ h : \text{Planck constant} \end{array}$$

We were able to manage the **6c**-catalyzed cyclization of **1a** to reach the quasi-steady-state kinetic at different temperatures, for example, 280.6 K, 294.2 K, 301.2 K, 312.3 K, 323.4 K.^{125,126} Collaborating with my colleague Dr. Markus Leutzsch, the reaction rate constants of the reactions could be readily calculated according to the ¹H NMR kinetic measurements (Table 4.3).

Table 4.3 Reaction rate constant at different temperature

<i>T</i> (K)	280.6	294.2	301.2	312.3	323.4
<i>1/T</i> (K ⁻¹)	0.003564	0.0034	0.00332	0.003202	0.003092
<i>k</i> (s ⁻¹)	5.17372E-05	0.000301076	0.000493541	0.001958173	0.004711654
$\ln(kh/k_B T)$	-39.2662417	-37.5522139	-37.0815238	-35.7398133	-34.896584

According to the Eyring plot, we were able to generate a function between the rate constant and the temperature (Figure 4.8). We could determine the activation enthalpy ΔH^\ddagger (18.47 ± 0.73 kcal/mol at 298.15 K) and the activation free energy ΔG^\ddagger (22.08 ± 1.46 kcal/mol at 298.15 K) of the rate-determining step of this reaction which referred to the release of catalyst **6c** from the covalent adduct **7c** (Table 4.4).

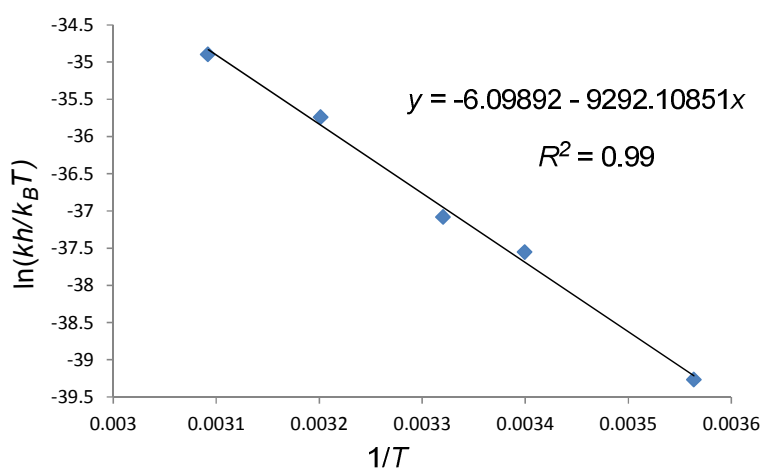


Figure 4.8 Eyring plot.

4 RESULTS AND DISCUSSION

Table 4.4 Calculation of activation parameters at 298.15 K.

ΔH^\ddagger	77258.88 ± 3072.25 J/mol	18.47 ± 0.73 kcal/mol
ΔS^\ddagger	-50.71 ± 10.20 J/(K·mol)	-0.0121 ± 0.0024 kcal/(K·mol)
ΔG^\ddagger	92377.84 ± 6112.89 J/mol	22.08 ± 1.46 kcal/mol

Discussion

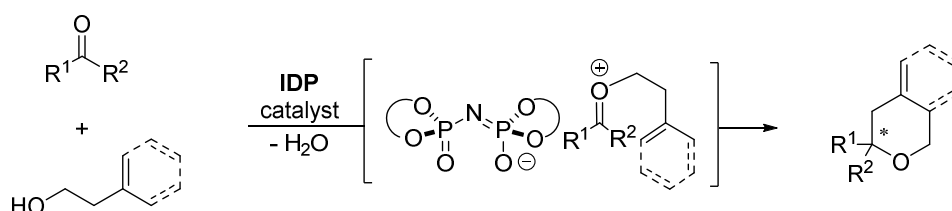
In this part of the PhD work, the first organocatalytic asymmetric intramolecular carbonyl–ene reaction of olefinic aldehydes was successfully developed, and diverse *trans*-configured pyrrolidines, tetrahydrofuranes, and cyclopentanes were obtained in good yields, with good to excellent diastereoselectivities and enantioselectivities. To the best of our knowledge, for the first time, high *trans*-diastereoselectivities up to 50:1 dr were achieved in this asymmetric carbonyl–ene cyclization. Unactivated substrates such as **1g-i** without Thorpe–Ingold-type substitutions were also compatible under the optimized reaction conditions.

Moreover, we could show that this chiral imidodiphosphate catalyzed asymmetric intramolecular carbonyl–ene reaction proceeds through a covalent intermediate, which is generated from the catalyst and cyclized substrate. A subsequent release of free catalyst from this covalent intermediate afforded the desired product. It needs to be addressed that the bifunctional property of the catalyst plays a crucial role for the catalytic cycle.

4 RESULTS AND DISCUSSION

4.2 Organocatalytic Asymmetric Transformations via Oxocarbenium Ions

As reactive intermediates, oxocarbenium ions are used in several types of transformations. Our confined chiral acid imidodiphosphates (IDPs) have been successfully utilized in the asymmetric acetalization of small substrates via an oxocarbenium ion intermediate. Presumably, these confined acid IDPs offer potential for other asymmetric transformations. We hypothesized that the reactive oxocarbenium ions could be further trapped by a less nucleophilic sp^2 -hybridized alkene group or an arene group instead of a reactive hydroxyl group (Scheme 4.4). Probably, asymmetric reactions, such as enantioselective Prins cyclizations and *oxa*-Pictet–Spengler reactions could be realized using our confined chiral acids as catalysts.



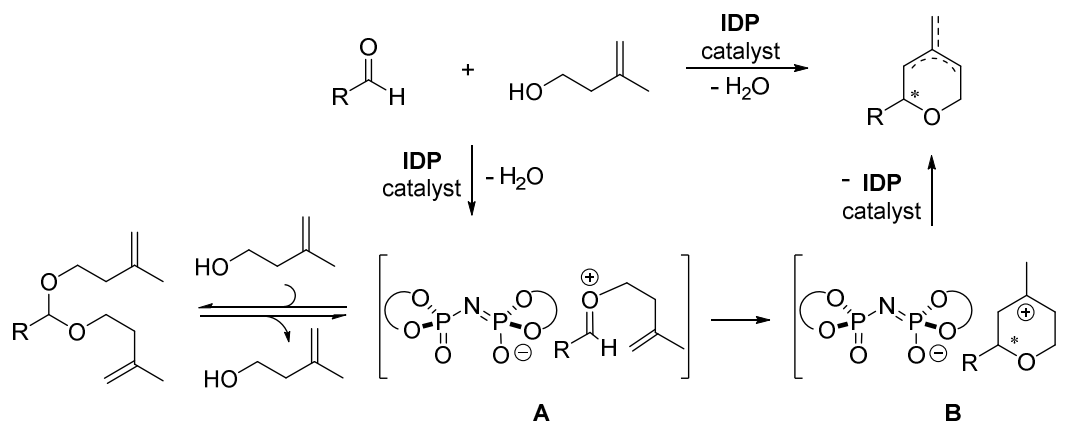
Scheme 4.4 IDP-catalyzed reactions between carbonyls and homoallylic alcohols.

4.2.1 Catalytic Asymmetric Prins Cyclization

(with Dr. Philip S. J. Kaib and Dr Gavin Chit Tsui)

A highly enantioselective Prins cyclization between aldehydes and homoallylic alcohols was investigated, effecting functionalized tetrahydropyrans (THPs).^{127–129} Despite tremendous applications of the Prins cyclization in natural product synthesis,^{130–133} a highly enantioselective catalytic Prins cyclization has not been reported.^{134,135} As shown in Scheme 4.5, we assumed that an oxocarbenium ion pair **A** could be readily formed according to our previous studies in IDP-catalyzed asymmetric acetalization. Probably, the oxocarbenium ion could be attracted by another intermolecular homoallylic alcohol, generating the undesired side product acetals. Presumably, the equilibrium between the oxocarbenium ion and the acetal could occur. The oxocarbenium ion could be trapped by the intramolecular nucleophilic alkene group generating another intermediate tertiary carbocation ion pair **B**.^{136–138} An exocyclic or endocyclic alkene Prins product would be obtained after the release of the catalyst, since the deprotonation could proceed either at the primary or the secondary carbon.

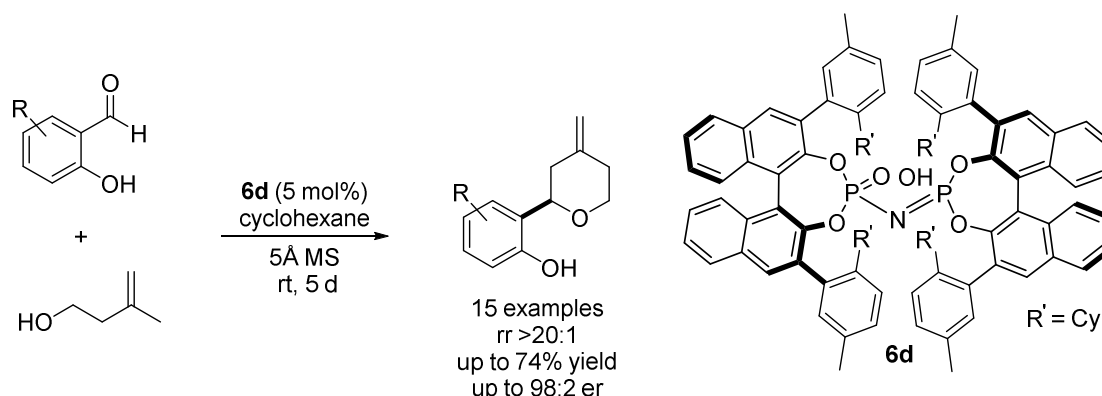
4 RESULTS AND DISCUSSION



Scheme 4.5 IDP-catalyzed Prins cyclization.

4.2.1.1 Reaction Design and Initial Study

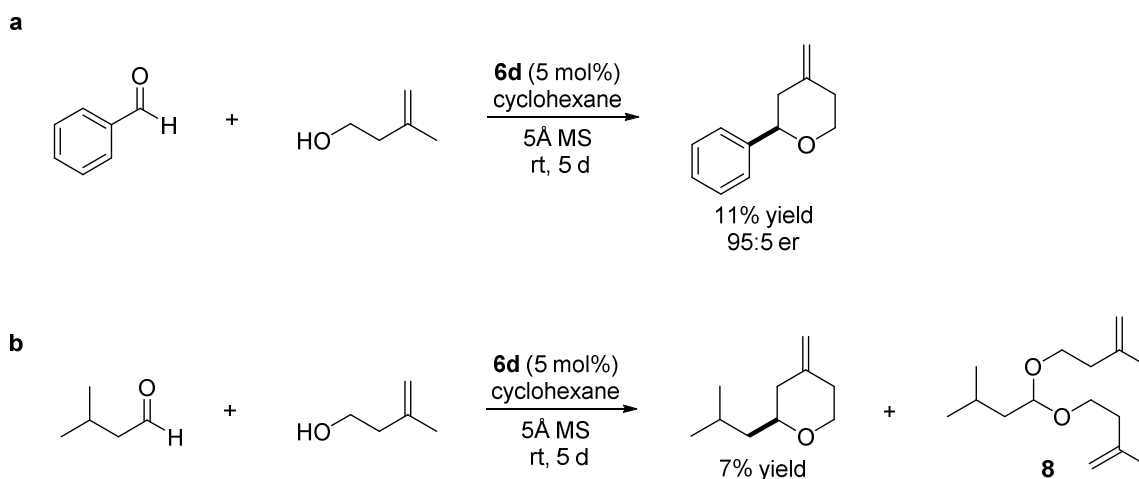
We began our investigation of the Prins cyclization with aldehydes and 3-methyl-3-buten-1-ol. Our confined IDP **6d** showed a good enantiocontrol in the asymmetric Prins cyclization of salicylaldehydes with 3-methyl-3-buten-1-ol in high yields, with excellent regio- and enantioselectivities. (Scheme 4.6).



Scheme 4.6 IDP-catalyzed Prins cyclization (with Dr Gavin Chit Tsui).

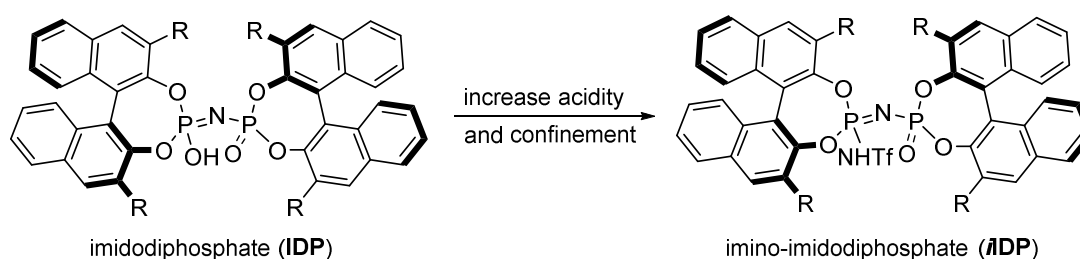
Unfortunately, under the optimized reaction conditions, benzaldehyde gave a poor yield, but a good enantioselectivity (11% yield, 95:5 er) (Scheme 4.7a). Aliphatic isovaleraldehyde turned out to be even less reactive (7% yield), the acetal **8** was obtained as the main product (Scheme 4.7b).

4 RESULTS AND DISCUSSION



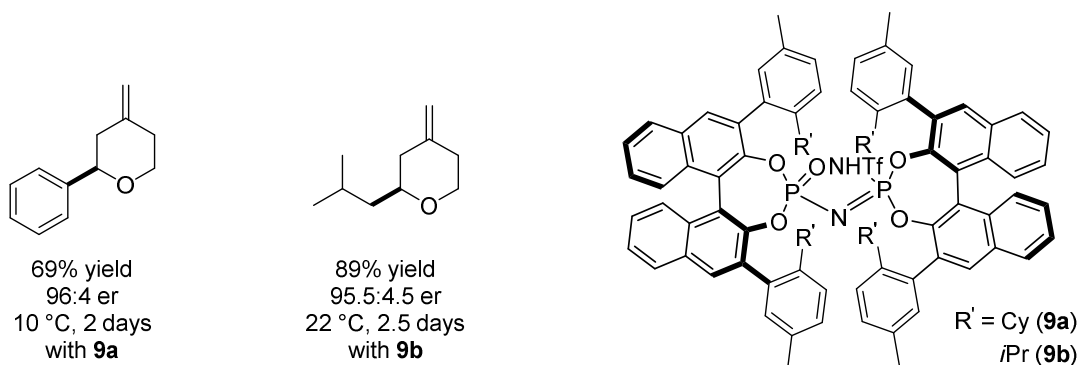
Scheme 4.7 IDP-catalyzed Prins cyclization of simple aldehydes.

We speculated that the poor activities of simple aldehydes could be due to the insufficient acidity of the IDP catalyst **6d**. To address this issue, we presumed that the replacement of one oxo-group in IDP with a stronger electron withdrawing group, such as an NSO_2CF_3 (*NTf*)-group, would lead to a more acidic and confined imino-imidodiphosphate (*i*IDP) **9** (Scheme 4.8).



Scheme 4.8 Highly acidic and confined Brønsted acid *i*IDP (*Dr. Philip S. J. Kaib*).

Both aromatic and aliphatic aldehydes proved suitable substrates for *i*IDP-catalyzed Prins cyclization, displaying high enantioselectivities and good yields (Scheme 4.9).



Scheme 4.9 Exploration of Brønsted acid *i*IDPs.

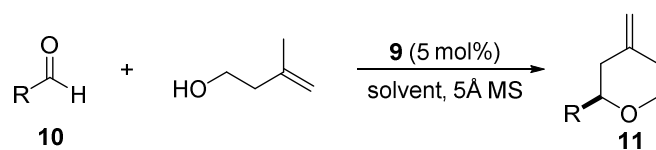
4 RESULTS AND DISCUSSION

4.2.1.2 Substrate Scope, Gram-Scale Synthesis, and Derivatizations

Various linear, α -, and β -branched aliphatic aldehydes turned out to be suitable substrates for catalyst **9a** under the optimized reaction conditions (Table 4.5, entries 1–8) and excellent enantioselectivities and good yields were generally obtained. THP products **11** were obtained in good to excellent regiomer ratios (rr; ratio of exo- to endocyclic isomers) of up to >20:1. 2-Phenylacetaldehyde (**10h**) was converted with reasonable enantioselectivity (90:10 er) (Table 4.5, entry 8). α,β -unsaturated aldehyde **10i** required a higher catalyst loading of *i*IDP **9b** and a prolonged reaction time to achieve high yield and enantioselectivity (Table 4.5, entry 9). Aromatic aldehydes, such as benzaldehyde, were selectively converted to the corresponding THPs, such as **11j**, which was isolated in 69% yield and with an excellent enantiomeric ratio of 96:4 (Table 4.5, entry 10). Systematic substitutions of the benzaldehyde core in *ortho*, *meta*, and *para*-position with electron donating and electron withdrawing groups were tolerated by catalyst **9b**. For instance, THPs **11k–11p** were obtained in good yields (65–86%), high to excellent enantiomeric ratios (up to 96.5:3.5 er) and high to excellent regioselectivities (up to >20:1) (Table 4.5, entries 11–16). Moreover, heterocyclic aromatic aldehydes **10q** and **10r** successfully furnished the desired Prins cyclization products **11q** and **11r** (Table 4.5, entries 17–18).

4 RESULTS AND DISCUSSION

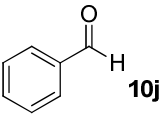
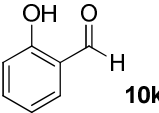
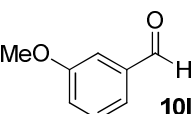
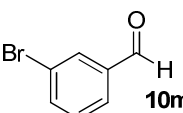
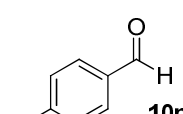
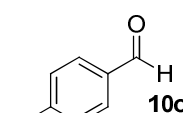
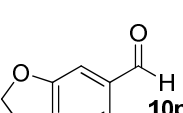
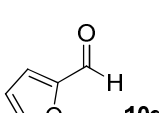
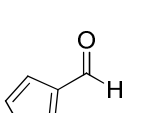
Table 4.5 Reaction scope.^a



entry	t (d)	T (°C)	aldehyde 10	yield (%) ^b	er ^c	rr ^d
1	2.5	22		89	95.5:4.5	9:1
2	7	10		60	95:5	10:1
3	7	0		85	95:5	>20:1
4	7	22		60	98:2	>20:1
5	7	22		94	95:5	9:1
6	3	22		85	95:5	13:1
7	3	22		90	98:2	20:1
8	2	22		80	90:10	>20:1
9 ^e	7	-30		87	95:5	11:1

4 RESULTS AND DISCUSSION

Continuing **Table 4.5** Reaction scope.^a

entry	t (d)	T (°C)	aldehyde 10	yield (%) ^b	er ^c	rr ^d
10	2	10		69	96:4	>20:1
11	2	0		80	95.5:4.5	>20:1
12	2	0		65	95:5	12:1
13	5	10		73	95:5	15:1
14	2	10		81	96:4	>20:1
15	2	10		86	96.5:3.5	>20:1
16	2	0		68	94:6	16:1
17	2	10		73	95:5	13:1
18	5	0		82	95:5	14:1

^aUnless otherwise indicated, all reactions were carried out with **10** (0.12 mmol), 3-methyl-3-buten-1-ol (0.1 mmol), *i*IDP catalyst **9** (5 mol%), and 50 mg of 5 Å molecular sieves in 1.0 mL of solvent (0.1 M); cyclohexane was used as solvent when T ≥ 10°C,

4 RESULTS AND DISCUSSION

methylcyclohexane was used as solvent when $T < 10^{\circ}\text{C}$; catalyst **9b** was used to afford products **11a–11h**, catalyst **9a** was used to afford **11i–11r**; ^bIsolated yields of **11h** and **11j–11r** are given, yields of the volatile products **11a–11g** and **11i** were determined by ¹H-NMR of the reaction mixtures using $\text{CHCl}_2\text{CHCl}_2$ as internal standard. ^cDetermined by GC analysis. ^dThe regiomer ratio (rr) between exo- and endocyclic alkenes was determined by GC analysis. ^e10 mol% catalyst was used.

The absolute configuration of **11o** was determined as *R* using single-crystal X-ray diffraction analysis (Figure 4.9).

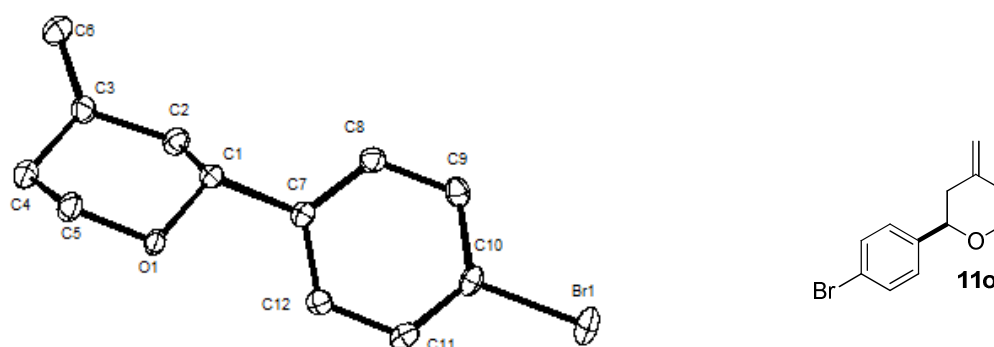
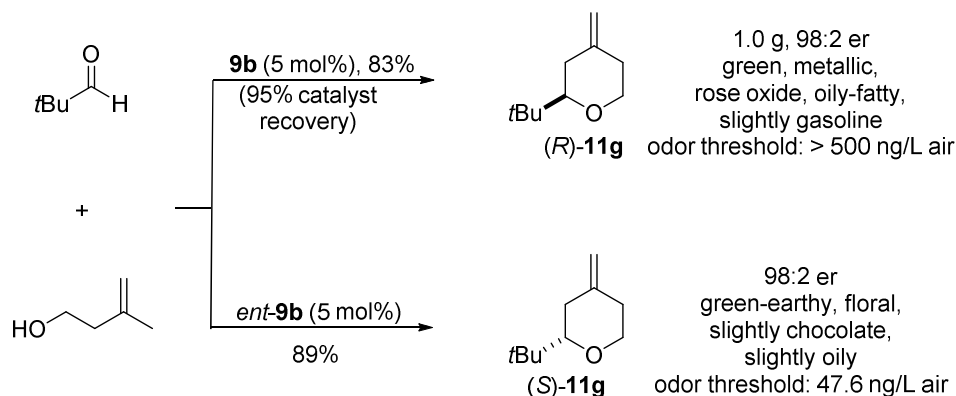


Figure 4.9 X-ray crystal structure of **11o**.

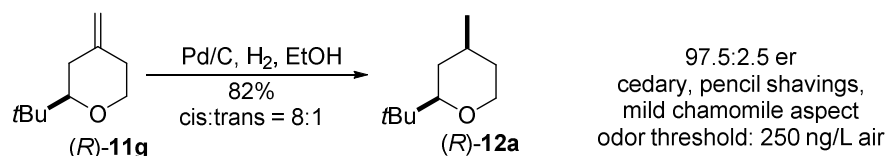
This methodology is quite robust, and a gram-scale asymmetric Prins cyclization of pivalaldehyde **10g** was achieved (Scheme 4.10a). 1.0 gram of 4-methylenetetrahydropyran (*R*)-**11g** was obtained in a 83% yield and 98:2 er. With a variety of scented THPs in hand, we collaborated with the perfumery company Givaudan to explore the olfactory properties of our products. The olfactory investigation of undiscovered compound **11g** was carried out. Unfortunately, (*R*)-**11g** (odor threshold > 500 ng/L air) proved to be too weak to serve in perfumery (Scheme 4.10a). (*S*)-**11g** could be furnished using the corresponding enantiomer of catalyst **9b** (98:2 er). As shown in Scheme 4.10a, (*S*)-**11g** had a floral and slightly chocolate smell (odor threshold 47.6 ng/L air), which was more than ten times stronger compared to (*R*)-**11g**. After the hydrogenation process of (*R*)-**11g**, *cis*-**12a** was obtained as a major product with an excellent 97:3 er. Compared to (*R*)-**11g**, *cis*-**12a** was five times weaker (odor threshold 250 ng/L air).

4 RESULTS AND DISCUSSION

a. Gram-Scale Experiment and Synthesis of Both Enantiomers



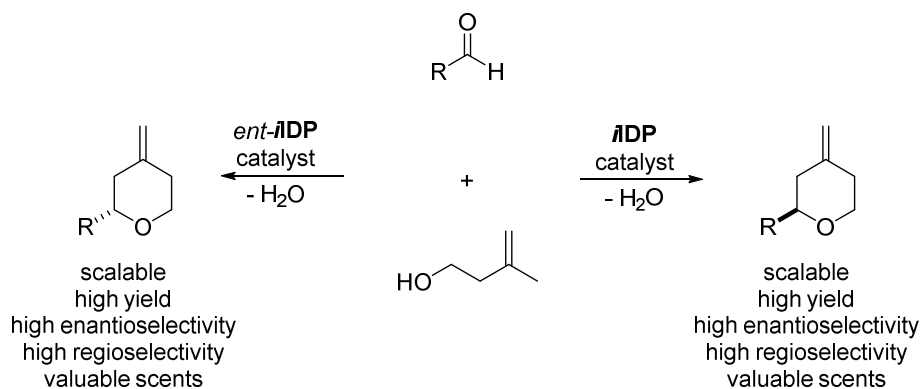
b. Derivatization



Scheme 4.10 Access to different scents.

4.2.1.3 Discussion

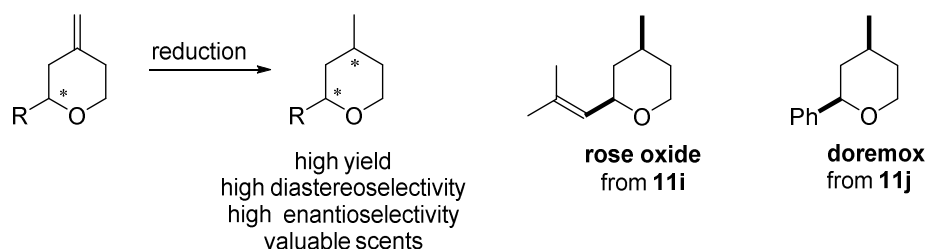
The first general catalytic asymmetric Prins cyclization was successfully developed (Scheme 4.11). Diverse scented THP products were obtained via the Prins cyclization of commercially available aldehydes and homoallylic alcohols, in good to excellent yields and with good to excellent regio- and enantioselectivities. This methodology is quite practical and scalable. Both enantiomerically enriched enantiomers could be obtained using different enantiomers of imino-imidodiphosphates. It is worth mentioning that these newly developed, more acidic and confined imino-imidodiphosphates (*i*IDPs) catalysts were the key to this highly enantioselective Prins cyclization.



Scheme 4.11 *i*IDP-catalyzed Prins cyclization.

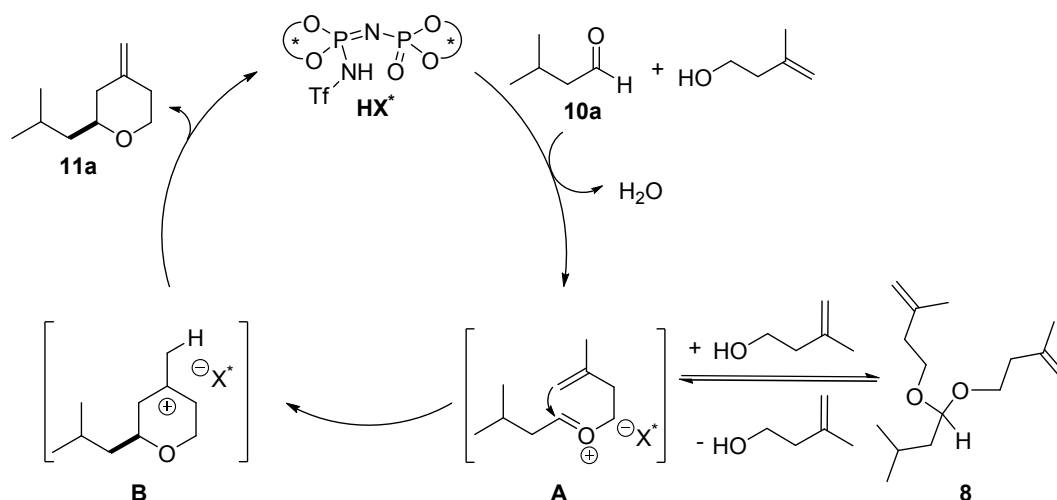
4 RESULTS AND DISCUSSION

The diverse tetrahydropyran products themselves already showed interesting olfactory properties. Valuable fragrant compounds such as rose oxide and doremix could be obtained, after a simple diastereoselective hydrogenation of the corresponding Prins cyclization products **11i** and **11j**.



Scheme 4.12 Derivatization to different scented compounds.

A plausible mechanism of this asymmetric Prins cyclization was proposed (Scheme 4.13). The imino-imidodiphosphate (*i*IDP) acid catalyzed the initial condensation of aldehyde **1a** and a homoallylic alcohol affording an ion pair of the oxocarbenium ion **A** and a chiral imino-imidodiphosphate counteranion. Acetal **8** was detected as soon as all the reagents were mixed, because ion pair **A** could be trapped by another molecule of the homoallylic alcohol acting as a nucleophile. In the equilibrium, acetal **8** could be fully consumed since oxocarbenium ion **A** could be further attacked by an intramolecular alkene group forming the tertiary carbocation **B**. In the following deprotonation step, the confined imino-imidodiphosphate counteranion kinetically prefers removing a proton at the primary carbon so that the exocyclic alkene product **11a** was furnished as the major product.



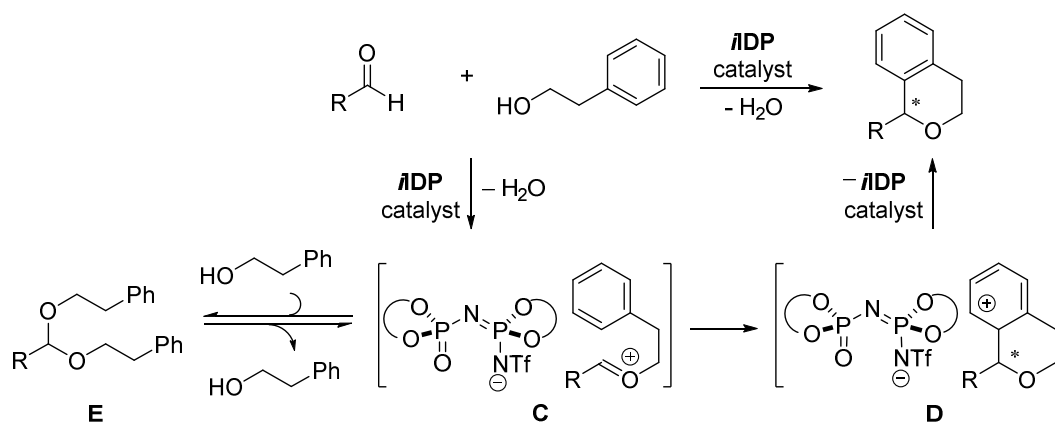
Scheme 4.13 Proposed catalytic cycle.

4 RESULTS AND DISCUSSION

4.2.2 Catalytic Asymmetric *Oxa*-Pictet–Spengler Reaction

(with Dr. Sayantani Das)

Encouraged by the results of our imino-imidodiphosphate (*i*IDP) catalyzed asymmetric Prins cyclization, we envisioned an acid-catalyzed enantioselective *oxa*-Pictet–Spengler reaction between aldehydes and aryl ethanols.^{139–141} As shown in Scheme 4.14, presumably, the readily formed oxocarbenium ion of **C** could be attracted by an intramolecular arene, generating another ion pair **D**. Valuable bioactive enantiomerically enriched isochromans could be obtained after a subsequent rearomatization.^{142–145} Probably, the oxocarbenium ion of **C** could be trapped by another intermolecular homobenzyl alcohol, and the undesirable side product acetal **E** would be generated.



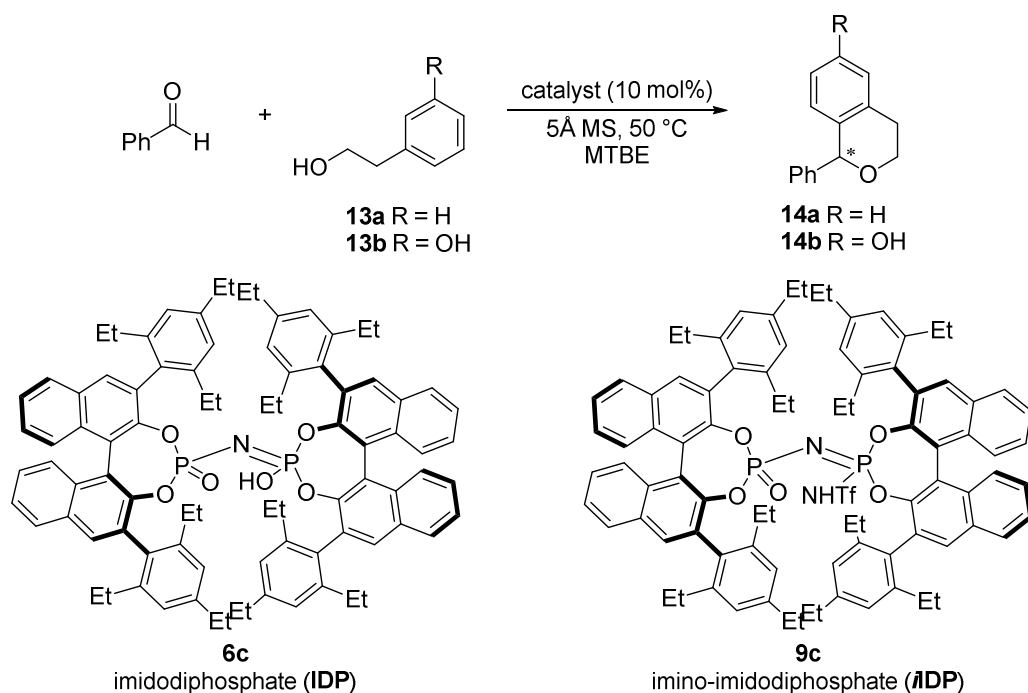
Scheme 4.14 *i*IDP-catalyzed *oxa*-Pictet–Spengler reaction.

4.2.1.1 Reaction Design and Initial Study

The investigation of chiral imidodiphosphate (IDP) catalyzed *oxa*-Pictet–Spengler reaction was carried out using isovaleraldehyde and phenylethanol **13a**.^{146,147} Unfortunately, the desired product was not obtained using IDP **6c** as catalyst (Table 4.6, entry 1). We hypothesized that the introduction of a hydroxyl group at the *meta* position of phenylethanol **13a** would increase the nucleophilicity of the arene. Indeed, using 3-(2-hydroxyethyl) phenol **13b** as substrate, the desired product **14b** was obtained in a promising yield and with a high enantioselectivity (32%, 94:6 er). Remarkably, using imino-imidodiphosphate (*i*IDP) **9c** as the catalyst, **14b** was obtained with a high enantioselectivity (95:5 er) but a low yield of 53% (Table 4.6, entry 3).

4 RESULTS AND DISCUSSION

Table 4.6 Optimization of reaction conditions^a



entry	substrate	catalyst	time	yield(%) ^b	er
1 ^c	13a	6c	72 h	0	N.D.
2	13b	6c	72 h	32	94:6
3	13b	9c	72 h	53	95:5

^aReactions on a 0.02 mmol scale (0.2 M). ^bNMR yield. ^cDCE was used as solvent.

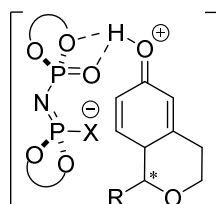
4.2.2.2 Catalyst Design, Synthesis, and Substrate Scope

Catalyst Design

As shown in Table 4.6, the modification of our confined IDP catalysts indeed improved the enantioselectivity of this Brønsted acid catalyzed *oxa*-Pictet–Spengler reaction.^{148–151} We speculated that a potential hydrogen bond would be formed between the hydroxyl group in **13b** and the basic site of the IDP derivatives, under the assumption that the bifunctional property of IDP derivatives was crucial for this asymmetric *oxa*-Pictet–Spengler reaction. We assumed that the basicity of *i*IDP **9c** was not strong enough for the rearomatization step, which resulted in the low yield of this reaction. Probably, a

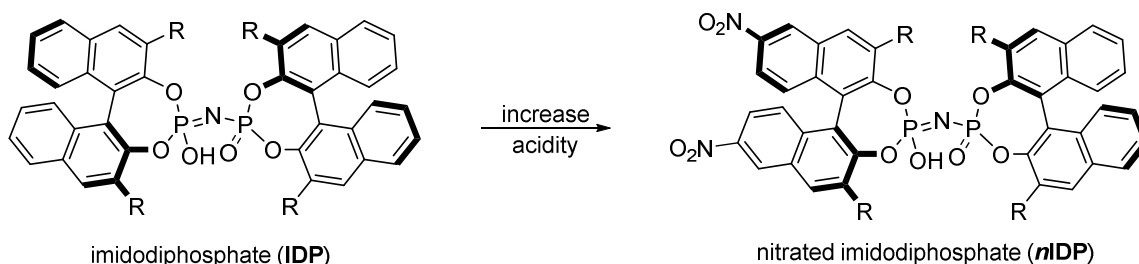
4 RESULTS AND DISCUSSION

subtle modulation of IDP might enable both high yield and enantioselectivity of this *oxa*-Pictet–Spengler reaction.



Scheme 4.15 Rearomatization step.

The acidity of the imidodiphosphates (IDPs) could be increased by introducing nitro groups on one side of the BINOL backbones. The chiral environment of this newly designed nitrated imidodiphosphates (*n*IDPs) would interact more closely with intermediates leading to a highly enantioselective control. Probably, the basicity of this new Brønsted acidic *n*IDPs would be enough for the rearomatization step resulting in an ideally high yield.

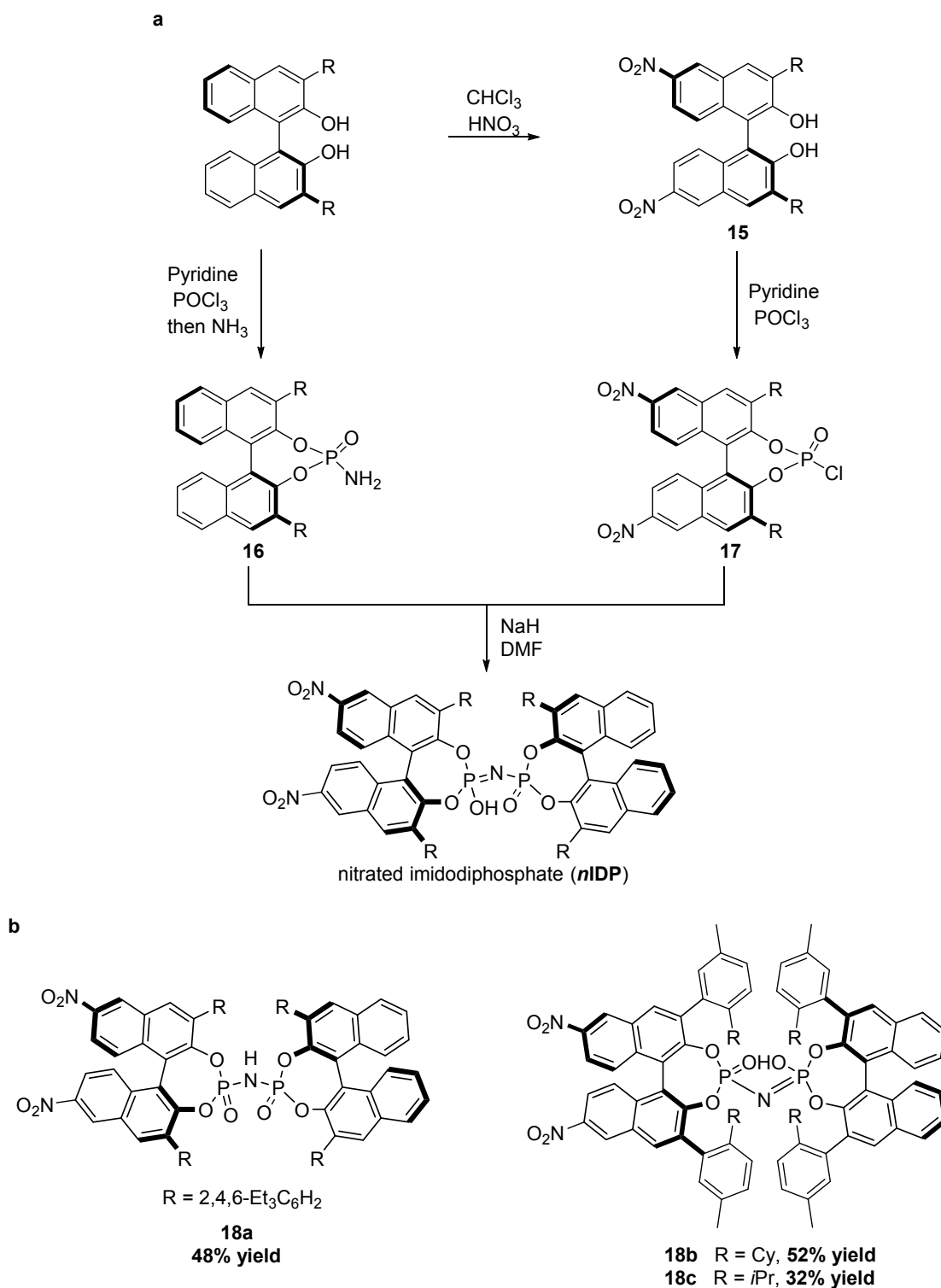


Scheme 4.16 Stronger confined Brønsted acid.

Catalyst Synthesis

Compared to the synthesis of the corresponding IDP catalyst, an additional step of nitration of the corresponding BINOL was required. Starting from the laboratory available 3,3'-substituted BINOL derivatives, the corresponding nitrated BINOL **15** could be easily obtained in one step. The remaining steps were similar to the synthesis of IDP, and the nitrated imidodiphosphates could be rapidly formed through the coupling of **16** and **17** under basic conditions. Subsequent to column chromatography, the mixture of nitrated imidodiphosphate and its salts were acidified by 6 M aqueous HCl. A class of nitrated imidodiphosphates **18a–18c** were successfully obtained (Scheme 4.17).

4 RESULTS AND DISCUSSION

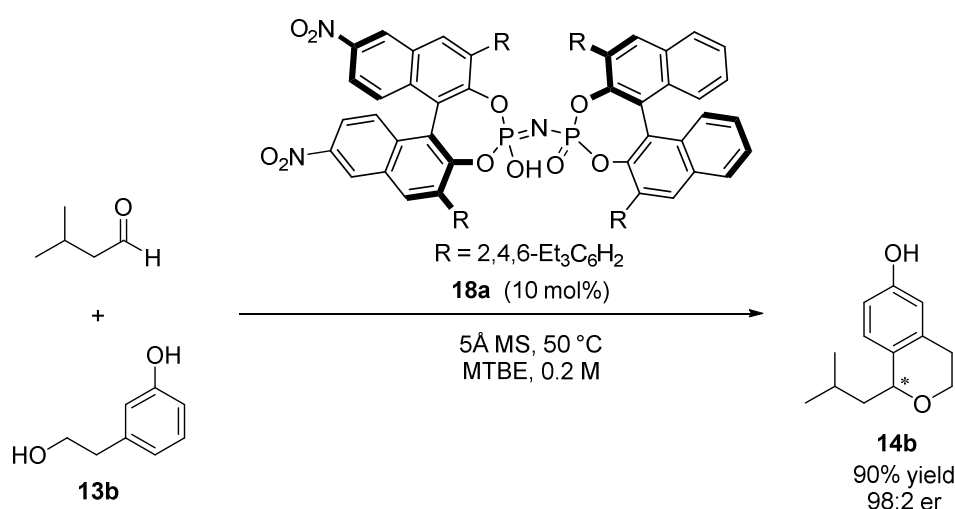


Scheme 4.17 Synthesis of nitrated imidodiphosphates (*nIDPs*).

4 RESULTS AND DISCUSSION

Application of *n*IDP in the *Oxa*-Pictet–Spengler Reaction

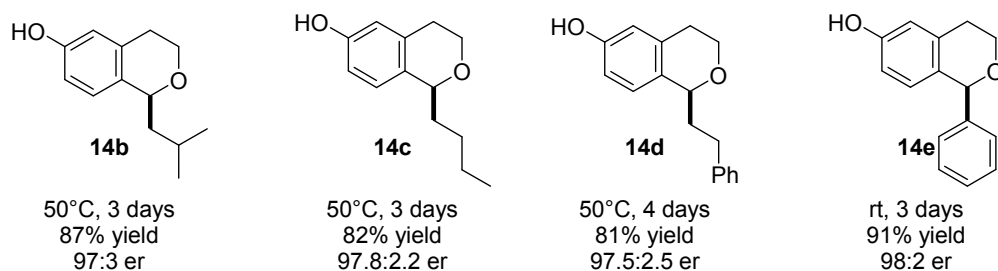
Based on initial results, nitrated imidodiphosphate **18a** with bulky 2,4,6-Et₃C₆H₂-substituents at the 3,3'-positions of the BINOL backbones was subsequently utilized in this asymmetric *oxa*-Pictet–Spengler reaction (Scheme 4.18). Gratifyingly, the desired product **14b** was obtained with a high yield of 90% and with an excellent enantioselectivity 98:2 er. The rational design and synthesis of *n*IDP was crucial to realize this highly enantioselective *oxa*-Pictet–Spengler reaction.



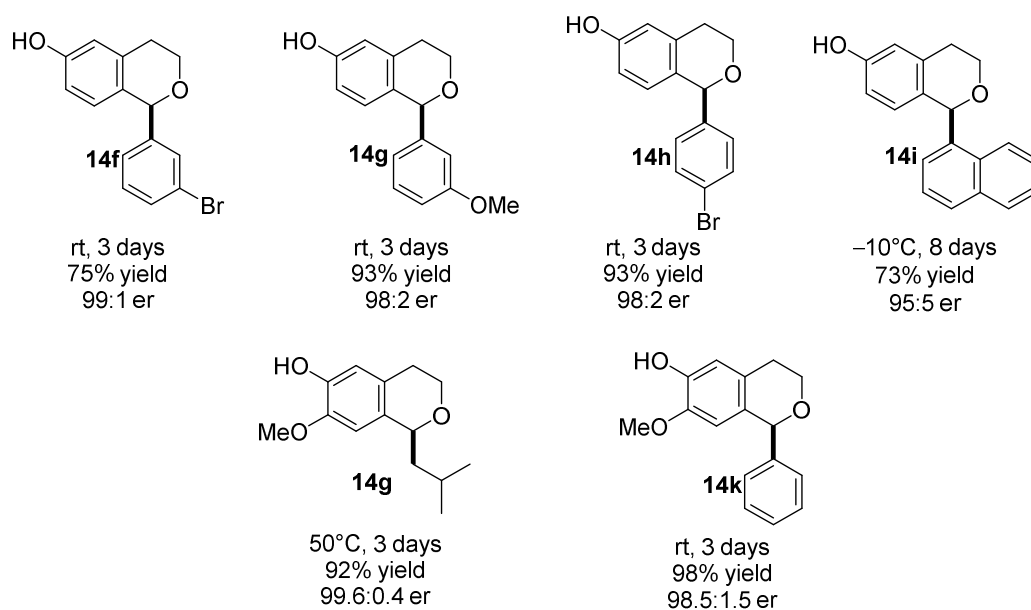
Scheme 4.18 Utilization of nitrated imidodiphosphate (*n*IDP).

Reaction Scope

Under the optimized reaction conditions, the scope of this reaction was explored next. As shown in Scheme 4.19, both aliphatic and aromatic aldehydes were compatible with this highly enantioselective *oxa*-Pictet–Spengler reaction (**14b–14i**). Other phenol derivatives were also explored and products **14g–14k** were obtained in excellent yields (92–98%) and enantioselectivities (up to >99:1 er).

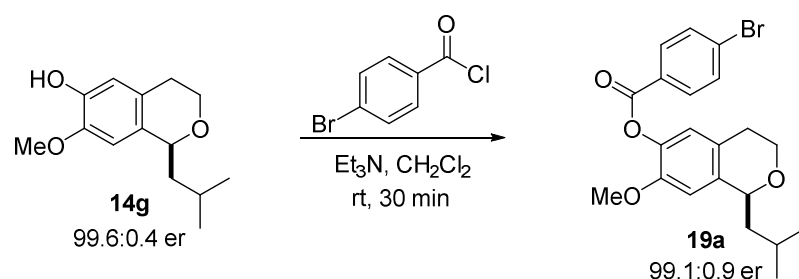


4 RESULTS AND DISCUSSION



Scheme 4.19 Reaction scope.

19a could be readily furnished after one simple derivatization of *oxa*-Pictet–Spengler reaction product **14g** (Scheme 4.20). The absolute configuration of **19a** was determined as *R* by single-crystal X-ray diffraction analysis (Figure 4.10).



Scheme 4.20 Derivatization.

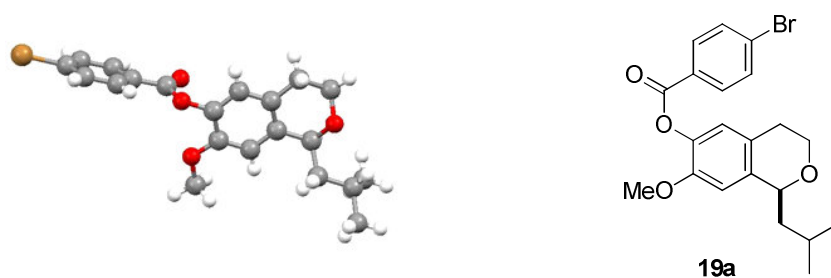


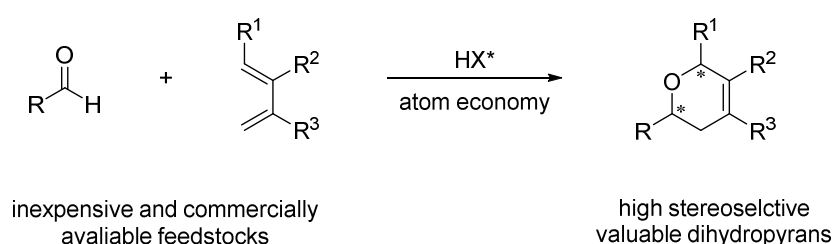
Figure 4.10 Absolute configuration of **19a**.

4 RESULTS AND DISCUSSION

4.3 Asymmetric [4+2]-Cycloaddition Reaction of Dienes with Aldehydes

4.3.1 Reaction Design and Initial Study

Encouraged by the work on the asymmetric intramolecular carbonyl–ene cyclization, Prins cyclization, and *oxa*-Pictet–Spengler reaction during my PhD study, we recognized the potential for Brønsted acids in a direct intermolecular asymmetric cycloaddition between simple alkenes and aldehydes. As shown in Scheme 4.21, a fundamental [4+2]-cycloaddition of dienes with aldehydes is equally efficient to deliver valuable dihydropyran compounds.¹⁵²

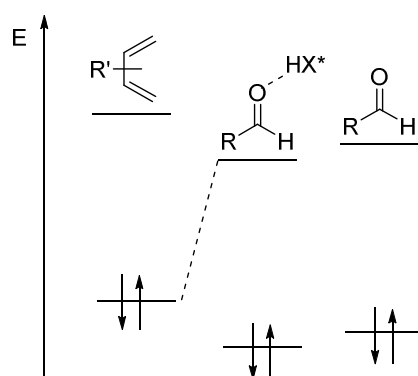


Scheme 4.21 Brønsted acid-catalyzed [4+2]-cycloaddition of dienes with aldehydes.

Catalytic and enantioselective variations of the [4+2]-cycloaddition of dienes with aldehydes have been investigated during the last 30 years, but current methodologies are limited to electron-biased substrates and therefore lack generality.¹⁵³ Despite the enormous potential of a general catalytic asymmetric [4+2]-cycloaddition of simple and electron-unbiased dienes with any type of aldehyde, such a process is entirely unknown. We reasoned that this is due to the inability of current catalysts to simultaneously reduce the large energy difference between the involved frontier orbitals of unactivated dienes and aldehydes, and due to various potential side reactions, such as Prins, carbonyl–ene, aldol, and/or cationic oligomerization reactions.

Strong Brønsted acids would be required to significantly lower the LUMO of the aldehyde (dienophile) and thereby narrowing the energy gap between the involved frontier orbitals¹⁵⁴ (Scheme 4.22). We further hypothesized that a highly confined chiral microenvironment of the catalyst would be essential to enable efficient stereocontrol with small and unfunctionalized substrates, and to preclude side reactions.

4 RESULTS AND DISCUSSION

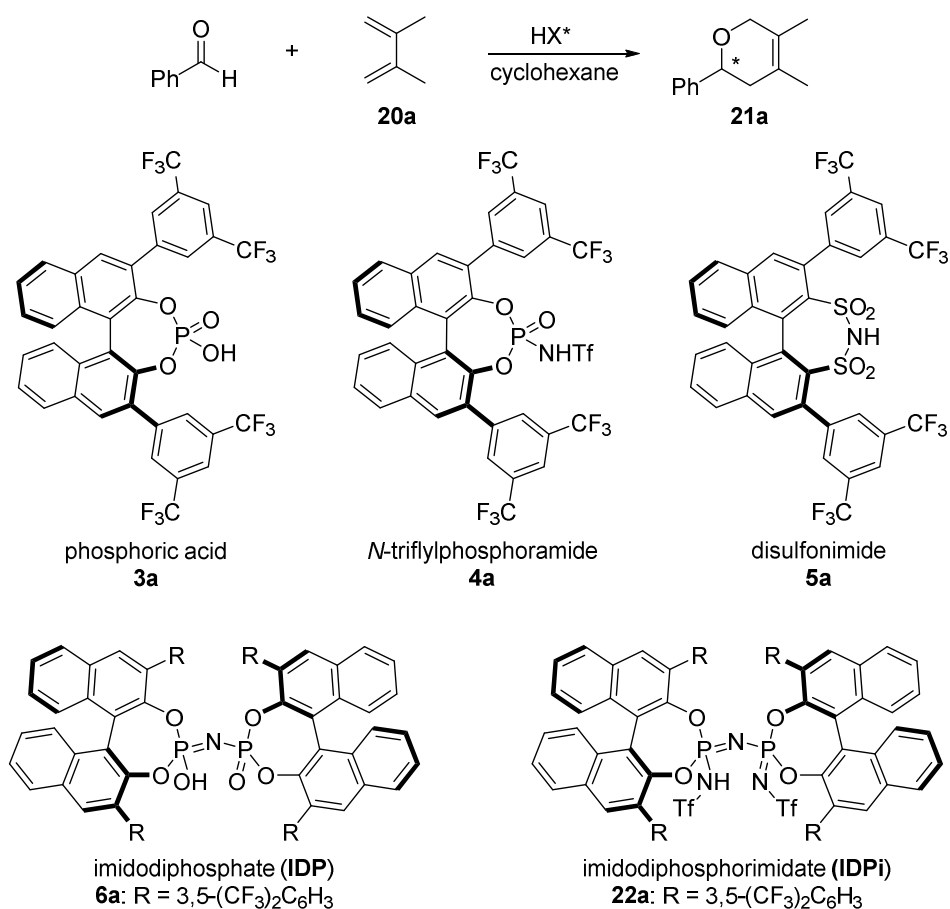


Scheme 4.22 FMOs of [4+2]-cycloaddition of diene with aldehyde.

We initially started with a chiral Brønsted acid catalyzed [4+2]-cycloaddition of 2,3-dimethyl-1,3-butadiene **20a** with benzaldehyde. Different chiral Brønsted acids, including phosphoric acid **3a**,³³ *N*-triflylphosphoramidate **4a**,⁵¹ disulfonimide **5a**,⁵⁵ and imidodiphosphate **6a**⁵⁹ with the same electron withdrawing substituents 3,5-(CF₃)₂C₆H₃ at the 3,3'-positions of the BINOL backbone were explored. However, the desired product **21a** (Table 4.7, entries 1, 3, and 4) was not observed due to the less nucleophilicity of 2,3-dimethyl-1,3-butadiene, when using phosphoric acid **3a**, disulfonimide **5a** and imidodiphosphate **6a**. Only trace of the desired [4+2]-cycloaddition product was detected using catalyst triflylphosphoramidate **4a**, even though a poor enantioselectivity of 64:36 er was observed (Table 4.7, entry 2). My colleague *Dr. Philip S. J. Kaib* creatively developed a method to replace both oxo groups with *N*-triflyl groups at the active site of imidodiphosphate, affording a new type of extremely acidic and confined Brønsted acid imidodiphosphorimidate (IDPi),¹⁵⁵ which would probably address both issues, the reactivity and the stereoselectivity in the [4+2]-cycloaddition. Imidodiphosphorimidate **22a** with 3,5-(CF₃)₂C₆H₃ substituents at the 3,3'-positions of BINOL backbones was directly tested. The obtained results were quite gratifying, a reaction with full conversion and hardly any side products was performed at room temperature with a promising enantioselectivity of 79:21 er (Table 4.7, entry 5).

4 RESULTS AND DISCUSSION

Table 4.7 Screening of different chiral Brønsted acids^a



entry	catalyst	HX* (mol%)	T/°C	t/h	conv. (%) ^b	er ^c
1	3a	5	22	24	n.r.	-
2	4a	5	22	24	10.5	64:36
3	5a	5	22	24	n.r.	-
4	6a	5	22	24	n.r.	-
5	22a	5	22	24	>95	79:21

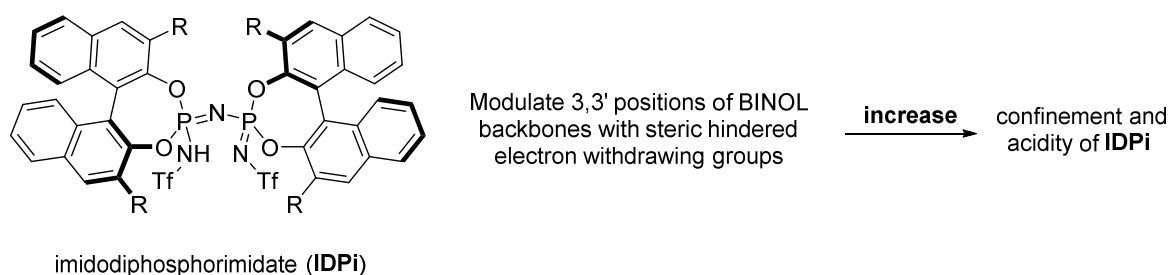
^aUnless otherwise indicated, reactions were performed with benzaldehyde (0.02 mmol), 2,3-dimethyl-1,3-butadiene (0.1 mmol), and catalyst (5 mol%) in 0.2 mL of solvent for 24 h at room temperature. ^bDetermined by ¹H NMR. ^cDetermined by HPLC analysis on chiral stationary phase.

4 RESULTS AND DISCUSSION

4.3.2 Catalyst Design and Synthesis

Catalyst Design

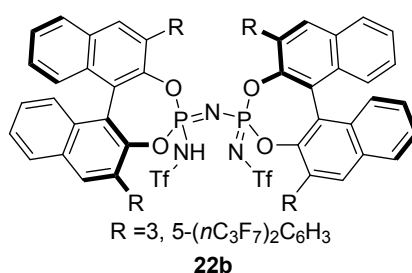
Encouraged by the promising results obtained with catalyst IDPi **22a**, we set out to modulate the IDPi catalyst. To enhance the acidity and the sterical hindrance of IDPi, we introduced bulkier electron withdrawing groups, such as 3,5-(C_nF_{2n+1})₂C₆H₃, 3,5-(SF₅)₂C₆H₃, 3,5-(NO₂)₂C₆H₃ substituents to the 3,3'-positions of imidodiphosphorimidate (IDPi) (Scheme 4.23).



Scheme 4.23 Modulation of IDPi.

Catalyst Synthesis

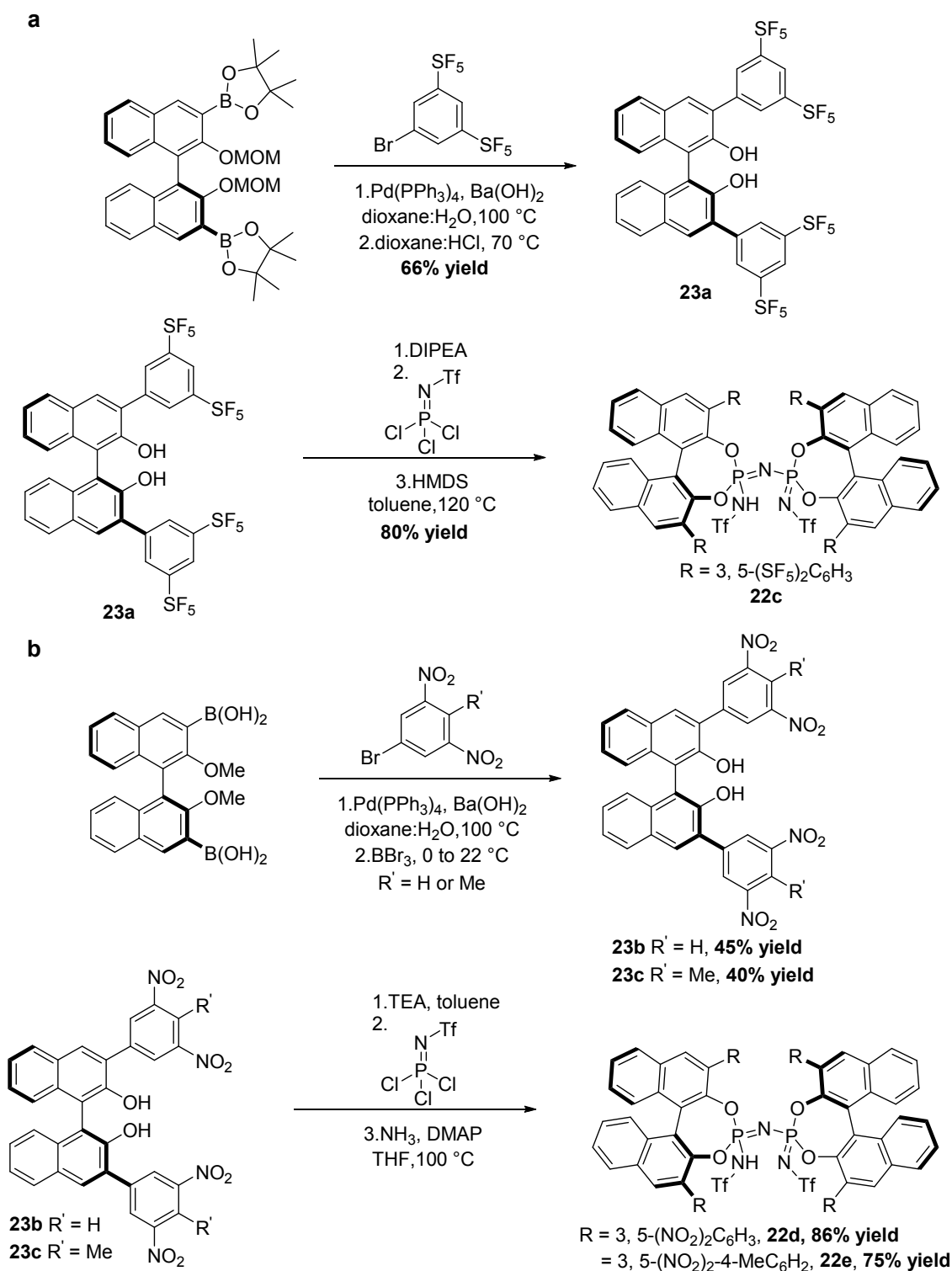
As mentioned above, the introduction of 3,5-(C_nF_{2n+1})₂C₆H₃ substituents were exploited. IDPi **22b** with 3,5-(nC₃F₇)₂C₆H₃ substituents were successfully synthesized by my colleague *Dr. Hyejin Kim* (Scheme 4.24). The characterization of **22b** will be disclosed in the upcoming publication.



Scheme 4.24 IDPi **22b** (*Dr. Hyejin Kim*).

According to the procedure for the synthesis of IDPi,¹⁵⁶ we started with the preparation of the corresponding BINOL. Even though it was reported the preparation of BINOL **23a** with 3,5-(SF₅)₂C₆H₃ substituents at the 3,3'-positions from the starting material 3,5-bis(pentafluorothio) bromo benzene, the yield was quite low around 22.5%. An optimization of the preparation of this BINOL was preformed, and an improved yield of

4 RESULTS AND DISCUSSION



Scheme 4.25 Synthesis of IDPi **22c–22e**.

66% was achieved from the starting material boronic ester, available in our laboratory¹⁵⁷ (Scheme 4.25a). Following the procedures of the IDPi catalyst synthesis, the new type of IDPi **22c** was afforded with an isolated yield of 80%. Similarly, using boronic acid available in our laboratory, the corresponding BINOL **23b** with 3,5-(NO₂)₂C₆H₃ substituents and **23c** with 3,5-(NO₂)₂-4-Me-C₆H₃ substituents could be obtained after the

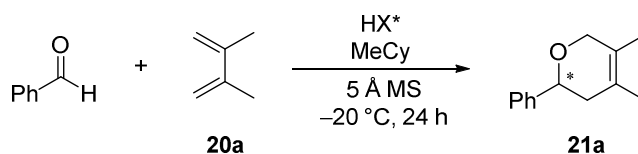
4 RESULTS AND DISCUSSION

Suzuki coupling respectively. Imidodiphosphorimidate **22d** and **22e** could be readily obtained after a further step (Scheme 4.25b).

4.3.3 Utilization of New Catalysts

We directly utilized these newly synthesized catalysts in the [4+2]-cycloaddition of 2,3-dimethyl-1,3-butadiene (**20a**) with benzaldehyde. Gratifyingly, all IDPis were able to catalyze the [4+2]-cycloaddition of 2,3-Dimethyl-1,3-butadiene with benzaldehyde (Table 4.8, entries 1–4). Excellent enantioselectivity of 98:2 er and >95% conv. could be achieved using catalyst **22c** at $-20\text{ }^{\circ}\text{C}$ (Table 4.8, entry 5). The reaction concentration could be increased to 0.3 M without diminishing the enantioselectivity (98:2 er) or the reactivity (> 95% conv.) for this [4+2]-cycloaddition of **20a** with benzaldehyde (Table 4.8, entry 6). The catalyst loading could be reduced to 0.2 mol%, and identically excellent results were achieved (Table 4.8, entry 7).

Table 4.8 Utilization of catalysts IDPis **22b-22e**^a



entry	T (°C)	catalyst	HX* (mol%)	C (M)	conv. (%) ^b	er ^c
1	22	22c	5	0.1	>95	90:10
2	22	22d	5	0.1	86	57:43
3	22	22e	5	0.1	75.6	60:40
4	-20	22b	1	0.1	88	90.5:9.5
5	-20	22c	1	0.1	>95	98:2
6 ^d	-20	22c	1	0.3	>95	98:2
7	-20	22c	0.2	0.3	>95	98:2

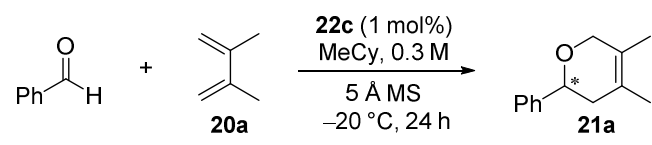
^aUnless otherwise indicated, reactions were performed with benzaldehyde (0.02 mmol), 2,3-dimethyl-1,3-butadiene (0.1 mmol), catalyst and 5 Å molecular sieves (70mg/mL) in solvent at $-20\text{ }^{\circ}\text{C}$ for 24 h. ^bDetermined by ^1H NMR. ^cDetermined by HPLC analysis on chiral stationary phase. ^dThe reaction was performed within 4 h.

4 RESULTS AND DISCUSSION

Optimization of the Amount of Diene

The amount of diene was optimized and could be reduced to 1.2 equiv. with an excellent enantiomeric ratio 98:2 and full conversion (Table 4.9, entry 3). The reaction was also performed well with excess amount of benzaldehyde. **21a** was obtained with similarly excellent enantioselectivity and conversion (Table 4.9, entry 4).

Table 4.9 The ratio of substrates^a



entry	C (M)	PhCHO (mmol)	20a (mmol)	conv. (%) ^b	er ^c
1	0.3	0.1	0.5	>95	98:2
2	0.3	0.1	0.25	>95	98:2
3	0.3	0.1	0.12	>95	98:2
4	0.3	0.12	0.1	>95	98:2

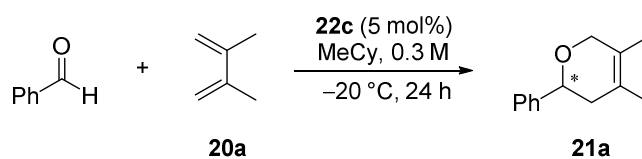
^aUnless otherwise indicated, reactions were performed with benzaldehyde, 2,3-dimethyl-1,3-butadiene, catalyst and 5 Å molecular sieves (70mg/mL) in solvent at -20 °C for 24 h. ^bDetermined by ¹H NMR. ^cDetermined by HPLC analysis on chiral stationary phase.

The Role of Molecular Sieves

Apparently 5 Å molecular sieves with a formula of 0.7CaO•0.30Na₂O•Al₂O₃•2.0SiO₂•4.5H₂O contain a lot of metal sources, a possible Brønsted acid assisted Lewis acid activation or the reverse way, a Lewis acid assisted Brønsted acid activation might happen. Comparative reactions were carried out (Table 4.10). According to the excellent results shown in Table 4.10, we could give a conclusion that a pure Brønsted acid **22c** could catalyze this highly enantioselective [4+2]-cycloaddition of 2,3-dimethyl-1,3-butadiene **20a** with benzaldehyde.

4 RESULTS AND DISCUSSION

Table 4.10 Comparative reactions^a



entry	5 Å M.S.	22c (mol%)	C (M)	conv. (%) ^b	er ^c
1	21 mg	5	0.3	>95	98:2
2	–	5	0.3	92	97.5:2.5

^aUnless otherwise indicated, reactions were performed with benzaldehyde (0.1 mmol), 2,3-dimethyl-1,3-butadiene (0.5 mmol), catalyst and 21 mg of 5 Å molecular sieves in 0.3 mL of MeCy at –20 °C for 24 h. ^bDetermined by ¹H NMR. ^cDetermined by HPLC analysis on chiral stationary phase.

4.3.4 Substrate Scope of Aromatic Aldehydes

With the optimized reaction conditions, various aromatic aldehydes were explored. Since fluorinated compounds have attracted the interest of chemists already for a long time due to their potential bio-activity, aldehydes with systematic fluoride substitution at *ortho*, *meta*, and *para*-position of the benzaldehyde ring were mainly exploited (Table 4.11, entries 2–4). All of them turned out to be suitable substrates for catalyst **22c** with excellent enantioselectivities and high yields except the moderate 92.5:7.5 er of **22b** (Table 4.11, entry 2). Both, the electron-deficient 4-Br benzaldehyde and electron-rich 4-Me benzaldehyde delivered the desired products with high enantioselectivities, even though a slightly higher catalyst loading of 3 mol% was used (Table 4.11, entries 5–6). We tried to optimize the reaction conditions to achieve a high yield of **21e** but failed. This low yield might be probably due to the low solubility of 4-Br benzaldehyde at –60 °C (Table 4.11, entry 5). However, traces of product **21g** were detected with the optimized reaction conditions using 4-MeO benzaldehyde as the substrate. We reasoned the poor reactivity to the high basicity of 4-MeO benzaldehyde, which might inhibit the activity of Brønsted acid **22c** (Table 4.11, entry 7). Heterocyclic aromatic aldehyde 2-thiophenecarboxaldehyde also successfully furnished the desired [4+2]-cycloaddition product with an excellent 99.5:0.5 enantiomeric ratio (Table 4.11, entry 8). Moderate yield was obtained, even though we extended the reaction time. The absolute

4 RESULTS AND DISCUSSION

configuration of **21e** was determined as *R* by single-crystal X-ray diffraction analysis (Figure 4.11).

Table 4.11 Scope of aromatic aldehydes^a

$\text{R-CHO} + \text{20a} \xrightarrow[\text{5 \AA MS}]{\text{22c, MeCy, 0.3 M}} \text{21}$
 R = Aryl

entry	22c (mol%)	20a (mmol)	21	yield (%) ^b	er ^c
1	0.2	0.12	 21a	97	98:2
2 ^d	1.0	0.2	 21b	81	92.5:7.5
3	1.0	0.2	 21c	94.5	98:2
4	1.0	0.2	 21d	89	97:3
5 ^e	3.0	1.0	 21e	36	95:5
6 ^e	3.0	0.5	 21f	93	96:4
7	3.0	0.5	 21g	–	–
8 ^d	1.0	0.2	 21h	48	99.5:0.5

4 RESULTS AND DISCUSSION

^aUnless otherwise indicated, reactions were performed with aldehyde (0.1 mmol), 2,3-dimethyl-1,3-butadiene (0.12–1.0 mmol), **22c** (0.2–3 mol%) and 5 Å molecular sieves (70mg/mL) in MeCy at –20 °C for 24 h. ^bIsolated yield. ^cDetermined by HPLC analysis on chiral stationary phase. ^dThe reaction was performed at –10 °C for 3 days. ^eThe reaction was performed at –60 °C for 6 days.

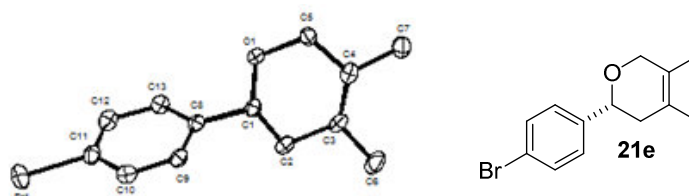


Figure 4.11 X-ray crystal structure of **21e**.

4.3.5 Substrate Scope of Aliphatic Aldehydes

Subsequently, aliphatic aldehydes were investigated next. Using the optimized conditions for aromatic aldehydes, the desired [4+2]-cycloaddition product could be obtained in generally high enantioselectivity but with low conversion in the reaction between isovaleraldehyde and **20a** (Table 4.12, entry 1). The trimerization of isovaleraldehyde turned out to be the main product. But the trimerization of isovaleraldehyde was reversible and no obvious trimerization product **25a** was observed when we performed the reaction at room temperature (Table 4.12, entry 2). Good enantioselectivity and conversion could be achieved when we reduced the catalyst loading to 1 mol% and increased the diene amount to 10 equiv. (Table 4.12, entry 3).

Table 4.12 Initial exploration with **22c**^a

entry	T (°C)	t (h)	conv. of 21i (%) ^b	er of 21i ^c	conv. of 25 (%) ^b
1	–40	52	8	96:4	92
2	22	20	87	88.5:11.5	–
3 ^d	–20	52	>95	93:7	–

4 RESULTS AND DISCUSSION

^aUnless otherwise indicated, reactions were performed with isovaleraldehyde (0.02 mmol), 2,3-dimethyl-1,3-butadiene (0.1 mmol), **22c** (3 mol%) and 5 Å molecular sieves (70mg/mL) in MeCy at -20 °C for 24 h. ^bDetermined by ¹H NMR. ^cDetermined by HPLC analysis on chiral stationary phase. ^dThe reaction was performed with 1 mol% catalyst loading and 10 equiv. of 2,3-dimethyl-1,3-butadiene.

In order to increase the enantioselectivity in the [4+2]-cycloaddition between isovaleraldehyde and 2,3-dimethyl-1,3-butadiene, we screened other IDPis. Gratifyingly, using the catalyst IDPi **22b** with 3,5-(C₃F₇)₂C₆H₃ substituents, we were able to increase the enantioselectivity to 94.4:5.6 er with excellent 91% isolated yield (Table 4.13, entry 1). Various aliphatic aldehydes were explored using **22b** as the catalyst. Both linear aldehydes valeraldehyde and decyl aldehyde, proved to be suitable substrates under the

Table 4.13 Scope of aliphatic aldehydes^a

entry	T (°C)	t (h)	21	yield (%) ^b	er ^c
1	-20	70		91	94:6
2	-20	48		87	97:3
3	-20	48		94	97:3
4	-10	67		83	97:3
5	-10	48		73	96:4

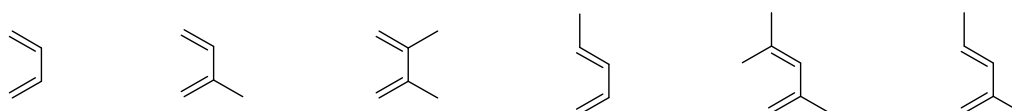
^aUnless otherwise indicated, reactions were performed with aldehyde (0.3 mmol), 2,3-dimethyl-1,3-butadiene (3.0 mmol), **22b** (1.0 mol%) and 5 Å molecular sieves (70mg/mL) in MeCy. ^bIsolated yield. ^cDetermined by HPLC analysis on chiral stationary phase.

4 RESULTS AND DISCUSSION

optimized reaction conditions, and the desired products **21j** and **21k** were obtained in excellent enantioselectivities and yields (Table 4.13, entries 2 and 3). The α -branched aliphatic aldehyde isobutyraldehyde was compatible with **22b** and furnished the product **21i** with 83% yield and 97.4:2.6 er after increasing the reaction temperature to $-10\text{ }^{\circ}\text{C}$ (Table 4.13, entry 4). The slightly larger aliphatic substrate 3-phenylpropionaldehyde was next exploited. The trimerization product of 3-phenylpropionaldehyde was detected as the main product when the reaction was performed at $-20\text{ }^{\circ}\text{C}$. Nevertheless, **21m** could be obtained in good enantioselectivity of 95.5:4.5 er (Table 4.13, entry 5).

4.3.6 Diene Scope

The initial objective of this part of the doctoral work was to achieve a highly enantioselective asymmetric [4+2]-cycloaddition of simple dienes with aldehydes. Both aliphatic and aromatic aldehydes were compatible in this asymmetric [4+2]-cycloaddition as shown above under the optimized reaction conditions. The scope of dienes was investigated next. Inexpensive and commercially available simple dienes, such as butadiene, isoprene, 1,3-pentadiene and trisubstituted diene 2,4-dimethyl-1,3-pentadiene were all explored (Scheme 4.26).



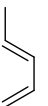
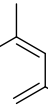
Scheme 4.26 Scope of dienes.

Starting with butadiene, however, the desired product was not obtained even after increasing the reaction temperature to $50\text{ }^{\circ}\text{C}$ with an increased catalyst loading (Table 4.14, entry 1). We also performed the reaction at high pressure which was known to accelerate the HDA reaction of butadiene, but the desired [4+2]-cycloaddition product was not observed except the polymerization of butadiene. Other new types of catalyst motifs might be required regarding the reactivity of butadiene, for example, a combination of IDPi with Lewis acid. Isoprene was investigated next, whose nucleophilicity is similar to the standard diene 2,3-dimethyl-1,3-butadiene. Excellent yield and enantioselectivity were achieved using **22c** as catalyst (98:2 er, 87% yield). Using *trans*-1,3-pentadiene as substrate, the *trans*-diastereoselective [4+2]-cycloaddition product was obtained with high enantioselectivity $>99.5:0.5$ er (Table 4.14, entry 3). But the isolated yield was quite low despite a full conversion of the benzaldehyde. This was

4 RESULTS AND DISCUSSION

due to the side reaction, the Prins reaction. Trisubstituted 2,4-dimethyl-1,3-pentadiene was tested next. After reducing the concentration and lowering the temperature, 82% yield and 96:4 er were achieved (Table 4.14, entry 4). Another *trans*-2-methyl-1,3-pentadiene was also investigated, affording the desired cycloadduct in good yield and enantioselectivity, yet moderate diastereoselectivity. The absolute configuration of **21o** was determined as *trans*-2*R*,6*S*, and the absolute configuration of **21q** was determined as *cis*-2*R*,6*R* by comparison with the reported specific rotation values.¹⁵⁸

Table 4.14 Scope of diene^a

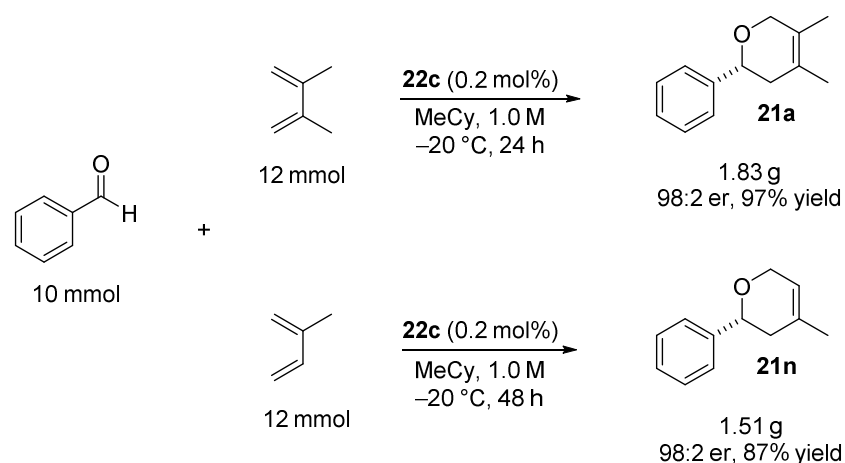
entry	catalyst (mol%)	C (M)	T (°C)	t (h)	20 (mmol)	yield (%) ^b	dr ^c	er ^d
1	22c , 3 mol%	22	50	72	 1.0 mmol 20b	—	—	—
2	22c , 1 mol%	0.3	-20	48	 0.2 mmol 20c	97	—	98:2
3	22b , 3 mol%	0.3	-30	72	 0.5 mmol 20d	20	<i>trans</i> : <i>cis</i> = 22:1	99:1 er _{<i>trans</i>}
4	22b , 2 mol%	0.01	-45	48	 0.5 mmol 20e	82	—	96:4
5	22b , 3 mol%	0.3	-30	72	 0.5 mmol 20f	81	<i>trans</i> : <i>cis</i> = 1:7	96:4 er _{<i>cis</i>}

^aUnless otherwise indicated, reactions were performed with aldehyde (0.1 mmol), diene (0.12–1.0 mmol), **22b** (1.0 mol%) and 70mg/mL 5 Å molecular sieves in MeCy. ^bIsolated yield. ^cDetermined by ¹H NMR. ^dDetermined by HPLC analysis on chiral stationary phase.

4 RESULTS AND DISCUSSION

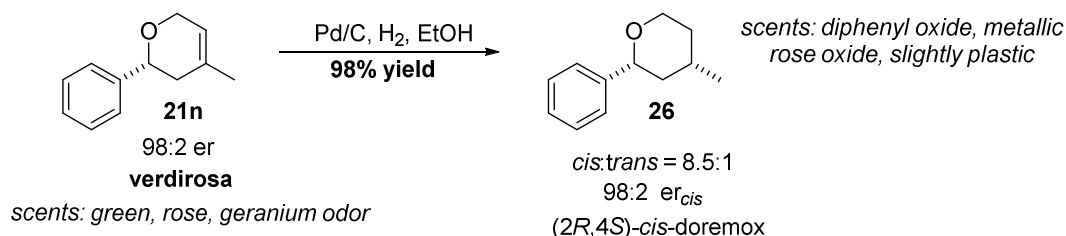
4.3.7 Gram-Scale Synthesis and Derivatization

This methodology is quite practical and scalable as shown in scheme 4.27. Gram-scale [4+2]-cycloaddition reactions proceeded well for both cases 2,3-dimethyl-1,3-butadiene **20a** and isoprene **20b** with benzaldehyde. Excellent enantioselectivity of 98:2 er was generally obtained and high yields (Scheme 4.27). Additionally, the catalyst **22c** could be easily recovered in a high yield of 97% through column chromatography without losing activity after acidification with 6 M HCl aq.



Scheme 4.27 Gram-scale synthesis.

Doremox is one of the most common commercial fragrances. (2*R*,4*S*)-*cis*-doremox could be readily afforded as main product with one simple hydrogenation step of the [4+2]-cycloaddition product **21n** (Scheme 4.28). (2*S*,4*R*)-*cis*-doremox is the nicest and strongest scent among the four diastereoisomers. The precursor of (2*S*,4*R*)-*cis*-doremox could be obtained from *ent*-**21n**.



Scheme 4.28 Derivatization.

4 RESULTS AND DISCUSSION

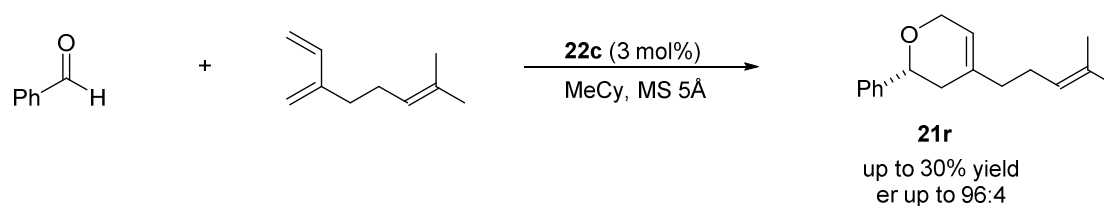
4.3.8 Discussion

The first highly enantioselective [4+2]-cycloaddition between simple dienes and aldehydes was presented in this chapter (Scheme 4.29). For the first time, a general asymmetric catalytic [4+2]-cycloaddition between dienes and aldehydes was achieved. Valuable dihydropyrans could be readily obtained in high stereo selectivities and yields from inexpensive commercial aldehydes and naturally abundant dienes. This methodology was quite practical and could be easily performed on a gram scale. The catalyst could be recovered and acidified with a high yield of 97%. This methodology provided the most straight forward and atom-economical synthesis of valuable fragrances. Since dihydropyran compounds were important scaffolds in natural products and pharmaceuticals, this methodology could in principle be utilized in organic synthesis.



Scheme 4.29 Asymmetric catalytic HDA reaction.

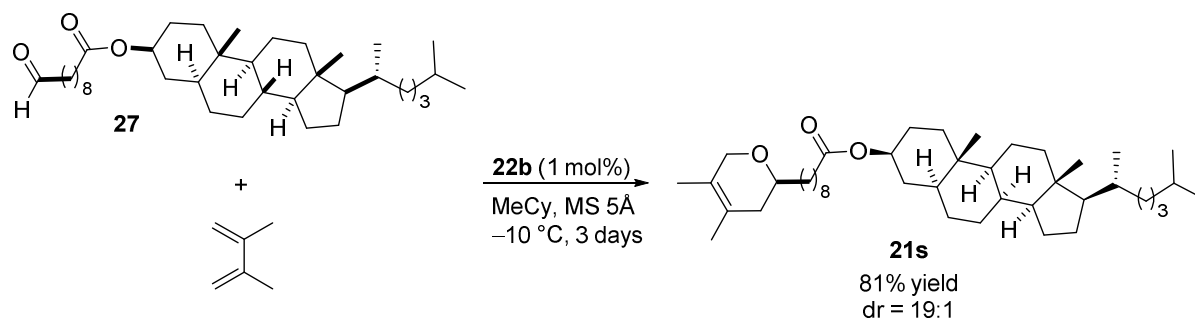
Although the substrate scope of this reaction is quite general, the basic aldehyde is not compatible with the reaction conditions (Table 4.11, entry 7). We reasoned this to a potential hydrogen bond between IDPi and the basic substituents of the aldehydes which might reduce the high acidity of IDPi. Another assumption is that the energy of the LUMO of the aldehyde was too high. To solve this problem, either the development of new catalysts or the optimization of the reaction conditions might be necessary. Large dienes were also investigated, for example beta-myrcene which is one of the common terpenes (Scheme 4.30). The enantioselectivity was very good, but the isolated yield was quite low, which is due to the side Prins reaction.



Scheme 4.30 Large diene.

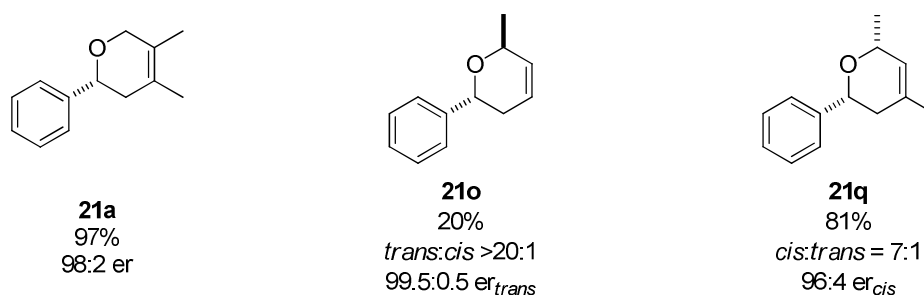
4 RESULTS AND DISCUSSION

Aliphatic aldehydes were well tolerated under the optimized reaction conditions (Table 4.13). To investigate the potential of this confined catalyst **22b** further, large substrate, such as dihydrocholesterol-derivatized aldehyde **27** synthesized. Subsequently, aldehyde **27** was performed with 2,3-dimethyl-1,3-butadiene **20a** using catalyst **22b**. The desired [4+2]-cycloadduct was afforded in a good yield of 81% with excellent diastereoselectivity.



Scheme 4.31 Large aldehyde.

Despite the important synthetic value of this Brønsted acid-catalyzed asymmetric [4+2]-cycloaddition reaction, the different diastereoselectivities were obtained by the variation of the dienes (**21o** and **21q**), which triggered closer investigations to achieve a mechanistic understanding of this reaction.



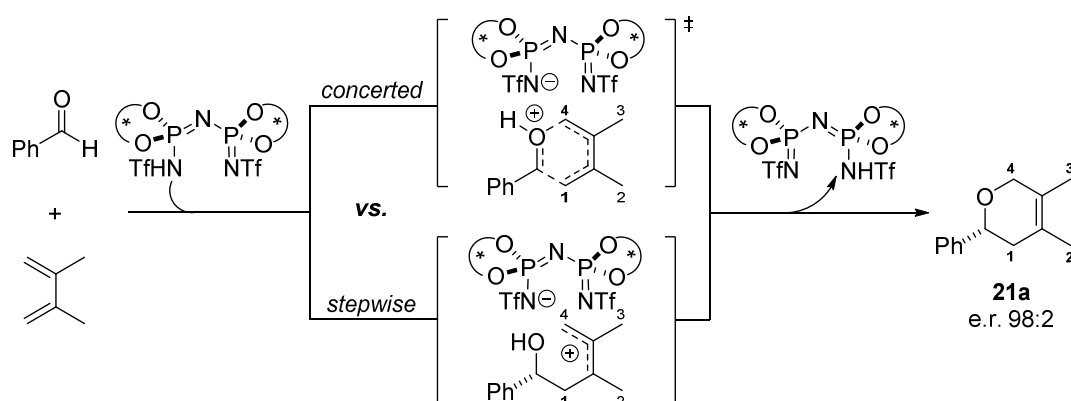
Scheme 4.32 Asymmetric catalytic [4+2]-cycloaddition.

Mechanistic Studies

We initially envisioned two mechanistic scenarios for the described Brønsted acid-catalyzed [4+2]-cycloaddition reaction: a concerted, pericyclic reaction or a stepwise, carbocationic pathway (Scheme 4.33). The protonation of benzaldehyde will result in the lowering of its LUMO promoting an electronically-matched interaction with the HOMO of the diene. A subsequent concerted [4+2]-cycloaddition could furnish the corresponding *hetero*-Diels–Alder adduct **21a** after deprotonation. Alternatively, a

4 RESULTS AND DISCUSSION

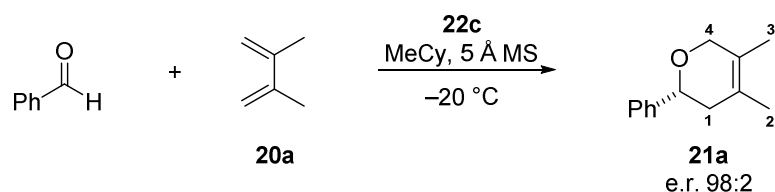
stepwise pathway proceeding via a carbocation intermediate, which undergoes an intramolecular nucleophilic attack, can be envisioned.^{159–161}



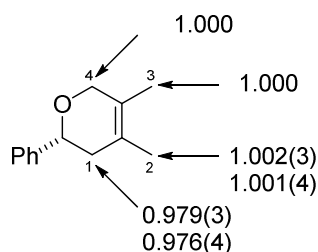
Scheme 4.33 Proposed reaction mechanism

The precise determination of the kinetic isotope effect (KIE), which is defined as the ratio of the rate constant of the lighter isotope (k_L) to the rate constant of the heavier isotope (k_H), can provide some detailed information about the reaction mechanism.¹⁶² In 1995, the Singleton group reported a practical KIE measurement at natural isotopic abundance, which has been successfully used to elucidate the mechanism of many reactions.^{163–165} To elucidate the reaction mechanism, an intramolecular ^{13}C kinetic isotope effect (KIE, $k^{12}\text{C}/k^{13}\text{C}$) experiment of the reaction leading to product **21a** was conducted at the natural isotopic abundance.^{166,167} The relative ^{13}C compositions of **20a** at C3 and C4 were respectively assigned to be 1.000 in this intramolecular KIE measurement. The ^{13}C KIE at C2 of 0.998(3)–0.999(4) indicated that the NMR measurements were accurately performed, since a negligible ^{13}C KIE at C2 would be expected for either of the envisioned mechanisms. We observed a substantial ^{13}C KIE at C1 of 1.022(3)–1.025(4), which suggested that the reaction proceeds via a stepwise mechanism. However, the observed KIE is also consistent with a concerted, though highly asynchronous pathway.

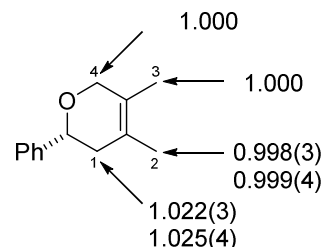
4 RESULTS AND DISCUSSION



a. ^{13}C relative compositions

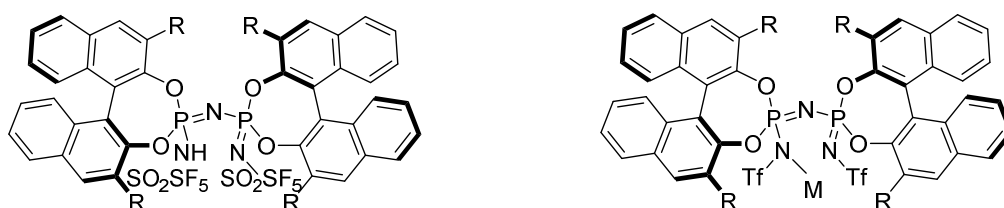


b. Intramolecular ^{13}C KIEs



Scheme 4.34 Intramolecular ^{13}C KIEs. (The values above were measured at $15 \pm 0.6\%$ completion of **20a**, the values below were measured at $16 \pm 0.8\%$ completion of **20a**.)

A series of highly acidic and confined IDP*i*s were synthesized in this hetero-Diels–Alder reaction between dienes and aldehydes, which could be utilized in other challenging asymmetric transformations. The main effort of the modulation of IDP*i* here is the introduction of 3,5-(EWG) $_2\text{C}_6\text{H}_3$ substituents at the 3,3'-positions of the BINOL backbones. The reactivity and stereoselectivity of this [4+2]-cycloaddition was dramatically improved using 3,5-(SF_5) $_2\text{C}_6\text{H}_3$ substituents. This indicated that the replacement of the oxo group at the active site of IDP*i* with $N\text{-SO}_2\text{SF}_5$ would make the active site even more compact and acidic. In principle, we could also replace the active “H” site with metal species, which might enable us to perform more fascinating asymmetric transformations.



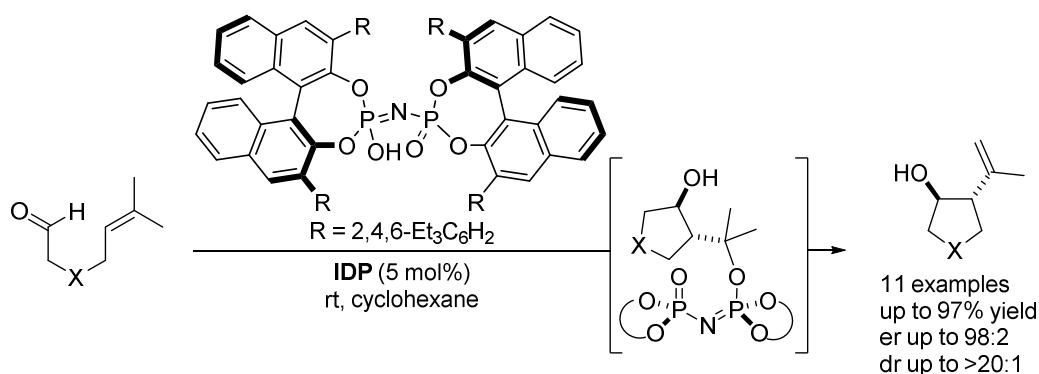
Scheme 4.35 Highly acidic confined acids.

5 SUMMARY

5.1 Organocatalytic Asymmetric Carbonyl–Ene Cyclization

Intramolecular carbonyl-ene cyclizations are widely used in the synthesis of cyclic compounds. Complementary to Jacobsen's work on an asymmetric *cis*-diastereoselective intramolecular carbonyl–ene cyclization reaction catalyzed by a chiral dimeric chromium complex, this PhD work describes the first organocatalytic highly enantioselective and *trans*-diastereoselective intramolecular carbonyl–ene cyclization of olefinic aldehydes without Thorpe–Ingold-type substitutions.

Mechanistic studies including ESI-MS, NMR, DFT calculations, unanimously supported an unexpected step-wise mechanism, suggesting that the reaction proceeds *via* a “catalyst-substrate” covalent intermediate.



1. The first organocatalytic highly enantioselective carbonyl–ene cyclization.
2. High *trans*-diastereoselectivities.
3. The first highly enantioselective carbonyl–ene cyclization of unactivated substrates.
4. Novel step-wise mechanism *via* a covalent intermediate.

Scheme 5.1 Brønsted acid-catalyzed asymmetric carbonyl–ene cyclization.

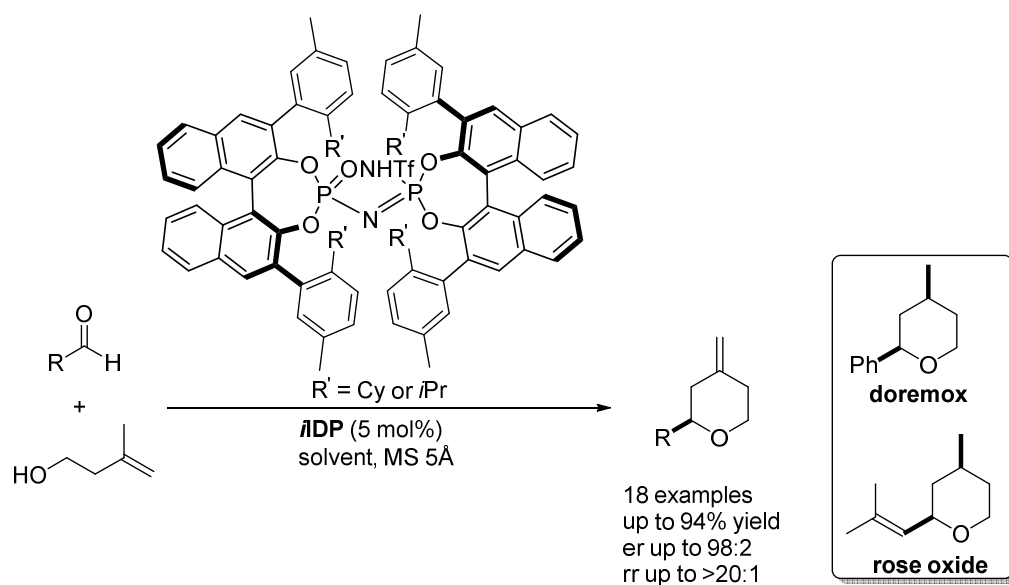
5 SUMMARY

5.2 Organocatalytic Asymmetric Transformations *via* Oxocarbenium Ions

5.2.1 A General Organocatalytic Asymmetric Prins Cyclization

(with Dr. Philip S. J. Kaib)

Functionalized chiral tetrahydropyrans (THPs) are valuable motifs in natural products and fragrances, which could potentially be readily synthesized using the Prins cyclization between aldehydes and homoallylic alcohols. Although the Prins cyclization has been frequently used in organic synthesis, enantioselective variants of the Prins cyclization have been rarely investigated. In 2015, the first highly enantioselective Prins cyclization was developed in the List group utilizing activated salicylaldehydes as substrates. In this part of the presented doctoral work, a new chiral Brønsted acid imino-imidodiphosphate (*i*IDP) was developed to realize a broad range of substrate scope, representing the first general and highly enantioselective Prins cyclization. This methodology provides a straightforward access to a variety of fragrances, including rose oxide and doremoz.



1. The first general highly enantioselective Prins cyclization.
2. High regioselectivities.
3. A straightforward approach to scent chemicals such as doremoz and rose oxide.

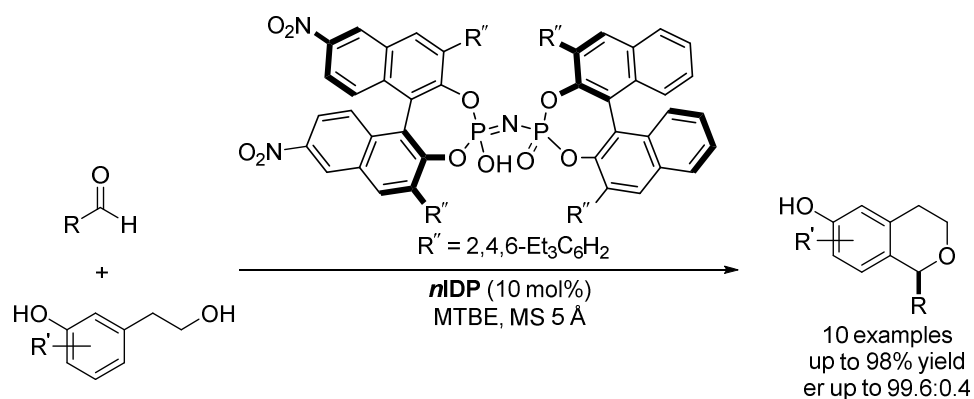
Scheme 5.2 A general Brønsted acid-catalyzed asymmetric Prins cyclization.

5 SUMMARY

5.2.2 Organocatalytic Asymmetric *Oxa*-Pictet–Spengler Reaction

(with Dr. Sayantani Das)

Chiral isochromans are important scaffolds in many natural bio-active compounds and could be efficiently afforded through an enantioselective *oxa*-Pictet–Spengler reaction between aldehydes and aryl ethanols. Our newly developed Brønsted acid, nitrated imidodiphosphate (*n*IDP), proved to be a suitable catalyst for this enantioselective *oxa*-Pictet–Spengler reaction. Diverse isochromans were obtained in high yields with excellent regio- and enantioselectivities. Interestingly, the bifunctional property of the *n*IDP catalyst was crucial in this transformation.



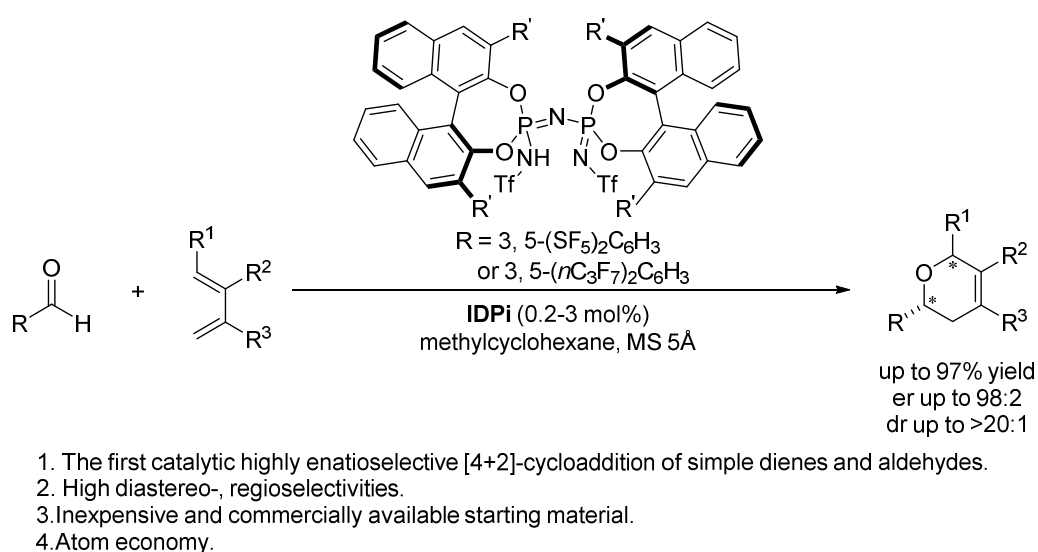
1. The first organocatalytic highly enantioselective *oxa*-Pictet–Spengler reaction.
2. High regioselectivities.
3. A broad substrate scope of diverse aldehydes.

Scheme 5.3 Brønsted acid-catalyzed asymmetric *oxa*-Pictet–Spengler reaction.

5 SUMMARY

5.3 Catalytic Asymmetric [4+2]-Cycloaddition of Dienes with Aldehydes

The [4+2]-cycloaddition between dienes and aldehydes is a direct and elegant approach to construct dihydropyrans. To achieve good yields and stereoselectivities, either highly activated aldehydes or engineered dienes were required in previous reports. In this thesis, the first highly general, efficient and enantioselective [4+2]-cycloaddition of simple dienes with aldehydes was developed, using our newly-developed imidodiphosphorimidates (IDPis) as catalysts. This methodology is very practical, scalable and atom-economical. A broad range of substrates are compatible with the optimized reaction conditions, including aliphatic and aromatic aldehydes as well as a variety of simple dienes. A diverse set of functionalized dihydropyran compounds were obtained in moderate to high yields and high stereoselectivities. Significantly, this method provided the most elegant and enantioselective access to valuable scented dihydropyran compounds.



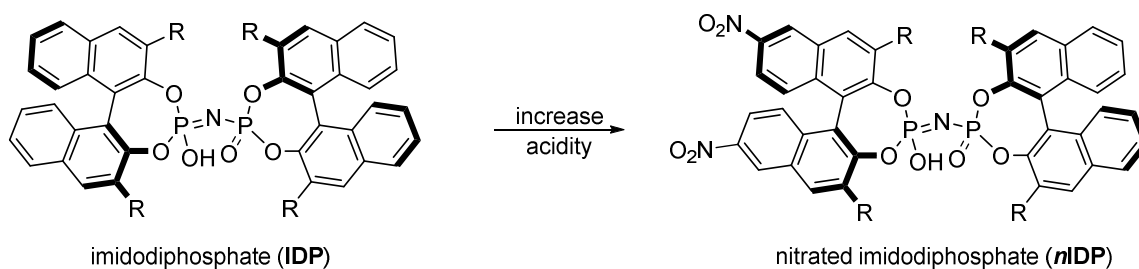
Scheme 5.4 Catalytic asymmetric [4+2]-cycloaddition of dienes with aldehydes.

5 SUMMARY

5.4 Highly Acidic and Confined Brønsted Acids

Highly acidic and confined Brønsted acids were designed and synthesized in this doctoral work to achieve a variety of highly enantioselective cyclization reactions of unactivated aldehydes and inactive nucleophilic alkenes. The effort has mainly been put in modulating the skeleton of our previously-developed confined Brønsted acidic imidodiphosphates (IDPs), which showed their privilege in asymmetric reactions of small-sized substrates.

As demonstrated in this dissertation, imidodiphosphates proved to be quite tunable. We successfully introduced electron withdrawing groups at the 6,6' positions of the BINOL backbone of imidodiphosphate (IDP), resulting in the nitrated imidodiphosphate (*n*IDP) (Scheme 5.5). Remarkably, this novel catalyst *n*IDP turned out to be more acidic without diminishing the inherent confinement of its parent IDP. Nitrated imidodiphosphate (*n*IDP) has been applied to a highly enantioselective *oxa*-Pictet–Spengler reaction of aldehydes and homobenzyl alcohol.

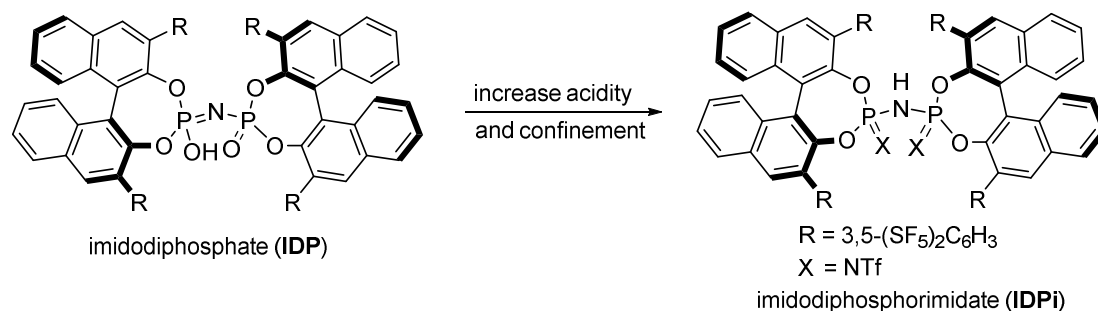


Scheme 5.5 Highly acidic and confined Brønsted acid *n*IDP.

The modulation of the 3,3'-positions of the BINOL backbone has been extensively studied in phosphoric acid catalysis, which has proven to be closely related to the acidity and sterical hindrance of chiral acids. Throughout this doctoral investigation, the substituents at the 3,3'-positions of the BINOL backbone of IDP are crucial to the reactivity and stereoselectivity in the reactions. The ideal substituents are supposed to improve both acidity and confinement of the chiral acid. Strong electron-withdrawing substituents, for example, 3,5-(SF₅)₂C₆H₃, emerged as excellent candidates. In combination with my colleagues' intelligent design of the replacement of the oxo group with a *N*-Tf group, super acidic but sterically hindered imidodiphosphorimidates (IDPis) have been developed in this doctoral work (Scheme 5.6). These rationally designed

5 SUMMARY

imidodiphosphorimidates (IDPis) enabled a general and highly enantioselective [4+2]-cycloaddition of simple dienes with aldehydes.



Scheme 3.7 Highly acidic and confined Brønsted acid IDPi.

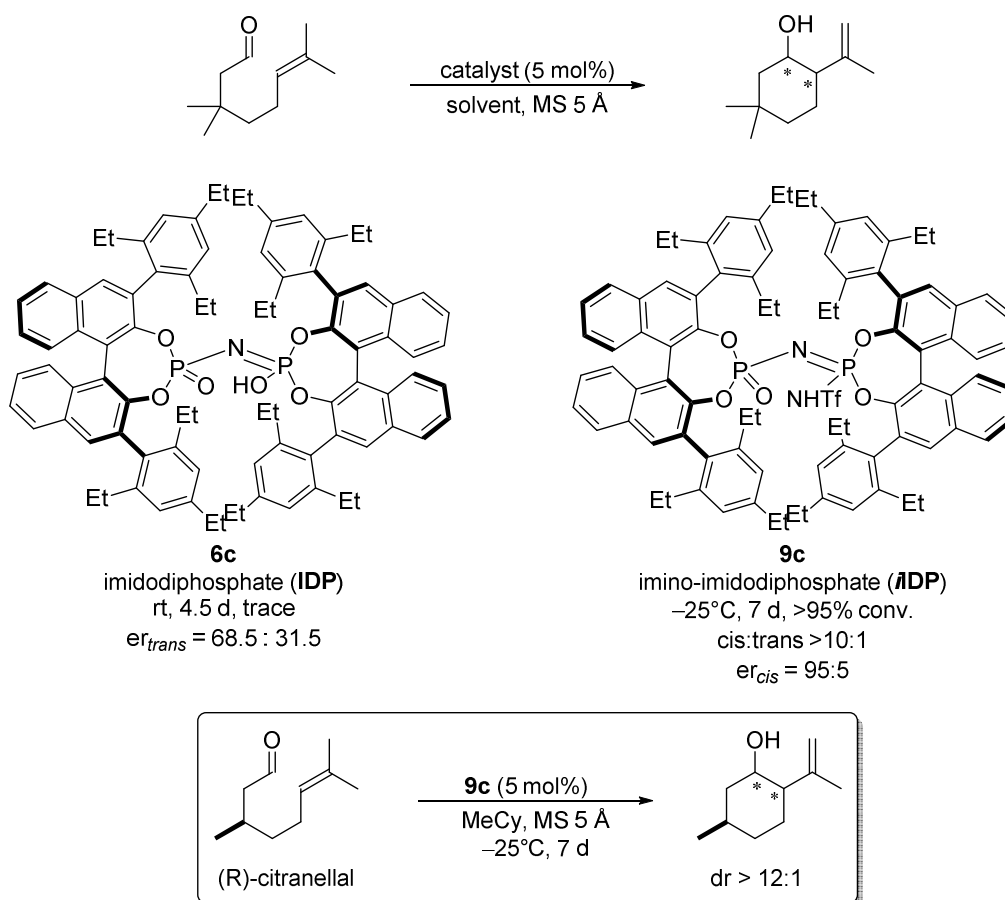
This work has been disclosed in the following publications:

1. “Confined Acid-Catalyzed Asymmetric Carbonyl–Ene Cyclization” L. Liu, M. Leutzsch, Y. Zheng, W. M. Alachraf, W. Thiel, B. List, *J. Am. Chem. Soc.* **2015**, 13268–13271.
2. “The Organocatalytic Asymmetric Prins Cyclization” T. G. Chit, L. Liu, B. List, *Angew. Chem. Int. Ed.* **2015**, 7703–7706.
3. “A General Catalytic Asymmetric Prins Cyclization” L. Liu,⁺ P. Kaib,⁺ A. Tap, B. List, *J. Am. Chem. Soc.* **2016**, 10822–10825. (⁺equal contribution)
4. “Nitrated Confined Imidodiphosphates Enable a Catalytic Asymmetric Oxa-Pictet–Spengler Reaction” S. Das,⁺ L. Liu,⁺ Y. Zheng, W. M. Alachraf, W. Thiel, C. K. De, and B. List, *J. Am. Chem. Soc.* **2016**, 9429–9432. (⁺equal contribution)
5. “Catalytic Asymmetric [4+2]-Cycloaddition of Dienes with Aldehydes”, L. Liu, H. Kim, Y. Xie, C. Farès, P. S. J. Kaib, R. Goddard, B. List, *J. Am. Chem. Soc.* **2017**, 139, 13656–13659.

6 OUTLOOK

6.1 A Highly Enantioselective Synthesis of Menthol

In our initial exploration of asymmetric intramolecular carbonyl–ene cyclizations, I focused on the construction of six-membered all carbon rings and aimed at an entioselective access to menthol. The initial results demonstrated that the chiral pockets of imidodiphosphates (IDPs) were not compact enough to differentiate and minimize the transition states of six membered rings, so that moderate enantioselectivity was achieved (Scheme 6.1a). Later, using newly developed imino-imidodiphosphates (*i*IDPs) as catalysts, high enantio- and diastereoselectivity were achieved (Scheme 6.1a). However the reaction time is relatively long. High diastereoselectivity was also obtained using (*R*)-citronellal as the substrate after 7 days (Scheme 6.1b). On the basis of these initial results, we presumed that chiral Brønsted acids would enable a highly enantioselective intramolecular carbonyl–ene cyclization to construct optically active six-membered cyclic compounds.

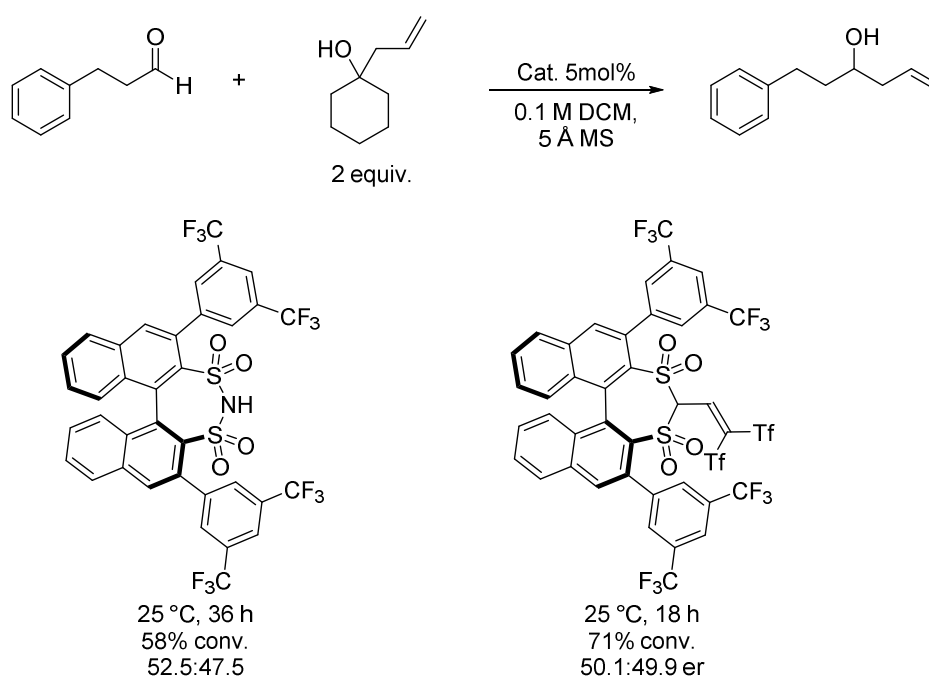


Scheme 6.1 Brønsted acid-catalyzed asymmetric carbonyl–ene cyclization.

6 OUTLOOK

6.2 An Organocatalytic Asymmetric Allylation of Aldehydes

Encouraged by the success of the asymmetric Prins cyclization in our laboratory, we hypothesized an asymmetric allylation of aldehydes via *oxa*-Cope rearrangement between aldehydes and tertiary homoallylic alcohols (Scheme 6.2). Gratifying, the desired product could be obtained with stronger Brønsted acids disulfonimide (DSI) and binaphthyl-allyl-tetrasulfones C–H acid (BALT), even though enantioselectivities were poor. Presumably, a highly enantioselective *oxa*-Cope rearrangement could be achieved with the development of new types of chiral Brønsted acids.



Scheme 6.2 Catalytic asymmetric allylation of aldehydes.

7 EXPERIMENTAL PART

7.1 General Experimental Conditions

Solvents and Reagents

All solvents were obtained by distillation over appropriate drying agent and then kept under an atmosphere of argon with the help of technicians in our laboratory: diethyl ether, tetrahydrofuran, toluene, cyclohexane, methylcyclohexane and methylcyclohexane (sodium), chloroform, dichloromethane, triethylamine (calcium hydride), ethanol (magnesium), 1,4-dioxane, MTBE, di(*n*-butyl)ether, DMF, acetonitrile, and DMSO were purchased from Sigma-Aldrich and used as received. Aldehydes were distilled and stored under argon in flame-dried Schlenk flasks prior to use. Other commercial reagents were purchased from different commercial suppliers and used without further purification unless indicated.

Inert Gas Atmosphere

Air and moisture-sensitive reactions were conducted in flame-dried round-bottom or Schlenk flasks under argon atmosphere. Argon was obtained from *Air Liquide* with higher than 99.5% purity.

Thin Layer Chromatography (TLC) and Preparative Thin Layer Chromatography

Silica gel pre-coated plastic sheets (Polygram SIL G/UV₂₅₄, 0.2 mm, with fluorescent indicator; Macherey-Nagel) plastic sheets or silica gel pre-coated glass plates SIL G-25 UV₂₅₄ and SIL G-100 UV₂₅₄ with 0.25 mm and 1.0 mm SiO₂ layers (Macherey-Nagel) were used. The visualization was accomplished by irradiation with UV-light ($\lambda = 254$ nm or 366 nm) and/or by staining reagents. Phosphomolybdic acid (PMA) stain: PMA (10 g) was dissolved in EtOH (100 mL). Anisaldehyde stain: Anisaldehyde (0.5 mL) and glacial acetic acid (10 mL) were dissolved in MeOH (85 mL), then concentrated H₂SO₄ (5.0 mL) was added carefully to the mixture.

7 EXPERIMENTAL PART

Flash Column Chromatography

Column chromatography was performed under Merck silica gel (60 Å, 230–400 mesh, particle size 0.040–0.063 mm) or aluminum oxide (neutral, activated, Brockmann I, Sigma-Aldrich) using technical grade solvents. Elution was accelerated using compressed air.

Nuclear Magnetic Resonance Spectroscopy (NMR)

Proton and carbon NMR spectra were recorded on Bruker AV-500, Bruker AV-400 or Bruker AV-300 spectrometer in deuterated solvents. Proton chemical shifts are reported in ppm (δ) relative to tetramethylsilane (TMS) with the solvent resonance employed as the internal standard (CDCl_3 δ 7.26 ppm; CD_2Cl_2 δ 5.32 ppm). Data are reported as follows: chemical shift, multiplicity (s = singlet, d = doublet, t = triplet, q = quartet, p = pentet, s = sextet, h = heptet, m = multiplet, br = broad), coupling constants (Hz) and integration. ^{13}C chemical shifts are reported in ppm from tetramethylsilane (TMS) with the solvent resonance as the internal standard (CDCl_3 δ 77.16 ppm; CD_2Cl_2 δ 53.84 ppm). ^{15}N , ^{19}F , and ^{31}P NMR spectra were referenced in ppm from MeNO_2 , CCl_3F , and H_3PO_4 , respectively.

High Pressure Liquid Chromatography (HPLC)

Shimadzu LC-20AD liquid chromatograph (SIL-20AC auto sampler, CMB-20A communication bus module, DGU-20A5 degasser, CTO-20AC column oven, SPD-M20A diode array detector), Shimadzu LC-20AB liquid chromatograph (SIL-20ACHT auto sampler, DGU-20A5 degasser, CTO-20AC column oven, SPD-M20A diode array detector), or Shimadzu LC-20AB liquid chromatograph (reversed phase, SIL-20ACHT auto sampler, CTO-20AC column oven, SPD-M20A diode array detector) using Daicel columns with a chiral stationary phase. All solvents used were HPLC-grade solvents purchased from Sigma-Aldrich. The enantiomeric ratios were determined by comparing the samples with the appropriate racemic mixtures. The enantiomeric ratios of chiral molecules were determined using corresponding chiral columns. Detail conditions are given in the individual experiment.

7 EXPERIMENTAL PART

Gas Chromatography (GC)

Gas chromatography (GC) was performed on HP 6890 and 5890 Series instruments (carrier gas: hydrogen) equipped with a split-mode capillary injection system and a flame ionization detector (FID). The enantiomeric ratios were determined by comparing the samples with the appropriate racemic mixtures. The enantiomeric ratios of chiral molecules were determined using corresponding chiral columns. Detail conditions are given in the individual experiment.

Mass Spectrometry (MS)

Electron impact (EI) mass spectrometry (MS) was performed on a Finnigan MAT 8200 (70 eV) or MAT 8400 (70 eV) spectrometer. Electrospray ionization (ESI) mass spectrometry was conducted on a Bruker ESQ 3000 spectrometer. High resolution mass spectrometry (HRMS) was performed on a Finnigan MAT 95 (EI) or Bruker APEX III FTMS (7T magnet, ESI). The ionization method and mode of detection employed is indicated for the respective experiment and all masses are reported in atomic units per elementary charge (m/z) with an intensity normalized to the most intense peak.

Specific Rotation ($[\alpha]$)

Optical rotations were measured with a Rudolph RA Autopol IV Automatic Polarimeter at 20 or 25 °C with a sodium lamp (sodium D line, $\lambda = 589$ nm). Measurements were performed in an acid resistant 1 mL cell (50 mm length) with concentrations (g/(100 mL)) reported in the corresponding solvent .

X-Ray Crystallography

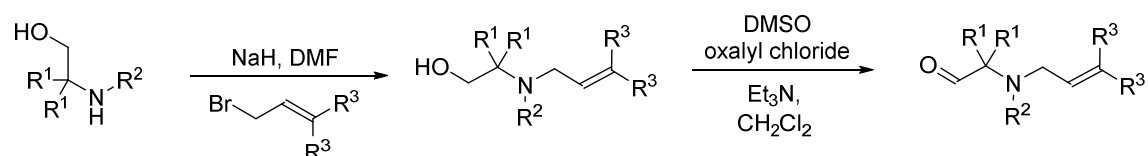
The crystals were grown as specified in the synthetic protocol. X-ray crystal structure analyses were performed on a Bruker-AXS Kappa Mach2 APEX-II diffractometer, equipped with an Incoatec Microfocus λ Mo radiation X-ray source. Data were face-indexed absorption corrected and scaled using the program SADABS (Bruker AXS, 2014). The structure was refined using the programs SHELXS and SHELXL, both programs from G. M. Sheldrick (Göttingen, 2014). The X-ray crystal structure analyses were performed by the X-ray department of the Max-Planck-Institut für Kohlenforschung.

7 EXPERIMENTAL PART

7.2 Organocatalytic Asymmetric Carbonyl–Ene Cyclization

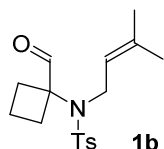
7.2.1 Substrates Synthesis

Synthesis of **1b-1f** and **1h**



General procedure: The corresponding aminoalcohol compound (1 equiv.) was dissolved in DMF (0.5 M), and NaH (60% dispersion in mineral oil, 1 equiv.) was added portionwise at 0 °C under argon atmosphere. The bubbling solution was stirred for 30 min at room temperature before allyl bromide (1.1 equiv) was added. The solution was stirred at room temperature until full consumption of the starting material. After the addition of H₂O, the aqueous phase was extracted with CH₂Cl₂. The combined organic layers were washed with H₂O, brine and dried by Na₂SO₄, then concentrated with a rotary evaporator. The crude mixture was purified by column chromatography on silica gel using EtOAc/hexane as the eluent. The obtained alcohol was used for the next Swern oxidation step. To a solution of DMSO (2.6 equiv.) in CH₂Cl₂ (0.5 M) at –78°C was added oxalyl chloride (1.3 equiv.). After 30 min, the solution of alcohol (1 equiv) in CH₂Cl₂ (1.0 M) was added. After another 30 min, triethylamine (6 equiv.) was added. The cold bath was removed and the reaction was quenched by the addition of H₂O. The reaction mixture was extracted with CH₂Cl₂ and the combined organic layer was washed with H₂O, brine and dried over Na₂SO₄, then concentrated with a rotary evaporator. The desired aldehyde was purified by column chromatography on silica gel using EtOAc/hexane as the eluent.

7 EXPERIMENTAL PART



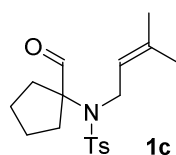
N-(1-Formylcyclobutyl)-4-methyl-*N*-(3-methylbut-2-en-1-yl)benzenesulfonamide.

Prepared according to general procedure. White solid, 54%.

¹H NMR (300 MHz, CD₂Cl₂): δ 9.68 (s, 1H), 7.70 (d, *J* = 8.3 Hz, 2H), 7.34 (d, *J* = 8.0 Hz, 2H), 7.30 (d, *J* = 8.0 Hz, 2H), 5.11 (app. t, *J* = 6.8 Hz, 1H), 3.91 (d, *J* = 6.8 Hz, 2H), 2.43 (s, 3H), 2.37–2.20 (m, 4H), 1.88–1.68 (m, 2H), 1.67 (d, *J* = 1.1 Hz, 3H), 1.60 (s, 3H).

¹³C NMR (75 MHz, CD₂Cl₂): δ 199.8, 144.0, 139.7, 136.8, 130.1, 127.4, 121.4, 68.6, 44.7, 29.3, 25.8, 21.7, 18.0, 14.3.

HRMS (ESI+) (*m/z*): calculated for C₁₇H₂₃N₁O₃S₁Na₁ [M+Na]⁺: 344.129085; found: 344.129100.



N-(1-Formylcyclopentyl)-4-methyl-*N*-(3-methylbut-2-en-1-yl)benzenesulfonamide.

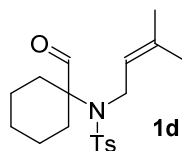
Prepared according to general procedure. White solid, 50%.

¹H NMR (500 MHz, CD₂Cl₂): δ 9.60 (s, 1H), 7.70 (d, *J* = 8.3 Hz, 2H), 7.32 (d, *J* = 8.1 Hz, 2H), 5.15 (app. t, *J* = 6.2 Hz, 1H), 3.90 (d, *J* = 6.2 Hz, 2H), 2.42 (s, 3H), 2.10–2.05 (m, 2H), 1.78–1.73 (m, 2H), 1.67 (d, *J* = 1.1 Hz, 3H), 1.59 (s, 3H), 1.57–1.51 (m, 4H).

¹³C NMR (126 MHz, CD₂Cl₂): δ 198.0, 144.2, 138.3, 134.9, 130.0, 128.0, 122.5, 77.1, 45.1, 32.5, 25.7, 24.0, 21.6, 18.0.

HRMS (ESI+) (*m/z*): calculated for C₁₈H₂₅N₁O₃S₁Na₁ [M+Na]⁺: 358.144735; found: 358.144700.

7 EXPERIMENTAL PART



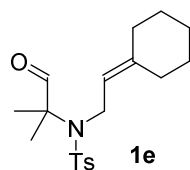
N-(1-Formylcyclohexyl)-4-methyl-*N*-(3-methylbut-2-en-1-yl)benzenesulfonamide.

Prepared according to general procedure. White solid, 73%.

¹H NMR (500 MHz, CDCl₃): δ 9.69 (s, 1H), 7.72 (d, *J* = 8.3 Hz, 2H), 7.28 (d, *J* = 8.3 Hz, 2H), 5.15 (app. t, *J* = 6.2 Hz, 1H), 3.84 (d, *J* = 6.2 Hz, 2H), 2.41 (s, 3H), 2.17 (d, *J* = 13.4 Hz, 2H), 1.69 (td, *J* = 12.6, 3.8 Hz, 2H), 1.64 (s, 3H), 1.60–1.49 (m, 8H), 1.17–1.07 (m, 1H).

¹³C NMR (126 MHz, CDCl₃): δ 200.0, 143.4, 138.1, 133.8, 129.5, 127.8, 122.6, 68.8, 43.4, 31.1, 25.6, 24.8, 22.5, 21.5, 17.8.

HRMS (ESI+) (*m/z*): calculated for C₁₉H₂₇N₁O₃S₁Na₁ [M+Na]⁺: 372.160386; found: 372.160520.



N-(2-Cyclohexylideneethyl)-4-methyl-*N*-(2-methyl-1-oxopropan-2-yl)benzenesulfonamide.

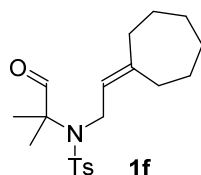
Prepared according to general procedure. White solid, 41%.

¹H NMR (500 MHz, CD₂Cl₂): δ 9.60 (s, 1H), 7.75 (d, *J* = 8.3 Hz, 2H), 7.34 (d, *J* = 8.0 Hz, 2H), 5.05 (app. t, *J* = 6.5 Hz, 1H), 3.83 (d, *J* = 6.5 Hz, 2H), 2.42 (s, 3H), 2.05 (td, *J* = 24, 6.1 Hz, 4H), 1.52–1.43 (m, 6H), 1.36 (s, 6H).

¹³C NMR (126 MHz, CD₂Cl₂): δ 198.8, 144.4, 142.3, 137.8, 130.0, 128.3, 119.1, 67.3, 42.8, 37.2, 29.0, 28.5, 27.5, 26.9, 22.4, 21.6.

HRMS (ESI+) (*m/z*): calculated for C₁₉H₂₇N₁O₃S₁Na₁ [M+Na]⁺: 372.160385; found: 372.160090.

7 EXPERIMENTAL PART



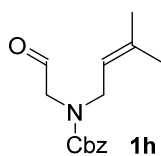
N-(2-Cycloheptylideneethyl)-4-methyl-*N*-(2-methyl-1-oxopropan-2-yl)benzenesulfonamide.

Prepared according to general procedure. White solid, 42%.

¹H NMR (500 MHz, CD₂Cl₂): δ 9.63 (s, 1H), 7.77 (d, *J* = 8.3 Hz, 2H), 7.36 (d, *J* = 8.0 Hz, 2H), 5.10 (app. t, *J* = 6.0 Hz, 1H), 3.83 (d, *J* = 6.0 Hz, 2H), 2.45 (s, 3H), 2.16–2.12 (m, 4H), 1.52–1.47 (m, 8H), 1.36 (s, 6H).

¹³C NMR (126 MHz, CD₂Cl₂): δ 198.8, 144.4, 143.9, 137.7, 130.0, 128.3, 122.7, 67.3, 43.2, 37.8, 30.5, 30.1, 29.7, 29.4, 27.0, 22.4, 21.6.

HRMS (ESI+) (*m/z*): calculated for C₂₀H₂₉N₁O₃S₁Na₁ [M+Na]⁺: 386.176035; found: 386.176120.



Benzyl (3-methylbut-2-en-1-yl)(2-oxoethyl)carbamate.

Prepared according to general procedure. White oil, 46%.

The NMR signals are reported as observed . The signals belong to two different rotamers.

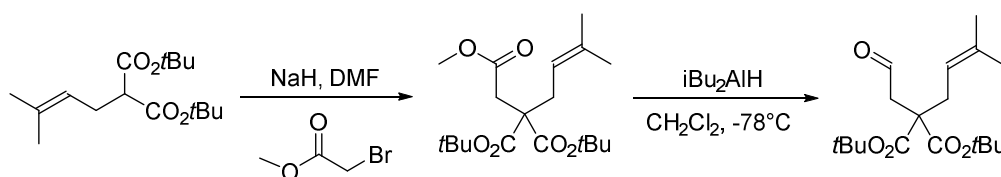
¹H NMR (500 MHz, CD₂Cl₂): δ 9.53–9.52 (m, 1H), 7.38–7.29 (m, 5H), 5.16–5.10 (m, 3H), 3.99–3.91 (m, 4H), 1.71–1.72 (m, 3H), 1.64–1.57 (m, 3H).

¹³C NMR (75 MHz, CD₂Cl₂): δ 199.2, 156.8, 156.1, 138.1, 137.5, 137.2, 136.2, 128.9, 128.4, 128.2, 120.5, 119.7, 119.6, 67.8, 57.0, 56.3, 46.2, 25.8, 18.0, 17.9.

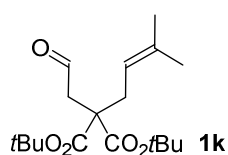
HRMS (ESI+) (*m/z*): calculated for C₁₅H₁₉ N₁O₃Na₁ [M+Na]⁺: 284.125713; found: 284.125770.

7 EXPERIMENTAL PART

Synthesis of **1k**



General procedure: To a solution of di-*tert*-butyl-malonate (4 mL, 15 mmol) in DMF (75 mL), sodium hydride (719 mg, 18 mmol) was added at 0°C . After stirring for one hour, 10 mmol of methylbromacetate was added to this reaction mixture. The reaction was stirred at r.t. for 6 h, then was diluted with 30 mL a.q. NaHCO_3 and extracted by 2 x 90 mL MTBE. The organic layer was rinsed with H_2O (2 x 150 mL) and brine (2 x 150 mL), then dried over Na_2SO_4 , filtered, and concentrated *in vacuo*. The product was isolated by flash chromatography (2–5% ethyl acetate/hexanes) as a colorless and viscous oil (780 mg, 2.19 mmol, 44% yield). To a solution of 2,2-di-*tert*-butyl 1-methyl 5-methylhex-4-ene-1,2,2-tricarboxylate (749 mg, 2.1 mmol) in CH_2Cl_2 (20 mL, 0.1 M), diisobutylaluminum hydride (4.6 mL, 4.6 mmol, 1M in hexane) was added at -78°C . The reaction mixture was stirred for 4 h at -78°C . The reaction was quenched by adding 0.1 mL H_2O , 0.1 mL 15% aqueous NaOH, and 0.4 mL H_2O waiting 5 minutes between each addition. The resulting suspension was carefully dried over Mg_2SO_4 and filtered, rinsed with CH_2Cl_2 then concentrated with a rotary evaporator. The product was obtained by flash chromatography (hexane/ether = 95/5) as an clear oil (200 mg, 0.61 mmol, 29% yield).



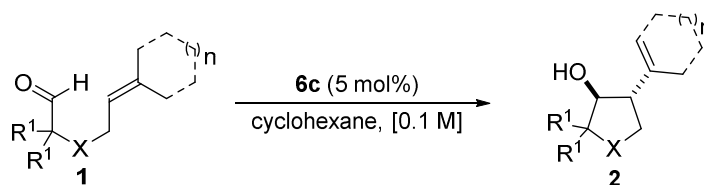
Di-*tert*-butyl 2-(3-methylbut-2-en-1-yl)-2-(2-oxoethyl)malonate.

$^1\text{H NMR}$ (500 MHz, CD_2Cl_2): δ 9.68 (t, $J = 2.0$ Hz, 1H), 5.0 (app. t, $J = 7.8$ Hz, 1H), 2.72 (d, $J = 2.0$ Hz, 2H), 2.59 (d, $J = 7.7$ Hz, 2H), 1.69 (d, $J = 0.9$ Hz, 3H), 1.59 (s, 3H), 1.43 (s, 18H).

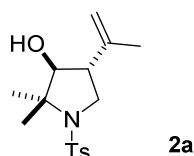
$^{13}\text{C NMR}$ (126 MHz, CD_2Cl_2): δ 200.3, 169.8, 136.5, 118.3, 82.4, 56.5, 46.7, 33.0, 27.9, 26.1, 18.2. **HRMS** (ESI+) (m/z): calculated for $\text{C}_{18}\text{H}_{30}\text{O}_5\text{Na}_1$ $[\text{M}+\text{Na}]^+$: 349.198544; found: 349.19841.

7 EXPERIMENTAL PART

7.2.2 Products



Unless specified otherwise, aldehyde **1** (0.1 mmol) was added to catalyst **6d** (0.005 mmol, 5 mol%) in cyclohexane (0.1 M). The mixture was stirred vigorously at room temperature. Purification was performed by column chromatography or preparative thin layer chromatography on silica gel using EtOAc/hexane as the eluent.



(3*S*,4*R*)-2,2-Dimethyl-4-(prop-1-en-2-yl)-1-tosylpyrrolidin-3-ol.

Prepared according to general procedure. 30.0 mg white solid, 97%.

¹H NMR (500 MHz, CDCl₃): δ 7.73 (d, *J* = 8.3 Hz, 2H), 7.29 (d, *J* = 8.1 Hz, 2H), 4.92 (t, *J* = 1.4 Hz, 1H), 4.89 (s, 1H), 3.63 (d, *J* = 10.4 Hz, 1H), 3.57 (t, *J* = 9.1 Hz, 1H), 3.06 (t, *J* = 10.1 Hz, 1H), 2.62 (q, *J* = 10.2 Hz, 1H), 2.41 (s, 3H), 1.71 (s, 3H), 1.50 (s, 3H), 1.27 (s, 3H).

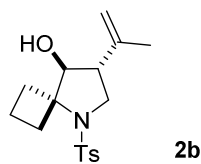
¹³C NMR (126 MHz, CDCl₃): δ 143.0, 141.3, 138.2, 129.5, 127.2, 113.9, 80.4, 65.9, 48.6, 48.1, 26.5, 21.6, 21.5, 19.8.

HRMS (ESI+) (*m/z*): calculated for C₁₆H₂₃N₁O₃S₁Na₁ [M+Na]⁺: 332.129130; found: 332.129085.

HPLC The enantiomeric ratio was measured by HPLC analysis using Chiralpak AS-3R, CH₃CN/ H₂O = 35:65, Flow rate = 1.0 mL/min, λ = 220 nm, t_R = 17.7 min (minor) and t_R = 18.9 min (major). er = 97.5:2.5.

[α]_D²⁵ = -19.1 (*c* 0.70, CH₂Cl₂).

7 EXPERIMENTAL PART



(7*R*,8*S*)-7-(prop-1-en-2-yl)-5-tosyl-5-azaspiro[3.4]octan-8-ol.

Prepared according to general procedure. 26 mg white solid, 81%.

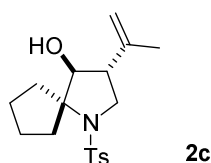
¹H NMR (500 MHz, CDCl₃): δ 7.73 (d, *J* = 8.3 Hz, 2H), 7.30 (d, *J* = 7.5 Hz, 2H), 4.92–4.90 (m, 2H), 3.84 (d, *J* = 8.7 Hz, 1H), 3.60 (dd, *J* = 9.6, 8.2 Hz, 1H), 3.19–3.13 (m, 2H), 2.65–2.61 (m, 1H), 2.52 (q, *J* = 8.6 Hz, 1H), 2.42 (s, 3H), 2.29–2.23 (m, 1H), 2.09–2.03 (m, 1H), 1.82 (tq, *J* = 10.8, 3.6 Hz, 1H), 1.72 (s, 3H), 1.70–1.64 (m, 1H).

¹³C NMR (126 MHz, CDCl₃): δ 143.1, 141.1, 138.2, 129.7, 126.9, 113.7, 79.8, 67.7, 49.3, 49.0, 32.5, 29.9, 21.5, 20.3, 13.5.

HRMS (ESI+) (*m/z*): calculated for C₁₇H₂₃N₁O₃S₁Na₁ [M+Na]⁺: 344.129085; found: 344.128960.

HPLC The enantiomeric ratio was measured by Heart-Cut HPLC analysis using Chiralpak OJ-3R, CH₃CN/ H₂O = 40:60, Flow rate = 1.0 mL/min, λ = 220 nm, *t_R* = 9.3 min (major) and *t_R* = 10.8 min (minor). er = 97:3.

[α]_D²⁵ = −8.8 (*c* 0.80, CH₂Cl₂).



(3*R*,4*S*)-3-(Prop-1-en-2-yl)-1-tosyl-1-azaspiro[4.4]nonan-4-ol.

Prepared according to general procedure. 27.8 mg white solid, 83%.

¹H NMR (500 MHz, CDCl₃): δ 7.72 (d, *J* = 8.3 Hz, 2H), 7.30 (d, *J* = 8.1 Hz, 2H), 4.92–4.91 (m, 1H), 4.89–4.88 (m, 1H), 3.78 (d, *J* = 10.0 Hz, 1H), 3.58 (t, *J* = 9.1 Hz, 1H), 3.10 (t, *J* = 9.9 Hz, 1H), 2.62–2.52 (m, 2H), 2.42 (s, 3H), 2.02–1.89 (m, 3H), 1.86–1.79 (m, 1H), 1.71 (s, 3H), 1.69–1.58 (m, 3H), 1.53–1.45 (m, 1H).

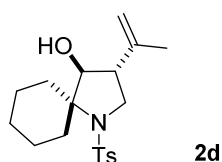
7 EXPERIMENTAL PART

^{13}C NMR (126 MHz, CDCl_3): δ 143.0, 141.3, 138.3, 129.6, 127.1, 113.9, 81.2, 75.7, 49.6, 48.7, 36.7, 33.3, 25.9, 25.3, 21.5, 19.9.

HRMS (ESI+) (m/z): calculated for $\text{C}_{18}\text{H}_{25}\text{N}_1\text{O}_3\text{S}_1\text{Na}_1$ $[\text{M}+\text{Na}]^+$: 358.144735; found: 358.144700.

HPLC The enantiomeric ratio was measured by Heart-Cut HPLC analysis using Chiralpak OJ-3R, $\text{CH}_3\text{CN}/\text{H}_2\text{O} = 40:60$, Flow rate = 1.0 mL/min, $\lambda = 220$ nm, $t_{\text{R}} = 15.2$ min (minor) and $t_{\text{R}} = 15.5$ min (major). er = 95.5:4.5.

$[\alpha]_{\text{D}}^{25} = -11.6$ (c 0.78, CH_2Cl_2).



(3R,4S)-3-(prop-1-en-2-yl)-1-tosyl-1-azaspiro[4.5]decan-4-ol.

The reaction was performed at 10°C for 5 days. 27.0 mg white solid, 77%.

^1H NMR (500 MHz, CDCl_3): δ 7.73 (d, $J = 8.3$ Hz, 2H), 7.28 (d, $J = 8.0$ Hz, 2H), 4.91–4.89 (m, 1H), 4.89–4.88 (m, 1H), 4.00 (d, $J = 7.0$ Hz, 1H), 3.55 (dd, $J = 9.7, 7.8$ Hz, 1H), 3.24 (dd, $J = 9.7, 8.9$ Hz, 1H), 2.62 (q, $J = 7.9$ Hz, 1H), 2.41 (s, 3H), 2.27–2.39 (m, 2H), 1.91 (d, $J = 12.1$ Hz, 1H), 1.74 (s, 3H), 1.70–1.61 (m, 6H), 1.44 (tq, $J = 13.4, 3.2$ Hz, 1H), 1.33–1.27 (m, 1H).

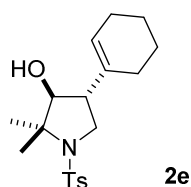
^{13}C NMR (126 MHz, CDCl_3): δ 142.8, 141.7, 138.7, 129.5, 127.2, 113.2, 81.1, 70.2, 51.2, 48.4, 36.4, 31.7, 24.7, 23.9, 23.7, 21.5, 20.7.

HRMS (ESI+) (m/z): calculated for $\text{C}_{19}\text{H}_{27}\text{N}_1\text{O}_3\text{S}_1\text{Na}_1$ $[\text{M}+\text{Na}]^+$: 372.160386; found: 372.160520.

HPLC The enantiomeric ratio was measured by Heart-Cut HPLC analysis using Chiralpak OJ-3R, $\text{CH}_3\text{CN}/\text{H}_2\text{O} = 50:50$, Flow rate = 1.0 mL/min, $\lambda = 220$ nm, $t_{\text{R}} = 38.4$ min (minor) and $t_{\text{R}} = 38.9$ min (major). er = 95:5.

$[\alpha]_{\text{D}}^{25} = -1.8$ (c 0.33, CH_2Cl_2).

7 EXPERIMENTAL PART



(3*S*,4*R*)-4-(Cyclohex-1-en-1-yl)-2,2-dimethyl-1-tosylpyrrolidin-3-ol.

Prepared according to general procedure. 28.0 mg white solid, 80%.

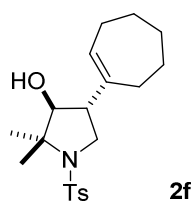
¹H NMR (500 MHz, CDCl₃): δ 7.72 (d, *J* = 7.0 Hz, 2H), 7.28 (d, *J* = 8.5 Hz, 2H), 5.61 (br. s, 1H), 3.63 (d, *J* = 10.4 Hz, 1H), 3.55 (t, *J* = 9.5 Hz, 1H), 3.01 (dt, *J* = 10.6, 1.2 Hz, 1H), 2.51 (q, *J* = 9.8 Hz, 1H), 2.41 (s, 3H), 2.00 (d, *J* = 1.6 Hz, 2H), 1.89 (br. s, 2H), 1.72 (br. s, 1H), 1.64–1.55 (m, 4H), 1.49 (s, 3H), 1.27 (s, 3H).

¹³C NMR (126 MHz, CDCl₃): δ 142.8, 138.3, 133.3, 129.5, 127.2, 125.3, 79.9, 65.8, 49.0, 48.1, 26.6, 25.6, 25.2, 22.7, 22.3, 21.5, 21.4.

HRMS (ESI+) (*m/z*): calculated for C₁₉H₂₇N₁O₃S₁Na₁ [M+Na]⁺: 372.160385; found: 372.160500.

HPLC The enantiomeric ratio was measured by HPLC analysis using Chiralpak AS-3R, CH₃CN/ H₂O = 70:30, Flow rate = 1.0 mL/min, λ = 220 nm, t_R = 3.4 min (major) and t_R = 3.7 min (minor). er = 92:8.

[α]_D²⁵ = -15.3 (*c* 0.34, CH₂Cl₂).



(3*S*,4*R*)-4-(Cyclohept-1-en-1-yl)-2,2-dimethyl-1-tosylpyrrolidin-3-ol.

Prepared according to general procedure. 35.0 mg white solid, 96%.

¹H NMR (500 MHz, CDCl₃): δ 7.73 (d, *J* = 8.3 Hz, 2H), 7.29 (d, *J* = 8.0 Hz, 2H), 5.77 (t, *J* = 6.6 Hz, 1H), 3.55 (d, *J* = 10.2 Hz, 1H), 3.48 (t, *J* = 9.3 Hz, 1H), 3.02 (t, *J* = 9.9 Hz, 1H), 2.52 (q, *J* = 9.8 Hz, 1H), 2.42 (s, 3H), 2.11 (q, *J* = 6.5 Hz, 2H), 2.05 (dd, *J* = 5.8, 4.1 Hz, 2H), 1.77–1.72 (m, 3H), 1.63 (br. s, 1H), 1.50 (s, 3H), 1.48–1.40 (m, 4H), 1.23 (s, 3H).

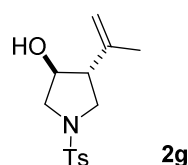
7 EXPERIMENTAL PART

^{13}C NMR (126 MHz, CDCl_3): δ 142.9, 140.0, 138.3, 131.5, 129.5, 127.2, 79.8, 65.6, 51.0, 47.9, 32.7, 28.8, 28.3, 27.1, 26.9, 26.7, 21.5, 21.1.

HRMS (ESI+) (m/z): calculated for $\text{C}_{20}\text{H}_{29}\text{N}_1\text{O}_3\text{S}_1\text{Na}_1$ $[\text{M}+\text{Na}]^+$: 386.176035; found: 386.175930.

HPLC The enantiomeric ratio was measured by HPLC analysis using Chiralpak OJ-3R, $\text{CH}_3\text{CN}/\text{H}_2\text{O} = 50:50$, Flow rate = 1.0 mL/min, $\lambda = 220$ nm, $t_{\text{R}} = 9.2$ min (major) and $t_{\text{R}} = 9.9$ min (minor). er = 95.5:4.5.

$[\alpha]_{\text{D}}^{25} = -23.4$ (c 1.0, CH_2Cl_2).



(3*S*,4*R*)-4-(Prop-1-en-2-yl)-1-tosylpyrrolidin-3-ol.

The reaction was performed at room temperature for 3 days then at 50 °C for 2 days in the presence of 6d (7.5 mol%). 24.0 mg white solid, 85%. Running the reaction at 50 °C from the start gave lower enantioselectivity.

^1H NMR (500 MHz, CDCl_3): δ 7.74 (d, $J = 8.3$ Hz, 2H), 7.34 (d, $J = 7.9$ Hz, 2H), 4.84–4.83 (m, 1H), 4.75–4.73 (m, 1H), 4.10 (p, $J = 5.0$ Hz, 1H), 3.60 (dd, $J = 10.4$, 6.1 Hz, 1H), 3.52 (dd, $J = 10.1$, 8.1 Hz, 1H), 3.21 (dd, $J = 10.1$, 7.4 Hz, 1H), 3.12 (dd, $J = 10.4$, 5.5 Hz, 1H), 2.55 (q, $J = 7.3$ Hz, 1H), 2.44 (s, 3H), 1.69 (s, 3H).

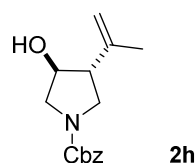
^{13}C NMR (126 MHz, CDCl_3): δ 143.7, 141.6, 133.6, 129.74, 129.73, 127.6, 112.9, 73.1, 54.0, 53.4, 49.7, 21.5, 20.7.

HRMS (ESI+) (m/z): calculated for $\text{C}_{14}\text{H}_{19}\text{N}_1\text{O}_3\text{S}_1\text{Na}_1$ $[\text{M}+\text{Na}]^+$: 304.097786; found: 304.097580.

HPLC The enantiomeric ratio was measured by HPLC analysis using Chiralpak OJ-3R, $\text{CH}_3\text{CN}/\text{H}_2\text{O} = 25:75$, Flow rate = 1.0 mL/min, $\lambda = 220$ nm, $t_{\text{R}} = 22.8$ min (major) and $t_{\text{R}} = 25.4$ min (minor). er = 98:2.

$[\alpha]_{\text{D}}^{25} = -13.0$ (c 1.0, CH_2Cl_2).

7 EXPERIMENTAL PART



Benzyl (3*S*,4*R*)-3-hydroxy-4-(prop-1-en-2-yl)pyrrolidine-1-carboxylate.

The reaction was performed at room temperature for 3 days then at 50 °C for 8 days in the presence of 6d (7.5 mol%). 19.0 mg White solid, 73%.

The NMR signals of major diastereomer are reported as observed . The signals belong to two different rotamers (ratio ~ 1:1).

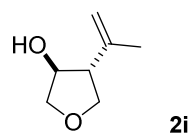
¹H NMR (500 MHz, CDCl₃): δ 7.36–7.31 (m, 5H), 5.13 (s, 2H), 4.90 (d, *J* = 3.6 Hz, 1H), 4.84 (d, *J* = 11.8 Hz, 1H), 4.23 (ddd, *J* = 12.1, 6.1, 2.2 Hz, 1H), 3.77–3.86 (m, 2H), 3.42–3.36 (m, 1H), 3.33–3.27 (m, 1H), 2.68 (s, *J* = 8.8 Hz, 1H), 2.30 (br. s, 1H), 1.76 (s, 3H).

¹³C NMR (126 MHz, CDCl₃): δ 154.9, 142.3, 142.2, 136.8, 128.5, 128.0, 127.9, 127.8, 112.6, 112.5, 73.1, 72.4, 66.9, 66.8, 53.1, 52.6, 52.5, 52.2, 48.2, 48.0, 23.0, 21.0, 20.9.

HRMS (ESI+) (*m/z*): calculated for C₁₅H₁₉N₁O₃Na₁ [M+Na]⁺: 284.125713; found: 284.125710.

HPLC The enantiomeric ratio was measured by Heart-Cut HPLC analysis using Chiralpak OJ-3R , CH₃CN/ H₂O = 70:30, Flow rate = 1.0 mL/min, λ = 220 nm, t_R = 17.1 min (major) and t_R = 17.8 min (minor). er = 98:2.

[α]_D²⁵ = -8.6 (*c* 0.95, CH₂Cl₂).



(3*S*,4*R*)-4-(Prop-1-en-2-yl)tetrahydrofuran-3-ol.

The reaction was performed under neat condition. White oil, 78% NMR yield using 1,1,2,2-tetrachloroethane used as internal standard.

¹H NMR (500 MHz, CD₂Cl₂): δ 4.84–4.83 (m, 1H), 4.81–4.80 (m, 1H), 4.29–4.26 (m, 1H), 4.05 (dd, *J* = 9.2, 7.5 Hz, 1H), 3.90 (dd, *J* = 9.6, 5.3 Hz, 1H), 3.68 (dd, *J* = 8.8, 6.3

7 EXPERIMENTAL PART

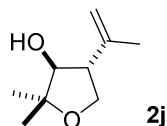
Hz, 1H), 3.65 (dd, $J = 9.5, 3.2$ Hz, 1H), 2.69 (dt, $J = 6.8, 3.8$ Hz, 1H), 1.93 (d, $J = 5.0$ Hz, 1H), 1.77 (t, $J = 1.1$ Hz, 3H).

^{13}C NMR (126 MHz, CD_2Cl_2): δ 144.1, 111.5, 76.4, 75.1, 71.3, 56.2, 21.5.

HRMS (ESI+) (m/z): calculated for $\text{C}_7\text{H}_{12}\text{O}_2\text{Na}_1$ $[\text{M}+\text{Na}]^+$: 151.072949; found: 151.073020.

GC The enantiomeric ratio was measured by GC analysis on Hydrodex-gamma-TBDAC-CD column: $t_{\text{R}} = 11.1$ min (major) and $t_{\text{R}} = 12.1$ min (minor). er = 97:3.

$[\alpha]_{\text{D}}^{25} = -20$ (c 0.33, CH_2Cl_2).



(3*S*,4*R*)-2,2-Dimethyl-4-(prop-1-en-2-yl)tetrahydrofuran-3-ol.

The reaction was performed under neat condition. 14mg white oil, 90%.

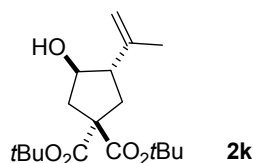
^1H NMR (500 MHz, CDCl_3): δ 4.89–4.87 (m, 2H), 3.96 (t, $J = 8.9$ Hz, 1H), 3.80 (dd, $J = 8.6, 5.1$ Hz, 1H), 3.65 (t, $J = 9.1$ Hz, 1H), 2.83 (q, $J = 9.0$ Hz, 1H), 1.77 (s, 3H), 1.75 (d, $J = 5.4$ Hz, 1H), 1.29 (s, 3H), 1.18 (s, 3H).

^{13}C NMR (126 MHz, CDCl_3): δ 142.6, 112.6, 81.1, 80.9, 66.7, 54.1, 26.6, 21.4, 19.9.

HRMS (ESI+) (m/z): calculated for $\text{C}_9\text{H}_{16}\text{O}_2\text{Na}_1$ $[\text{M}+\text{Na}]^+$: 179.104249; found: 179.104430.

GC The enantiomeric ratio was measured by GC analysis on Hydrodex-BTBDAC-G-589 column: $t_{\text{R}} = 33.0$ min (minor) and $t_{\text{R}} = 36.0$ min (major).

$[\alpha]_{\text{D}}^{25} = -30.5$ (c 0.42, CH_2Cl_2). er = 98:2.



Di-*tert*-butyl (3*R*,4*S*)-3-hydroxy-4-(prop-1-en-2-yl)cyclopentane-1,1-dicarboxylate.

7 EXPERIMENTAL PART

The reaction was performed at room temperature for 3 days then at 50 °C for 2 days in the presence of 6d (7.5 mol%). 26.5 mg white oil, 81%.

¹H NMR (500 MHz, CDCl₃): δ 4.81 (br s, 2H), 4.04 (q, *J* = 7.1 Hz, 1H), 2.52–2.38 (m, 3H), 2.23 (br. s, 1H), 2.09 (dd, *J* = 13.3, 10.8 Hz, 1H), 2.02–1.98(m, 1H), 1.75 (t, *J* = 0.9 Hz, 3H), 1.46 (s, 9H), 1.44 (s, 9H).

¹³C NMR (126 MHz, CDCl₃): δ 172.2, 171.1, 144.4, 111.5, 81.6, 81.3, 74.9, 58.3, 54.8, 41.2, 35.9, 27.8, 20.3.

HRMS (ESI+) (*m/z*): calculated for C₁₈H₃₀O₅Na₁ [M+Na]⁺: 349.198544; found: 349.198320.

GC The enantiomeric ratio was measured by GC analysis on BGB-176/BGB-15-G-618 column: *t_R* = 53.3 min (minor) and *t_R* = 53.8 min (major). er = 98:2.

$[\alpha]_{\text{D}}^{25} = -6.0$ (*c* 0.6, CH₂Cl₂).

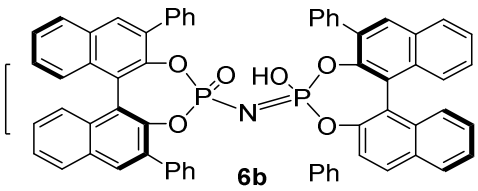
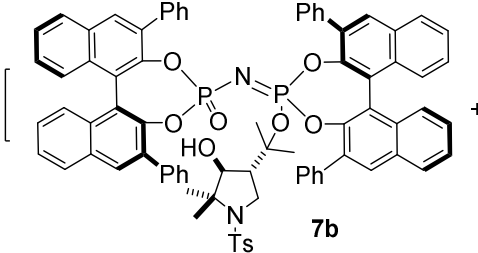
7.2.3 Mechansitic Studies

ESI-MS Studies

In order to elucidate the reaction mechanism, we performed electrospray ionization mass spectroscopy (ESI-MS) studies using the cyclization of olefinic aldehyde **1a** as a model reaction. For this purpose, we carried out two reactions: One experiment was the cyclization of **1a** in the presence of catalytic amounts of catalyst **6b** under the optimized reaction conditions, and the other experiment was performed in the presence of catalytic amounts of catalyst **6c**. General procedure: substrate **1a** (15.5 mg, 0.05mmol) and dry cyclohexane (0.5 mL) were added to a vial, then catalyst **6b** (2.5 mg, 2.5 μ mol) or **6c** (3.3 mg, 2.5 μ mol) were added at 22 °C. Samples of the reaction mixtures were monitored at different time during the initial 24h. The selected spectra Figure S1, Figure S2, and the HRMS data of the catalyst **6b**, **6c**, and intermediate **7b**, **7c** were summarized in Table S1 and Table S2. The ESI-MS obtained revealed the characteristic signals of free catalysts **6b** and **6c**. As soon as substrate **1a**, catalyst **6b** were combined under the optimized reaction conditions, the new peak at m/z 1291.3 could be detected which matches the mass of the covalent the intermediate $[\mathbf{7b} + \text{H}]^+$ generated from substrate **1a** and the corresponding catalyst **6b**. Interestingly, the fact that the intermediate **7b** could be easily detected under the reaction conditions, while the catalyst **6b** remained below the detection limit, suggested that the elimination of catalyst **6b** from **7b** could be the rate-determining step of the whole reaction.

7 EXPERIMENTAL PART

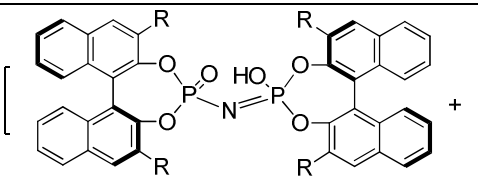
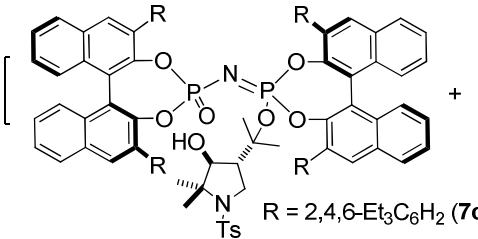
Table 7.1 High-Resolution Mass Data^a

species	formula	HRMS calcd	HRMS found	deviation [ppm]
 6b	$C_{64}H_{42}NO_6P_2$	982.24819	982.24816	0.03
 7b	$C_{80}H_{65}N_2O_9P_2S$	1291.38805	1291.38801	0.03

^aThe reaction was performed using catalyst **6b** (2.45 mg, 2.5 μ mol), **1a** (15.5 mg, 0.05mmol) in dry cyclohexane (0.5 mL) at room temperature and samples of the reaction mixtures were monitored at different time during the initial 24 h.

As soon as substrate **1a**, catalyst **6c** were combined under the optimized reaction conditions, the new peak at m/z 1627.7 could be detected which match the masses of the covalent the intermediate [**7c** + H]⁺ generated from substrate **1a** and the corresponding catalyst **6c**.

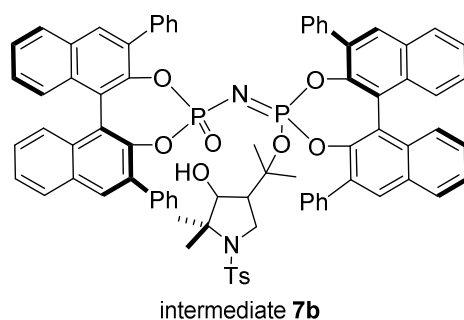
Table 7.2 High-Resolution Mass Data^a

species	formula	HRMS calcd	HRMS found	deviation [ppm]
 R = 2,4,6-Et ₃ C ₆ H ₂ (6c)	$C_{88}H_{90}NO_6P_2$	1318.62379	1318.62370	0.07
 R = 2,4,6-Et ₃ C ₆ H ₂ (7c)	$C_{104}H_{113}N_2O_9P_2S$	1627.76365	1627.76362	0.02

7 EXPERIMENTAL PART

^aThe reaction was performed using catalyst **6c** (3.3 mg, 2.5 μmol), **1a** (15.5 mg, 0.05 mmol) in dry cyclohexane (0.5 mL) at room temperature and samples of the reaction mixtures were monitored at different time during the initial 24 h.

Characterization of Intermediate **7b**

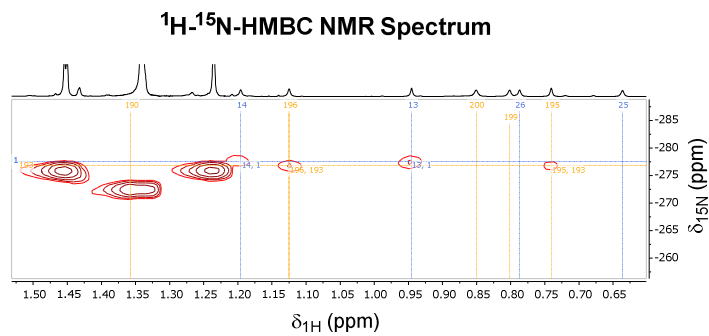
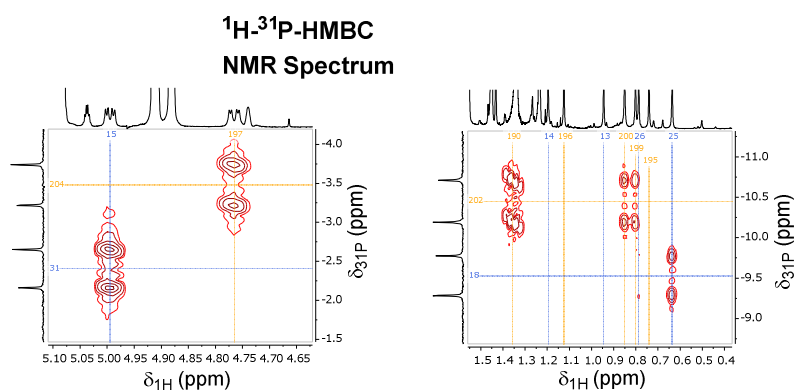
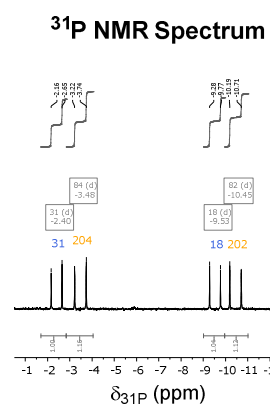
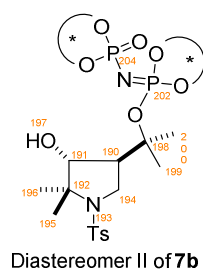
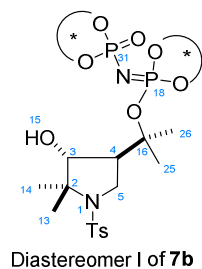


The detected intermediate **7b** were further characterized by ^1H , ^{13}C , ^1H - ^1H NOESY, ^1H - ^{13}C HMBC, ^1H - ^{31}P HMBC and ^1H - ^{15}N HMBC NMR experiments of reaction mixture. The ^{15}N , ^{13}C and ^{31}P spectra of intermediate **7b** were referenced indirectly to the referenced proton frequency with the ϵ -scale with the factors 0.10136767 for ^{15}N ($\delta(\text{MeNO}_2) = 0$ ppm), 0.25145020 for ^{13}C ($\delta(\text{Me}_4\text{Si}) = 0$ ppm) and 0.40480742 for ^{31}P ($\delta(\text{H}_3\text{PO}_0) = 0$ ppm). The ^{15}N chemical shifts were determined from the indirect dimension of a ^1H - ^{15}N HMBC. The absolute configuration of two diastereomers of **7b** was not determined.

HRMS (ESI+) (m/z): calculated for $\text{C}_{80}\text{H}_{65}\text{N}_2\text{O}_9\text{P}_2\text{S}_1$ $[\text{M}+\text{H}]^+$: 1291.38805; found: 1291.38801.

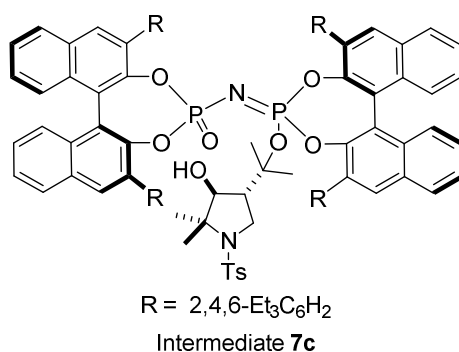
7 EXPERIMENTAL PART

Selected NMR spectra of intermediate **7b**



7 EXPERIMENTAL PART

Characterization of Intermediate 7c

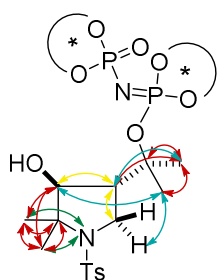
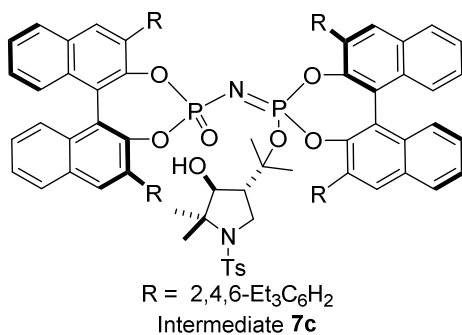


The detected intermediate **7c** were further characterized by ¹H, ¹³C, ¹H-¹H NOESY, ¹H-¹³C HMBC, ¹H-³¹P HMBC and ¹H-¹⁵N HMBC NMR experiments of reaction mixture. The ¹⁵N, ¹³C- and ³¹P spectra of intermediate **7c** were referenced indirectly to the referenced proton frequency with the ϵ -scale with the factors 0.10136767 for ¹⁵N ($\delta(\text{MeNO}_2) = 0$ ppm), 0.25145020 for ¹³C ($\delta(\text{Me}_4\text{Si}) = 0$ ppm) and 0.40480742 for ³¹P ($\delta(\text{H}_3\text{PO}_0) = 0$ ppm). The ¹⁵N chemical shifts were determined from the indirect dimension of a ¹H-¹⁵N HMBC. The absolute configuration of two diastereomers of **7c** was not determined.

HRMS (ESI+) (m/z): calculated for C₁₀₄H₁₁₃N₂O₉P₂S₁ [M+H]⁺: 1627.76365; found: 1627.76362.

7 EXPERIMENTAL PART

Selected NMR spectra of intermediate **7c**



Connections showing J-couplings

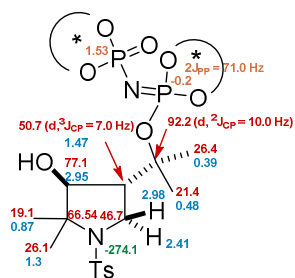
¹H-¹H-COSY

¹H-¹⁵N-HMBC

¹H-¹³C-HMBC

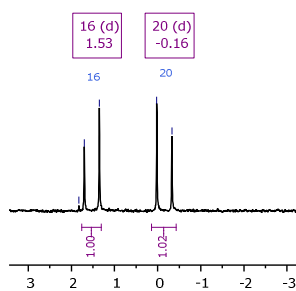
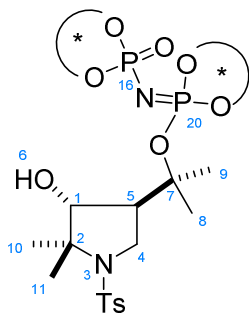
Connections showing close distances of atoms

¹H-¹H-NOESY



³¹P NMR Spectrum

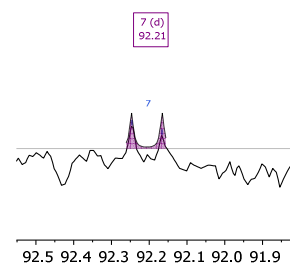
1.53
1.270
1.35
0.02
-0.35



δ_{31P} (ppm)

¹³C NMR Spectrum

92.25 [7]
92.17 [7]

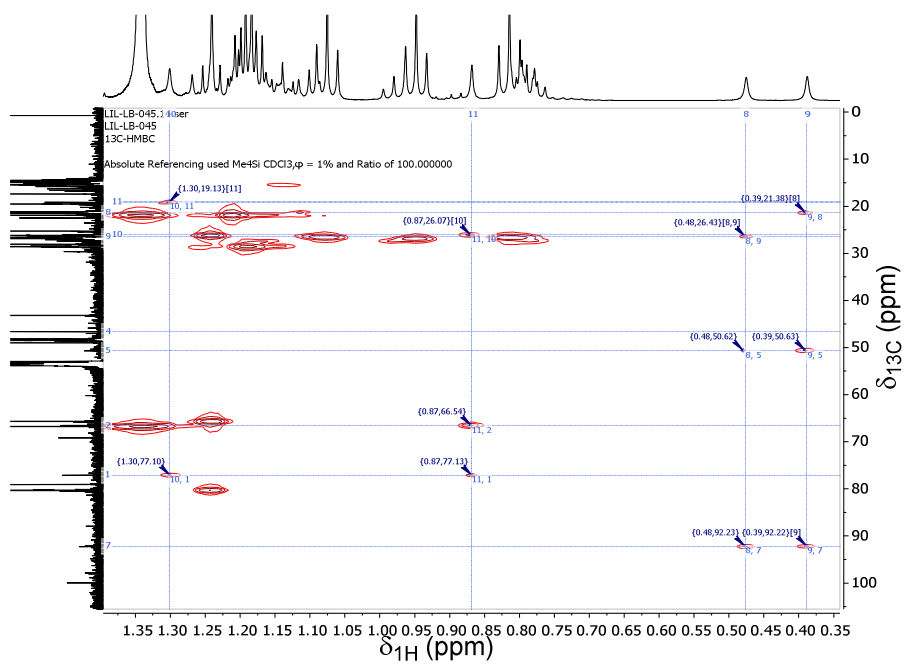


δ_{13C} (ppm)

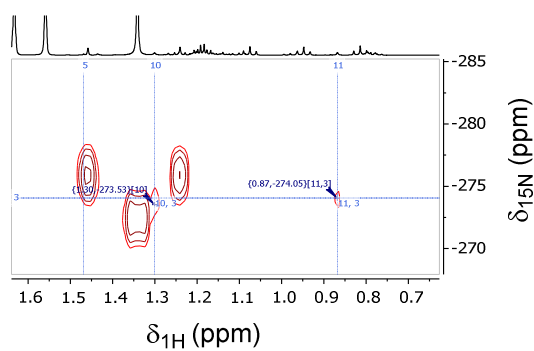
7 EXPERIMENTAL PART

Selected NMR spectra of intermediate **7c**

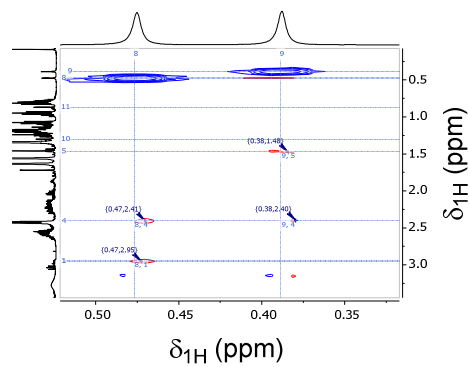
^1H - ^{13}C -HMBC NMR Spectrum



^1H - ^{15}N -HMBC NMR Spectrum



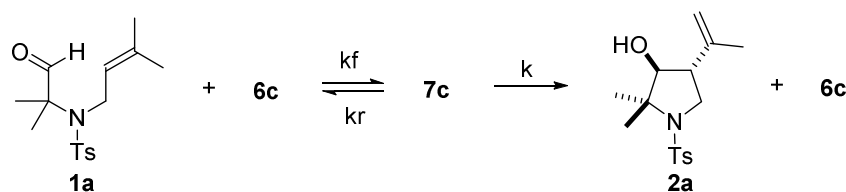
^1H - ^1H -NOESY NMR Spectrum



7 EXPERIMENTAL PART

Eyring Equation Studies

The activation parameters of the elimination of catalyst **6c** from **7c** were determined by measuring the rate constant as a function of temperatures on the basis of Eyring equation (equation 4.1). By reducing the loading of the catalyst **6c** to 1 mol%, all the catalyst **6c** could be saturated to the intermediate **7c**. Subsequently, the concentration of **7c** did not change in the beginning of the reaction, so the reaction rate to generate the product **2a** reached V_{max} in the beginning of the reaction ($d[2a] = k [7c] dt$). We carried out the following reactions: substrate **1a** (235.2 mg, 0.76 mmol) and dry CD_2Cl_2 (0.5 mL) were added to a dry NMR tube, then catalyst **6c** (10 mg, 7.6 μ mol) was added at $-78^\circ C$. Then the reaction was performed at various temperatures. The total volume of sample was 0.7 ml at $22^\circ C$ and we ignored the changes of volume at different temperatures. 1H and ^{31}P NMR spectra of the reaction mixtures were monitored at different time. The kinetic data of time versus $[2a]$ were provided, and the $[2a]$ was determined by several different signals. $V_{max} = k [7c]$, $[7c] = 0.01086$ M. The obtained NMR data was analyzed with the reaction monitoring plugin of MestReNova 9.1 and Origin 2015G 32Bit.



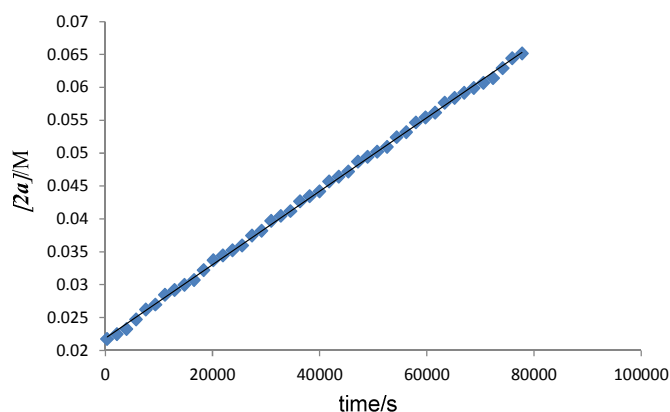
7 EXPERIMENTAL PART

Temperature 280.6 K:

Substrate **1a** (235.2 mg, 0.76 mmol) and dry CD₂Cl₂ (0.5 mL) were added to a dry NMR tube, then catalyst **6c** (10 mg, 7.6 μmol) was added at -78°C. The reaction was conducted at 280.6 K as internally monitored.³ ¹H NMR spectra of the reaction mixtures were monitored at different time. The kinetic datas of time versus *[2a]* were provided, and the *[2a]* was determined by several different signals. $V_{max} = k [7c]$, $[7c] = 0.01086$ M.

$$k = 5.17372\text{E-}05 \text{ s}^{-1}$$

	1	2	3	average
V_m	5.69E-07	5.57E-07	5.59E-07	5.61718E-07
R^2	0.99524	0.99024	0.99921	0.994897



time/s	<i>[2a]</i> /M		
	1	2	3
383	0.026207	0.028453	0.021714
2183	0.026207	0.028453	0.022463
3983	0.026207	0.029202	0.023212
5783	0.028453	0.029951	0.024709
7583	0.0307	0.031448	0.026207
9383	0.029951	0.031448	0.026956
11183	0.032197	0.034443	0.028453
12983	0.032946	0.035192	0.029202
14783	0.032946	0.035192	0.029951
16583	0.032946	0.037438	0.0307
18383	0.03669	0.038187	0.032197

7 EXPERIMENTAL PART

20183	0.037438	0.040433	0.033695
21983	0.038187	0.041931	0.034443
23783	0.038187	0.040433	0.035192
25583	0.038936	0.041931	0.035941
27383	0.041182	0.04268	0.037438
29183	0.041182	0.044177	0.038187
30983	0.043429	0.045675	0.039685
32783	0.043429	0.045675	0.040433
34583	0.044177	0.049419	0.041182
36383	0.047172	0.050167	0.04268
38183	0.047172	0.049419	0.043429
39983	0.04867	0.050916	0.044177
41783	0.049419	0.051665	0.045675
43583	0.050167	0.051665	0.046424
45383	0.051665	0.053163	0.047172
47183	0.052414	0.056158	0.04867
48983	0.052414	0.055409	0.049419
50783	0.053911	0.058404	0.050167
52583	0.05466	0.058404	0.050916
54383	0.056906	0.056158	0.052414
56183	0.056906	0.06065	0.053163
57983	0.059901	0.062148	0.05466
59783	0.06065	0.06065	0.055409
61583	0.06065	0.062897	0.056158
63383	0.061399	0.062148	0.057655
65183	0.062897	0.065143	0.058404
66983	0.064394	0.065143	0.059153
68783	0.064394	0.067389	0.059901
70583	0.062897	0.064394	0.06065
72383	0.064394	0.065892	0.061399
74183	0.067389	0.068138	0.062897
75983	0.069635	0.068138	0.064394
77783	0.068887	0.072631	0.065143

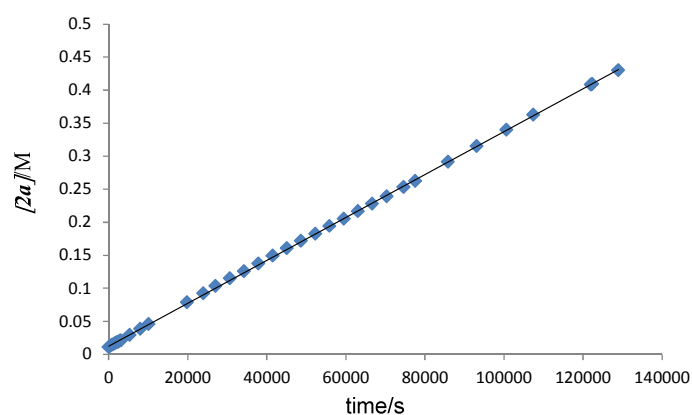
7 EXPERIMENTAL PART

Temperature 294.2 K:

Substrate **1a** (235.2 mg, 0.76 mmol) and dry CD₂Cl₂ (0.5 mL) were added to a dry NMR tube, then catalyst **6c** (10 mg, 7.6 μmol) was added at -78°C. The reaction was conducted at 294.2 K measured by thermometer. ¹H NMR spectra of the reaction mixtures were monitored at different time. The kinetic datas of time versus *[2a]* were provided, and the *[2a]* was determined by several different signals. $V_{max} = k [7c]$, $[7c] = 0.01086$ M. ¹H NMR kinetics study also followed.

$$k = 0.000301 \text{ s}^{-1}$$

	1	2	3	average
V_m	3.25E-06	3.29E-06	3.27E-06	3.26883E-06
R^2	0.99988	0.9999	0.99988	0.999887



time/s	<i>[2a]</i> /M		
	1	2	3
0	0.010483	0.013478	2.097E-02
360	0.012729	0.015724	2.471E-02
780	0.014227	0.016473	2.471E-02
1200	0.014975	0.01797	2.621E-02
1560	0.016473	0.018719	2.621E-02
1980	0.01797	0.020217	2.845E-02

7 EXPERIMENTAL PART

2340	0.018719	0.020966	2.920E-02
2760	0.020217	0.022463	3.070E-02
3120	0.020966	0.023212	3.145E-02
5280	0.029202	0.031448	4.043E-02
8040	0.038187	0.040433	4.867E-02
10080	0.045675	0.047921	5.616E-02
19830	0.078621	0.081616	8.985E-02
23880	0.092099	0.094345	1.026E-01
27060	0.10333	0.105576	1.138E-01
30660	0.114562	0.117557	1.250E-01
34260	0.125793	0.129537	1.363E-01
37860	0.137025	0.14002	1.475E-01
41460	0.149005	0.152749	1.595E-01
45060	0.160236	0.163232	1.707E-01
48660	0.171468	0.175212	1.820E-01
52260	0.181951	0.185695	1.924E-01
55860	0.193931	0.198424	2.044E-01
59460	0.205163	0.209655	2.164E-01
63060	0.216394	0.220887	2.276E-01
66660	0.227626	0.232118	2.381E-01
70320	0.238857	0.244099	2.508E-01
74580	0.253084	0.258325	2.643E-01
77580	0.262069	0.266562	2.733E-01
85860	0.291271	0.297261	3.033E-01
93060	0.315232	0.32197	3.280E-01
100620	0.339941	0.34668	3.527E-01
107460	0.362404	0.369892	3.751E-01
121980	0.408079	0.416315	4.208E-01
122340	0.408828	0.417064	4.223E-01

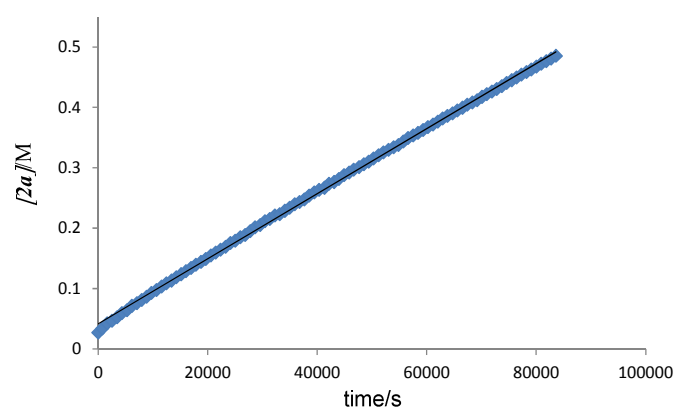
7 EXPERIMENTAL PART

Temperature 301.2 K:

Substrate **1a** (235.2 mg, 0.76 mmol) and dry CD₂Cl₂ (0.5 mL) were added to a dry NMR tube, then catalyst **6c** (10 mg, 7.6 μmol) was added at -78°C. The reaction was conducted at 301.2 K as internally monitored.⁴ ¹H NMR spectra of the reaction mixtures were monitored at different time. The kinetic datas of time versus $[2a]$ were provided, and the $[2a]$ was determined by several different signals. $V_{max} = k [7c]$, $[7c] = 0.01086$ M.

$$k = 0.000493541 \text{ s}^{-1}$$

	1	2	3	average
V_m	5.38E-06	5.38E-06	5.31E-06	5.35845E-06
R^2	0.99904	0.99888	0.99867	0.998863



time/s	$[2a]/M$		
	1	2	3
0	0.026956	0.014975	0.013478
780	0.033695	0.021714	0.019468
1680	0.041931	0.028453	0.026207
2580	0.046424	0.034443	0.032946
3480	0.052414	0.040433	0.038936
4380	0.059153	0.046424	0.044926
5280	0.063645	0.051665	0.050167
6180	0.071133	0.057655	0.056158
7080	0.075626	0.063645	0.062148

7 EXPERIMENTAL PART

7980	0.080867	0.068887	0.067389
8880	0.086108	0.074877	0.072631
9780	0.092847	0.080118	0.078621
10680	0.09734	0.086857	0.084611
11580	0.10333	0.090601	0.089103
12480	0.108571	0.096591	0.095094
13380	0.113064	0.101833	0.100335
14280	0.118305	0.106325	0.105576
15180	0.123547	0.112315	0.110818
16080	0.128788	0.117557	0.116059
16980	0.13403	0.122798	0.1213
17880	0.139271	0.128039	0.126542
18780	0.143764	0.132532	0.131034
19680	0.149005	0.137773	0.136276
20580	0.154246	0.143015	0.141517
21480	0.159488	0.148256	0.14601
22380	0.16398	0.153498	0.151251
23280	0.169222	0.158739	0.156493
24180	0.175212	0.165478	0.161734
25080	0.178956	0.168473	0.166227
25980	0.184946	0.175212	0.171468
26880	0.18869	0.178207	0.175961
27780	0.19468	0.183448	0.181202
28680	0.201419	0.189438	0.186443
29580	0.205163	0.193931	0.190936
30480	0.211153	0.199172	0.196177
31380	0.214897	0.204414	0.20067
32280	0.220887	0.208906	0.205911
33180	0.223133	0.21265	0.210404
34080	0.228374	0.217143	0.214897
34980	0.233616	0.222384	0.220138
35880	0.239606	0.226877	0.224631
36780	0.24335	0.232118	0.229872

7 EXPERIMENTAL PART

37680	0.247094	0.236611	0.233616
38580	0.253833	0.241103	0.238857
39480	0.259074	0.246345	0.24335
40380	0.263567	0.250837	0.248591
41340	0.266562	0.256079	0.253084
42180	0.2733	0.260571	0.257576
43080	0.276296	0.265813	0.262069
43980	0.281537	0.270305	0.26731
44940	0.287527	0.275547	0.271803
45840	0.29202	0.280039	0.276296
46680	0.296512	0.284532	0.281537
47640	0.301005	0.289773	0.28603
48540	0.305498	0.294266	0.290522
49440	0.30999	0.299507	0.295015
50340	0.315232	0.304	0.299507
51240	0.320473	0.308493	0.304749
52140	0.324966	0.312985	0.308493
53040	0.329458	0.318227	0.313734
53940	0.333951	0.322719	0.318227
54840	0.337695	0.327212	0.322719
55740	0.342936	0.331704	0.327212
56640	0.348926	0.336946	0.332453
57540	0.353419	0.341438	0.336197
58440	0.357163	0.345931	0.34069
59340	0.362404	0.350424	0.345931
60240	0.366897	0.354916	0.350424
61140	0.371389	0.359409	0.354167
62040	0.375882	0.36465	0.359409
62940	0.381123	0.369892	0.363901
63840	0.385616	0.372887	0.368394
64740	0.390108	0.377379	0.372138
65640	0.394601	0.382621	0.377379
66540	0.399094	0.387113	0.381872

7 EXPERIMENTAL PART

67440	0.404335	0.391606	0.386365
68340	0.408079	0.396099	0.390857
69240	0.411823	0.400591	0.394601
70140	0.417064	0.406581	0.399842
71040	0.421557	0.410325	0.404335
71940	0.426049	0.414818	0.408828
72840	0.430542	0.41931	0.41332
73740	0.435034	0.423054	0.417064
74640	0.440276	0.428296	0.421557
75540	0.444768	0.432788	0.426798
76440	0.449261	0.436532	0.430542
77340	0.453754	0.441773	0.435034
78240	0.458246	0.446266	0.439527
79140	0.462739	0.450759	0.44402
80040	0.467232	0.455251	0.448512
80940	0.471724	0.458995	0.452256
81840	0.476217	0.463488	0.456749
82740	0.480709	0.46798	0.461241
83640	0.485202	0.473222	0.465734

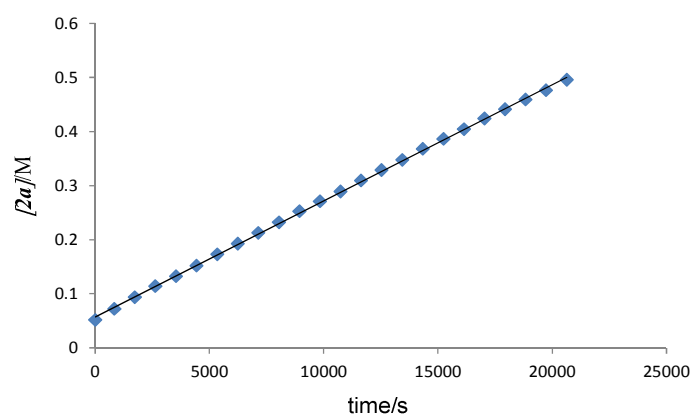
7 EXPERIMENTAL PART

Temperature 312.3 K:

Substrate **1a** (235.2 mg, 0.76 mmol) and dry CD₂Cl₂ (0.5 mL) were added to a dry NMR tube, then catalyst **6c** (10 mg, 7.6 μmol) was added at -78°C. The reaction was conducted at 312.3 K.⁴ ¹H NMR spectra of the reaction mixtures were monitored at different time. The kinetic datas of time versus *[2a]* were provided, and the *[2a]* was determined by several different signals. $V_{max} = k [7c]$, $[7c] = 0.01086$ M.

$$k = 0.001958173 \text{ s}^{-1}$$

	1	2	3	average
V_m	2.15E-5	2.13E-05	2.10E-05	0.0000212602
R^2	0.99963	0.99967	0.99964	0.999647



time/s	<i>[2a]</i> /M		
	1	2	3
0	0.051665	0.068887	0.050916
840	0.071882	0.087606	0.071133
1740	0.093596	0.107074	0.092099
2640	0.113813	0.128039	0.111567
3540	0.132532	0.149005	0.131034
4440	0.152	0.166975	0.150502
5340	0.172966	0.187192	0.170719
6240	0.192433	0.207409	0.190187
7140	0.21265	0.226877	0.208906
8040	0.232118	0.245596	0.228374

7 EXPERIMENTAL PART

8940	0.252335	0.265813	0.247094
9840	0.271054	0.284532	0.265813
10740	0.289025	0.304	0.284532
11640	0.309241	0.323468	0.304
12540	0.328709	0.342187	0.322719
13440	0.347429	0.361655	0.341438
14340	0.367645	0.379626	0.359409
15240	0.386365	0.399842	0.378128
16140	0.404335	0.417813	0.396099
17040	0.423803	0.435783	0.414818
17940	0.441025	0.453754	0.432788
18840	0.458995	0.473222	0.450759
19740	0.476217	0.488946	0.46798
20640	0.495685	0.507665	0.485951

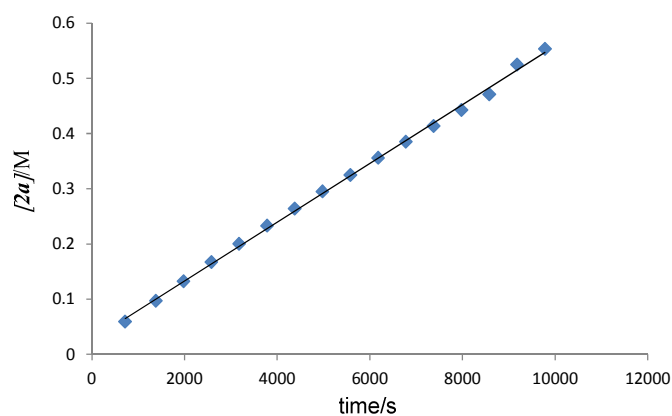
7 EXPERIMENTAL PART

Temperature 323.4 K:

Substrate **1a** (235.2 mg, 0.76 mmol) and dry CD_2Cl_2 (0.5 mL) were added to a dry NMR tube, then catalyst **6c** (10 mg, 7.6 mmol) was added at -78°C .⁴ ^1H NMR spectra of the reaction mixtures were monitored at different time. The kinetic datas of time versus $[\mathbf{2a}]$ were provided, and the $[\mathbf{2a}]$ was determined by several different signals. $V_{max} = k [\mathbf{7c}]$. $[\mathbf{7c}] = 0.01086 \text{ M}$.

$$k = 0.004711654 \text{ s}^{-1}$$

	1	2	3	average
V_m	5.32E-05	5.03E-05	5.00E-05	5.11551E-05
R^2	0.99835	0.99831	1	0.998887



7 EXPERIMENTAL PART

time/s	$[2\alpha]/M$		
	1	2	3
720	0.059153	0.04867	0.059153
1380	0.096591	0.083862	0.092099
1980	0.132532	0.117557	0.122049
2580	0.166975	0.149754	0.152
3180	0.199921	0.181202	0.181951
3780	0.232867	0.211901	0.211901
4380	0.264315	0.241852	0.241852
4980	0.295015	0.271054	0.271803
5580	0.324966	0.299507	0.301754
6180	0.355665	0.327961	0.331704
6780	0.384867	0.355665	0.361655
7380	0.41332	0.383369	0.392355
7980	0.442522	0.410325	0.422305
8580	0.470975	0.437281	0.452256
9180	0.524887	0.489695	0.482207
9780	0.55334	0.515153	0.512158

7 EXPERIMENTAL PART

Eyring Plot

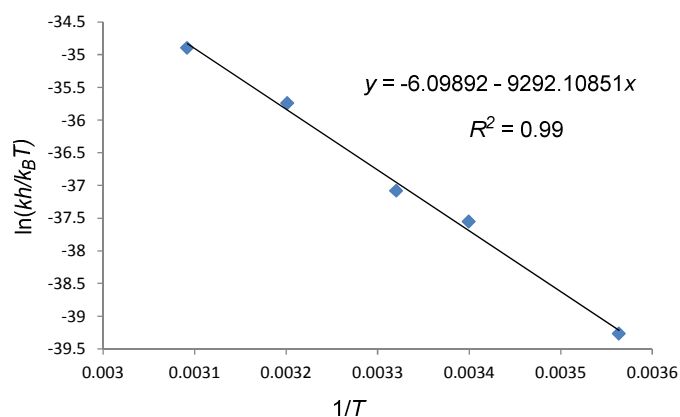
$$\ln(kh/k_B T) = -\Delta H/RT + \Delta S/R$$

Boltzmann Constant $k_B = 1.3806488 \times 10^{-23} \text{ J/K}$,

Planck Constant $h = 6.62606957 \times 10^{-34} \text{ J}\cdot\text{s}$.

1 kcal = 4184 J, $R = 8.314462175 \text{ J/(K}\cdot\text{mol)}$.

T (K)	280.6	294.2	301.2	312.3	323.4
1/T (K ⁻¹)	0.003564	0.0034	0.00332	0.003202	0.003092
k (s ⁻¹)	5.17372E-05	0.000301076	0.000493541	0.001958173	0.004711654
$\ln(kh/k_B T)$	-39.2662417	-37.5522139	-37.0815238	-35.7398133	-34.896584



slope = $-\Delta H/R = -9292.10851 \pm 369.50685$, intercept = $\Delta S/R = -6.09892 \pm 1.22658$.

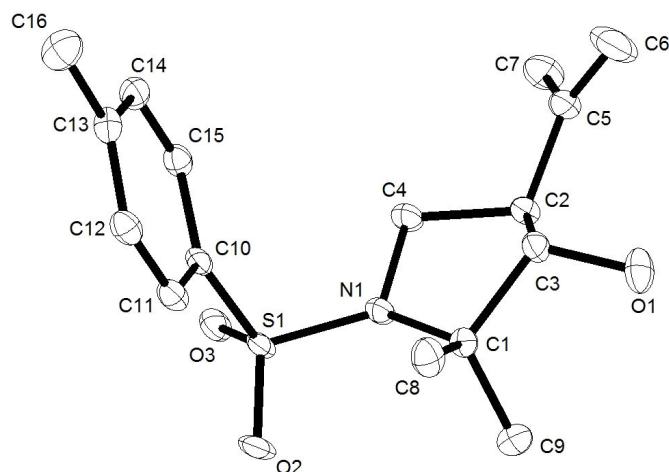
Calculation of activation parameters at 298.15 K

ΔH	$77258.88 \pm 3072.25 \text{ J/mol}$	$18.47 \pm 0.73 \text{ kcal/mol}$
ΔS	$-50.71 \pm 10.20 \text{ J/(K}\cdot\text{mol)}$	$-0.0121 \pm 0.0024 \text{ kcal/(K}\cdot\text{mol)}$
ΔG	$92377.84 \pm 6112.89 \text{ J/mol}$	$22.08 \pm 1.46 \text{ kcal/mol}$

7 EXPERIMENTAL PART

7.2.4 X-Ray Data

X-ray structural analysis parameter for 2a:



Crystal data and structure refinement.

Identification code	9037sadabs	
Empirical formula	$C_{13} H_{23} N O_3 S_1$	
Color	colourless	
Formula weight	$309.41 \text{ g}\cdot\text{mol}^{-1}$	
Temperature	100 K	
Wavelength	1.54178 \AA	
Crystal system	TRICLINIC	
Space group	$p 1$, (no. 1)	
Unit cell dimensions	$a = 8.8573(4) \text{ \AA}$	$\alpha = 100.3631(12)^\circ$.
	$b = 11.7268(5) \text{ \AA}$	$\beta = 92.9867(11)^\circ$.
	$c = 15.6313(7) \text{ \AA}$	$\gamma = 90.2474(12)^\circ$.
Volume	$1594.78(12) \text{ \AA}^3$	
Z	4	
Density (calculated)	$1.289 \text{ Mg}\cdot\text{m}^{-3}$	
Absorption coefficient	1.883 mm^{-1}	
F(000)	664 e	
Crystal size	$0.8 \times 0.2 \times 0.16 \text{ mm}^3$	
θ range for data collection	3.832 to 67.596° .	
Index ranges	$-10 \leq \eta \leq 10$, $-13 \leq \kappa \leq 14$, $-18 \leq \lambda \leq 18$	
Reflections collected	72019	
Independent reflections	9536 [$R_{\text{int}} = 0.0369$]	
Reflections with $I > 2\sigma(I)$	9493	
Completeness to $\theta = 67.596^\circ$	96.7 %	

7 EXPERIMENTAL PART

Absorption correction	Gaussian	
Max. and min. transmission	0.80136 and 0.36318	
Refinement method	Full-matrix least-squares on F ²	
Data / restraints / parameters	9536 / 3 / 809	
Goodness-of-fit on F ²	1.020	
Final R indices [I>2σ(I)]	R ₁ = 0.0402	wR ² = 0.1049
R indices (all data)	R ₁ = 0.0403	wR ² = 0.1050
Absolute structure parameter	0.010(12)	
Extinction coefficient	0	
Largest diff. peak and hole	0.493 and -0.435 e·Å ⁻³	

7 EXPERIMENTAL PART

Selected bond lengths [Å] and angles [°].

C(1)-C(2)	1.559(4)	C(1)-C(8)	1.523(5)
C(1)-C(9)	1.517(5)	C(1)-N(1)	1.506(4)
C(2)-C(3)	1.522(4)	C(2)-O(1)	1.418(4)
C(3)-C(4)	1.535(4)	C(3)-C(5)	1.511(4)
C(4)-N(1)	1.480(4)	C(5)-C(6)	1.314(6)
C(5)-C(7)	1.511(5)	C(6)-H(6A)	0.89(5)
C(6)-H(6B)	0.95(6)	C(10)-C(11)	1.396(4)
C(10)-C(15)	1.398(5)	C(10)-S(1)	1.761(4)
C(11)-C(12)	1.381(5)	C(12)-C(13)	1.398(5)
C(13)-C(14)	1.401(5)	C(13)-C(16)	1.506(6)
C(14)-C(15)	1.376(5)	N(1)-S(1)	1.613(3)
O(2)-S(1)	1.432(2)	O(3)-S(1)	1.442(2)
C(33)-C(34)	1.544(5)	C(33)-C(40)	1.532(4)
C(33)-C(41)	1.525(4)	C(33)-N(3)	1.503(4)
C(34)-C(35)	1.528(4)	C(34)-O(7)	1.415(4)
C(35)-C(36)	1.528(5)	C(35)-C(37)	1.504(5)
C(36)-N(3)	1.483(4)	C(37)-C(38)	1.505(5)
C(37)-C(39)	1.313(6)	C(39)-H(39A)	0.93(5)
C(39)-H(39B)	1.02(7)	C(42)-C(43)	1.398(4)
C(42)-C(47)	1.397(5)	C(42)-S(3)	1.765(3)
C(43)-C(44)	1.381(5)	C(44)-C(45)	1.400(5)
C(45)-C(46)	1.397(4)	C(45)-C(48)	1.508(5)
C(46)-C(47)	1.379(5)	N(3)-S(3)	1.611(3)
O(8)-S(3)	1.443(2)	O(9)-S(3)	1.431(2)
C(17)-C(18)	1.564(5)	C(17)-C(24)	1.519(5)
C(17)-C(25)	1.521(4)	C(17)-N(2)	1.509(4)
C(18)-C(19)	1.521(5)	C(18)-O(4)	1.409(4)
C(19)-C(20)	1.537(4)	C(19)-C(21)	1.512(5)
C(20)-N(2)	1.484(4)	C(21)-C(22)	1.324(6)
C(21)-C(23)	1.501(5)	C(22)-H(22A)	0.98(5)
C(22)-H(22B)	0.97(7)	C(26)-C(27)	1.397(4)
C(26)-C(31)	1.393(5)	C(26)-S(2)	1.772(3)

7 EXPERIMENTAL PART

C(27)-C(28)	1.380(5)	C(28)-C(29)	1.403(5)
C(29)-C(30)	1.393(5)	C(29)-C(32)	1.505(5)
C(30)-C(31)	1.386(5)	N(2)-S(2)	1.622(3)
O(5)-S(2)	1.444(2)	O(6)-S(2)	1.430(3)
C(49)-C(50)	1.565(4)	C(49)-C(56)	1.522(5)
C(49)-C(57)	1.521(4)	C(49)-N(4)	1.508(4)
C(50)-C(51)	1.516(4)	C(50)-O(10)	1.412(4)
C(51)-C(52)	1.534(5)	C(51)-C(53)	1.517(4)
C(52)-N(4)	1.486(4)	C(53)-C(54)	1.324(5)
C(53)-C(55)	1.490(5)	C(54)-H(54A)	0.95(5)
C(54)-H(54B)	0.98(5)	C(58)-C(59)	1.391(5)
C(58)-C(63)	1.395(4)	C(58)-S(4)	1.775(3)
C(59)-C(60)	1.381(5)	C(60)-C(61)	1.404(4)
C(61)-C(62)	1.387(5)	C(61)-C(64)	1.510(5)
C(62)-C(63)	1.383(5)	N(4)-S(4)	1.615(3)
O(11)-S(4)	1.433(2)	O(12)-S(4)	1.446(3)
C(8)-C(1)-C(2)	110.1(3)	C(9)-C(1)-C(2)	112.7(3)
C(9)-C(1)-C(8)	110.6(3)	N(1)-C(1)-C(2)	99.8(2)
N(1)-C(1)-C(8)	114.8(3)	N(1)-C(1)-C(9)	108.5(3)
C(3)-C(2)-C(1)	104.8(2)	O(1)-C(2)-C(1)	111.6(3)
O(1)-C(2)-C(3)	113.5(3)	C(2)-C(3)-C(4)	100.7(2)
C(5)-C(3)-C(2)	118.1(3)	C(5)-C(3)-C(4)	111.2(3)
N(1)-C(4)-C(3)	102.9(2)	C(3)-C(5)-C(7)	114.0(3)
C(6)-C(5)-C(3)	123.9(4)	C(6)-C(5)-C(7)	122.1(4)
C(5)-C(6)-H(6A)	119(3)	C(5)-C(6)-H(6B)	128(4)
H(6A)-C(6)-H(6B)	113(5)	C(11)-C(10)-C(15)	120.1(3)
C(11)-C(10)-S(1)	120.4(3)	C(15)-C(10)-S(1)	119.5(2)
C(12)-C(11)-C(10)	119.3(3)	C(11)-C(12)-C(13)	121.5(3)
C(12)-C(13)-C(14)	118.1(3)	C(12)-C(13)-C(16)	121.5(3)
C(14)-C(13)-C(16)	120.4(3)	C(15)-C(14)-C(13)	121.2(3)
C(14)-C(15)-C(10)	119.8(3)	C(1)-N(1)-S(1)	125.1(2)
C(4)-N(1)-C(1)	112.4(2)	C(4)-N(1)-S(1)	119.1(2)
N(1)-S(1)-C(10)	107.83(15)	O(2)-S(1)-C(10)	

7 EXPERIMENTAL PART

108.57(15)	O(2)-S(1)-N(1)	108.06(14)	O(2)-
S(1)-O(3)	119.10(14)	O(3)-S(1)-C(10)	
106.38(15)	O(3)-S(1)-N(1)	106.45(13)	C(40)-
C(33)-C(34)	113.1(3)	C(41)-C(33)-C(34)	110.0(3)
C(41)-C(33)-C(40)	110.0(3)	N(3)-C(33)-C(34)	100.3(2)
N(3)-C(33)-C(40)	108.4(3)	N(3)-C(33)-C(41)	114.9(3)
C(35)-C(34)-C(33)	104.6(3)	O(7)-C(34)-C(33)	111.7(3)
O(7)-C(34)-C(35)	113.8(3)	C(36)-C(35)-C(34)	100.6(2)
C(37)-C(35)-C(34)	118.4(3)	C(37)-C(35)-C(36)	112.0(3)
N(3)-C(36)-C(35)	103.1(3)	C(35)-C(37)-C(38)	114.1(3)
C(39)-C(37)-C(35)	123.9(3)	C(39)-C(37)-C(38)	122.0(4)
C(37)-C(39)-H(39A)	123(3)	C(37)-C(39)-H(39B)	125(4)
H(39A)-C(39)-H(39B)	111(5)	C(43)-C(42)-S(3)	120.3(2)
C(47)-C(42)-C(43)	120.1(3)	C(47)-C(42)-S(3)	119.5(2)
C(44)-C(43)-C(42)	119.5(3)	C(43)-C(44)-C(45)	121.1(3)
C(44)-C(45)-C(48)	121.2(3)	C(46)-C(45)-C(44)	118.3(3)
C(46)-C(45)-C(48)	120.4(3)	C(47)-C(46)-C(45)	121.4(3)
C(46)-C(47)-C(42)	119.5(3)	C(33)-N(3)-S(3)	125.5(2)
C(36)-N(3)-C(33)	111.9(3)	C(36)-N(3)-S(3)	119.1(2)
N(3)-S(3)-C(42)	108.05(16)	O(8)-S(3)-C(42)	
106.21(15)	O(8)-S(3)-N(3)	106.32(14)	O(9)-
S(3)-C(42)	108.41(14)	O(9)-S(3)-N(3)	
107.90(15)	O(9)-S(3)-O(8)	119.49(15)	C(24)-
C(17)-C(18)	109.8(3)	C(24)-C(17)-C(25)	110.3(3)
C(25)-C(17)-C(18)	112.6(3)	N(2)-C(17)-C(18)	99.0(2)
N(2)-C(17)-C(24)	111.0(3)	N(2)-C(17)-C(25)	113.7(3)
C(19)-C(18)-C(17)	105.8(3)	O(4)-C(18)-C(17)	113.8(3)
O(4)-C(18)-C(19)	114.8(3)	C(18)-C(19)-C(20)	101.7(3)
C(21)-C(19)-C(18)	115.8(3)	C(21)-C(19)-C(20)	113.1(3)
N(2)-C(20)-C(19)	104.0(3)	C(22)-C(21)-C(19)	119.2(3)
C(22)-C(21)-C(23)	121.1(3)	C(23)-C(21)-C(19)	119.7(3)
C(21)-C(22)-H(22A)	124(3)	C(21)-C(22)-H(22B)	126(4)
H(22A)-C(22)-H(22B)	111(5)	C(27)-C(26)-S(2)	119.4(3)
C(31)-C(26)-C(27)	120.6(3)	C(31)-C(26)-S(2)	120.0(2)

7 EXPERIMENTAL PART

C(28)-C(27)-C(26)	119.3(3)	C(27)-C(28)-C(29)	121.2(3)
C(28)-C(29)-C(32)	120.5(3)	C(30)-C(29)-C(28)	118.3(3)
C(30)-C(29)-C(32)	121.3(3)	C(31)-C(30)-C(29)	121.4(3)
C(30)-C(31)-C(26)	119.1(3)	C(17)-N(2)-S(2)	125.2(2)
C(20)-N(2)-C(17)	113.0(2)	C(20)-N(2)-S(2)	117.6(2)
N(2)-S(2)-C(26)	108.65(15)	O(5)-S(2)-C(26)	
105.82(15)	O(5)-S(2)-N(2)	106.10(13)	O(6)-
S(2)-C(26)	108.45(15)	O(6)-S(2)-N(2)	
108.06(15)	O(6)-S(2)-O(5)	119.38(15)	C(56)-
C(49)-C(50)	112.2(3)	C(57)-C(49)-C(50)	109.4(3)
C(57)-C(49)-C(56)	110.4(3)	N(4)-C(49)-C(50)	99.3(2)
N(4)-C(49)-C(56)	113.9(3)	N(4)-C(49)-C(57)	111.2(3)
C(51)-C(50)-C(49)	105.3(3)	O(10)-C(50)-C(49)	113.7(3)
O(10)-C(50)-C(51)	114.7(3)	C(50)-C(51)-C(52)	102.1(3)
C(50)-C(51)-C(53)	116.4(3)	C(53)-C(51)-C(52)	112.5(3)
N(4)-C(52)-C(51)	103.8(3)	C(54)-C(53)-C(51)	119.0(3)
C(54)-C(53)-C(55)	122.0(3)	C(55)-C(53)-C(51)	118.9(3)
C(53)-C(54)-H(54A)	120(3)	C(53)-C(54)-H(54B)	121(3)
H(54A)-C(54)-H(54B)	120(4)	C(59)-C(58)-C(63)	120.6(3)
C(59)-C(58)-S(4)	119.2(2)	C(63)-C(58)-S(4)	120.1(3)
C(60)-C(59)-C(58)	119.5(3)	C(59)-C(60)-C(61)	120.8(3)
C(60)-C(61)-C(64)	119.9(3)	C(62)-C(61)-C(60)	118.5(3)
C(62)-C(61)-C(64)	121.6(3)	C(63)-C(62)-C(61)	121.6(3)
C(62)-C(63)-C(58)	118.9(3)	C(49)-N(4)-S(4)	125.8(2)
C(52)-N(4)-C(49)	112.7(3)	C(52)-N(4)-S(4)	117.4(2)
N(4)-S(4)-C(58)	108.42(15)	O(11)-S(4)-C(58)	108.40(15)
O(11)-S(4)-N(4)	107.89(14)	O(11)-S(4)-O(12)	119.51(15)
O(12)-S(4)-C(58)	106.07(15)	O(12)-S(4)-N(4)	106.14(14)

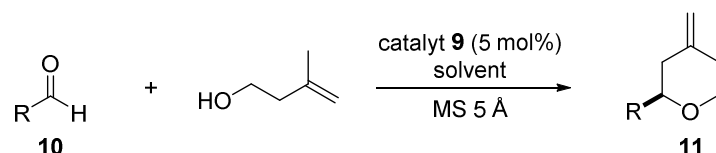
Symmetry transformations used to generate equivalent atoms

7 EXPERIMENTAL PART

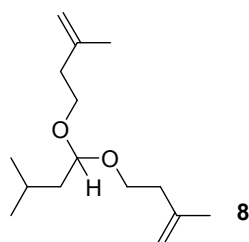
7.3 Organocatalytic Asymmetric Transformations via Oxocarbenium Ions

7.3.1 Prins Cyclization

7.3.1.1 Products



Unless specified otherwise, aldehyde **10** (0.12 mmol) and 3-methyl-3-buten-1-ol (0.10 mmol) were added to a mixture of catalyst **9** (0.005 mmol, 5 mol%) and 50 mg 5 Å molecular sieves in anhydrous solvent (0.1 M). Purification was performed by column chromatography or preparative thin layer chromatography on silica gel using pentane/diethyl ether = 95/5 as the eluent. Due to the concentration and separation issue, only the enantiomeric ratios of minor endocyclic alkene isomers of **11e**, **11f**, **11i**, **11l**, **11m**, **11p–11r** were provided.



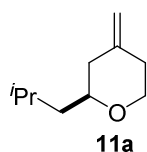
2-methyl-4-(3-methyl-1-((3-methylbut-3-en-1-yl)oxy)butoxy)but-1-ene

¹H NMR (500 MHz, CDCl₃): δ 4.77–4.78 (m, 2H), 4.73–4.74 (m, 2H), 4.59 (t, *J* = 6.0 Hz, 1 H), 3.66–3.70 (m, 2H), 3.52–3.57 (m, 2H), 2.29 (t, *J* = 7.0 Hz, 4H), 1.75 (br s, 6H), 1.69–1.73 (m, 1H), 1.50 (dd, *J* = 6.9 Hz, *J* = 6.0 Hz, 2H), 0.91 (s, 3H), 0.90 (s, 3H). The spectra is not clean because a little amount of impurity **11a** was exist, which is similar polarity to **8** during column chromatography.

¹³C NMR (126 MHz, CDCl₃): δ 143.0, 111.6, 101.9, 63.7, 42.2, 38.1, 24.5, 23.0, 22.9. The spectra is not clean because a little amount of impurity **3a** was exist, which is similar polarity to **B** during column chromatography.

HRMS (ESI+) (*m/z*): calculated for C₁₅H₂₈O₂Na₁ [M+Na]⁺: 263.1981; found: 263.1979.

7 EXPERIMENTAL PART



(*S*)-2-Isobutyl-4-methylenetetrahydro-2*H*-pyran

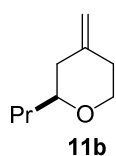
Prepared at 22 °C in cyclohexane. A colorless oil was obtained. Due to the volatile nature of the product, the yield was determined by ^1H NMR spectroscopy of the reaction mixture using $\text{CHCl}_2\text{CHCl}_2$ as internal standard. The major isomer was obtained in 89% NMR yield. The regiomer ratio of the isolated compound is 9:1 which was determined by GC analysis.

^1H NMR (500 MHz, CDCl_3): δ 4.72–4.70 (m, 2H), 4.05 (ddd, $J = 10.9\text{Hz}, 5.6\text{Hz}, 1.6\text{Hz}$, 1H), 3.4–3.2 (m, 2H), 2.34–2.10 (m, 3H), 1.99–1.91 (m, 1H), 1.83–1.74 (m, 1H), 1.56–1.46 (m, 1H), 1.25–1.16 (m, 1H), 0.91 (d, $J = 3.3\text{ Hz}$, 3H), 0.89 (d, $J = 3.3\text{ Hz}$, 3H).

^{13}C NMR (126 MHz, CDCl_3): δ 145.0, 108.1, 68.7, 45.5, 41.6, 35.3, 24.3, 23.2, 22.3.

HRMS (EI) (m/z): calculated for $\text{C}_{10}\text{H}_{18}\text{O}_1$ [M]: 154.1357; found: 154.1356.

GC The enantiomeric ratio was measured by GC analysis on Hydrodex-gamma-TBDACD column: $t_{\text{R}} = 32.17\text{ min}$ (major) and $t_{\text{R}} = 34.50\text{ min}$ (minor), er = 95.5:4.5.



(*S*)-4-Methylene-2-propyltetrahydro-2*H*-pyran

Prepared at 10 °C in cyclohexane. A colorless oil was obtained. Due to the volatile nature of the product, the yield was determined by ^1H NMR spectroscopy of the reaction mixture using $\text{CHCl}_2\text{CHCl}_2$ as internal standard. The major isomer was obtained in 60% NMR yield. The regiomer ratio of the isolated compound is 10:1 which was determined by GC analysis.

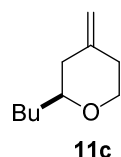
^1H NMR (300 MHz, CD_2Cl_2): δ 4.71–4.68 (m, 2H), 4.01 (ddd, $J = 10.9\text{ Hz}, 5.5\text{ Hz}, 1.7\text{ Hz}$, 1H), 3.32 (ddd, $J = 13.7\text{ Hz}, 10.9\text{ Hz}, 2.9\text{ Hz}$, 1H), 3.24–3.16 (m, 1H), 2.32–2.09 (m, 3H), 1.98–1.89 (m, 1H), 1.49–1.30 (m, 4H), 0.91 (t, $J = 7.1\text{ Hz}$, 3H).

7 EXPERIMENTAL PART

^{13}C NMR (75 MHz, CD_2Cl_2): δ 145.9, 108.0, 79.0, 69.0, 41.6, 38.9, 35.8, 19.1, 14.3.

HRMS (EI) (m/z): calculated for $\text{C}_9\text{H}_{17}\text{O}_1$ [M]: 141.1273; found: 141.1275.

GC The enantiomeric ratio was measured by GC analysis on Lipodex-G/in G-566 column: $t_{\text{R}} = 10.38$ min (minor) and $t_{\text{R}} = 11.27$ min (major), er = 95:5.



(*S*)-2-Butyl-4-methylenetetrahydro-2*H*-pyran

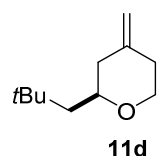
Prepared at 0 °C in methylcyclohexane. A colorless oil was obtained. Due to the volatile nature of the product, the yield was determined by ^1H NMR spectroscopy of the reaction mixture using $\text{CHCl}_2\text{CHCl}_2$ as internal standard. The major isomer was obtained in 85% NMR yield. The regioisomeric ratio of the isolated compound is >20:1 which was determined by GC analysis.

^1H NMR (500 MHz, CDCl_3): δ 4.72–4.69 (m, 2H), 4.06 (ddd, $J = 10.9$ Hz, 5.6 Hz, 1.4 Hz, 1H), 3.36 (ddd, $J = 13.6$ Hz, 10.9 Hz, 2.7 Hz, 1H), 3.24–3.19 (m, 1H), 2.32–2.26 (m, 1H), 2.22 (td, $J = 13.3$ Hz, 1.9 Hz, 1H), 2.15–2.11 (m, 1H), 1.99–1.94 (m, 1H), 1.48–1.28 (m, 6H), 0.90 (t, $J = 7.0$ Hz, 3H).

^{13}C NMR (126 MHz, CDCl_3): δ 145.1, 108.3, 79.0, 68.8, 41.3, 36.1, 35.4, 27.8, 22.9, 14.2.

HRMS (EI) (m/z): calculated for $\text{C}_{10}\text{H}_{18}\text{O}_1$ [M]: 154.1357; found: 154.1355.

GC The enantiomeric ratio was measured by GC analysis on Hydrodex-beta-TBDAC-CD column: $t_{\text{R}} = 13.51$ min (major) and $t_{\text{R}} = 14.80$ min (minor), er = 95:5.



(*S*)-4-Methylene-2-neopentyltetrahydro-2*H*-pyran

Prepared at 22 °C in cyclohexane. A colorless oil was obtained. Due to the volatile nature of the product, the yield was determined by ^1H NMR spectroscopy of the reaction

7 EXPERIMENTAL PART

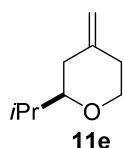
mixture using $\text{CHCl}_2\text{CHCl}_2$ as internal standard. The major isomer was obtained in 60% NMR yield. The regiomer ratio of the isolated compound is >20:1 which was determined by GC analysis.

^1H NMR (500 MHz, CDCl_3): δ 4.71–4.69 (m, 2H), 4.03 (ddd, $J = 11.1$ Hz, 5.7 Hz, 1.1 Hz, 1H), 3.4–3.3 (m, 2H), 2.31–2.24 (m, 1H), 2.14–2.11 (m, 2H), 2.04–1.99 (m, 1H), 1.53 (q, 8.0 Hz, 1H), 1.25 (dd, 14.5 Hz, 2.6 Hz, 1H), 0.93 (s, 9H).

^{13}C NMR (126 MHz, CDCl_3): δ 145.3, 108.1, 76.8, 68.4, 49.9, 42.8, 35.0, 30.2, 30.1.

HRMS (EI) (m/z): calculated for $\text{C}_{11}\text{H}_{20}\text{O}_1$ [M]: 168.1514; found: 168.1512.

GC The enantiomeric ratio was measured by GC analysis on Hydrodex-gamma-TBDAC-CD column: $t_{\text{R}} = 14.86$ min (major) and $t_{\text{R}} = 16.37$ min (minor), er = 98:2.



(*R*)-2-Isopropyl-4-methylenetetrahydro-2*H*-pyran

Prepared at 22 °C in cyclohexane. A colorless oil was obtained. Due to the volatile nature of the product, the yield was determined by ^1H NMR spectroscopy of the reaction mixture using $\text{CHCl}_2\text{CHCl}_2$ as internal standard. The major isomer was obtained in 94% NMR yield. The regioisomeric ratio of the isolated compound is 9:1 which was determined by GC analysis.

^1H NMR (300 MHz, CD_2Cl_2): δ 4.71–4.70 (m, 2H), 4.03 (ddd, $J = 10.9$ Hz, 5.6 Hz, 1.6 Hz, 1H), 3.03 (ddd, $J = 13.7$ Hz, 10.8 Hz, 2.9 Hz, 1H), 2.91 (ddd, $J = 11.1$ Hz, 6.2 Hz, 2.4 Hz, 1H), 2.31–2.19 (m, 2 H), 2.15–2.09 (m, 1H), 2.01–1.92 (m, 1H), 1.66 (q, 6.6 Hz, 1H), 0.92 (d, 6.8 Hz, 3H), 0.90 (d, 6.8 Hz, 3H).

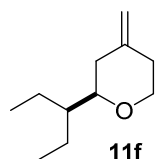
^{13}C NMR (126 MHz, CD_2Cl_2): δ 146.2, 108.1, 84.3, 69.2, 38.4, 35.9, 33.6, 18.7, 18.5.

HRMS (EI) (m/z): calculated for $\text{C}_9\text{H}_{16}\text{O}_1$ [M]: 140.1201; found: 140.1200.

GC The enantiomeric ratio was measured by GC analysis on Cyclodextrin-H/in OV-1701 column: $t_{\text{R}} = 11.34$ min (minor) and $t_{\text{R}} = 13.50$ min (major), er (exocyclic alkene isomer) = 95:5; $t_{\text{R}} = 15.53$ min (minor) and $t_{\text{R}} = 16.87$ min (major), er (endocyclic alkene isomer 1) =

7 EXPERIMENTAL PART

77:23; $t_R = 23.18$ min (minor) and $t_R = 25.19$ min (major), er (endocyclic alkene isomer 2) = 76:24.



(*R*)-4-Methylene-2-(pentan-3-yl)tetrahydro-2*H*-pyran

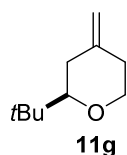
Prepared at 22 °C in cyclohexane. A colorless oil was obtained. Due to the volatile nature of the product, the yield was determined by ^1H NMR spectroscopy of the reaction mixture using $\text{CHCl}_2\text{CHCl}_2$ as internal standard. The major isomer was obtained in 85% NMR yield. The regiomer ratio of the isolated compound is 13:1 which was determined by GC analysis.

^1H NMR (500 MHz, CD_2Cl_2): δ 4.71–4.69 (m, 2H), 4.02 (ddd, $J = 10.8$ Hz, 5.7 Hz, 1.2 Hz, 1H), 3.29 (ddd, $J = 13.5$ Hz, 10.8 Hz, 2.7 Hz, 1H), 3.16 (ddd, $J = 11.2$ Hz, 5.4 Hz, 2.3 Hz, 1H), 2.28–2.21 (m, 1H), 2.18 (td, $J = 13.1$ Hz, 1.9 Hz, 1H), 2.14–2.10 (m, 1H), 2.04–1.99 (m, 1H), 1.51–1.25 (m, 5H), 0.89–0.85 (m, 6H).

^{13}C NMR (126 MHz, CD_2Cl_2): δ 146.4, 108.1, 80.9, 69.3, 46.3, 38.3, 35.9, 22.0, 21.8, 11.69, 11.65.

HRMS (EI) (m/z): calculated for $\text{C}_{11}\text{H}_{20}\text{O}_1$ [M]: 168.1514; found: 168.1513.

GC The enantiomeric ratio was measured by GC analysis on C-DEXTRIN-H/in G-632 column: $t_R = 10.92$ min (minor) and $t_R = 11.71$ min (major), er (exocyclic alkene isomer) = 95:5; $t_R = 12.18$ min (minor) and $t_R = 13.26$ min (major), er (endocyclic alkene isomer 1) = 80:20; $t_R = 16.24$ min (minor) and $t_R = 17.27$ min (major), er (endocyclic alkene isomer 2) = 77:23.



(*R*)-2-(*tert*-Butyl)-4-methylenetetrahydro-2*H*-pyran

Prepared at 22 °C in cyclohexane. A colorless oil was obtained. Due to the volatile nature of the product, the yield was determined by ^1H NMR spectroscopy of the reaction

7 EXPERIMENTAL PART

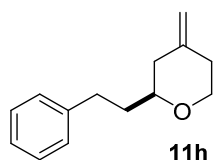
mixture using $\text{CHCl}_2\text{CHCl}_2$ as internal standard. The major isomer was obtained in 90% NMR yield. The regiomer ratio of the isolated compound is 20:1 which was determined by GC analysis. The corresponding enantiomer could be achieved using *ent*-**9b**.

^1H NMR (500 MHz, CD_2Cl_2): δ 4.71–4.69 (m, 2H), 4.05 (ddd, $J = 13.5$ Hz, 10.8 Hz, 1.0 Hz, 1H), 3.29 (ddd, $J = 13.5$ Hz, 10.8 Hz, 2.7 Hz, 1H), 2.8 (dd, $J = 11.5$ Hz, 2.2 Hz, 1H), 2.27–2.19 (m, 2H), 2.13–2.09 (m, 1H), 2.01–1.96 (m, 1H), 0.89 (s, 9H).

^{13}C NMR (126 MHz, CD_2Cl_2): δ 146.7, 108.1, 87.2, 69.5, 35.94, 35.88, 34.4, 26.1.

HRMS (EI) (m/z): calculated for $\text{C}_{10}\text{H}_{18}\text{O}_1$ [M]: 154.1357; found: 154.1356.

GC The enantiomeric ratio was measured by GC analysis on Lipodex-G/in G-566 column: using catalyst **9b** $t_{\text{R}} = 9.07$ min (minor) and $t_{\text{R}} = 9.73$ min (major), er = 98:2; using catalyst *ent*-**9b** $t_{\text{R}} = 9.14$ min (major) and $t_{\text{R}} = 10.21$ min (minor), er = 98:2.



(*S*)-4-Methylene-2-phenethyltetrahydro-2*H*-pyran

Prepared at 22 °C in cyclohexane. A colorless oil was obtained. 80% Isolated yield was obtained using pentane/diethylether = 95/5 as the eluents. The regiomer ratio of the isolated compound is >20:1 which was determined by GC analysis.

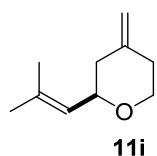
^1H NMR (500 MHz, CDCl_3): δ 7.30–7.27 (m, 2H), 7.22–7.17 (m, 3H), 4.70 (qd, $J = 10.3$ Hz, 1.8 Hz, 2H), 4.10 (ddd, $J = 10.9$ Hz, 5.6 Hz, 1.5 Hz, 1H), 3.38 (ddd, $J = 13.6$ Hz, 11.0 Hz, 2.7 Hz, 1H), 3.27–3.22 (m, 1H), 2.82–2.76 (m, 1H), 2.70–2.64 (m, 1H), 2.35–2.28 (m, 1H), 2.22 (td, $J = 13.2$ Hz, 1.8 Hz, 1H), 2.17–2.13 (m, 1H), 2.05–2.00 (m, 1H), 1.92–1.84 (m, 1H), 1.77–1.70 (m, 1H).

^{13}C NMR (126 MHz, CDCl_3): δ 144.8, 142.3, 128.6, 128.5, 125.9, 108.5, 77.9, 68.8, 41.3, 38.1, 35.4, 31.9.

HRMS (ESI+) (m/z): calculated for $\text{C}_{19}\text{H}_{28}\text{O}_2\text{Na}_1$ [$\text{M}+\text{Na}$] $^+$: 311.1981; found: 311.1980.

GC The enantiomeric ratio was measured by GC analysis on Hydrodex-beta-TBDAC-CD column: $t_{\text{R}} = 23.11$ min (major) and $t_{\text{R}} = 23.68$ min (minor), er = 90:10.

7 EXPERIMENTAL PART



(*R*)-4-Methylene-2-(2-methylprop-1-en-1-yl)tetrahydro-2*H*-pyran

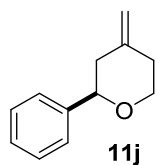
Prepared at $-30\text{ }^{\circ}\text{C}$ in methylcyclohexane. A colorless oil was obtained. Due to the volatile nature of the product, the yield was determined by ^1H NMR spectroscopy of the reaction mixture using $\text{CHCl}_2\text{CHCl}_2$ as internal standard. The major isomer was obtained in 87% NMR yield. The regiomer ratio of the isolated compound is 11:1 which was determined by GC analysis.

^1H NMR (500 MHz, CDCl_3): δ 5.23–5.19 (m, 1H), 4.75–4.71 (m, 2H), 4.07 (ddd, $J = 10.9\text{ Hz}, 5.6\text{ Hz}, 1.5\text{ Hz}, 1\text{H}$), 3.97 (ddd, $J = 10.9\text{ Hz}, 8.2\text{ Hz}, 2.8\text{ Hz}, 1\text{H}$), 3.43 (ddd, $J = 13.6\text{ Hz}, 11.0\text{ Hz}, 2.7\text{ Hz}, 1\text{H}$), 2.34–2.27 (m, 1H), 2.20–2.06 (m, 3H), 1.73 (d, $J = 1.3\text{ Hz}, 3\text{H}$), 1.69 (d, $J = 1.3\text{ Hz}, 3\text{H}$).

^{13}C NMR (126 MHz, CDCl_3): δ 144.6, 136.2, 125.6, 108.5, 75.8, 68.5, 41.3, 35.0, 25.7, 18.5.

HRMS (ESI+) (m/z): calculated for $\text{C}_{10}\text{H}_{16}\text{O}_1\text{Na}_1$ [$\text{M}+\text{Na}$] $^+$: 175.1093; found: 175.1095.

GC The enantiomeric ratio was measured by GC analysis on Hydrodex-gamma-TBDAC-CD column: $t_{\text{R}} = 14.90\text{ min}$ (major) and $t_{\text{R}} = 16.20\text{ min}$ (minor), *er* (exocyclic alkene isomer) = 95:5; $t_{\text{R}} = 21.77\text{ min}$ (major) and $t_{\text{R}} = 22.44\text{ min}$ (minor), *er* (endocyclic alkene isomer 1) = 52:48; $t_{\text{R}} = 24.52\text{ min}$ and $t_{\text{R}} = 25.41\text{ min}$, *er* (endocyclic alkene isomer 2) = 50:50.



(*R*)-4-Methylene-2-phenyltetrahydro-2*H*-pyran

Prepared at $10\text{ }^{\circ}\text{C}$ in cyclohexane. A colorless oil was obtained. 69% isolated yield was obtained using pentane/diethylether = 95/5 as the eluents (due to the volatile nature of the product, the yield was also determined by ^1H NMR spectroscopy of the reaction mixture using $\text{CHCl}_2\text{CHCl}_2$ as internal standard. The major isomer was obtained in 97% NMR

7 EXPERIMENTAL PART

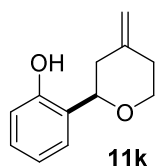
yield). The regiomer ratio of the isolated compound is >20:1 which was determined by GC analysis.

¹H NMR (500 MHz, CDCl₃): δ 7.39–7.34 (m, 4H), 7.30–7.26 (m, 1H), 4.81 (qd, *J* = 7.3 Hz, 1.8 Hz, 2H), 4.30 (dd, *J* = 11.3 Hz, 2.5 Hz, 1H), 4.24 (ddd, *J* = 10.8 Hz, 5.7 Hz, 1.0 Hz, 1H), 3.56 (ddd, *J* = 13.5 Hz, 11.0 Hz, 2.7 Hz, 1H), 2.48–2.40 (m, 2H), 2.36–2.30 (m, 1H), 2.25–2.22 (m, 1H).

¹³C NMR (126 MHz, CDCl₃): δ 144.6, 142.5, 128.5, 127.7, 126.0, 109.0, 81.1, 69.3, 43.3, 35.1.

HRMS (EI) (*m/z*): calculated for C₁₂H₁₄O₁ [M]: 174.1044; found: 174.1041.

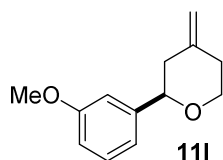
GC The enantiomeric ratio was measured by GC analysis on Hydrodex-beta-TBDAC-CD column: *t_R* = 15.02 min (major) and *t_R* = 15.94 min (minor), er = 96:4.



(*R*)-2-(4-Methylenetetrahydro-2*H*-pyran-2-yl)phenol Prepared at 0 °C in methylcyclohexane. A colorless oil was obtained. 80% Isolated yield was obtained using pentane:diethyl ether 95:5 as the eluents. The regiomer ratio of the isolated compound is >20:1 which was determined by GC analysis.

HRMS (ESI+) (*m/z*): calculated for C₁₂H₁₄O₂Na₁ [M+Na]⁺: 213.0885; found: 213.0888.

GC The enantiomeric ratio was measured by GC analysis on Hydrodex-gamma-TBDAC-CD column: *t_R* = 16.04 min (major) and *t_R* = 16.53 min (minor), er = 95.5:4.5.



(*R*)-2-(3-Methoxyphenyl)-4-methylenetetrahydro-2*H*-pyran

Prepared at 0 °C in methylcyclohexane. A colorless oil was obtained. 65% Isolated yield was obtained using pentane/diethylether = 95/5 as the eluents. The regiomer ratio of the isolated compound is 12:1 which was determined by GC analysis.

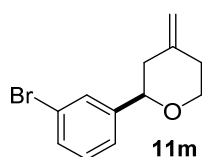
7 EXPERIMENTAL PART

¹H NMR (500 MHz, CDCl₃): δ 7.28–7.24 (m, 1H), 6.95–6.94 (m, 2H), 6.82 (dd, *J* = 8.2 Hz, 0.95 Hz, 1H), 4.81 (qd, *J* = 3.2 Hz, 1.8 Hz, 2H), 4.27 (dd, *J* = 11.2 Hz, 2.5 Hz, 1H), 4.23 (ddd, *J* = 11.0 Hz, 5.7 Hz, 1.1 Hz, 1H), 3.82 (s, 3H), 3.55 (ddd, *J* = 13.6 Hz, 11.0 Hz, 2.6 Hz, 1H), 2.48–2.40 (m, 2H), 2.34–2.29 (m, 1H), 2.24–2.21 (m, 1H).

¹³C NMR (126 MHz, CDCl₃): δ 159.8, 144.6, 144.1, 129.5, 118.3, 113.4, 111.3, 109.1, 80.9, 69.2, 55.4, 43.3, 35.1.

HRMS (ESI+) (*m/z*): calculated for C₁₃H₁₆O₂Na₁ [M+Na]⁺: 227.1042; found: 227.1044.

GC The enantiomeric ratio was measured by GC analysis on Hydrodex-beta-TBDAC-CD column column: *t_R* = 80.12 min (major) and *t_R* = 82.53 min (minor), *er* (exocyclic alkene isomer) = 95:5; *t_R* = 101.56 min (minor) and *t_R* = 113.69 min (major), *er* (endocyclic alkene isomer) = 54:46.



(*R*)-2-(3-bromophenyl)-4-methylenetetrahydro-2*H*-pyran

Prepared at 10 °C in cyclohexane. A colorless oil was obtained. 73% Isolated yield was obtained using pentane/diethylether = 95/5 as the eluents. The regiomeric ratio of the isolated compound is 15:1 which was determined by GC analysis.

¹H NMR (500 MHz, CDCl₃): δ 7.55 (t, *J* = 1.7 Hz, 1H), 7.40 (qd, *J* = 7.9 Hz, 1.2 Hz, 1H), 7.29–7.28 (m, 1H), 7.23–7.20 (m, 1H), 4.82 (qd, *J* = 7.8 Hz, 1.7 Hz, 2H), 4.28–4.21 (m, 2H), 3.54 (ddd, *J* = 13.6 Hz, 11.0 Hz, 2.6 Hz, 1H), 2.47–2.38 (m, 2H), 2.29–2.21 (m, 2H).

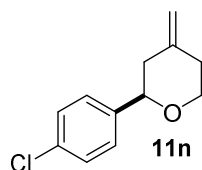
¹³C NMR (126 MHz, CDCl₃): δ 144.8, 144.1, 130.7, 130.1, 129.1, 124.5, 122.7, 109.4, 80.1, 69.3, 43.2, 35.0.

HRMS (ESI+) (*m/z*): calculated for C₁₂H₁₃Br₁O₁Na₁ [M+Na]⁺: 275.0042; found: 275.0042.

GC The enantiomeric ratio was measured by GC analysis on Hydrodex-beta-TBDAC-CD column column: *t_R* = 38.84 min (major) and *t_R* = 40.29 min (minor), *er* (exocyclic alkene

7 EXPERIMENTAL PART

isomer) = 95:5; t_R = 46.66 min (minor) and t_R = 49.94 min (major), er (endocyclic alkene isomer) = 57:43.



(*R*)-2-(4-chlorophenyl)-4-methylenetetrahydro-2*H*-pyran

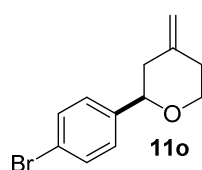
Prepared at 10 °C in cyclohexane. A colorless oil was obtained. 81% Isolated yield was obtained using pentane/diethylether = 95/5 as the eluents. The regiomic ratio of the isolated compound is >20:1 which was determined by GC analysis.

¹H NMR (500 MHz, CDCl₃): δ 7.33–7.29 (m, 4H), 4.82 (qd, J = 7.1 Hz, 1.8 Hz, 2H), 4.27 (dd, J = 11.3 Hz, 2.6 Hz, 1H), 4.22 (ddd, J = 11.0 Hz, 5.7 Hz, 1.1 Hz, 1H), 3.54 (ddd, J = 13.6 Hz, 11.0 Hz, 2.7 Hz, 1H), 2.45–2.38 (m, 2H), 2.29–2.21 (m, 2H).

¹³C NMR (126 MHz, CDCl₃): δ 144.2, 141.0, 133.3, 128.7, 127.4, 109.3, 80.2, 69.2, 43.3, 35.0.

HRMS (ESI+) (m/z): calculated for C₁₂H₁₃Cl₁O₁Na₁ [M+Na]⁺: 208.0654; found: 208.0653.

GC The enantiomeric ratio was measured by GC analysis on Hydrodex-beta-TBDAC-CD column column: t_R = 71.63 min (minor) and t_R = 72.40 min (major), er = 96:4.



(*R*)-2-(4-bromophenyl)-4-methylenetetrahydro-2*H*-pyran

Prepared at 10 °C in cyclohexane. A colorless oil was obtained. 86% Isolated yield was obtained using pentane/diethylether = 95/5 as the eluents. The regiomic ratio of the isolated compound is >20:1 which was determined by GC analysis.

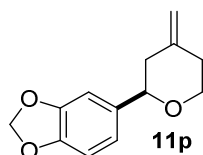
¹H NMR (500 MHz, CDCl₃): δ 7.49–7.46 (m, 2H), 7.26–7.24 (m, 2H), 4.82 (qd, J = 8.8 Hz, 1.7 Hz, 2H), 4.26–4.20 (m, 2H), 3.54 (ddd, J = 13.6 Hz, 11.1 Hz, 2.6 Hz, 1H), 2.45–2.38 (m, 2H), 2.28–2.21 (m, 2H).

7 EXPERIMENTAL PART

^{13}C NMR (126 MHz, CDCl_3): δ 144.1, 141.6, 131.6, 127.7, 121.4, 109.3, 80.2, 69.2, 43.2, 35.0.

HRMS (EI) (m/z): calculated for $\text{C}_{12}\text{H}_{13}\text{Br}_1\text{O}_1$ [M]: 252.0149; found: 252.0150.

GC The enantiomeric ratio was measured by GC analysis on Hydrodex-beta-TBDAC-CD column column: $t_{\text{R}} = 97.26$ min (minor) and $t_{\text{R}} = 98.48$ min (major), er = 96.5:3.5.



(*R*)-5-(4-methylenetetrahydro-2*H*-pyran-2-yl)benzo[d][1,3]dioxole

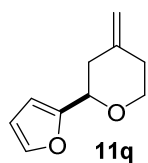
Prepared at 0 °C in methylcyclohexane. A colorless oil was obtained. 68% Isolated yield was obtained using pentane/diethylether = 95/5 as the eluents. The regiomeric ratio of the isolated compound is 16:1 which was determined by GC analysis.

^1H NMR (500 MHz, CDCl_3): δ 6.90 (d, $J = 1.6$ Hz, 1H), 6.83–6.81 (m, 1H), 6.78–6.77 (m, 1H), 5.94 (s, 2H), 4.80 (qd, $J = 9.5$ Hz, 1.8 Hz, 2H), 4.22–4.19 (m, 2H), 3.53 (ddd, $J = 13.6$ Hz, 11.0 Hz, 2.7 Hz, 1H), 2.44–2.37 (m, 2H), 2.32–2.26 (m, 1H), 2.23–2.19 (m, 1H).

^{13}C NMR (126 MHz, CDCl_3): δ 147.8, 147.0, 144.6, 136.6, 119.4, 109.0, 108.2, 106.8, 101.1, 80.9, 69.2, 43.3, 35.1.

HRMS (ESI+) (m/z): calculated for $\text{C}_{13}\text{H}_{14}\text{O}_3\text{Na}_1$ [M+Na] $^+$: 241.0835; found: 241.0836.

GC The enantiomeric ratio was measured by GC analysis C-DEXTRIN H/in G-632 column column: $t_{\text{R}} = 55.76$ min (minor) and $t_{\text{R}} = 57.22$ min (major), er (exocyclic alkene isomer) = 94:6; $t_{\text{R}} = 73.98$ min (major) and $t_{\text{R}} = 86.96$ min (minor), er (endocyclic alkene isomer) = 51:49.



(*R*)-2-(furan-2-yl)-4-methylenetetrahydro-2*H*-pyran

7 EXPERIMENTAL PART

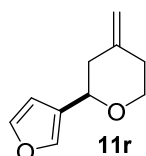
Prepared at 10 °C in cyclohexane. A colorless oil was obtained. 73% Isolated yield was obtained using pentane/diethylether = 95/5 as the eluents. The regiomic ratio of the isolated compound is 13:1 which was determined by GC analysis.

¹H NMR (500 MHz, CDCl₃): δ 7.40 (dd, *J* = 1.8 Hz, 0.85 Hz, 1H), 6.34 (dd, *J* = 3.3 Hz, 1.9 Hz, 1H), 6.31–6.30 (m, 1H), 4.82 (q, *J* = 1.7 Hz, 2H), 4.40 (dd, *J* = 10.8 Hz, 2.9 Hz, 1H), 4.12 (ddd, *J* = 11.0 Hz, 5.5 Hz, 2.1 Hz, 1H), 3.56 (ddd, *J* = 13.9 Hz, 11.1 Hz, 2.8 Hz, 1H), 2.61–2.56 (m, 1H), 2.52–2.49 (m, 1H), 2.44–2.37 (m, 1H), 2.23 (qd, *J* = 13.6 Hz, 2.3 Hz, 1H).

¹³C NMR (126 MHz, CDCl₃): δ 154.4, 143.5, 142.4, 110.2, 109.7, 106.9, 73.7, 68.7, 38.8, 35.0.

HRMS (EI) (*m/z*): calculated for C₁₀H₁₂O₂ [*M*]: 164.0837; found: 164.0835.

GC The enantiomeric ratio was measured by GC analysis on Hydrodex-beta-TBDAC-G-589 column: *t*_R = 19.24 min (major) and *t*_R = 24.92 min (minor), er (exocyclic alkene isomer) = 95:5; *t*_R = 27.47 min (minor) and *t*_R = 28.44 min (major), er (endocyclic alkene isomer 1) = 58:42; *t*_R = 28.97 min (major) and *t*_R = 29.58 min (minor), er (endocyclic alkene isomer 2) = 51:49.



(*R*)-2-(furan-3-yl)-4-methylenetetrahydro-2*H*-pyran

Prepared at 0 °C in methylcyclohexane. A colorless oil was obtained. 82% Isolated yield was obtained using pentane/diethylether = 95/5 as the eluents. The regiomic ratio of the isolated compound is 14:1 which was determined by GC analysis.

¹H NMR (500 MHz, CDCl₃): δ 7.41–7.39 (m, 2H), 6.43–6.42 (m, 1H), 4.81–4.79 (m, 2H), 4.30 (dd, *J* = 10.8 Hz, 2.7 Hz, 1H), 4.13 (ddd, *J* = 10.9 Hz, 5.4 Hz, 1.7 Hz, 1H), 3.53 (ddd, *J* = 13.8 Hz, 10.0 Hz, 2.8 Hz, 1H), 2.48–2.44 (m, 1H), 2.39–2.34 (m, 2H), 2.23–2.19 (m, 1H).

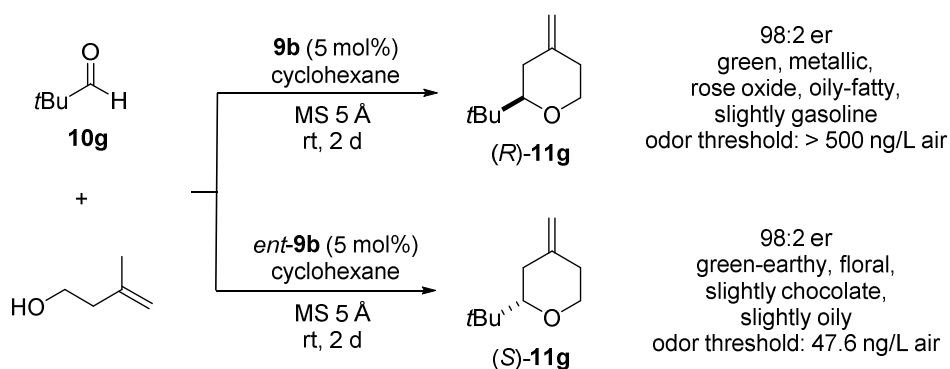
¹³C NMR (126 MHz, CDCl₃): δ 144.1, 143.3, 139.3, 127.0, 109.3, 108.9, 73.6, 68.8, 41.5, 35.1.

7 EXPERIMENTAL PART

HRMS (EI) (m/z): calculated for $C_{10}H_{12}O_2$ [M]: 164.0837; found: 164.0835.

GC The enantiomeric ratio was measured by GC analysis on Cyclodextrin-H/OV-1701 column: $t_R = 7.29$ min (minor) and $t_R = 7.77$ min (major), er (exocyclic alkene isomer) = 95:5; $t_R = 8.46$ min (minor) and $t_R = 8.66$ min (major), er (endocyclic alkene isomer 1) = 91:9; $t_R = 11.41$ min (minor) and $t_R = 14.11$ min (major), er (endocyclic alkene isomer 2) = 57:43.

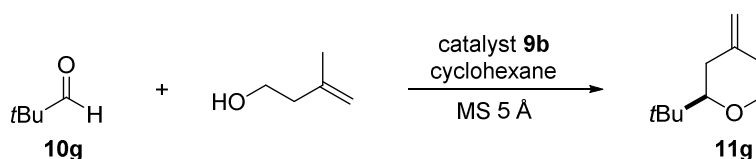
Synthesis of Both Enantiomers



Aldehyde **10g** (0.12 mmol) and 3-methyl-3-buten-1-ol (0.1 mmol) were added to a mixture of catalyst **9b** (5 μ mol, 5 mol%) and 50 mg 5 Å molecular sieves in anhydrous solvent (0.1 M). Purification was performed by chromatography on silica gel using pentane/diethylether = 95/5 as the eluent. The olfactory property of **(R)-11g** was measured by Givaudan (Switzerland). Using **ent-9b**, the corresponding enantiomer **(S)-11g** could be obtained.

7 EXPERIMENTAL PART

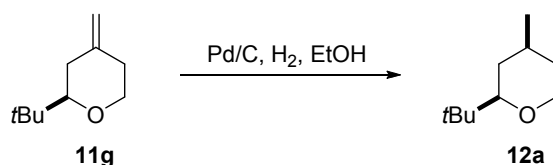
Gram-Scale Reaction



At room temperature, 4 g of 5 Å molecular sieves and catalyst **9b** (0.53 g/0.4 mmol) were added to 16 mL anhydrous cyclohexane and the mixture was stirred for 20 min. Then aldehyde **10g** (0.82 g/9.6 mmol) and 3-methyl-3-buten-1-ol (0.68 g/8.0 mmol) were added subsequently. The reaction was completed after 2 days. Purification of product **11g** was performed by column chromatography on silica gel using pentane/diethylether = 95/5 as the eluent. **11g** (1.02 g/6.6 mmol) was obtained after further distillation. The catalyst **9b** could be recycled by column chromatography on silica gel using hexane/ethyl acetate = 70:30 as the eluent giving a pale solid. The solid was dissolved in CH₂Cl₂ (5 mL) and stirred with 6 N aqueous HCl (5 mL) for 30 min. The organic layer was separated, washed with 6 N aqueous HCl (5 mL) and concentrated under reduced pressure to give the recycled catalyst **9b** (0.51 g, 95%).

The recycled catalyst **9b** was further used for another gram scale reaction. At room temperature, 4 g 5 Å molecular sieves and catalyst **9b** (0.10 g/0.08 mmol) were added to 16 ml anhydrous cyclohexane and the mixture was stirred for 20 min. Then aldehyde **10g** (0.82 g/9.6 mmol) and 3-methyl-3-buten-1-ol (0.68 g/8.0 mmol) were added subsequently. The reaction was completed after 7 days. Purification of product **11g** was performed by column chromatography on silica gel using pentane/diethylether = 95/5 as the eluent. **11g** (1.01 g/6.58 mmol) was obtained after further distillation.

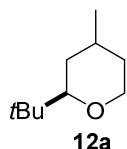
Derivatization



11g (100 mg, 0.65 mmol) was dissolved in dry, degassed ethanol (4 mL) at room temperature, then palladium (10%) on charcoal (40 mg) was added. An atmosphere of hydrogen was introduced and the resulting suspension was stirred at room temperature for 2 h. The reaction mixture was filtered over Celite, then concentrated with a rotary evaporator. The product **12a** was obtained by flash chromatography (pentane/diethylether

7 EXPERIMENTAL PART

= 95/5) as a clear oil (83 mg, 0.83 mmol, 82% yield). The *cis*-diastereomer was obtained as the major product, with a ratio of *cis:trans* = 8:1 which was determined by ¹H NMR spectroscopy. The olfactory property of **12a** was measured by Givaudan (Switzerland). The main isomer (2*R*, 4*S*)-2-(*tert*-butyl)-4-methyltetrahydro-2*H*-pyran **12a** smelled dry, woody-spicy, agrestic, slightly chocolate (order threshold: 250 ng/L air)



(2*R*, 4*S*)-2-(*tert*-Butyl)-4-methyltetrahydro-2*H*-pyran

¹H NMR (500 MHz, CD₂Cl₂): δ 3.94 (*cis* isomer, qd, *J* = 11.3, 1.4 Hz, 0.88H), 3.72 (*trans* isomer, ddq, *J* = 11.6 Hz, 5.3 Hz, 0.7 Hz, 0.11H), 3.64–3.59 (*trans* isomer, m, 0.11H), 3.34 (*cis* isomer, dt, *J* = 11.5 Hz, 2.2 Hz, 0.90H), 3.09 (*trans* isomer, dd, *J* = 11.9 Hz, 2.0 Hz, 0.11H), 2.83 (*cis* isomer, dd, *J* = 11.2 Hz, 1.6 Hz, 0.87H), 2.14–2.08 (*trans* isomer, m, 0.11H), 1.82–1.74 (*trans* isomer, m, 0.13H), 1.60–1.46 (m, *cis* isomer 2.5H and *trans* isomer 0.1H), 1.32 (*trans* isomer, qd, *J* = 13.1 Hz, 2.1 Hz, 0.12H), 1.22 (*trans* isomer, pd, *J* = 13.4 Hz, 1.9 Hz, 0.15H), 1.15–1.06 (*cis* isomer, m, 0.9H; δ at 1.08 *trans* isomer, d, *J* = 7.3 Hz, 0.39H), 0.93 (*cis* isomer, d, *J* = 6.4 Hz, 2.7H), 0.91–0.83 (*cis* isomer, m 0.94H; δ at 0.86 *cis* isomer, s, 8.2 H; δ at 0.84 *trans* isomer, s, 1.0H) (spectra complicated due to the presence of two diastereo isomers).

¹³C NMR (126 MHz, CD₂Cl₂): δ 85.8 (*cis* isomer), 79.7 (*trans* isomer), 68.7 (*cis* isomer), 63.7 (*trans* isomer), 35.4 (*cis* isomer), 35.0 (*cis* isomer), 34.2 (*cis* isomer), 34.15 (*trans* isomer), 32.1 (*trans* isomer), 31.8 (*trans* isomer), 31.1 (*cis* isomer), 26.3 (*cis* isomer), 26.2 (*trans* isomer), 25.7 (*trans* isomer), 22.8 (*cis* isomer), 17.8 (*trans* isomer).

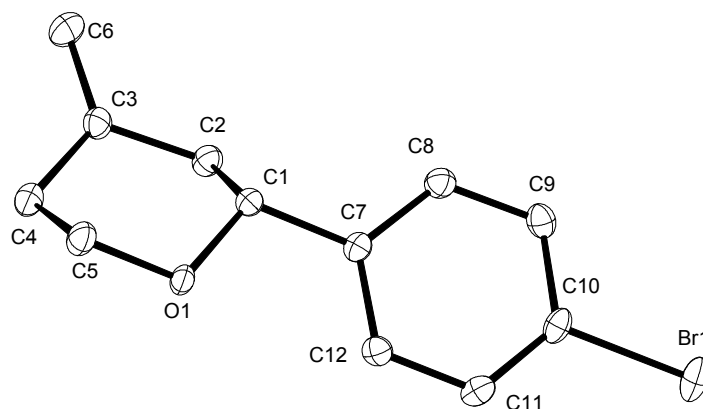
HRMS (EI) (*m/z*): calculated for C₁₀H₂₁O₁ [M]: 157.1592; found: 157.1591.

GC The enantiomeric ratio was measured by GC analysis on Hydrodex-gamma-TBDAC-CD column *t_R* (*cis*) = 11.08 min (major) and *t_R* (*cis*) = 11.95 min (minor), er = 97.5:2.5; *t_R* (*trans*) = 14.31 min (major) and *t_R* (*trans*) = 15.21 min (minor), er = 95.5:4.5.

7 EXPERIMENTAL PART

7.3.1.2 X-Ray Data

X-Ray Structural Analysis Parameter for 11o:



Crystal data and structure refinement:

Identification code	9749
Empirical formula	$C_{12}H_{13}Br_1O_1$
Color	colorless
Formula weight	$253.13 \text{ g} \cdot \text{mol}^{-1}$
Temperature	100 K
Wavelength	0.71073 \AA
Crystal system	MONOCLINIC
Space group	$P2_1$, (no. 4)
Unit cell dimensions	$a = 4.3752(18) \text{ \AA}$ $\alpha = 90^\circ$. $b = 9.783(4) \text{ \AA}$ $\beta = 98.083(6)^\circ$. $c = 12.561(5) \text{ \AA}$ $\gamma = 90^\circ$.
Volume	$532.3(4) \text{ \AA}^3$
Z	2
Density (calculated)	$1.579 \text{ Mg} \cdot \text{m}^{-3}$

7 EXPERIMENTAL PART

Absorption coefficient	3.825 mm ⁻¹	
F(000)	256 e	
Crystal size	0.275 x 0.220 x 0.040 mm ³	
θ range for data collection	1.638 to 30.841°.	
Index ranges	-6 \leq h \leq 6, -13 \leq k \leq 14, -17 \leq l \leq 18	
Reflections collected	10215	
Independent reflections	3321 [R _{int} = 0.0316]	
Reflections with I > 2 σ (I)	3036	
Completeness to $\theta = 27.500^\circ$	100.0 %	
Absorption correction	Gaussian	
Max. and min. transmission	0.86 and 0.48	
Refinement method	Full-matrix least-squares on F ²	
Data / restraints / parameters	3321 / 1 / 127	
Goodness-of-fit on F ²	1.174	
Final R indices [I > 2 σ (I)]	R ₁ = 0.0263	wR ² = 0.0744
R indices (all data)	R ₁ = 0.0319	wR ² = 0.0863
Absolute structure parameter	0.003(7)	
Largest diff. peak and hole	0.6 and -0.6 e · Å ⁻³	

Bond lengths [Å] and angles [°]

Br(1)-C(10)	1.898(3)	O(1)-C(1)	1.420(4)
O(1)-C(5)	1.435(5)	C(1)-C(2)	1.533(5)
C(1)-C(7)	1.516(5)	C(2)-C(3)	1.504(6)
C(3)-C(4)	1.496(6)	C(3)-C(6)	1.324(5)
C(4)-C(5)	1.519(6)	C(7)-C(8)	1.390(5)
C(7)-C(12)	1.392(5)	C(8)-C(9)	1.391(5)

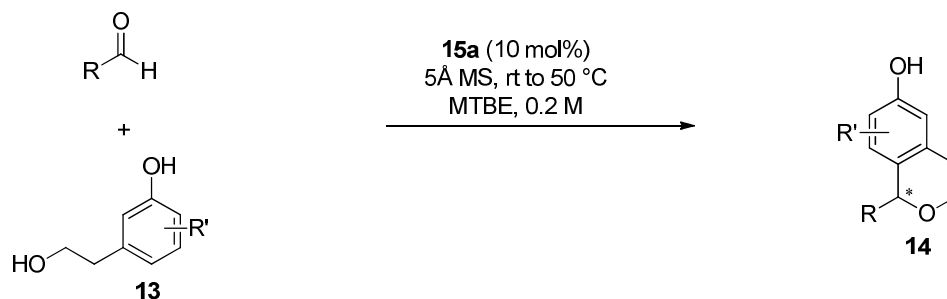
7 EXPERIMENTAL PART

C(9)-C(10)	1.399(6)	C(10)-C(11)	1.369(6)
C(11)-C(12)	1.396(5)		
C(1)-O(1)-C(5)	111.3(3)	O(1)-C(1)-C(2)	110.2(3)
O(1)-C(1)-C(7)	108.5(3)	C(7)-C(1)-C(2)	113.2(3)
C(3)-C(2)-C(1)	110.0(3)	C(4)-C(3)-C(2)	113.4(3)
C(6)-C(3)-C(2)	122.9(4)	C(6)-C(3)-C(4)	123.7(4)
C(3)-C(4)-C(5)	110.3(3)	O(1)-C(5)-C(4)	110.8(3)
C(8)-C(7)-C(1)	119.7(3)	C(8)-C(7)-C(12)	118.9(3)
C(12)-C(7)-C(1)	121.3(3)	C(7)-C(8)-C(9)	121.6(3)
C(8)-C(9)-C(10)	117.7(3)	C(9)-C(10)-Br(1)	118.4(3)
C(11)-C(10)-Br(1)	119.4(3)	C(11)-C(10)-C(9)	122.2(3)
C(10)-C(11)-C(12)	119.0(3)	C(7)-C(12)-C(11)	120.6(3)

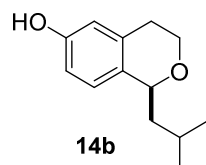
7 EXPERIMENTAL PART

7.3.2 Oxa-Pictet–Spengler Reaction

7.3.2.1 Products



A 2 mL GC vial was charged with starting material (0.1 mmol), catalyst (14.0 mg, 0.01 equiv., 10 mol%), molecular sieves 5 Å (50 mg) and a magnetic stirring bar at room temperature. Then 500 μ L (0.2 M) of MTBE was added followed by aldehyde (2.5 equiv., 0.25 mmol). The vial was filled with argon and sealed. It was then introduced to the desired temperature for the reaction. The progress of the reaction was monitored by TLC. For aromatic aldehydes, the reactions were quenched with trimethylamine. Purification was performed by column chromatography or preparative thin layer chromatography on silica gel using EtOAc/hexanes as eluents.



(*S*)-1-isobutylisochroman-6-ol

Prepared according to the general procedure. 18.0 mg yellow oil, 87%.

$^1\text{H NMR}$ (500 MHz, CDCl_3): δ 6.92 (d, $J = 8.5$ Hz, 1H), 6.65 (dd, $J = 8.4, 2.7$ Hz, 1H), 6.57 (d, $J = 2.7$ Hz, 1H), 4.72 (d, $J = 10.1$ Hz, 1H), 4.09 (ddd, $J = 11.5, 5.5, 1.8$ Hz, 1H), 3.75 (ddd, $J = 12.9, 8.8, 4.0$ Hz, 1H), 2.90 (ddd, $J = 16.3, 8.8, 5.3$ Hz, 1H), 2.66 (td, $J = 16.4, 4.2$ Hz, 1H), 2.08–1.86 (m, 1H), 1.75 (ddd, $J = 11.9, 10.2, 3.8$ Hz, 1H), 1.59–1.51 (m, 1H), 1.01 (d, $J = 6.6$ Hz, 3H), 0.95 (d, $J = 6.6$ Hz, 3H).

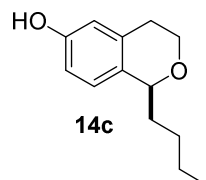
$^{13}\text{C NMR}$ (126 MHz, CDCl_3): δ 153.76, 135.45, 131.61, 126.21, 115.14, 113.48, 73.96, 62.74, 45.52, 29.37, 24.59, 24.12, 21.68.

HRMS (ESI+) (m/z): calculated for $\text{C}_{13}\text{H}_{18}\text{O}_2\cdot\text{H}$ $[\text{M}+\text{H}]^+$: 207.138070; found: 207.137955.

7 EXPERIMENTAL PART

HPLC The enantiomeric ratio was measured by HPLC analysis using ChiralpakOJ-3, heptane/ *i*PrOH = 85:15, flow rate = 1.0 mL/min, λ = 279 nm, t_R = 5.7 min (major) and t_R = 8.9 min (minor). er = 96.8:3.2.

$[\alpha]_D^{25} = -70.0$ (*c* 0.50, CHCl₃).



(*S*)-1-butylisochroman-6-ol

Prepared according to the general procedure. 17.0 mg colorless oil, 82%.

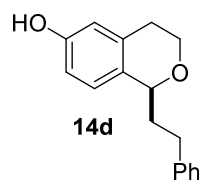
¹H NMR (500 MHz, CDCl₃): δ 6.95 (d, *J* = 6.4 Hz, 1H), 6.67 (dd, *J* = 8.4, 2.6 Hz, 1H), 6.57 (d, *J* = 2.6 Hz, 1H), 4.68 (dd, *J* = 7.9, 1.7 Hz, 1H), 4.1 (td, *J* = 5.6, 3.7 Hz, 1H), 3.74 (ddd, *J* = 12.6, 8.8, 3.7 Hz, 1H), 2.93 (ddd, *J* = 16.3, 9.5, 4.9 Hz, 1H), 2.62 (td, *J* = 16.3, 3.6 Hz, 1H), 1.94–1.82 (m, 1H), 1.81–1.70 (m, 1H), 1.51–1.30 (m, 4H), 0.91 (t, *J* = 7.3 Hz, 3H).

¹³C NMR (126 MHz, CDCl₃): δ 153.85, 135.61, 130.97, 126.22, 115.12, 113.58, 75.92, 63.14, 35.88, 29.41, 27.50, 22.95, 14.23.

HRMS (ESI+) (*m/z*): calculated for C₁₃H₁₈O₂H [M+H]⁺: 207.138000; found: 207.137955.

HPLC The enantiomeric ratio was measured by HPLC analysis using ChiralpakOD-3, heptane/ *i*PrOH = 95:5, flow rate = 0.5 mL/min, λ = 279 nm, t_R = 12.7 min (major) and t_R = 14.4 min (minor). er = 97.3:2.7.

$[\alpha]_D^{25} = -81.6$ (*c* 0.50, CHCl₃).



(*S*)-1-phenethylisochroman-6-ol

Prepared according to the general procedure. 20.5 mg yellow oil, 80.6%.

¹H NMR (500 MHz, CDCl₃): δ 7.28 (t, *J* = 7.7 Hz, 2H), 7.23 (d, *J* = 7.5 Hz, 2H), 7.18 (t, *J* = 7.4 Hz, 1H), 6.93 (d, *J* = 8.4 Hz, 1H), 6.65 (dd, *J* = 8.4, 2.6 Hz, 1H), 6.59 (d, *J* = 2.6 Hz, 1H), 4.78–4.63 (m, 1H), 4.23–4.09 (m, 1H), 3.85–3.71 (m, 1H), 2.97 (ddd, *J* = 16.4, 9.5, 5.4 Hz, 1H), 2.77 (t, *J* = 8.9 Hz, 2H), 2.65 (td, *J* = 16.4, 3.6 Hz, 1H), 2.63–2.13 (m, 1H), 2.13–1.97 (m, 1H), 1.62 (br s, 1H).

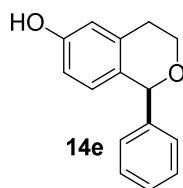
7 EXPERIMENTAL PART

^{13}C NMR (126 MHz, CDCl_3): δ 153.88, 142.54, 135.74, 123.62, 128.66, 128.48, 126.13, 125.86, 11.20, 113.63, 75.11, 63.23, 37.90, 31.50, 29.41.

HRMS (ESI+) (m/z): calculated for $\text{C}_{17}\text{H}_{18}\text{O}_2\text{Na}$ $[\text{M}+\text{Na}]^+$: 277.120080; found: 277.119899.

HPLC The enantiomeric ratio was measured by HPLC analysis using ChiralpakAD-3, heptane/ *i*PrOH = 90:10, flow rate = 1.0 mL/min, λ = 279 nm, t_{R} = 7.6 min (major) and t_{R} = 8.7 min (minor). er = 97.4:2.6.

$[\alpha]_{\text{D}}^{25} = -27.6$ (c 0.55, CHCl_3).



(S)-1-phenylisochroman-6-ol

Prepared according to the general procedure. 20.6 mg white solid, 91%.

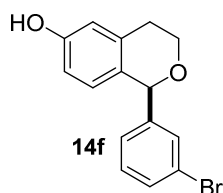
^1H NMR (500 MHz, CD_2Cl_2): δ 7.42–7.22 (m, 5H), 6.61 (d, J = 2.5 Hz, 1H), 6.58 (d, J = 8.4 Hz, 1H), 6.55 (dd, J = 8.4, 2.5 Hz, 1H), 5.65 (s, 1H), 5.12 (br s, 1H), 4.13 (ddd, J = 11.3, 5.6, 3.7 Hz, 1H), 3.87 (ddd, J = 13.6, 9.6, 4.0 Hz, 1H), 3.06 (ddd, J = 16.4, 9.5, 5.5 Hz, 1H), 2.73 (dd, J = 16.5, 3.8 Hz, 1H).

^{13}C NMR (126 MHz, CD_2Cl_2): δ 154.82, 143.26, 136.13, 123.32, 129, 30, 128.83, 128.63, 128.50, 79.87, 64.15, 29.48.

HRMS (ESI-) (m/z): calculated for $\text{C}_{15}\text{H}_{13}\text{O}_2$ $[\text{M}-\text{H}]^-$: 225.092080; found: 225.092105.

HPLC The enantiomeric ratio was measured by HPLC analysis using ChiralpakOD-3, heptane/ *i*PrOH = 90:10, flow rate = 1.0 mL/min, λ = 279 nm, t_{R} = 7.1 min (major) and t_{R} = 12.7 min (minor). er = 96.7:3.3.

$[\alpha]_{\text{D}}^{25} = -14.8$ (c 0.50, CHCl_3).



(S)-1-(3-bromophenyl)isochroman-6-ol

Prepared according to the general procedure. 22.8 mg yellow solid, 75%.

7 EXPERIMENTAL PART

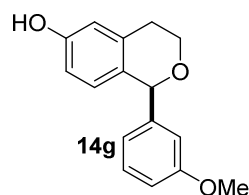
¹H NMR (500 MHz, CDCl₃): δ 7.49–7.41 (m, 2H), 7.26–7.17 (m, 2H), 6.65–6.52 (m, 3H), 5.64 (s, 1H), 4.99 (br s, 1H), 4.15 (ddd, *J* = 11.4, 5.6, 3.8 Hz, 1H), 3.89 (ddd, *J* = 13.5, 9.6, 4.1 Hz, 1H), 3.07 (ddd, *J* = 16.5, 9.5, 5.7 Hz, 1H), 2.74 (dd, *J* = 16.4, 3.9 Hz, 1H).

¹³C NMR (126 MHz, CDCl₃): δ 154.41, 144.67, 135.49, 131.92, 131.37, 130.11, 128.90, 128.27, 12.61, 122.69, 115.07, 113.73, 78.86, 63.84, 28.90.

HRMS (ESI+) (*m/z*): calculated for C₁₅H₁₃BrO₂.Na [M+Na]⁺: 326.999270; found: 326.999124.

HPLC The enantiomeric ratio was measured by HPLC analysis using Chiralpak AS-3, heptane/ *i*PrOH = 90:10, flow rate = 1.0 mL/min, λ = 279 nm, *t*_R = 5.2 min (major) and *t*_R = 5.9 min (minor). er = 99.2:0.8.

[α]_D²⁵ = -5.6 (*c* 0.50, CHCl₃).



(*S*)-1-(3-methoxyphenyl)isochroman-6-ol

Prepared according to the general procedure. 23.8 mg yellow oil, 93%.

¹H NMR (500 MHz, CDCl₃): δ 7.34–7.17 (m, 1H), 6.90 (d, *J* = 7.6 Hz, 1H), 6.88–6.80 (m, 2H), 6.63 (d, *J* = 8.4 Hz, 1H), 6.59 (d, *J* = 2.6 Hz, 1H), 6.54 (dd, *J* = 8.4, 2.6 Hz, 1H), 5.65 (s, 1H), 5.08 (br s, 1H), 4.16 (ddd, *J* = 11.4, 5.5, 3.9 Hz, 1H), 3.90 (ddd, *J* = 13.6, 9.5, 4.1 Hz, 1H), 3.78 (s, 3H), 3.06 (ddd, *J* = 16.4, 9.4, 5.6 Hz), 2.74 (dd, *J* = 16.4, 4.0, 1H).

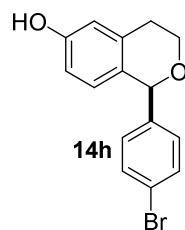
¹³C NMR (126 MHz, CDCl₃): δ 159.76, 154.31, 143.87, 135.41, 129.52, 129.48, 128.32, 121.41, 114.91, 114.38, 113.84, 113.57, 79.48, 63.78, 55.37, 29.00.

HRMS (ESI+) (*m/z*): calculated for C₁₆H₁₆O₃.Na [M+Na]⁺: 279.099350; found: 279.099164.

HPLC The enantiomeric ratio was measured by HPLC analysis using Chiralpak AD-3, heptane/ *i*PrOH = 94:6, flow rate = 1.0 mL/min, λ = 279 nm, *t*_R = 19.4 min (minor) and *t*_R = 20.6 min (major). er = 98.1:1.9.

[α]_D²⁵ = -14.4 (*c* 0.50, CHCl₃).

7 EXPERIMENTAL PART



(S)-1-(4-bromophenyl)isochroman-6-ol

Prepared according to the general procedure. 26.4 mg yellow solid, 87%.

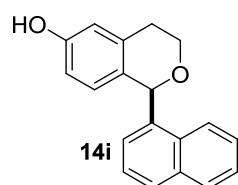
¹H NMR (500 MHz, CDCl₃): δ 7.46 (d, *J* = 8.4 Hz, 2H), 7.18 (d, *J* = 8.4 Hz, 2H), 6.89–6.31 (m, 3H), 5.64 (s, 1H), 5.13 (br s, 1H), 4.14 (ddd, *J* = 11.4, 5.4, 3.9 Hz, 1H), 3.90 (ddd, *J* = 13.5, 9.6, 4.0 Hz, 1H), 3.06 (ddd, *J* = 16.5, 9.6, 5.5 Hz, 1H), 2.73 (td, *J* = 16.5, 4.0 Hz, 1H).

¹³C NMR (126 MHz, CDCl₃): δ 154.42, 141.36, 135.45, 131.69, 130.66, 129.05, 128.23, 122.29, 115.02, 113.67, 78.88, 63.82, 28.95.

HRMS (ESI+) *m/z* calculated for C₁₅H₁₃BrO₂Na [M+Na]⁺: 326.999310; found: 326.999124.

HPLC The enantiomeric ratio was measured by HPLC analysis using Chiralpak AD-3, heptane/ *i*PrOH = 90:10, flow rate = 1.0 mL/min, λ = 279 nm, *t*_R = 4.9 min (major) and *t*_R = 5.3 min (minor). er = 98.2:1.8.

[α]_D²⁵ = +4.0 (*c* 0.50, CHCl₃).



(S)-1-(naphthalen-1-yl)isochroman-6-ol

Prepared according to the general procedure. 20.1 mg yellow solid, 73%.

¹H NMR (500 MHz, CDCl₃): δ 7.90–7.79 (m, 3H), 7.76 (s, 1H), 7.55–7.44 (m, 2H), 7.40 (dd, *J* = 8.6, 1.7 Hz, 1H), 6.64 (d, *J* = 2.5 Hz, 1H), 6.62 (d, *J* = 3.50 Hz, 1H), 6.53 (dd, *J* = 8.50, 2.6 Hz, 1H), 5.84 (s, 1H), 4.20 (ddd, *J* = 11.4, 5.6, 3.8 Hz, 1H), 3.95 (ddd, *J* = 13.6, 9.6, 4.40 Hz, 1H), 3.12 (ddd, *J* = 16.5, 9.5, 5.5 Hz, 1H), 2.76 (dd, *J* = 16.5, 3.8, 1H).

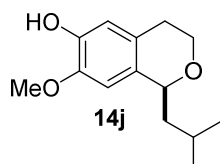
¹³C NMR (126 MHz, CDCl₃): δ 154.29, 139.72, 135.59, 133.37, 133.20, 129.67, 128.56, 128.50, 128.21, 128.16, 127.82, 126.53, 126.23, 114.98, 113.60, 79.74, 63.89, 29.07.

7 EXPERIMENTAL PART

HRMS (ESI+) m/z calculated for $C_{19}H_{16}O_2Na$ $[M+Na]^+$: 299.104430; found: 299.104249.

HPLC The enantiomeric ratio was measured by HPLC analysis using Chiralpak AD-3, heptane/ i PrOH = 94:6, flow rate = 1.0 mL/min, λ = 279 nm, t_R = 12.3 min (major) and t_R = 13.5 min (minor). er = 95.4:4.6.

$[\alpha]_D^{25} = +25.4$ (c 0.27, $CHCl_3$).



(*S*)-1-isobutyl-7-methoxyisochroman-6-ol

Prepared according to the general procedure. 21.7 mg white solid, 92%.

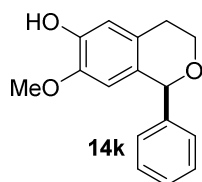
1H NMR (500 MHz, CD_2Cl_2): δ 6.61 (s, 1H), 6.53 (s, 1H), 5.53 (br s, 1H), 4.67 (dd, J = 10.4, 2.0 Hz, 1H), 4.07–3.99 (m, 1H), 3.84 (s, 3H), 3.69 (ddd, J = 12.8, 8.7, 4.1 Hz, 1H), 2.79 (tddd, J = 16.2, 8.7, 5.3, 1.0 Hz, 1H), 2.58 (dd, J = 16.1, 4.4 Hz, 1H), 2.01–1.87 (m, 1H), 1.71 (ddd, J = 14.4, 10.4, 3.9 Hz, 1H), 1.54 (ddd, J = 14.2, 9.9, 2.9 Hz, 1H), 1.01 (d, J = 6.7 Hz, 3H), 0.95 (d, J = 6.7 Hz, 3H).

^{13}C NMR (126 MHz, $CDCl_3$): δ 145.64, 144.47, 131.27, 127.16, 124.68, 107.84, 74.14, 63.12, 56.63, 45.83, 28.99, 25.05, 24.30, 21.80.

HRMS (ESI-) m/z calculated for $C_{14}H_{19}O_3$ $[M-H]^-$: 235.133940; found: 235.133970.

HPLC The enantiomeric ratio was measured by HPLC analysis using OD-3, heptane/ i PrOH = 95:5, flow rate = 1 mL/min, λ = 279 nm t_R = 5.8 min (major) and t_R = 7.0 min (minor). er = 99.6:0.4.

$[\alpha]_D^{25} = -116.4$ (c 0.50, $CHCl_3$).



(*S*)-7-methoxy-1-phenylisochroman-6-ol

Prepared according to the general procedure. 25.0 mg yellow solid, 98%.

1H NMR (500 MHz, $CDCl_3$): δ 7.43–7.28 (m, 5H), 6.73 (s, 1H), 6.21 (s, 1H), 5.67 (s, 1H), 5.56 (br s, 1H), 4.13 (ddd, J = 11.3, 5.3, 4.3 Hz, 1H), 3.88 (ddd, J = 13.3, 9.1, 4.1

7 EXPERIMENTAL PART

Hz, 1H), 3.36 (s, 3H), 3.01 (ddd, $J = 16.20, 9.1, 5.4$ Hz, 1H), 2.71 (dd, $J = 16.1, 4.2$ Hz, 1H).

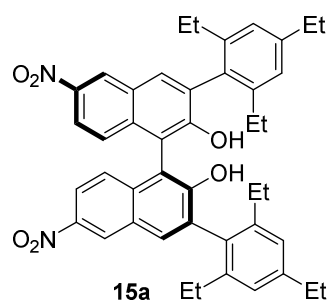
^{13}C NMR (126 MHz, CDCl_3): δ 159.76, 154.31, 143.87, 135.41, 129.52, 129.48, 128.32, 121.41, 114.91, 114.38, 113.84, 113.57, 79.48, 63.78, 55.37, 29.00.

HRMS (ESI+) (m/z): calculated for $\text{C}_{16}\text{H}_{16}\text{O}_3\text{Na}$ $[\text{M}+\text{Na}]^+$: 279.099230; found: 279.099164.

HPLC The enantiomeric ratio was measured by HPLC analysis using ChiralpakAD-3, heptane/ *i*PrOH = 95:5, flow rate = 1.0 mL/min, $\lambda = 279$ nm, $t_{\text{R}} = 11.8$ min (major) and $t_{\text{R}} = 16.2$ min (minor). er = 98.8:1.2.

$[\alpha]_{\text{D}}^{25} = -60.3$ (c 0.60, CHCl_3).

7.3.2.2 Catalysts synthesis



(1*S*,3'*S*)-6,6'-Dinitro-3,3'-bis(2,4,6-triethylphenyl)-[1,1'-binaphthalene]-2,2'-diol

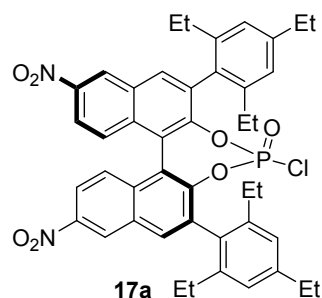
A solution of HNO_3 (94 μL , 2 mmol) in CHCl_3 (1.3 mL) was added dropwise to the solution of corresponding BINOL (570mg, 0.94 mmol) in CHCl_3 (5.6 mL) at -40 °C under argon. After 20 min at 0 °C, the solution was warmed up to room temperature for further 20 min. The reaction was cooled to 0 °C, and then water (45 mL) was carefully added, and the mixture was extracted with CH_2Cl_2 (45 \times 3 mL). The organic layer was collected, dried (MgSO_4), filtered, and the solvent was removed under reduced pressure. The residue was purified by column chromatography on silica gel using 50% CH_2Cl_2 /hexane as the eluent yielding the title compound as a yellow solid (504mg, 77%).

^1H NMR (500 MHz, CD_2Cl_2): δ 8.87 (d, $J = 1.5$ Hz, 2H), 8.09 (dd, $J = 9.2$ Hz, 1.7 Hz, 2H), 8.02 (br s, 2H), 7.34 (d, $J = 9.2$ Hz, 2H), 7.14 (d, $J = 7.8$ Hz, 4H), 5.43 (br s, 2H), 2.71 (q, $J = 7.5$ Hz, 4H), 2.54–2.31 (m, 8H), 1.30 (t, $J = 7.5$ Hz, 6H), 1.11 (t, $J = 7.4$ Hz, 6H), 1.02 (t, $J = 7.4$ Hz, 6H).

^{13}C NMR (126 MHz, CD_2Cl_2): δ 154.1, 146.2, 144.4, 144.1, 144.0, 136.9, 133.3, 131.8, 129.7, 127.9, 126.8, 126.7, 126.0, 125.6, 120.5, 114.5, 29.2, 27.4, 27.3, 15.7, 15.6.

7 EXPERIMENTAL PART

HRMS (ESI⁻) (*m/z*): calculated for C₄₄H₄₃N₂O₆ [M-H]⁻: 695.312662; found: 695.312750.



(2*S*,4*R*,11*bS*)-4-chloro-9,14-dinitro-2,6-bis(2,4,6-triethylphenyl)dinaphtho[2,1-*d*:1',2'-*f*][1,3,2]dioxaphosph-epine 4-oxide

To a solution of **15a** (350 mg, 0.50 mmol) in pyridine (1.6 mL) under argon was added POCl₃ (466 μL, 5.0 mmol) at room temperature. The mixture was stirred at room temperature for 5 h and then concentrated to dryness under vacuum. The residue was passed through a short silica gel column using 40% CH₂Cl₂/hexane as the eluent yielding the title compound as a colorless solid (350 mg, 90%).

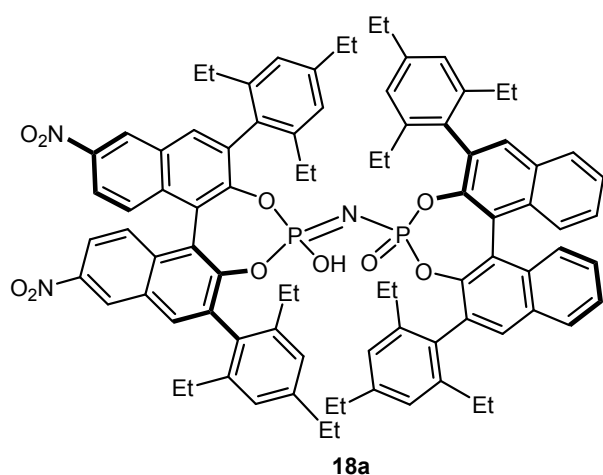
¹H NMR (600 MHz, CDCl₃): δ 8.94 (dd, *J* = 6.1 Hz, 2.3 Hz, 2H), 8.20 (d, *J* = 17.4 Hz, 2H), 8.15 (dq, *J* = 9.4 Hz, 0.9 Hz, 2H), 7.36 (dd, *J* = 9.3 Hz, 6.8 Hz, 2H), 7.13 (d, *J* = 28.4 Hz, 2H), 7.02 (d, *J* = 7.9 Hz, 2H), 2.74–2.69(m, 4H), 2.56–2.24(m, 8H), 1.36–1.31 (m, 6H), 1.27 (t, *J* = 7.5 Hz, 3H), 1.21 (t, *J* = 7.6 Hz, 3H), 7.36 (dt, *J* = 7.6 Hz, 4.0 Hz, 6H).

¹³C NMR (151 MHz, CDCl₃): δ 148.0, 147.9, 147.8, 145.9, 145.2, 144.9, 143.0, 142.5, 142.0, 141.7, 135.6, 135.5, 135.3, 135.1, 134.7, 134.6, 134.4, 134.3, 130.7, 130.4, 130.0, 129.8, 128.3, 128.2, 125.64, 125.62, 125.3, 125.1, 125.0, 124.7, 122.0, 121.9, 121.84, 121.82, 120.7, 120.6, 28.81, 28.80, 27.5, 27.0, 26.8, 16.1, 15.3, 15.2, 15.18, 14.7, 14.5.

³¹P NMR (202 MHz, CDCl₃): δ 6.52 (s).

HRMS (ESI⁺) (*m/z*): calculated for C₄₄H₄₂N₂O₇P₁Na₁ [M+Na]⁺: 799.231039; found: 799.230700.

7 EXPERIMENTAL PART



4-((4-hydroxy-9,14-dinitro-2,6-bis(2,4,6-triethylphenyl)-415-dinaphtho[2,1-d:1',2'-][1,3,2]dioxaphosphepin-4-ylidene)amino)-2,6-bis(2,4,6-triethylphenyl)dinaphtho[2,1-d:1',2'-f][1,3,2]dioxaphosphepine 4-oxide

Sodium hydride (60% dispersion in mineral oil, 48 mg, 1.2 mmol) was added to a solution of **16a** (250 mg, 0.32 mmol) and **17a** (203 mg, 0.30 mmol) in DMF (3 ml) under argon at room temperature. After 2.5 h at room temperature, 10% aqueous HCl solution (1 mL) was added. The organic layer was separated and the solvent was removed under reduced pressure. The residue was purified by column chromatography on silica gel using 5–15% ethyl acetate/hexane as the eluents giving a colorless solid. The solid was dissolved in CH₂Cl₂ (5 mL) and stirred with 6N aqueous HCl (5 mL) for 1 h. The organic layer was separated, washed with 6N aqueous HCl (5 mL) and concentrated under reduced pressure to give the title compound as a pale yellow solid (206 mg, 48%).

¹H NMR (500 MHz, CD₂Cl₂): δ 8.87 (d, *J* = 2.3 Hz, 1H), 8.84 (d, *J* = 2.3 Hz, 1H), 8.15 (dd, *J* = 9.3 Hz, 2.4 Hz, 1H), 8.05 (br s, 1H), 7.97 (dd, *J* = 9.4 Hz, 2.4 Hz, 1H), 7.90 (t, *J* = 8.4 Hz, 2H), 7.84 (d, *J* = 14.5 Hz, 2H), 7.61 (br s, 1H), 7.56–7.53(m, 1H), 7.48–7.42(m, 4H), 7.25–7.21(m, 1H), 7.06 (t, *J* = 9.8 Hz, 2H), 6.98 (d, *J* = 4.9 Hz, 2H), 6.87–6.86(m, 4H), 6.44 (br s, 1H), 6.33 (br s, 1H), 2.63–2.49(m, 8H), 2.29–2.09(m, 10H), 2.05–1.90(m, 3H), 1.78–1.71 (m, 1H), 1.22–1.15(m, 12H), 1.09 (q, *J* = 7.7 Hz, 6H), 0.98–0.92(m, 7H), 0.86–0.79(m, 7H), 0.08–0.01(m, 6H).

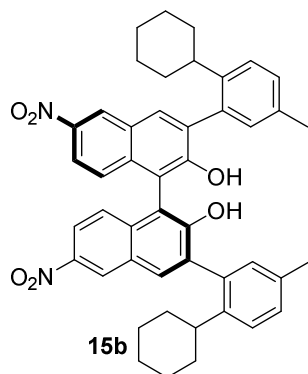
¹³C NMR (126 MHz, CD₂Cl₂): δ 150.4, 150.3, 149.5, 149.4, 146.1, 146.0, 145.8, 145.7, 145.67, 145.59, 145.0, 144.7, 144.6, 144.3, 144.1, 144.0, 143.71, 143.70, 143.4, 143.0, 142.9, 142.3, 136.3, 136.27, 135.8, 135.77, 135.7, 135.3, 135.2, 134.5, 133.3, 133.28, 133.0, 132.9, 132.7, 132.6, 132.0, 131.9, 131.88, 131.7, 130.6, 130.0, 128.9, 128.3, 127.8, 127.3, 127.0, 126.9, 126.4, 126.2, 126.0, 125.8, 125.7, 125.6, 125.4, 125.2, 125.1, 125.08, 124.9, 122.8, 122.7, 122.5, 122.2, 120.5, 120.3, 30.2, 29.2, 29.19, 29.18, 29.1,

7 EXPERIMENTAL PART

27.5, 27.45, 27.4, 27.22, 27.2, 27.1, 24.1, 17.8, 17.77, 16.3, 16.0, 15.9, 15.8, 15.6, 15.5, 15.4, 15.3, 15.1.

^{31}P NMR (202 MHz, CD_2Cl_2): δ 5.90 (d, $J = 86.0$, 1P), 3.54 (d, $J = 85.5$, 1P).

HRMS (ESI $^-$) (m/z): calculated for $\text{C}_{88}\text{H}_{86}\text{N}_3\text{O}_{10}\text{P}_2$ $[\text{M}-\text{H}]^-$: 1406.579400; found: 1406.579070.



(*S*)-3,3'-bis(2-cyclohexyl-5-methylphenyl)-6,6'-dinitro-[1,1'-binaphthalene]-2,2'-diol

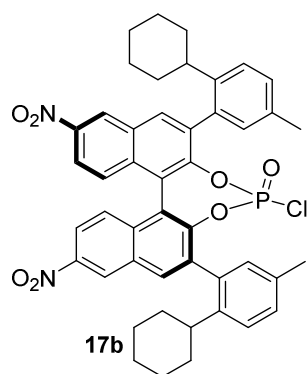
A solution of HNO_3 (63 μL , 1.4 mmol) in CHCl_3 (1 mL) was added dropwise to a solution of corresponding BINOL (441mg, 0.70 mmol) in CHCl_3 (4.2 mL) at -40 $^\circ\text{C}$ under argon. Then the solution was warmed up to room temperature for further 30 min. The reaction was cooled to 0 $^\circ\text{C}$, and water (35 mL) was carefully added, and the mixture was extracted with CH_2Cl_2 (3×35 mL). The organic layer was collected, dried over MgSO_4 , filtered, and the solvent was removed under reduced pressure. The residue was purified by column chromatography on silica gel using 50% CH_2Cl_2 /hexane as the eluent yielding the title compound as a yellow solid (434 mg, 86%).

^1H NMR (300 MHz, CDCl_3 , major): δ 8.87–8.85 (m, 2H), 8.12–8.00 (m, 4H), 7.40–7.28 (m, 6H), 7.22 (br s, 1H), 7.16–7.15 (m, 1H), 5.37–5.29 (m, 2H), 2.50–2.37 (m, 8H), 1.82–1.54 (m, 11H), 1.45–0.87 (m, 9H).

^{13}C NMR (75 MHz, CDCl_3 , major): δ 153.4, 153.3, 153.2, 144.43, 144.4, 144.36, 144.3, 144.29, 144.2, 144.1, 136.6, 136.5, 136.45, 136.4, 136.36, 133.2, 133.0, 132.97, 132.93, 132.89, 132.6, 132.3, 131.2, 130.8, 130.7, 127.7, 127.5, 127.47, 127.2, 127.1, 127.07, 125.9, 125.6, 125.4, 120.6, 120.5, 114.1, 114.06, 113.9, 41.4, 41.3, 41.04, 41.0, 35.3, 35.1, 35.0, 34.96, 34.0, 27.3, 27.0, 26.9, 26.1, 21.1, 21.0.

HRMS (ESI $^-$) (m/z): calculated for $\text{C}_{46}\text{H}_{43}\text{N}_2\text{O}_6$ $[\text{M}-\text{H}]^-$: 719.3126; found: 719.3127.

7 EXPERIMENTAL PART



(4*R*,11*bS*)-4-chloro-2,6-bis(2-cyclohexyl-5-methylphenyl)-9,14-dinitrodinaphtho[2,1-*d*:1',2'-*f*][1,3,2]dioxaphosphine 4-oxide

POCl₃ (96 μL, 0.77 mmol) was added to a solution of **15b** (184 mg, 0.256 mmol) in pyridine (0.8 mL) under argon at room temperature. The mixture was stirred at room temperature for 5 h and then concentrated to dryness under vacuum. The residue was filtered over a short silica gel column using 40% CH₂Cl₂/hexane as the eluent yielding the title compound as a pale yellow solid (170 mg, 83%).

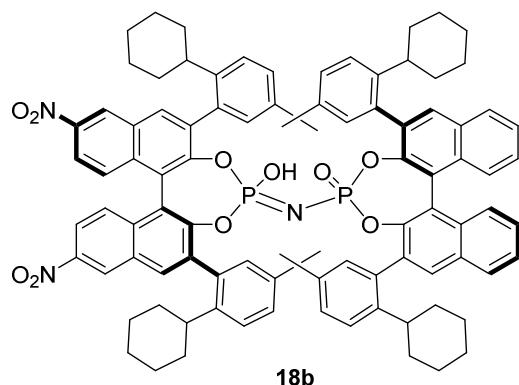
¹H NMR (300 MHz, CDCl₃): δ 9.05–8.91 (m, 2H), 8.25–8.12 (m, 4H), 7.48–7.27 (m, 6.5H), 7.22–7.05 (m, 1.4H), 2.39–2.19 (m, 8H), 2.01–1.56 (m, 9H), 1.51–0.77 (m, 11H) (spectra complicated due to presence of rotamers).

¹³C NMR (126 MHz, CDCl₃): δ 147.54, 147.5, 147.44, 147.41, 147.3, 146.2, 146.1, 146.03, 146.01, 143.9, 143.87, 143.5, 143.4, 142.8, 142.7, 136.9, 136.86, 136.7, 136.67, 136.6, 135.5, 135.3, 135.1, 135.0, 135.0, 134.96, 134.8, 134.7, 134.5, 134.4, 134.3, 134.2, 134.1, 133.2, 133.0, 132.9, 132.5, 132.4, 132.0, 131.9, 131.7, 131.6, 131.5, 131.4, 130.93, 130.90, 130.86, 130.4, 130.3, 130.2, 130.1, 130.0, 128.5, 128.4, 128.2, 128.0, 127.8, 127.7, 127.6, 127.5, 126.3, 125.9, 125.4, 125.3, 125.2, 125.1, 125.0, 122.8, 122.5, 121.7, 121.5, 121.47, 121.4, 121.36, 120.92, 120.87, 120.67, 120.6, 41.7, 41.6, 41.5, 41.47, 40.9, 40.8, 40.7, 37.7, 37.6, 36.7, 36.6, 35.5, 35.46, 35.0, 34.9, 34.0, 33.9, 33.5, 33.3, 33.27, 33.24, 32.6, 27.3, 27.2, 27.08, 27.06, 26.9, 26.7, 26.68, 26.6, 26.5, 26.1, 26.07, 25.95, 25.93, 24.3, 20.89, 20.86, 19.7 (spectra complicated due to presence of rotamers and unassigned C–P-coupling).

³¹P NMR (202 MHz, CDCl₃): δ 6.75, 6.58 (major), 6.38, 6.23 (spectra complicated due to the presence of rotamers).

7 EXPERIMENTAL PART

HRMS (ESI+) (m/z): calculated for $C_{46}H_{42}N_2O_7P_1Na_1$ $[M+Na]^+$: 823.2310; found: 823.2308.



4-((2,6-bis(2-cyclohexyl-5-methylphenyl)-4-hydroxy-9,14-dinitro-4,5-dinaphtho[2,1-d:1',2'-f][1,3,2]dioxaphosphepin-4-ylidene)amino)-2,6-bis(2-cyclohexyl-5-methylphenyl)dinaphtho[2,1-d:1',2'-f][1,3,2]dioxaphosphepine 4-oxide

Sodium hydride (60% dispersion of in mineral oil, 12 mg, 0.32 mmol) was added to a solution of **16b** (70 mg, 0.088 mmol) and **17b** (55 mg, 0.08 mmol) in DMF (0.8 mL) under argon at room temperature. After 2.5 h at room temperature, 10% aqueous HCl solution (0.1 mL) was added. The solvent was removed under reduced pressure. The residue was purified by column chromatography on silica gel using 10–20% ethyl acetate/hexane as the eluents giving a pale yellow solid. The solid was dissolved in CH_2Cl_2 (2 mL) and stirred with 6N aqueous HCl (2 mL) for 30 min. The organic layer was separated, washed with 6N aqueous HCl (2 mL) and concentrated under reduced pressure to give the title compound as a pale yellow solid (60 mg, 52%).

¹H NMR (500 MHz, CD_2Cl_2): δ 9.01–8.83(m, 2H), 8.26–5.69(m, 28H), 2.91–2.38(m, 2H), 2.34–2.21(m, 3H), 2.18–1.68(m, 17H), 1.63–0.33(m, 34H) (spectra complicated due to presence of rotamers).

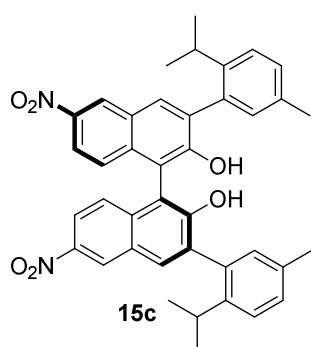
¹³C NMR (126 MHz, CD_2Cl_2): δ 148.8, 148.6, 147.3, 146.2, 146.18, 146.0, 145.7, 144.4, 144.1, 144.0, 143.9, 143.7, 143.6, 143.1, 143.0, 137.1, 136.7, 136.5, 136.1, 135.8, 135.6, 135.4, 135.3, 135.1, 135.0, 134.8, 134.7, 134.66, 134.5, 134.4, 134.1, 134.09, 133.7, 133.3, 133.2, 133.1, 132.9, 132.7, 132.4, 132.3, 132.2, 132.0, 131.9, 131.8, 131.7, 131.6, 131.5, 131.4, 131.2, 131.1, 130.8, 130.4, 130.3, 130.1, 130.0, 129.9, 129.7, 129.5, 129.2, 129.1, 128.8, 128.7, 128.6, 128.5, 128.3, 128.2, 128.0, 127.9, 127.8, 127.5, 127.4, 127.3, 127.2, 127.1, 126.9, 125.7, 125.5, 125.4, 125.3, 125.0, 123.7, 123.4, 123.3, 122.4, 122.2,

7 EXPERIMENTAL PART

121.8, 121.7, 120.5, 120.3, 120.1, 119.9, 119.8, 41.7, 41.6, 41.5, 41.3, 41.2, 41.1, 40.7, 40.4, 40.3, 40.2, 40.1, 39.9, 39.2, 37.8, 37.4, 36.9, 36.5, 36.3, 35.9, 35.8, 35.6, 35.2, 34.9, 34.5, 34.1, 34.0, 33.8, 33.3, 33.1, 32.5, 32.3, 31.4, 30.5, 29.9, 29.85, 29.7, 27.6, 27.5, 27.4, 27.37, 27.2, 27.15, 27.1, 27.0, 26.9, 26.5, 26.4, 26.2, 23.1, 21.4, 21.2, 21.14, 21.1, 21.0, 20.7, 20.65, 20.5, 20.3 (spectra complicated due to presence of rotamers and unassigned C–P-coupling).

^{31}P NMR (202 MHz, CD_2Cl_2): δ 3.84–0.58 (m, 1P), –1.17–2.30 (m, 1P).

HRMS (ESI[–]) m/z calculated for $\text{C}_{92}\text{H}_{86}\text{N}_3\text{O}_{10}\text{P}_2$ $[\text{M}–\text{H}]^-$: 1454.5794; found: 1454.5790.



(*S*)-3,3'-Bis(2-isopropyl-5-methylphenyl)-6,6'-dinitro-[1,1'-binaphthalene]-2,2'-diol

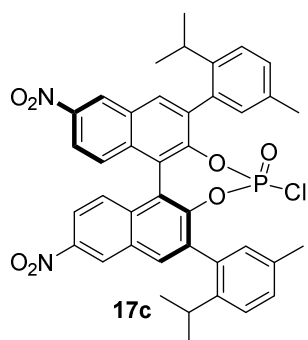
A solution of HNO_3 (90 μL , 2.0 mmol) in CHCl_3 (1.35 mL) was added dropwise to a solution of corresponding BINOL (525 mg, 0.953 mmol) in CHCl_3 (6.6 mL) at -40 °C under argon. Then the solution was warmed up to room temperature for further 30 min. The reaction was cooled to 0 °C, water (45 mL) was carefully added, and the mixture was extracted with CH_2Cl_2 (45 \times 3 mL). The organic layer was collected, dried over MgSO_4 , filtered, and the solvent was removed under reduced pressure. The residue was purified by column chromatography on silica gel using 50% CH_2Cl_2 /hexane as the eluent yielding the title compound as a yellow solid (340 mg, 56%).

^1H NMR (500 MHz, CDCl_3): δ 8.86–8.85 (m, 2H), 8.10–8.07 (m, 4H), 7.34–7.27 (m, 8H), 7.22 (br s, 1H), 5.55–5.54 (m, 2H), 2.98–2.97 (m, 2H), 2.26–2.18 (m, 6H), 1.31–0.1.30 (m, 12H) (spectra complicated due to presence of rotamers).

^{13}C NMR (126 MHz, CDCl_3): δ 153.2, 151.7, 147.6, 144.2, 136.4, 134.4, 134.3, 133.3, 132.7, 130.9, 128.5, 127.6, 126.0, 125.6, 125.4, 120.6, 113.9, 33.8, 24.1, 19.5 (spectra complicated due to presence of rotamers).

7 EXPERIMENTAL PART

HRMS (ESI+) (m/z): calculated for $C_{40}H_{36}N_2O_6Na_1$ $[M+Na]^+$: 663.2465; found: 663.2467.



(4*R*,11*bS*)-4-chloro-2,6-bis(2-isopropyl-5-methylphenyl)-9,14-dinitrodinaphtho[2,1-*d*:1',2'-*f*][1,3,2]dioxaphosphepine 4-oxide

$POCl_3$ (92 μ L, 0.99 mmol) was added to a solution of **15c** (210 mg, 0.328 mmol) in pyridine (1.0 mL) under argon at room temperature. The mixture was stirred at room temperature for 5 h and then concentrated to dryness under vacuum. The residue was passed through a short silica gel column using 40% CH_2Cl_2 /hexane as the eluent yielding the title compound as a pale yellow solid (193 mg, 82%).

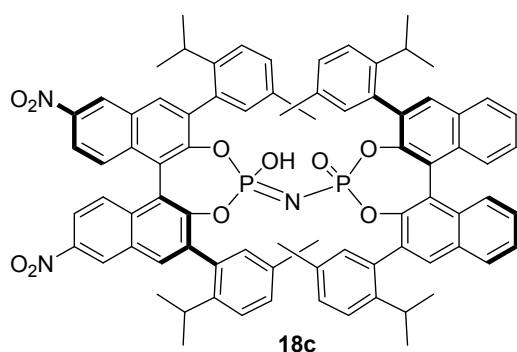
1H NMR (300 MHz, CD_2Cl_2): δ 9.00–8.99 (m, 2H), 8.30–8.21 (m, 2H), 8.16–8.12 (m, 2H), 7.52–7.28 (m, 6H), 7.22–7.10 (m, 2H), 3.69–2.68 (m, 2H), 2.39–2.32 (m, 6H), 1.49–0.99 (m, 12H) (spectra complicated due to presence of rotamers).

^{13}C NMR (126 MHz, CD_2Cl_2): δ 147.7, 147.65, 146.4, 145.0, 144.5, 137.1, 136.9, 135.7, 135.5, 135.4, 135.0, 134.8, 133.6, 133.5, 132.3, 132.27, 132.1, 132.0, 131.5, 131.3, 130.7, 130.5, 130.4, 129.0, 128.8, 127.1, 126.8, 125.8, 125.7, 125.6, 125.5, 125.4, 122.1, 121.9, 120.9, 120.88, 31.1, 30.9, 30.4, 30.0, 27.0, 25.9, 25.4, 25.1, 23.8, 23.5, 23.3, 22.9, 21.0, 20.96 (spectra complicated due to presence of rotamers and unassigned C–P-coupling).

^{31}P NMR (202 MHz, CD_2Cl_2): δ 6.79 (major), 6.62, 6.42 (spectra complicated due to the presence of rotamers).

HRMS (ESI+) (m/z): calculated for $C_{40}H_{34}N_2O_7Cl_1P_1Na_1$ $[M+Na]^+$: 743.1684; found: 743.1687.

7 EXPERIMENTAL PART



4-((4-hydroxy-2,6-bis(2-isopropyl-5-methylphenyl)-9,14-dinitro-415-dinaphtho[2,1-d:1',2'-f][1,3,2]dioxaphosphepin-4-ylidene)amino)-2,6-bis(2-isopropyl-5-methylphenyl)dinaphtho[2,1-d:1',2'-f][1,3,2]dioxaphosphepine 4-oxide

Sodium hydride (60% dispersion of in mineral oil, 24 mg, 0.60 mmol) was added to a solution of **16c** (120.0 mg, 0.166 mmol) and **17c** (92.5 mg, 0.151 mmol) in DMF (1.5 mL) under argon at room temperature. After 3 h at room temperature, 10% aqueous HCl solution (0.1 mL) was added. The solvent was removed under reduced pressure. The residue was purified by column chromatography on silica gel using 10–20% ethyl acetate/hexane as the eluents giving a pale yellow solid. The solid was dissolved in CH₂Cl₂ (2 mL) and stirred with 6N aqueous HCl (2 mL) for 30 min. The organic layer was separated, washed with 6N aqueous HCl (2 mL) and concentrated under reduced pressure to give the title compound as a pale yellow solid (62 mg, 32%).

¹H NMR (500 MHz, CD₂Cl₂, major): δ 9.08–8.23 (m, 2H), 8.45–5.74 (m, 28H), 2.91–2.02 (m, 10H), 1.93–1.26 (m, 6H), 1.20–0.15 (m, 24H).

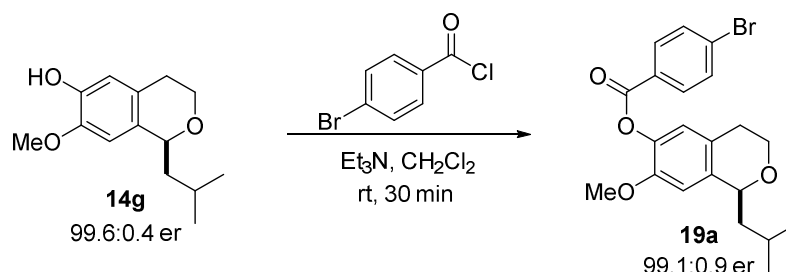
¹³C NMR (126 MHz, CD₂Cl₂, major): δ 145.7, 144.5, 135.5, 135.3, 135.1, 135.0, 134.8, 134.7, 134.1, 133.0, 132.8, 132.7, 132.6, 132.2, 131.5, 131.0, 130.6, 130.2, 130.1, 130.0, 129.6, 129.3, 129.1, 129.0, 128.9, 128.8, 128.7, 128.2, 127.4, 127.3, 127.2, 127.1, 127.07, 127.0, 126.8, 126.79, 126.64, 126.6, 126.4, 126.3, 126.26, 125.8, 125.7, 125.5, 125.44, 125.42, 125.4, 125.3, 125.1, 120.3, 30.8, 30.78, 30.7, 30.6, 30.5, 30.2, 30.0, 25.4, 25.3, 25.1, 25.0, 24.9, 24.89, 24.83, 24.8, 24.67, 24.65, 24.2, 24.0, 23.7, 23.6, 23.56, 23.2, 23.16, 23.1, 23.0, 22.8, 21.2, 21.1, 21.06, 21.04, 21.0, 20.8, 20.7, 20.6, 20.54, 20.53, 1.18.

³¹P NMR (202 MHz, CD₂Cl₂): δ 12.30–9.45 (m, 2P).

7 EXPERIMENTAL PART

HRMS (ESI⁻) (*m/z*): calculated for C₈₀H₇₀N₃O₁₀P₂ [M-H]⁻: 1294.4531; found: 1294.4550.

7.3.2.2 X-Ray Data



A 2 mL GC vial was charged with starting material **14g** (0.08 mmol), followed by triethylamine (1.2 equiv, 0.10 mmol), 4-bromobenzoylchloride (1.2 equiv, 0.10 mmol) and a magnetic stirring bar at room temperature. The vial was filled with argon and sealed. It was then stirred at room temperature for half an hour. The progress of the reaction was monitored by TLC. Purification of **19a** was performed by column chromatography or preparative thin layer chromatography on silica gel using EtOAc/hexanes as the eluents.

(S)-1-isobutyl-7-methoxyisochroman-6-yl 4-bromobenzoate **19a**

¹H NMR (500 MHz, CD₂Cl₂): δ 8.04 (dd, *J* = 8.7, 2.0 Hz, 2H), 7.68 (dd, *J* = 8.8, 2.0 Hz, 2H), 6.88 (s, 1H), 6.69 (s, 1H), 4.76 (dd, *J* = 10.4, 2.0 Hz, 1H), 4.13–4.03 (m, 1H), 3.77 (s, 3H), 3.76–3.69 (m, 1H), 2.93–2.79 (m, 1H), 2.66 (dd, *J* = 16.0, 4.4 Hz, 1H), 2.06–1.92 (m, 1H), 1.80 (ddd, *J* = 14.2, 10.5, 3.9 Hz, 1H), 1.60 (ddd, *J* = 12.0, 9.9, 2.9 Hz, 1H), 1.04 (d, *J* = 6.7 Hz, 3H), 0.98 (d, *J* = 6.7 Hz, 3H).

¹³C NMR (126 MHz, CD₂Cl₂): δ 164.51, 149.77, 138.46, 138.41, 132.34, 132.04, 128.96, 128.89, 126.83, 123.12, 109.44, 74.09, 62.78, 56.42, 45.52, 28.59, 24.94, 24.11, 21.59.

HRMS (ESI⁺) (*m/z*): calculated for C₂₁H₂₃O₄Br₁Na₁ [M+Na]⁺: 441.067410; found 441.067204. The enantiomeric ratio was measured by HPLC analysis using Chiralpak AD-3, heptane/ *i*PrOH = 70:30, flow rate = 1.0 mL/min, λ = 279 nm, t_R = 4.0 min (minor) and t_R = 5.2 min (major). er = 99.1:0.9.

7 EXPERIMENTAL PART

X-Ray structural analysis parameter for 19a:

Crystal data and structure refinement

Identification code	9920
Empirical formula	C ₂₁ H ₂₃ BrO ₄
Color	colorless
Formula weight	419.30 g · mol ⁻¹
Temperature	100.15 K
Wavelength	0.71073 Å
Crystal system	Orthorhombic
Space group	P2 ₁ 2 ₁ 2 ₁ , (no. 19)
Unit cell dimensions	a = 5.4738(5) Å α = 90°. b = 7.8392(11) Å β = 90°. c = 45.290(3) Å γ = 90°.
Volume	1943.4(4) Å ³
Z	4
Density (calculated)	1.433 Mg · m ⁻³
Absorption coefficient	2.138 mm ⁻¹
F(000)	864 e
Crystal size	0.18 x 0.12 x 0.06 mm ³
θ range for data collection	2.637 to 31.097°.
Index ranges	-7 ≤ h ≤ 7, -11 ≤ k ≤ 11, -65 ≤ l ≤ 65
Reflections collected	31126
Independent reflections	6225 [R _{int} = 0.0748]
Reflections with I > 2σ(I)	4759
Completeness to θ = 25.242°	99.8 %

7 EXPERIMENTAL PART

Absorption correction	Gaussian	
Max. and min. transmission	0.89 and 0.75	
Refinement method	Full-matrix least-squares on F^2	
Data / restraints / parameters	6225 / 0 / 238	
Goodness-of-fit on F^2	1.112	
Final R indices [$I > 2\sigma(I)$]	$R_1 = 0.0478$	$wR^2 = 0.1213$
R indices (all data)	$R_1 = 0.0759$	$wR^2 = 0.1534$
Absolute structure parameter	-0.031(7)	
Largest diff. peak and hole	0.7 and -1.2 e · Å ⁻³	

7 EXPERIMENTAL PART

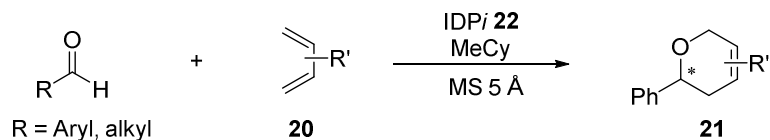
Bond lengths [Å] and angles [°].

Br(1)-C(19)	1.903(4)	O(1)-C(5)	1.433(6)
O(1)-C(6)	1.432(6)	O(2)-C(2)	1.350(6)
O(2)-C(10)	1.428(6)	O(3)-C(1)	1.402(5)
O(3)-C(15)	1.364(6)	O(4)-C(15)	1.196(6)
C(1)-C(2)	1.401(7)	C(1)-C(9)	1.376(7)
C(2)-C(3)	1.380(6)	C(3)-C(4)	1.405(7)
C(4)-C(5)	1.527(6)	C(4)-C(8)	1.390(7)
C(5)-C(11)	1.524(7)	C(6)-C(7)	1.517(7)
C(7)-C(8)	1.511(7)	C(8)-C(9)	1.403(6)
C(11)-C(12)	1.537(7)	C(12)-C(13)	1.521(8)
C(12)-C(14)	1.548(8)	C(15)-C(16)	1.485(6)
C(16)-C(17)	1.396(6)	C(16)-C(21)	1.385(6)
C(17)-C(18)	1.388(6)	C(18)-C(19)	1.383(7)
C(19)-C(20)	1.376(7)	C(20)-C(21)	1.383(6)
C(6)-O(1)-C(5)	111.5(4)	C(2)-O(2)-C(10)	117.2(4)
C(15)-O(3)-C(1)	114.3(3)	C(2)-C(1)-O(3)	118.5(4)
C(9)-C(1)-O(3)	119.6(4)	C(9)-C(1)-C(2)	121.9(4)
O(2)-C(2)-C(1)	115.9(4)	O(2)-C(2)-C(3)	126.2(4)
C(3)-C(2)-C(1)	117.9(4)	C(2)-C(3)-C(4)	121.2(4)
C(3)-C(4)-C(5)	120.3(4)	C(8)-C(4)-C(3)	119.9(4)
C(8)-C(4)-C(5)	119.7(4)	O(1)-C(5)-C(4)	111.2(4)
O(1)-C(5)-C(11)	105.5(4)	C(11)-C(5)-C(4)	113.8(4)
O(1)-C(6)-C(7)	109.9(4)	C(8)-C(7)-C(6)	111.3(4)
C(4)-C(8)-C(7)	121.4(4)	C(4)-C(8)-C(9)	119.1(4)
C(9)-C(8)-C(7)	119.5(4)	C(1)-C(9)-C(8)	119.8(4)
C(5)-C(11)-C(12)	114.4(4)	C(11)-C(12)-C(14)	112.5(5)
C(13)-C(12)-C(11)	110.1(5)	C(13)-C(12)-C(14)	112.6(6)
O(3)-C(15)-C(16)	112.9(4)	O(4)-C(15)-O(3)	122.5(4)
O(4)-C(15)-C(16)	124.6(4)	C(17)-C(16)-C(15)	123.1(4)
C(21)-C(16)-C(15)	117.1(4)	C(21)-C(16)-C(17)	119.8(4)
C(18)-C(17)-C(16)	120.0(4)	C(19)-C(18)-C(17)	118.6(4)
C(18)-C(19)-Br(1)	119.8(4)	C(20)-C(19)-Br(1)	118.0(3)
C(20)-C(19)-C(18)	122.2(4)	C(19)-C(20)-C(21)	118.7(4)
C(20)-C(21)-C(16)	120.6(4)		

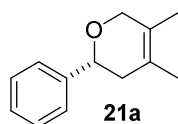
7 EXPERIMENTAL PART

7.4 Catalytic Asymmetric [4+2]-Cycloaddition Reaction of Dienes with Aldehydes

7.4.1 Products



Unless specified otherwise, aldehyde (0.1 mmol) and diene (0.12–1.0 mmol) were added to a mixture of catalyst **22** (0.2–3 mol%) and 70 mg/mL 5 Å molecular sieves in anhydrous MeCy (0.01–1.0 M). Purification was performed by column chromatography or preparative thin layer chromatography on silica gel using 2–6% diethyl ether/pentane as the eluent.



(*R*)-4,5-dimethyl-2-phenyl-3,6-dihydro-2H-pyran

Aldehyde (0.1 mmol) and diene (0.2 mmol) were added to a mixture of catalyst **22c** (1 mol%) and 5 Å molecular sieves (21 mg) in anhydrous MeCy (0.3 mL) at -78 °C, then the reaction mixture was stirred at -20 °C for 24 h. **21a** was obtained as a colorless oil (18.2 mg, 0.097 mmol, 97%).

^1H NMR (600 MHz, CD_2Cl_2): δ 7.39–7.34 (m, 4H), 7.28 (tt, $J = 7.1, 1.6$ Hz, 1H), 4.54 (dd, $J = 10.6, 3.5$ Hz, 1H), 4.21 (pd, $J = 15.5, 1.0$ Hz, 1H), 4.09 (d, $J = 15.5$ Hz, 1H), 2.30–2.24 (m, 1H), 2.10 (dd, $J = 16.7, 0.6$ Hz, 1H), 1.72 (br s, 3H), 1.62–1.616 (m, 3H).

^{13}C NMR (151 MHz, CD_2Cl_2): δ 143.5, 128.6, 127.6, 126.2, 125.0, 124.2, 76.5, 70.6, 39.0, 18.5, 14.0.

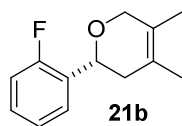
HRMS (ESI+) (m/z): calculated for $\text{C}_{13}\text{H}_{16}\text{O}_1\text{Na}_1$ [$\text{M}+\text{Na}$] $^+$: 211.1093; found: 211.1092.

$[\alpha]_D^{20}$: +224 ($c = 0.50$, CHCl_3).

GC: The enantiomeric ratio was measured by GC analysis on a chiral column (Hydrodex-gamma-TBDAC column: 25.0 m; i.D. 0.25mm); FID; Temperature: 220 °C (injector), 350

7 EXPERIMENTAL PART

°C (detector), 100 °C (108 min, iso); Gas: H₂ (0.50 bar); t_R = 88.43 min (major) and t_R = 92.67 min (minor), er = 98:2.



(*R*)-2-(2-fluorophenyl)-4,5-dimethyl-3,6-dihydro-2H-pyran

Aldehyde (0.1 mmol) and diene (0.2 mmol) were added to a mixture of catalyst **22c** (1 mol%) and 5 Å molecular sieves (21 mg) in anhydrous MeCy (0.3 mL) at -78 °C, then the reaction mixture was stirred at -10 °C for 72 h. **21b** was obtained as a colorless oil (16.6 mg, 0.081 mmol, 81%).

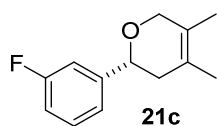
¹H NMR (500 MHz, CDCl₃): δ 7.51 (dt, *J* = 7.5, 1.6 Hz, 1H), 7.25–7.22 (m, 1H), 7.15 (dt, *J* = 7.6, 0.8 Hz, 1H), 7.01 (ddd, *J* = 10.2, 8.2, 0.8 Hz, 1H), 4.86 (dd, *J* = 10.6, 3.6 Hz, 1H), 4.24 (d, *J* = 15.5 Hz, 1H), 4.12 (d, *J* = 15.5 Hz, 1H), 2.28–2.22 (m, 1H), 2.14 (d, *J* = 16.6 Hz, 1H), 1.69 (br s, 3 H), 1.60 (br s, 3 H).

¹³C NMR (126 MHz, CDCl₃): δ 160.7, 158.7, 130.0, 129.9, 129.6, 128.8, 128.7, 128.4, 127.24, 127.20, 126.4, 124.48, 124.45, 124.0, 115.3, 115.1, 70.4, 70.35, 70.33, 37.7, 18.4, 14.0.

HRMS (ESI+) (*m/z*): calculated for C₁₃H₁₅O₁F₁Na₁ [M+Na]⁺: 229.09991; found: 229.09996.

[α]_D²⁰: +178.4 (*c* = 0.50, CHCl₃).

HPLC: The enantiomeric ratio was measured by HPLC analysis using Chiralpak IA-3, i.D. 4.6 mm. Heptane/ *i*PrOH = 99.5:0.5, flow rate = 1.0 mL/min, λ = 254 nm, t_R = 4.1 min (major) and t_R = 4.5 min (minor), er = 92:8.



(*R*)-2-(3-fluorophenyl)-4,5-dimethyl-3,6-dihydro-2H-pyran

7 EXPERIMENTAL PART

Aldehyde (0.1 mmol) and diene (0.2 mmol) were added to a mixture of catalyst **22c** (1 mol%) and 5 Å molecular sieves (21 mg) in anhydrous MeCy (0.3 mL) at $-78\text{ }^{\circ}\text{C}$, then the reaction mixture was stirred at $-20\text{ }^{\circ}\text{C}$ for 24 h. **21c** was obtained as a colorless oil (19.5 mg, 0.0945 mmol, 94.5%).

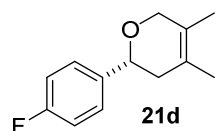
$^1\text{H NMR}$ (500 MHz, CDCl_3): δ 7.30 (dt, $J = 7.9, 2.0$ Hz, 1H), 7.14–7.09 (m, 2H), 6.95 (ddt, $J = 8.9, 2.5, 0.5$ Hz, 1H), 4.54 (dd, $J = 10.6, 3.8$ Hz, 1H), 4.20 (td, $J = 15.6, 1.1$ Hz, 1H), 4.10 (d, $J = 15.5$ Hz, 1H), 2.29–2.22 (m, 1H), 2.09 (d, $J = 16.6$ Hz, 1H), 1.69 (br s, 3H), 1.59 (br s, 3H).

$^{13}\text{C NMR}$ (126 MHz, CDCl_3): δ 164.0, 162.1, 145.54, 145.49, 129.96, 129.90, 124.7, 123.7, 121.46, 121.45, 114.4, 114.2, 113.0, 112.8, 75.71, 75.70, 70.4, 38.6, 18.5, 14.0.

HRMS (ESI+) (m/z): calculated for $\text{C}_{13}\text{H}_{15}\text{O}_1\text{F}_1\text{Na}_1$ $[\text{M}+\text{Na}]^+$: 229.0999; found: 229.1001.

$[\alpha]_D^{20}$: +184 ($c = 0.50$, CHCl_3).

HPLC: The enantiomeric ratio was measured by HPLC analysis using Chiralpak IA-3, i.D. 4.6 mm. Heptane/ *i*PrOH = 99.5:0.5, flow rate = 1.0 mL/min, $\lambda = 220$ nm, $t_R = 4.5$ min (major) and $t_R = 4.9$ min (minor), er = 98:2.



(*R*)-2-(4-fluorophenyl)-4,5-dimethyl-3,6-dihydro-2H-pyran

Aldehyde (0.1 mmol) and diene (0.2 mmol) were added to a mixture of catalyst **22c** (1 mol%) and 5 Å molecular sieves (21 mg) in anhydrous MeCy (0.3 mL) at $-78\text{ }^{\circ}\text{C}$, then the reaction mixture was stirred at $-20\text{ }^{\circ}\text{C}$ for 24 h. **21d** was obtained as a colorless oil (16 mg, 0.089 mmol, 89%).

$^1\text{H NMR}$ (500 MHz, CDCl_3): δ 7.34 (dt, $J = 5.6, 2.0$ Hz, 2H), 7.02 (tt, $J = 6.8, 2.9$ Hz, 2H), 4.52 (dd, $J = 10.6, 3.5$ Hz, 1H), 4.20 (td, $J = 15.5, 1.1$ Hz, 1H), 4.10 (d, $J = 15.5$ Hz, 1H), 2.30–2.24 (m, 1H), 2.07 (d, $J = 16.7$ Hz, 1H), 1.69 (br s, 3H), 1.59 (br s, 3H).

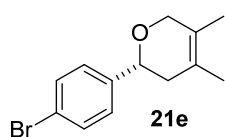
7 EXPERIMENTAL PART

^{13}C NMR (126 MHz, CDCl_3): δ 163.2, 161.3, 138.63, 138.60, 127.7, 127.6, 124.7, 123.8, 115.4, 115.2, 75.8, 70.4, 38.7, 18.5, 14.0.

HRMS (ESI+) (m/z): calculated for $\text{C}_{13}\text{H}_{15}\text{O}_1\text{F}_1\text{Na}_1$ $[\text{M}+\text{Na}]^+$: 229.0999; found: 229.1001.

$[\alpha]_D^{20}$: +164 ($c = 0.50$, CHCl_3).

HPLC: The enantiomeric ratio was measured by HPLC analysis using Chiralpak IA-3, i.D. 4.6 mm. Heptane/ *i*PrOH = 99.5:0.5, flow rate = 1.0 mL/min, $\lambda = 220$ nm, $t_R = 5.0$ min (major) and $t_R = 5.5$ min (minor), er = 97:3.



(*R*)-2-(4-bromophenyl)-4,5-dimethyl-3,6-dihydro-2H-pyran

Aldehyde (0.1 mmol) and diene (1.0 mmol) were added to a mixture of catalyst **22c** (3 mol%) and 5 Å molecular sieves (21 mg) in anhydrous MeCy (0.3 mL) at -78 °C, then the reaction mixture was stirred at -60 °C for 6 days. **21e** was obtained as a colorless oil (9.6 mg, 0.036 mmol, 36%).

^1H NMR (500 MHz, CDCl_3): δ 7.47 (dt, $J = 8.5, 2.4$ Hz, 2H), 7.25 (dt, $J = 8.4, 1.5$ Hz, 2H), 4.50 (dd, $J = 10.6, 3.5$ Hz, 1H), 4.19 (td, $J = 15.6, 1.1$ Hz, 1H), 4.09 (d, $J = 15.6$ Hz, 1H), 2.26–2.20 (m, 1H), 2.07 (d, $J = 16.7$ Hz, 1H), 1.68 (br s, 3H), 1.59 (br s, 3H).

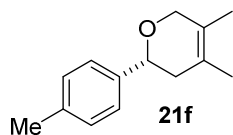
^{13}C NMR (126 MHz, CDCl_3): δ 141.9, 131.6, 127.7, 124.7, 123.7, 121.2, 75.7, 70.4, 38.6, 18.5, 14.0.

HRMS (ESI+) (m/z): calculated for $\text{C}_{13}\text{H}_{16}\text{O}_1\text{Br}_1$ $[\text{M}+\text{H}]^+$: 267.0379; found: 267.0380.

$[\alpha]_D^{20}$: +154 ($c = 0.50$, CHCl_3).

HPLC: The enantiomeric ratio was measured by HPLC analysis using Chiralpak IA-3, i.D. 4.6 mm. Heptane/ *i*PrOH = 99.5:0.5, flow rate = 1.0 mL/min, $\lambda = 254$ nm, $t_R = 5.6$ min (major) and $t_R = 6.2$ min (minor), er = 95:5.

7 EXPERIMENTAL PART



(*R*)-4,5-dimethyl-2-(*p*-tolyl)-3,6-dihydro-2H-pyran

Aldehyde (0.1 mmol) and diene (0.5 mmol) were added to a mixture of catalyst **22c** (3 mol%) and 5 Å molecular sieves (21 mg) in anhydrous MeCy (0.3 mL) at -78 °C, then the reaction mixture was stirred at -60 °C for 6 days. **21f** was obtained as a colorless oil (18.9 mg, 0.093 mmol, 93%).

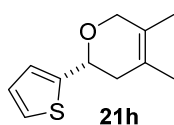
$^1\text{H NMR}$ (500 MHz, CD_2Cl_2): δ 7.23 (d, $J = 8.0$ Hz, 2H), 7.15 (d, $J = 8.0$ Hz, 2H), 4.48 (dd, $J = 10.6, 3.5$ Hz, 1H), 4.17 (d, $J = 15.5$ Hz, 1H), 4.05 (d, $J = 15.5$ Hz, 1H), 2.33 (s, 3H), 2.26–2.21 (m, 1H), 2.06 (d, $J = 16.7$ Hz, 1H), 1.69 (br s, 3H), 1.59 (br s, 3H).

$^{13}\text{C NMR}$ (126 MHz, CD_2Cl_2): δ 140.4, 137.3, 129.2, 126.1, 124.9, 124.2, 76.4, 70.6, 38.9, 21.2, 18.5, 13.9.

HRMS (ESI+) (m/z): calculated for $\text{C}_{14}\text{H}_{18}\text{O}_1\text{Na}_1$ [$\text{M}+\text{Na}$] $^+$: 225.1250; found: 225.1250.

$[\alpha]_D^{20}$: +184 ($c = 0.50$, CHCl_3).

HPLC: The enantiomeric ratio was measured by HPLC analysis using Chiralpak IA-3, i.D. 4.6 mm. Heptane/ *i*PrOH = 99.5:0.5, flow rate = 1.0 mL/min, $\lambda = 254$ nm, $t_R = 5.4$ min (major) and $t_R = 6.2$ min (minor), er = 95:5.



(*R*)-4,5-dimethyl-2-(thiophen-2-yl)-3,6-dihydro-2H-pyran

Aldehyde (0.1 mmol) and diene (0.2 mmol) were added to a mixture of catalyst **4c** (1 mol%) and 5 Å molecular sieves (21 mg) in anhydrous MeCy (0.3 mL) at -78 °C, then the reaction mixture was stirred at -10 °C for 72 h. **3g** was obtained as a colorless oil (9.3 mg, 0.048 mmol, 48%).

$^1\text{H NMR}$ (500 MHz, CD_2Cl_2): δ 7.25 (dd, $J = 4.5, 1.0$ Hz, 1H), 6.98–6.96 (m, 2H), 4.49 (dd, $J = 10.0, 3.7$ Hz, 1H), 4.17 (d, $J = 15.6$ Hz, 1H), 4.02 (d, $J = 15.5$ Hz, 1H), 2.42–2.36 (m, 1H), 2.21 (d, $J = 16.6$ Hz, 1H), 1.70 (br s, 3H), 1.57 (br s, 3H).

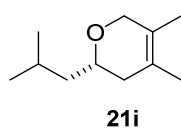
7 EXPERIMENTAL PART

^{13}C NMR (126 MHz, CD_2Cl_2): δ 146.6, 126.8, 124.9, 124.8, 124.0, 123.6, 72.4, 70.2, 38.6, 18.4, 13.9.

HRMS (ESI+) (m/z): calculated for $\text{C}_{11}\text{H}_{14}\text{O}_1\text{S}_1\text{Na}_1$ $[\text{M}+\text{Na}]^+$: 217.0658; found: 217.0659.

$[\alpha]_D^{20}$: +64 ($c = 0.50$, CHCl_3).

HPLC: The enantiomeric ratio was measured by HPLC analysis using Chiralpak IA-3, i.D. 4.6 mm. Heptane/ *i*PrOH = 99.5:0.5, flow rate = 1.0 mL/min, $\lambda = 220$ nm, $t_R = 5.6$ min (major) and $t_R = 6.0$ min (minor), er = 99.7:0.3.



(*S*)-2-isobutyl-4,5-dimethyl-3,6-dihydro-2H-pyran

Aldehyde (0.30 mmol) and diene (3.0 mmol) were added to a mixture of catalyst **22b** (1 mol%) and 5 Å molecular sieves (70 mg) in anhydrous MeCy (1.0 mL) at -78 °C, then the reaction mixture was stirred at -20 °C for 70 h. **21i** was obtained as a colorless oil (46 mg, 0.27 mmol, 91%).

^1H NMR (500 MHz, CD_2Cl_2): δ 3.91–3.75 (m, 2H), 3.42 (dddd, $J = 10.1, 8.2, 4.8, 3.6$ Hz, 1H), 1.84–1.76 (m, 1H), 1.73–1.66 (m, 2H), 1.54 (s, 3H), 1.44 (s, 3H), 1.37 (ddd, $J = 14.1, 8.2, 6.2$ Hz, 1H), 1.14 (ddd, $J = 13.7, 7.9, 4.8$ Hz, 1H), 0.82 (dd, $J = 6.7, 2.0$ Hz, 6H).

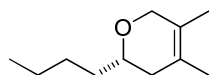
^{13}C NMR (126 MHz, CD_2Cl_2): δ 124.6, 123.7, 72.5, 69.7, 45.2, 37.3, 24.6, 23.1, 22.4, 18.2, 13.7.

HRMS (EI) (m/z): calculated for $\text{C}_{11}\text{H}_{20}\text{O}_1$ $[\text{M}]$: 168.1509; found 168.1510.

$[\alpha]_D^{25}$: +64.4 ($c = 0.30$, CH_2Cl_2).

GC: The enantiomeric ratio was measured by GC analysis on a chiral column (Cyclodextrin-H column: 25.0 m; i.D. 0.25mm); FID; Temperature: 220 °C (injector), 350 °C (detector), 75 °C (iso); Gas: H_2 (0.40 bar); $t_R = 20.68$ min (minor) and $t_R = 21.55$ min (major), er = 94:6.

7 EXPERIMENTAL PART



21j

(*S*)-2-butyl-4,5-dimethyl-3,6-dihydro-2H-pyran

Aldehyde (0.30 mmol) and diene (3.0 mmol) were added to a mixture of catalyst **22b** (1 mol%) and 5 Å molecular sieves (70 mg) in anhydrous MeCy (1.0 mL) at $-78\text{ }^{\circ}\text{C}$, then the reaction mixture was stirred at $-20\text{ }^{\circ}\text{C}$ for 48 h. **21j** was obtained as a colorless oil (44 mg, 0.26 mmol, 87%).

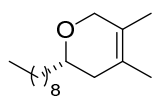
$^1\text{H NMR}$ (500 MHz, CD_2Cl_2): δ 3.91–3.76 (m, 2H), 3.33 (dddd, $J = 10.4, 7.4, 5.0, 3.6$ Hz, 1H), 1.86–1.76 (m, 1H), 1.71 (d, $J = 16.5$ Hz, 1H), 1.54 (s, 3H), 1.44 (s, 3H), 1.38–1.17 (m, 6H), 0.82 (t, $J = 7.1$ Hz, 3H).

$^{13}\text{C NMR}$ (126 MHz, CD_2Cl_2): δ 124.4, 123.4, 74.2, 69.6, 36.7, 35.6, 27.7, 22.8, 18.0, 13.8, 13.5.

HRMS (EI) (m/z): calculated for $\text{C}_{11}\text{H}_{20}\text{O}_1$ [M]: 168.1509; found 168.1508.

$[\alpha]_D^{25}$: +66.1 ($c = 0.36$, CH_2Cl_2).

GC: The enantiomeric ratio was measured by GC analysis on a chiral column (Cyclodextrin-H column: 25.0 m; i.D. 0.25mm); FID; Temperature: $230\text{ }^{\circ}\text{C}$ (injector), $350\text{ }^{\circ}\text{C}$ (detector), $115\text{ }^{\circ}\text{C}$ (10 min, iso) to $170\text{ }^{\circ}\text{C}$ ($8\text{ }^{\circ}\text{C}/\text{min}$, 3 min iso); Gas: H_2 (0.50 bar); $t_R = 4.21$ min (minor) and $t_R = 4.35$ min (major), er = 97:3.



21k

(*S*)-2-ethyl-4,5-dimethyl-3,6-dihydro-2H-pyran

Aldehyde (0.30 mmol) and diene (3.0 mmol) were added to a mixture of catalyst **22b** (1 mol%) and 5 Å molecular sieves (70 mg) in anhydrous MeCy (1.0 mL) at $-78\text{ }^{\circ}\text{C}$, then the reaction mixture was stirred at $-20\text{ }^{\circ}\text{C}$ for 48 h. **21k** was obtained as a colorless oil (67 mg, 0.28 mmol, 94%).

7 EXPERIMENTAL PART

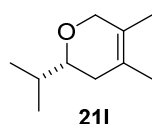
¹H NMR (500 MHz, CD₂Cl₂): δ 3.91–3.75 (m, 2H), 3.33 (dddd, *J* = 10.4, 7.2, 4.9, 3.4 Hz, 1H), 1.86–1.76 (m, 1H), 1.71 (d, *J* = 16.5 Hz, 1H), 1.54 (s, 3H), 1.45–1.39 (m, 4H), 1.36–1.29 (m, 2H), 1.24–1.16 (m, 13H), 0.80 (t, *J* = 6.9 Hz, 3H).

¹³C NMR (126 MHz, CD₂Cl₂): δ 126.3, 125.4, 76.1, 71.5, 38.6, 37.8, 33.8, 31.63, 31.55, 31.5, 31.2, 27.4, 24.6, 20.0, 15.8, 15.4.

HRMS (EI) (*m/z*): calculated for C₁₆H₃₀O₁ [M]: 238.2291; found 238.2288.

[α]_D²⁵: +118.0 (*c* = 0.36, CH₂Cl₂).

GC: The enantiomeric ratio was measured by GC analysis on a chiral column (Cyclodextrin-H column: 25.0 m; i.D. 0.25mm); FID; Temperature: 220 °C (injector), 350 °C (detector), 130 °C (40 min, iso); Gas: H₂ (0.50 bar); t_R = 34.49 min (minor) and t_R = 35.43 min (major), er = 97:3.



(*R*)-2-isopropyl-4,5-dimethyl-3,6-dihydro-2H-pyran

Aldehyde (0.30 mmol) and diene **2a** (3.0 mmol) were added to a mixture of catalyst **22b** (1 mol%) and 5 Å molecular sieves (70 mg) in anhydrous MeCy (1.0 mL) at –78 °C, then the reaction mixture was stirred at –10 °C for 70 h. **21I** was obtained as a colorless oil (38 mg, 0.25 mmol, 83%).

¹H NMR (500 MHz, CD₂Cl₂): δ 3.92–3.77 (m, 2H), 3.03 (ddd, *J* = 10.4, 6.8, 3.4 Hz, 1H), 1.90–1.82 (m, 1H), 1.69 (d, *J* = 16.5 Hz, 1H), 1.61–1.52 (m, 4H), 1.44 (dt, *J* = 2.3, 1.2 Hz, 3H), 0.83 (dd, *J* = 26.5, 6.8 Hz, 6H).

¹³C NMR (126 MHz, CD₂Cl₂): δ 124.4, 123.5, 79.3, 70.0, 33.7, 32.9, 18.4, 18.1, 17.9, 13.5.

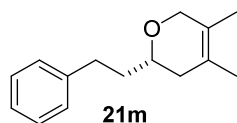
HRMS (ESI+) (*m/z*): calculated for C₁₀H₁₉O₁ [M+H]⁺: 155.1430; found 155.1432.

[α]_D²⁵: +163.2 (*c* = 0.32, CH₂Cl₂).

GC: The enantiomeric ratio was measured by GC analysis on a chiral column (Hydrodex-gamma-TBDAC column: 25.0 m; i.D. 0.25mm); FID; Temperature: 220 °C (injector), 350 °C

7 EXPERIMENTAL PART

(detector), 65 °C (25 min, iso) to 220 °C (8 °C/min, 5 min iso); Gas: H₂ (0.50 bar); t_R = 21.81 min (minor) and t_R = 23.46 min (major), er = 97:3.



(*S*)-4,5-dimethyl-2-phenethyl-3,6-dihydro-2H-pyran

Aldehyde (0.30 mmol) and diene (3.0 mmol) were added to a mixture of catalyst **22b** (1 mol%) and 5 Å molecular sieves (70 mg) in anhydrous MeCy (1.0 mL) at -78 °C, then the reaction mixture was stirred at -10 °C for 48 h. **21m** was obtained as a colorless oil (47 mg, 0.22 mmol, 73%).

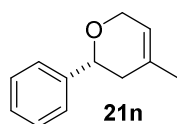
¹H NMR (500 MHz, CD₂Cl₂): δ 7.23–7.03 (m, 5H), 3.94–3.77 (m, 2H), 3.34 (dddd, *J* = 10.3, 8.0, 4.6, 3.5 Hz, 1H), 2.68 (ddd, *J* = 13.7, 9.8, 5.5 Hz, 1H), 2.58 (ddd, *J* = 13.7, 9.6, 6.9 Hz, 1H), 1.91–1.83 (m, 1H), 1.77–1.61 (m, 3H), 1.54 (s, 3H), 1.44 (s, 3H).

¹³C NMR (126 MHz, CD₂Cl₂): δ 142.5, 128.4, 128.2, 125.6, 124.4, 123.4, 73.2, 69.6, 37.5, 36.6, 31.7, 18.0, 13.5.

HRMS (EI) (*m/z*): calculated for C₁₅H₂₀O₁ [*M*]: 216.1509; found 216.1511.

[α]_D²⁵: +80.2 (*c* = 0.34, CH₂Cl₂).

GC: The enantiomeric ratio was measured by GC analysis on a chiral column (Cyclodextrin-H column: 25.0 m; i.D. 0.25mm); FID; Temperature: 230 °C (injector), 350 °C (detector), 125 °C (45 min, iso) to 170 °C (8 °C/min, 3 min iso); Gas: H₂ (0.60 bar); t_R = 37.79 min (minor) and t_R = 38.98 min (major), er = 96:4.



(*R*)-4-methyl-2-phenyl-3,6-dihydro-2H-pyran

Aldehyde (0.1 mmol) and diene (0.2 mmol) were added to a mixture of catalyst **22b** (1 mol%) and 5 Å molecular sieves (21 mg) in anhydrous MeCy (0.3 mL) at -78 °C, then the reaction mixture was stirred at -20 °C for 24 h. **21n** was obtained as a colorless oil (17 mg, 0.097 mmol, 97%).

7 EXPERIMENTAL PART

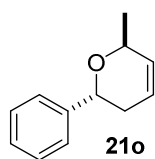
¹H NMR (500 MHz, CD₂Cl₂): δ 7.38–7.33 (m, 4H), 7.27 (tt, *J* = 8.6, 1.8 Hz, 1H), 5.51 (br s, 1H), 4.51 (dd, *J* = 10.4, 3.5 Hz, 1H), 4.29–4.28 (m, 2H), 2.28–2.22 (m, 1H), 2.10 (d, *J* = 16.8 Hz, 1H), 1.75 (br s, 3H).

¹³C NMR (126 MHz, CD₂Cl₂): δ 143.4, 132.5, 128.6, 127.7, 126.2, 120.2, 76.1, 66.8, 38.1, 23.0.

HRMS (ESI+) (*m/z*): calculated for C₁₂H₁₄O₁Na₁ [M+Na]⁺: 197.09368; found: 197.09366.

[α]_D²⁰: +161 (*c* = 0.50, CHCl₃).

GC: The enantiomeric ratio was measured by GC analysis on a chiral column (Hydrodex-gamma-TBDAC column: 25.0 m; i.D. 0.25mm); FID; Temperature: 220 °C (injector), 350 °C (detector), 115 °C (35 min, iso); Gas: H₂ (0.53 bar); t_R = 18.86 min (major) and t_R = 19.87 min (minor), er = 98:2.



(2*R*,6*S*)-6-methyl-2-phenyl-3,6-dihydro-2H-pyran

Aldehyde (0.2 mmol) and diene (2.0 mmol) were added to a mixture of catalyst **22b** (2 mol%) and 5 Å molecular sieves (42 mg) in anhydrous MeCy (0.6 mL) at –78 °C, then the reaction mixture was stirred at –20 °C for 72 h. **21o** was obtained as a colorless oil (7.0 mg, 0.04 mmol, 20%).

¹H NMR (500 MHz, CD₂Cl₂): δ 7.38–7.32 (m, 4H), 7.26 (tt, *J* = 7.2, 1.5 Hz, 1H), 5.93–5.88 (m, 1H), 5.78 (qd, *J* = 12.2, 2.0 Hz, 1H), 4.72 (t, *J* = 6.5 Hz, 1H), 4.46–4.41 (m, 1H), 2.26–2.23 (m, 2H), 1.30 (d, *J* = 6.8 Hz, 3H).

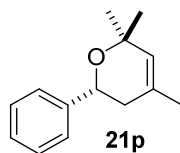
¹³C NMR (126 MHz, CD₂Cl₂): δ 143.4, 131.6, 128.6, 127.6, 126.6, 124.1, 69.9, 69.7, 32.6, 20.2.

HRMS (EI) (*m/z*): calculated for C₁₂H₁₄O₁ [M]: 174.1045; found: 174.1042.

[α]_D²⁰: +124 (*c* = 0.15, CHCl₃).

7 EXPERIMENTAL PART

GC: The enantiomeric ratio was measured by GC analysis on a chiral column (Hydrodex-gamma-TBDAC column: 25.0 m; i.D. 0.25mm); FID; Temperature: 220 °C (injector), 350 °C (detector), 110 °C (30 min, iso); 230 °C (8 min); Gas: H₂ (0.50 bar); t_R = 22.14 min (minor) and t_R = 23.39 min (major), er = 99:1.



(*R*)-4,6,6-trimethyl-2-phenyl-3,6-dihydro-2H-pyran

Aldehyde (0.1 mmol) and diene (0.5 mmol) were added to a mixture of catalyst **22b** (2 mol%) and 5 Å molecular sieves (700 mg) in anhydrous MeCy (10.0 mL) at -78 °C, then the reaction mixture was stirred at -45 °C for 48 h. **21p** was obtained as a colorless oil (16.5 mg, 0.082 mmol, 82%).

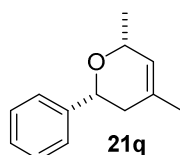
¹H NMR (500 MHz, CD₂Cl₂): δ 7.40–7.38 (m, 2H), 7.33 (dt, *J* = 7.4, 2.0 Hz, 2H), 7.26 (tt, *J* = 6.6, 1.4 Hz, 1H), 5.42 (t, *J* = 1.0 Hz, 1H), 4.69 (dd, *J* = 10.7, 3.3 Hz, 1H), 2.18–2.11 (m, 1H), 2.01 (dd, *J* = 16.7, 3.3 Hz, 1H), 1.72 (br s, 3H), 1.29 (d, *J* = 1.6 Hz, 6H).

¹³C NMR (126 MHz, CD₂Cl₂): δ 143.9, 130.6, 129.1, 128.6, 127.5, 126.5, 73.7, 71.1, 37.8, 30.1, 26.2, 23.1.

HRMS (ESI+) (*m/z*): calculated for C₁₄H₁₈O₁Na₁ [M+Na]⁺: 225.1250; found: 225.1248.

[α]_D²⁰: +80 (*c* = 0.50, CHCl₃).

GC: The enantiomeric ratio was measured by GC analysis on a chiral column (Cyclodextrin-H column: 25.0 m; i.D. 0.25mm); FID; Temperature: 220 °C (injector), 350 °C (detector), 90 °C (60 min, iso); Gas: H₂ (0.50 bar); t_R = 42.0 min (minor) and t_R = 45.2 min (major), er = 96:4.



(*2R,6R*)-4,6-dimethyl-2-phenyl-3,6-dihydro-2H-pyran

7 EXPERIMENTAL PART

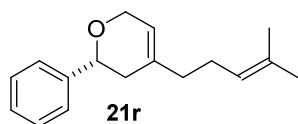
Aldehyde (0.1 mmol) and diene (0.5 mmol) were added to a mixture of catalyst **22b** (1 mol%) and 21 mg 5 Å molecular sieves in anhydrous MeCy (0.1 M) at $-78\text{ }^{\circ}\text{C}$, then the reaction mixture was stirred at $-40\text{ }^{\circ}\text{C}$ for 20 h. **21q** was obtained as a colorless oil in 81% yield.

$^1\text{H NMR}$ (300 MHz, CD_2Cl_2): δ 7.41–7.23 (m, 5H), 5.41 (tt, $J = 2.5, 1.4\text{ Hz}$, 1H), 4.56 (dd, $J = 10.5, 3.7\text{ Hz}$, 1H), 4.39–4.20 (m, 1H), 2.26–2.14 (m, 1H), 2.10–2.02 (m, 1H), 1.74–1.73 (m, 3H), 1.25 (d, $J = 6.6\text{ Hz}$, 3H).

$^{13}\text{C NMR}$ (75 MHz, CD_2Cl_2): δ 143.6, 132.5, 128.6, 127.6, 126.3, 125.6, 76.3, 72.0, 38.1, 22.9, 21.8.

HRMS (EI) m/z calculated for $\text{C}_{13}\text{H}_{16}\text{O}_1$ [M]: 188.11957; found: 188.11951.

The enantiomeric ratio was measured by GC analysis on Hydrodex-BTBDAC-G681 column: $t_{\text{R}} = 38.2\text{ min}$ (minor) and $t_{\text{R}} = 39.6\text{ min}$ (major), er = 96:4.



(*R*)-4,6,6-trimethyl-2-phenyl-3,6-dihydro-2H-pyran

Aldehyde (0.1 mmol) and diene (0.3 mmol) were added to a mixture of catalyst **22b** (2 mol%) and 5 Å molecular sieves (21 mg) in anhydrous MeCy (0.3 mL) at $-78\text{ }^{\circ}\text{C}$, then the reaction mixture was stirred at $-40\text{ }^{\circ}\text{C}$ for 4 days. **21r** was obtained as a colorless oil (8.7 mg, 0.036 mmol, 36%).

$^1\text{H NMR}$ (500 MHz, CD_2Cl_2): δ 7.38–7.32 (m, 4H), 7.27 (tt, $J = 6.2, 1.8\text{ Hz}$, 1H), 5.51 (q, $J = 1.2\text{ Hz}$, 1H), 5.13 (ddt, $J = 8.2, 2.8, 1.4\text{ Hz}$, 1H), 4.50 (dd, $J = 10.4, 3.5\text{ Hz}$, 1H), 4.31 (p, $J = 1.7\text{ Hz}$, 2H), 2.28–2.22 (m, 1H), 2.15–2.11 (m, 3H), 2.07–2.04 (m, 2H), 1.69 (d, $J = 0.9\text{ Hz}$, 3H), 1.62 (br s, 3H).

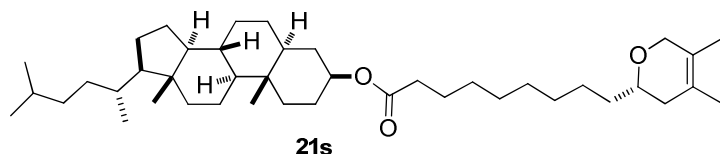
$^{13}\text{C NMR}$ (126 MHz, CD_2Cl_2): δ 143.5, 136.2, 132.1, 128.7, 128.6, 127.6, 126.2, 124.3, 119.9, 76.1, 66.8, 37.3, 36.7, 26.4, 25.8, 17.8.

HRMS (ESI+) (m/z): calculated for $\text{C}_{17}\text{H}_{22}\text{O}_1\text{Na}_1$ [M+Na] $^+$: 265.1563; found: 265.1562.

$[\alpha]_{\text{D}}^{20}$: +36 ($c = 0.45$, CHCl_3).

7 EXPERIMENTAL PART

GC: The enantiomeric ratio was measured by GC analysis on a chiral column (Hydrodex-gamma-TBDAC column: 25.0 m; i.D. 0.25mm); FID; Temperature: 220 °C (injector), 350 °C (detector), 130 °C (140 min, iso); Gas: H₂ (0.50 bar); t_R = 114.5 min (major) and t_R = 117.4 min (minor), er = 96:4.



(3*S*,5*S*,8*R*,9*S*,10*S*,13*R*,14*S*,17*R*)-10,13-dimethyl-17-((*R*)-5-methylhexan-2-yl)hexadecahydro-1*H*-cyclopenta[*a*]phenanthren-3-yl 9-((*S*)-4,5-dimethyl-3,6-dihydro-2*H*-pyran-2-yl)nonanoate

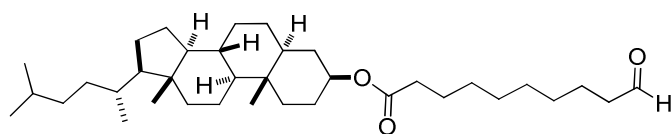
Aldehyde (0.1 mmol) and diene (1.0 mmol) were added to a mixture of catalyst **22b** (1 mol%) and 5 Å molecular sieves (21 mg) in anhydrous MeCy (0.3 mL) at -78 °C, then the reaction mixture was stirred at -10 °C for 72 h. **21s** was obtained as a colorless solid (52 mg, 0.081 mmol, 81%).

¹H NMR (500 MHz, CD₂Cl₂): δ 4.66 (hept, *J* = 5.0 Hz, 1H), 3.96 (td, *J* = 15.4, 0.9 Hz, 1H), 3.87 (d, *J* = 15.4 Hz, 1H), 3.43–3.38 (m, 1H), 2.23 (t, *J* = 7.4 Hz, 2H), 1.97 (td, *J* = 12.6, 3.3 Hz, 1H), 1.92–1.60 (m, 10H), 1.60–1.46 (m, 10.8H), 1.44–0.96 (m, 30.9H), 0.91 (d, *J* = 6.5 Hz, 3H), 0.86 (dd, *J* = 6.6, 2.0 Hz, 6H), 0.83 (s, 3H), 0.69–0.61 (m, 4H).

¹³C NMR (126 MHz, CD₂Cl₂): δ 173.5, 124.8, 123.9, 74.6, 73.7, 70.1, 56.9, 56.8, 54.7, 45.1, 43.0, 40.5, 39.9, 37.21, 37.19, 36.6, 36.32, 36.26, 35.93, 35.88, 35.1, 34.5, 32.5, 30.1, 29.9, 29.7, 29.5, 29.1, 28.6, 28.5, 28.0, 25.9, 25.5, 24.6, 24.3, 23.0, 22.7, 21.6, 18.9, 18.5, 14.0, 12.4, 12.3.

[α]_D²⁰: +32 (*c* = 0.50, CHCl₃).

HPLC: The diastereomeric ratio was measured by Heart-Cut-HPLC analysis using Chiralpak OD-3, i.D. 4.6 mm. Heptane/ *i*PrOH = 99:1, flow rate = 1.0 mL/min, λ = 204 nm, t_R = 4.0 min (major) and t_R = 4.7 min (minor), dr = 19:1.



Dihydrocholesterol-derivatized aldehyde **27**

7 EXPERIMENTAL PART

To a round-bottom flask were added dihydrocholesterol (1.2 g, 3.0 mmol, 1.0 equiv), 4-(dimethylamino)-pyridine (DMAP, 18.3 mg, 0.15 mmol, 0.05 equiv), benzene (18.0 mL), trimethylamine (TEA, 0.46 mL, 3.3 mmol, 1.1 equiv), and followed by the addition of 10-undecenoyl chloride (1.0 mL, 4.5 mmol, 1.5 equiv). The reaction mixture was stirred at room temperature overnight. The solvent was removed under reduced pressure and the residue was purified by column chromatography on silica gel using 5–10% ethyl acetate/hexanes as the eluent giving a colorless solid (0.98 g, 1.8 mmol, 59%). To a round bottom flask were added the obtained colorless solid (0.55 g, 1.0 mmol, 1.0 equiv), triphenylphosphine (Ph₃P, 0.80 g, 3.0 mmol, 3.0 equiv), and CH₂Cl₂ (10 mL), followed by the bubbling of the ozone at –40 °C until the starting material was fully consumed. The solvent was removed under reduced pressure and the residue was purified by column chromatography on silica gel using 5–10% ethyl acetate/hexanes as eluents giving a colorless solid **27** (0.38 g, 0.69 mmol, 69%).

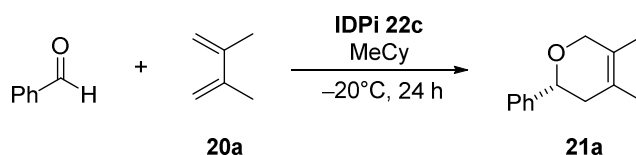
¹H NMR (500 MHz, CD₂Cl₂): δ 9.72 (s, 1H), 4.66 (hept, *J* = 4.6 Hz, 1H), 2.39 (dt, *J* = 7.4, 1.6 Hz, 2H), 2.23 (t, *J* = 7.5 Hz, 2H), 1.97 (td, *J* = 12.6, 3.2 Hz, 1H), 1.85–1.71 (m, 3H), 1.67–1.43 (m, 10.6H), 1.38–0.95 (m, 28H), 0.91 (d, *J* = 6.5 Hz, 3H), 0.86 (dd, *J* = 6.6, 1.9 Hz, 6H), 0.82 (s, 3H), 0.69–0.63 (m, 4H).

¹³C NMR (126 MHz, CD₂Cl₂): δ 203.1, 173.5, 73.7, 56.9, 56.7, 54.7, 45.1, 44.3, 43.0, 40.5, 39.9, 37.2, 36.6, 36.3, 35.92, 35.87, 35.0, 34.5, 32.5, 29.6, 29.50, 29.48, 29.4, 29.1, 28.6, 28.4, 28.0, 25.4, 24.6, 24.2, 23.0, 22.7, 22.5, 21.6, 18.9, 12.4, 12.2.

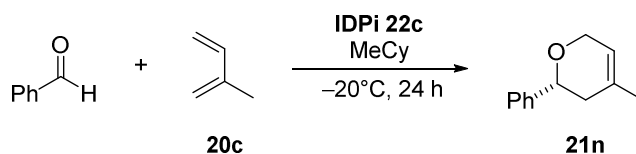
HRMS (ESI+) (*m/z*): calculated for C₃₇H₆₄O₃Na₁ [M+Na]⁺: 579.4748; found: 579.4756.

7 EXPERIMENTAL PART

Gram-Scale Reaction

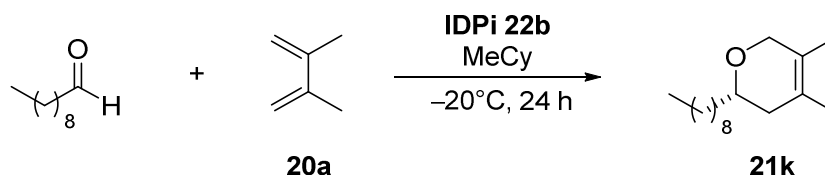


To a flame-dried schlenk, 700 mg 5 Å molecular sieves, catalyst **22c** (45 mg/0.02 mmol) and 10 mL anhydrous methylcyclohexane were added. The mixture was stirred for 5 min at room temperature. Then benzaldehyde (1.06 g/10.0 mmol) was added to the reaction mixture at -78 °C. Subsequently, 2,3-dimethyl-1,3-butadiene (985.8 mg/12.0 mmol) was dropped in slowly within 10 mins at -78 °C. The reaction was stirred at -20 °C for 1 day. Purification of product **21a** was performed by column chromatography on silica gel using pentane/diethyl ether = 100/2 as the eluent (1.825 g/9.7 mmol, 97% and 98:2 er). The catalyst **22c** could be recycled by column chromatography on silica gel using hexane/ethyl acetate = 50/50 as the eluent affording a white solid. The solid was dissolved in CH_2Cl_2 (10 mL) and stirred with 6 N aqueous HCl (10 mL) for 30 min. The organic layer was separated, washed with 6 N aqueous HCl (10 mL) and concentrated under reduced pressure to furnish the recycled catalyst **22c** (43.7 mg, 97%).



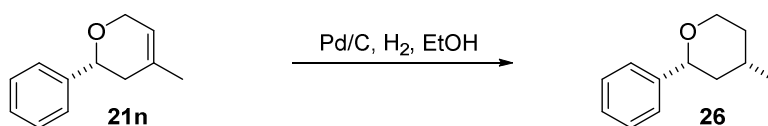
To a flame-dried schlenk, 700 mg 5 Å molecular sieves, catalyst **22c** (45 mg/0.02 mmol) and 10 mL anhydrous methylcyclohexane were added. The mixture was stirred for 5 min at room temperature. Then benzaldehyde (1.06 g/10.0 mmol) was added to the reaction mixture at -78 °C. Subsequently, isoprene **20c** (817.4 mg/12.0 mmol) was dropped in slowly within 10 mins at -78 °C. The reaction was stirred at -20 °C for 2 days. Purification of product **21n** was performed by column chromatography on silica gel using pentane/diethyl ether = 100/2 as the eluent (1.51 g/8.7 mmol, 87% and 98:2 er). The catalyst **22c** was recycled by column chromatography.

7 EXPERIMENTAL PART



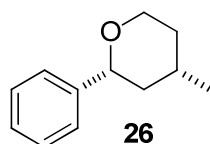
To a flame-dried schlenk, 1.05 g 5 Å molecular sieves, catalyst **22b** (104.8 mg/0.405 mmol), 15 ml anhydrous methylcyclohexane were added in sequence at room temperature. Then 2,3-dimethyl-1,3-butadiene (3.7 g/45.0 mmol) and decyl aldehyde (703.2 mg/4.5 mmol) was were added to the reaction mixture in sequence in the reaction mixture at $-20\text{ }^{\circ}\text{C}$. The reaction was performed for 2 days at $-20\text{ }^{\circ}\text{C}$. Purification of product **21k** was performed by column chromatography on silica gel using pentane/diethyl ether = 100/2 as the eluent (0.95 g/3.99 mmol, 89% and 96.5:3.5 er).

Derivatization



21n (31.5 mg, 0.18 mmol) was dissolved in anhydrous and degassed ethanol (1.0 mL) at room temperature, followed by the addition of palladium (10%) on charcoal (10.4 mg). An atmosphere of hydrogen was introduced and the resulting suspension was stirred at $-20\text{ }^{\circ}\text{C}$ for 2 h. The reaction mixture was warmed up to room temperature and performed overnight. The reaction mixture was filtered over Celite and the residue was purified by column chromatography on silica gel using 5% diethyl ether/pentane as the eluent affording Doremox **26** as a clear oil. (31 mg, 0.176 mmol, 98%, *cis:trans* = 8.5:1, 98:2 er_{*cis*}, 94.5:5.5 er_{*trans*}).

7 EXPERIMENTAL PART



(2*R*,4*S*)-4-methyl-2-phenyltetrahydro-2H-pyran

¹H NMR (600 MHz, CD₂Cl₂): δ 7.34–7.30 (m, 4H), 7.25–7.22 (m, 1H), 4.64 (*trans* isomer, dd, *J* = 9.9, 3.0 Hz, 0.12H), 4.29 (*cis* isomer, dd, *J* = 11.3, 2.2 Hz, 0.95H), 4.10 (*cis* isomer, ddd, *J* = 11.5, 4.7, 1.6 Hz, 0.97H), 3.81–3.79 (*trans* isomer, m, 0.24H), 3.57 (*cis* isomer, ddd, *J* = 12.4, 11.4, 2.2 Hz, 0.99H), 2.12–2.07 (*trans* isomer, m, 0.12H), 1.92–1.73 (m, 2.22H), 1.63–1.58 (m, 1.13H), 1.35–1.26 (m, 1.22H), 1.20–1.14 (m, 1.37H), 0.97 (d, *J* = 6.5 Hz, 3.0H), (spectra were complicated due to the presence of two diastereomers).

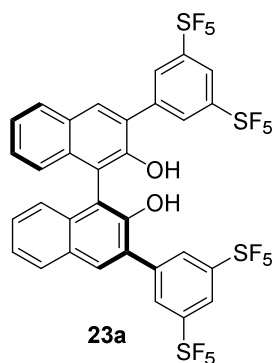
¹³C NMR (151 MHz, CD₂Cl₂): δ 144.1 (*cis* isomer), 143.8 (*trans* isomer), 128.54 (*trans* isomer), 128.52 (*cis* isomer), 127.5 (*cis* isomer), 127.3 (*trans* isomer), 126.4 (*trans* isomer), 126.2 (*cis* isomer), 80.0 (*cis* isomer), 74.2 (*trans* isomer), 68.8 (*cis* isomer), 63.3 (*trans* isomer), 43.3 (*cis* isomer), 39.6 (*trans* isomer), 34.9 (*cis* isomer), 32.4 (*trans* isomer), 31.2 (*cis* isomer), 25.9 (*trans* isomer), 22.5 (*cis* isomer), 18.5 (*trans* isomer), (spectra were complicated due to the presence of two diastereomers).

HRMS (ESI+) (*m/z*) calculated for C₁₂H₁₆O₁Na₁ [M+Na]⁺: 199.1093; found: 199.1094.

GC: The enantiomeric ratio was measured by GC analysis on a chiral column (Hydrodex-gamma-TBDAC column: 25.0 m; i.D. 0.25mm); FID; Temperature: 220 °C (injector), 350 °C (detector), 120 °C (30 min, iso); Gas: H₂ (0.50 bar); *t_R* (*cis*) = 17.04 min (minor) and *t_R* (*cis*) = 17.76 min (major), e.r. = 98:2; *t_R* (*trans*) = 19.45 min (major) and *t_R* (*trans*) = 21.17 min (minor), er = 94.5:5.5.

7 EXPERIMENTAL PART

7.4.2 Catalyst Synthesis



(*S*)-3,3'-bis(3,5-bis(pentafluoro- λ^6 -sulfanyl)phenyl)-[1,1'-binaphthalene]-2,2'-diol

To a three-necked round bottom flask with a condenser were added barium hydroxide octahydrate (2.3 g, 7.2 mmol, 4.5 equiv), a 1,4-dioxane/H₂O solution (3:1, 30 mL), (*S*)-2,2'-(2,2'-bis(methoxymethoxy)-[1,1'-binaphthyl]-3,3'-diyl)bis(4,4',5,5'-tetramethyl-1,3,2-dioxaborolane) (1.0 g, 1.6 mmol, 1.0 equiv), and 2,4-bis(pentafluorosulfanyl)bromobenzene (2.17 g, 5.3 mmol, 3.3 equiv). After degassing the reaction mixture with argon for 20 min, tetrakis(triphenylphosphine)palladium (0.14 g, 0.12 mmol, 0.075 equiv) was added. The mixture was refluxed for 24 h, then cooled to room temperature, and quenched with HCl (10 mL, 1.0 M, aq.). After extraction with CH₂Cl₂ (3×30 mL), the combined organic layers were successively washed with HCl (60 mL, 1.0 M, aq.), NaHCO₃ (60 mL, sat., aq.), and brine (60 mL). The organic layers were dried over Na₂SO₄, and concentrated under reduced pressure. 1,4-dioxane (90 mL) and HCl (30 mL, conc. aq.) were added to the residue and the reaction mixture was stirred at 70 °C for 5 h in a round bottom flask equipped with a condenser. After cooling to room temperature, the reaction solution was extracted with CH₂Cl₂ (3×100 mL). The organic layers were combined, dried over Na₂SO₄, and the solvent was removed under reduced pressure. The residue was purified by column chromatography on silica gel using 5–10% ethyl acetate/hexanes affording the title compound **23a** as a colorless solid (1.0 g, 1.06 mmol, 66%).

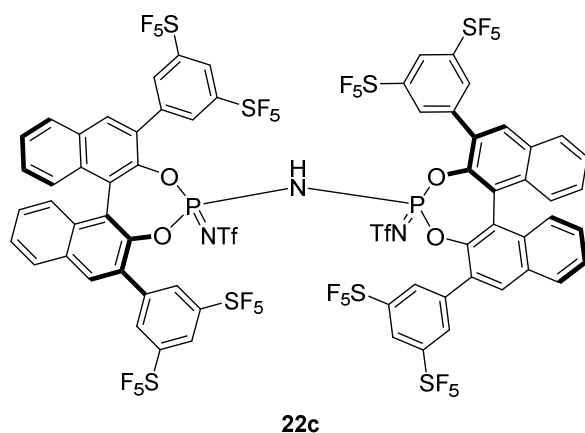
¹H NMR (500 MHz, CDCl₃): δ 8.33 (d, J = 1.9 Hz, 4H), 8.17 (t, J = 1.9 Hz, 2H), 8.10 (s, 2H), 8.02 (d, J = 7.9 Hz, 2H), 7.50 (ddd, J = 8.0, 6.9, 1.0 Hz, 2H), 7.44 (ddd, J = 8.3, 6.9, 1.3 Hz, 2H), 7.22 (d, J = 8.3 Hz, 2H), 5.39 (s, 2H).

7 EXPERIMENTAL PART

^{13}C NMR (126 MHz, CDCl_3): δ 153.9, 153.7, 153.6, 153.4, 153.3, 149.8, 139.6, 133.5, 132.7, 130.4, 129.6, 129.1, 127.1, 125.6, 124.1, 123.1, 111.9; δ 153.6 (p, $J = 18.8$ Hz).

^{19}F NMR (470 MHz, CDCl_3): δ 81.94 (p, $J = 150.5$ Hz), 63.09 (d, $J = 150.5$ Hz).

HRMS (ESI $^-$) (m/z): calculated for $\text{C}_{32}\text{H}_{17}\text{O}_2\text{F}_{20}\text{S}_4$ [$\text{M}-\text{H}$] $^-$: 940.9798; found 940.9803.



N-(((11*cS*)-2-(3,5-bis(pentafluoro- λ^6 -sulfanyl)phenyl)-4-(((11*cS*)-2-(3,5-bis(pentafluoro- λ^6 -sulfanyl)phenyl)-6-(3-(pentafluoro- λ^6 -sulfanyl)-5-((tetrafluoro- λ^5 -sulfanyl)-12-fluoranyl)phenyl)-4-(((trifluoromethyl)sulfonyl)imino)-4 λ^5 -dinaphtho[2,1-*d*:1',2'-*f*][1,3,2]dioxaphosphepin-4-yl)imino)-6-(3-(pentafluoro- λ^6 -sulfanyl)-5-((tetrafluoro- λ^5 -sulfanyl)- λ^2 -fluoranyl)phenyl)-415-dinaphtho[2,1-*d*:1',2'-*f*][1,3,2]dioxaphosphepin-4-yl)-1,1,1-trifluoromethanesulfonamide

In a flame-dried flask under argon, diol **23a** (0.1 g, 0.1 mmol, 2.1 equiv) was dissolved in toluene (1.4 mL). Subsequently, *N,N*-diisopropylethylamine (DIPEA, 0.14 mL, 0.80 mmol, 16.0 equiv), followed by trifluoromethylsulfonyl trichlorophosphazene ($\text{P}(\text{NTf})\text{Cl}_3$, 30.4 mg, 0.1 mmol, 2.1 equiv) were added and the solution was stirred at room temperature for 5 min. 1,1,1,3,3,3-hexamethyldisilazane (HMDS, 10.4 mg, 0.05 mmol, 1.0 equiv) was added to the reaction mixture, which was stirred at stirred at 120 °C for 12 h. The reaction mixture was cooled to room temperature and the solvent was removed under reduced pressure. The residue was purified by column chromatography on silica gel using 20–40% ethyl acetate/hexanes as the eluent affording a colorless solid. The solid was dissolved in CH_2Cl_2 (25 mL) and stirred with HCl (6.0 M, aq., 25 mL) for 30 min. The organic layer was separated, washed with HCl (6.0 M, aq., 25 mL), and

7 EXPERIMENTAL PART

concentrated under reduced pressure to provide compound **22c** as a colorless solid (90 mg, 0.04 mmol, 80%).

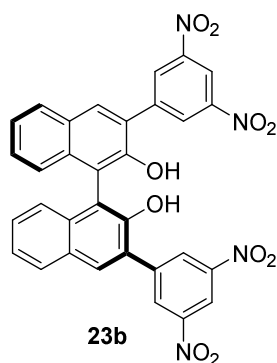
¹H NMR (500 MHz, CD₂Cl₂): δ 8.20 (br s, 2H), 8.18 (t, *J* = 1.75 Hz, 2H), 8.16–8.15 (m, 2H), 8.13 (br s, 2H), 7.97–7.94 (m, 2H), 7.92–7.91 (m, 2H), 7.87 (d, *J* = 1.60 Hz, 4H), 7.80–7.75 (m, 4H), 7.66 (t, *J* = 7.30 Hz, 2H), 7.48 (br s, 4H), 7.40–7.37 (m, 2H), 7.36 (s, 2H), 7.07 (d, *J* = 8.60 Hz, 2H), 6.58 (s, 2H), 4.93 (br s, 2H).

¹³C NMR (126 MHz, CD₂Cl₂): δ 154.0, 153.9, 153.8, 153.6, 144.0, 141.4, 138.6, 138.2, 134.0, 133.0, 132.6, 132.4, 132.3, 131.5, 130.84, 130.78, 130.1, 129.9, 129.61, 129.56, 128.7, 128.6, 127.9, 127.8, 127.14, 127.11, 124.5, 124.1, 123.9, 121.7, 120.3, 117.7.

¹⁹F NMR (470 MHz, CD₂Cl₂): δ 80.8 (sext, *J* = 152.0 Hz, 8F), 63.1 (d, *J* = 150.6 Hz, 16F), 62.3 (d, *J* = 150.0 Hz, 16F), –79.5 (s, 6F).

³¹P NMR (202 MHz, CD₂Cl₂): δ –15.3.

HRMS (ESI[–]) (*m/z*): calculated for C₆₆H₃₂N₃O₈F₄₆P₂S₁₀ [M–H][–]: 2249.8143; found: 2249.8128.



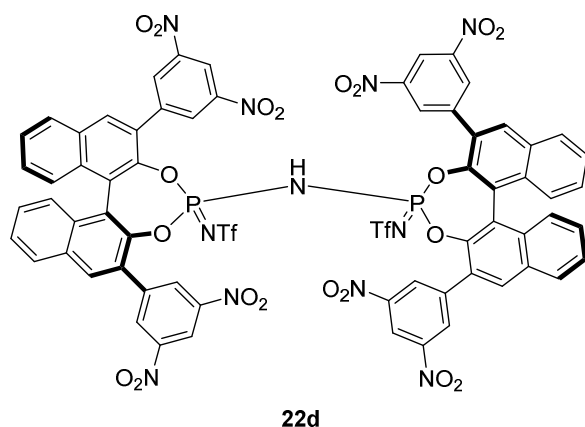
(*S*)-3,3'-bis(3,5-dinitrophenyl)-[1,1'-binaphthalene]-2,2'-diol

To a two-necked round flask with a condenser were added barium hydroxide octahydrate (1.76 mmol), a 1,4-dioxane/H₂O solution (3/1, 10 mL), (2,2'-dimethoxy-[1,1'-binaphthalene]-3,3'-diyl)diboronic acid (0.6 mmol) and 1-brom-3,5-dinitrobenzene (1.91 mmol), the mixture was degass by Ar₂ for 20min, then add tetrakis(triphenylphosphine)palladium (0.063 mmol), The mixture was refluxed at 70 °C for 48 h , then cooled to room temperature. The dioxane was removed, and the resulting residue was redissolved in CH₂Cl₂, washed with 1 N HCl solution and brine, dried over Na₂SO₄. The crude product as afforded as red oil which was purified by column

7 EXPERIMENTAL PART

chromatography with a eluent: hexane:ethylacetate 95:5–85:15. Remove the solvent under reduced pressure to give the methoxyl-protected title compound as a pale solid (0.362 mmol, 60.3%).

Under argon, add the protected compound 160 mg/0.25 mmol and dry CH₂Cl₂ 15 mL to a flamed schlenk. Then cool the reaction mixture to 0 °C. A solution of BBr₃ in CH₂Cl₂ (2.0 mL, 1.0 M, 8eq) was then added dropwise over 10 mins. The reaction mixture was stirred at room temperature for another 6 hours with a full conversion. Quench the reaction by slowly adding water. The reaction mixture was diluted with CH₂Cl₂, washed with water then brine. The combined organic layers were dried over Na₂SO₄, filtered and concentrated. The crude product was purified by silica flash column chromatography (4:1–3:1 CH₂Cl₂:hexane) affording the literature reported product **23b** (21.6 mmol, 86.3%).



N,N'-((11b*S*,11b'*S*)-azanediylbis(2,6-bis(3,5-dinitrophenyl)-4λ⁵-dinaphtho[2,1-d:1',2'-f][1,3,2]dioxaphosphepine-4-yl-4-ylidene))bis(1,1,1-trifluoromethanesulfonamide)

To a mixture of the 3, 3'-disubstituted BINOL **23b** (2.0 equiv.) and trifluoromethylsulfonyl trichlorophosphazene (P(NTf)Cl₃, 2.0 equiv.) in tetrahydrofuran (0.2 M) was added Et₃N (12 equiv.) at room temperature under argon atmosphere. After being stirred for 10 min, NH₃ in dioxane (1.0 equiv., 0.5 M), DMAP (0.4 equiv.) was added. After an additional stirring for 10 min at room temperature, the reaction mixture was heated to 70 °C for 45 hours. The solvent was removed by reduced pressure and the residue was purified by column chromatography on silica gel using 3% ethyl acetate/DCM as the eluents giving a pale yellow solid. The solid was dissolved in CH₂Cl₂ and stirred with 6 N aqueous HCl for 30 mins. The organic layer was separated, washed

7 EXPERIMENTAL PART

with 6 N aqueous HCl and concentrated under reduced pressure to give the title compound **22d** as a white solid (74%).

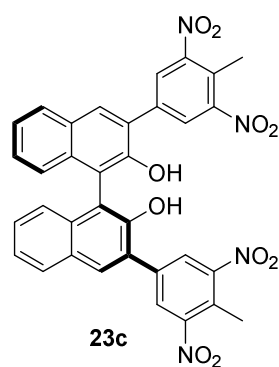
¹H NMR (600 MHz, CD₂Cl₂): δ 8.99 (t, *J* = 4.2 Hz, 2H), 8.69 (d, *J* = 2.4 Hz, 5H), 8.67 (t, *J* = 4.2 Hz, 2H), 8.20 (s, 2H), 8.13 (d, *J* = 8.4 Hz, 2H), 7.95 (d, *J* = 1.8 Hz, 5H), 7.93–7.90 (m, 2H), 7.88–7.85 (m, 5H), 7.80–7.77 (m, 2H), 7.66 (ddd, *J* = 7.8, 6.6, 1.2 Hz, 2H), 7.43 (ddd, *J* = 8.4, 7.2, 1.2 Hz, 2H), 7.31 (d, *J* = 7.8 Hz, 2H), 6.87 (s, 2H).

¹³C NMR (151 MHz, CD₂Cl₂): δ 148.69, 148.39, 143.91, 143.88, 143.85, 143.19, 143.15, 143.11, 139.76, 139.27, 133.06, 132.89, 132.42, 131.94, 131.48, 131.30, 130.93, 130.21, 129.63, 129.52, 129.22, 129.21, 129.20, 129.19, 129.18, 129.16, 129.15, 128.50, 127.75, 127.59, 127.50, 127.36, 123.74, 123.73, 123.72, 122.83, 122.47, 122.46, 122.45, 120.71, 118.58, 118.30, 118.05, 116.47.

³¹P NMR (202 MHz, CD₂Cl₂): δ –5.37 (S).

¹⁹F NMR (470 MHz, CD₂Cl₂): δ –79.9 (S).

HRMS (ESI[–]) (*m/z*): calculated for C₆₆H₃₂N₁₁O₂₄F₆P₂S₂ [M–H][–]: 1602.0448; found: 1602.0449.



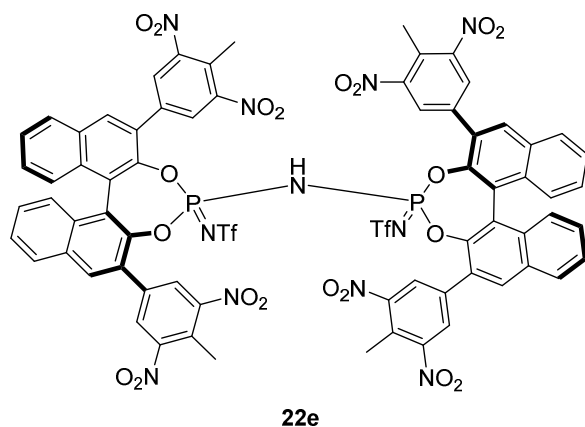
(*S*)-3,3'-bis(4-methyl-3,5-dinitrophenyl)-[1,1'-binaphthalene]-2,2'-diol

To a two-necked round flask with a condenser were added barium hydroxide octahydrate (1.76 mmol), a 1,4-dioxane/H₂O solution (3/1, 10 mL), (2,2'-dimethoxy-[1,1'-binaphthalene]-3,3'-diyl)diboronic acid (0.6 mmol) and 1-brom-3,5-dinitrotoluene (1.91 mmol), the mixture was degass by Ar₂ for 20min, then add tetrakis(triphenylphosphine)palladium (0.063 mmol), The mixture was refluxed at 70 °C for 48 h , then cooled to room temperature. The dioxane was removed, and the resulting residue was redissolved in CH₂Cl₂, washed with 1 N HCl solution and brine, dried over

7 EXPERIMENTAL PART

Na₂SO₄. The crude product as afforded as red oil which was purified by column chromatography with an eluent of 3–10% hexane:ethylacetate. Remove the solvent under reduced pressure to give the methoxyl-protected title compound as a pale solid (0.31 mmol, 52%).

Under argon, add the protected compound 138 mg/0.25 mmol and dry CH₂Cl₂ 12 ml to a flamed schlenk. Then cool the reaction mixture to 0 °C. A solution of BBr₃ in CH₂Cl₂ (1.6 mL, 1.0 M, 8eq) was then added dropwise over 10 mins. The reaction mixture was stirred at room temperature for another 6 hours with a full conversion. Quench the reaction by slowly adding water. The reaction mixture was diluted with CH₂Cl₂, washed with water then brine. The combined organic layers were dried over Na₂SO₄, filtered and concentrated. The crude product was purified by silica flash column chromatography with an eluent of 25–40% CH₂Cl₂:hexane, affording the literature reported product **23c** (0.155 mmol, 77.3%).



N,N'-((11bS,11b'S)-azanediylbis(2,6-bis(4-methyl-3,5-dinitrophenyl)-4λ⁵-dinaphtho[2,1-d:1',2'-f][1,3,2]dioxaphosphepine-4-yl-4-ylidene))bis(1,1,1-trifluoromethanesulfonamide)

To a mixture of the 3, 3'-disubstituted BINOL **23c** (2.0 equiv.) and trifluoromethylsulfonyl trichlorophosphazene (P(NTf)Cl₃, 2.0 equiv.) in tetrahydrofuran (0.2 M) was added Et₃N (12 equiv.) at room temperature under argon atmosphere. After being stirred for 10 min, NH₃ in dioxane (0.5 M, 1.0 equiv.), DMAP (0.4 equiv.) was added. After an additional stirring for 10 min at room temperature, the reaction mixture was heated to 70 °C for 45 hours. The solvent was removed by reduced pressure and the residue was purified by column chromatography on silica gel using 1–25% ethyl acetate/DCM as the eluents giving a pale yellow solid. The solid was dissolved in CH₂Cl₂ and stirred with 6N aqueous HCl for 30 mins. The organic layer was separated, washed

7 EXPERIMENTAL PART

with 6 N aqueous HCl and concentrated under reduced pressure to give the title **22e** compound as a white solid (75%).

¹H NMR (600 MHz, CD₂Cl₂): δ 8.36 (br s, 2H), 8.21 (s, 1H), 8.11 (d, *J* = 8.4 Hz, 1H), 8.03 (d, *J* = 8.4 Hz, 1H), 7.88 (ddd, *J* = 8.4, 6.6, 1.2 Hz, 1H), 7.67 (ddd, *J* = 8.4, 6.6, 1.2 Hz, 1H), 7.62 (ddd, *J* = 8.4, 6.6, 1.2 Hz, 1H), 7.42 (d, *J* = 9.0 Hz, 1H), 7.37 (ddd, *J* = 8.4, 7.2, 1.2 Hz, 1H), 7.24 (br s, 2H), 7.20 (d, *J* = 2.4 Hz, 1H), 6.90 (s, 1H), 2.62 (s, 3H), 2.29 (s, 3H).

¹³C NMR (151 MHz, CD₂Cl₂): δ 151.61, 151.54, 144.34, 144.30, 144.27, 143.25, 143.21, 143.17, 136.86, 135.83, 133.04, 132.73, 132.42, 131.89, 131.32, 131.11, 130.01, 129.59, 129.53, 129.52, 129.51, 129.50, 129.41, 129.08, 129.07, 129.06, 128.28, 127.61, 127.35, 127.22, 127.15, 127.12, 127.09, 126.75, 125.30, 123.86, 123.85, 123.84, 122.84, 122.15, 122.14, 122.13, 120.72, 118.59, 116.48, 15.23, 14.42.

³¹P NMR (202 MHz, CD₂Cl₂): δ -6.28 (S).

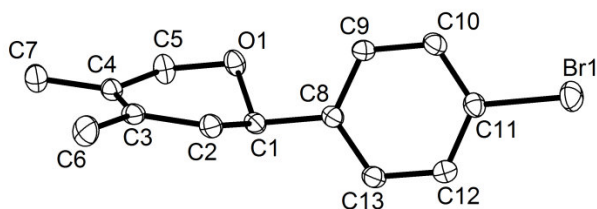
¹⁹F NMR (470 MHz, CD₂Cl₂): δ -79.86 (S).

HRMS (ESI) (*m/z*): calculated for C₇₀H₄₀N₁₁O₂₄F₆P₂S₂ [M-H]: 1658.1074; found: 1658.1087.

7 EXPERIMENTAL PART

7.4.3 X-Ray Data

X-ray structural analysis parameter for 21e:



Crystal data and structure refinement

Crystal data and structure refinement

Identification code	10450
Empirical formula	C ₁₃ H ₁₅ Br ₁ O ₁
Color	colourless
Formula weight	267.16 g·mol ⁻¹
Temperature	100(2) K
Wavelength	0.71073 Å
Crystal system	orthorhombic
Space group	<i>P</i> 2 ₁ 2 ₁ 2 ₁ , (no. 19)
Unit cell dimensions	<i>a</i> = 6.836(2) Å $\alpha = 90^\circ$ <i>b</i> = 11.5511(9) Å $\beta = 90^\circ$ <i>c</i> = 15.3107(9) Å $\gamma = 90^\circ$
Volume	1208.9(4) Å ³
<i>Z</i>	4
Density (calculated)	1.468 Mg·m ⁻³
Absorption coefficient	3.372 mm ⁻¹
<i>F</i> (000)	544 e
Crystal size	0.23 x 0.15 x 0.09 mm ³
θ range for data collection	3.528 to 33.119°.
Index ranges	-10 ≤ <i>h</i> ≤ 10, -17 ≤ <i>k</i> ≤ 17, -23 ≤ <i>l</i> ≤ 23
Reflections collected	65284
Independent reflections	4595 [<i>R</i> _{int} = 0.0406]
Reflections with <i>I</i> > 2σ(<i>I</i>)	4427
Completeness to $\theta = 25.242^\circ$	99.1 %
Absorption correction	Gaussian
Max. and min. transmission	0.75447 and 0.51719
Refinement method	Full-matrix least-squares on <i>F</i> ²
Data / restraints / parameters	4595 / 0 / 138

7 EXPERIMENTAL PART

Goodness-of-fit on F^2	1.109	
Final R indices [$I > 2\sigma(I)$]	$R_1 = 0.0203$	$wR^2 = 0.0521$
R indices (all data)	$R_1 = 0.0220$	$wR^2 = 0.0530$
Absolute structure parameter	-0.006(3)	
Extinction coefficient	0	
Largest diff. peak and hole	0.463 and -0.355 $e \cdot \text{\AA}^{-3}$	

7 EXPERIMENTAL PART

Atomic coordinates and equivalent isotropic displacement parameters (\AA^2).

U_{eq} is defined as one third of the trace of the orthogonalized U_{ij} tensor.

	x	y	z	U_{eq}
C(1)	0.2649(2)	0.3189(2)	0.5884(1)	0.018(1)
C(2)	0.0983(2)	0.3329(2)	0.6540(1)	0.020(1)
C(3)	0.0412(2)	0.4578(2)	0.6672(1)	0.021(1)
C(4)	0.1547(2)	0.5432(2)	0.6371(1)	0.021(1)
C(5)	0.3487(2)	0.5167(2)	0.5945(1)	0.023(1)
C(6)	-0.1475(3)	0.4750(2)	0.7163(2)	0.032(1)
C(7)	0.1107(3)	0.6705(2)	0.6422(1)	0.028(1)
C(8)	0.3544(2)	0.1997(1)	0.5929(1)	0.017(1)
C(9)	0.5089(2)	0.1772(2)	0.6500(1)	0.020(1)
C(10)	0.5871(2)	0.0659(2)	0.6570(1)	0.022(1)
C(11)	0.5082(2)	-0.0221(1)	0.6060(1)	0.020(1)
C(12)	0.3551(3)	-0.0018(1)	0.5486(1)	0.022(1)
C(13)	0.2789(2)	0.1097(2)	0.5422(1)	0.021(1)
Br(1)	0.6150(1)	-0.1736(1)	0.6157(1)	0.029(1)
O(1)	0.4148(2)	0.4013(1)	0.6078(1)	0.021(1)

Bond lengths [\AA] and angles [$^\circ$].

C(1)-O(1)	1.430(2)	C(1)-C(8)	1.508(2)
C(1)-C(2)	1.528(2)	C(2)-C(3)	1.507(2)
C(3)-C(4)	1.337(3)	C(3)-C(6)	1.506(2)
C(4)-C(7)	1.502(2)	C(4)-C(5)	1.509(2)
C(5)-O(1)	1.422(2)	C(8)-C(9)	1.396(2)
C(8)-C(13)	1.397(2)	C(9)-C(10)	1.397(2)
C(10)-C(11)	1.390(2)	C(11)-C(12)	1.387(2)
C(11)-Br(1)	1.9020(16)	C(12)-C(13)	1.393(2)
O(1)-C(1)-C(8)	107.89(12)	O(1)-C(1)-C(2)	109.09(13)
C(8)-C(1)-C(2)	111.72(13)	C(3)-C(2)-C(1)	112.47(14)
C(4)-C(3)-C(6)	124.83(17)	C(4)-C(3)-C(2)	120.68(14)
C(6)-C(3)-C(2)	114.48(16)	C(3)-C(4)-C(7)	126.01(15)
C(3)-C(4)-C(5)	120.57(15)	C(7)-C(4)-C(5)	113.41(15)
O(1)-C(5)-C(4)	114.07(14)	C(9)-C(8)-C(13)	119.29(15)
C(9)-C(8)-C(1)	120.38(14)	C(13)-C(8)-C(1)	120.29(14)

7 EXPERIMENTAL PART

C(8)-C(9)-C(10)	120.58(15)	C(11)-C(10)-C(9)	118.82(14)
C(12)-C(11)-C(10)	121.68(15)	C(12)-C(11)-Br(1)	119.63(13)
C(10)-C(11)-Br(1)	118.70(12)	C(11)-C(12)-C(13)	118.89(15)
C(12)-C(13)-C(8)	120.74(15)	C(5)-O(1)-C(1)	111.52(12)

Anisotropic displacement parameters (\AA^2).

The anisotropic displacement factor exponent takes the form:

$$-2\pi^2 [h^2 a^{*2} U_{11} + \dots + 2 h k a^* b^* U_{12}].$$

	U ₁₁	U ₂₂	U ₃₃	U ₂₃	U ₁₃	U ₁₂
C(1)	0.016(1)	0.021(1)	0.016(1)	0.000(1)	0.000(1)	0.003(1)
C(2)	0.015(1)	0.024(1)	0.021(1)	-0.002(1)	0.003(1)	0.001(1)
C(3)	0.015(1)	0.027(1)	0.019(1)	-0.005(1)	0.000(1)	0.002(1)
C(4)	0.019(1)	0.024(1)	0.019(1)	-0.004(1)	-0.002(1)	0.005(1)
C(5)	0.023(1)	0.020(1)	0.027(1)	0.004(1)	0.006(1)	0.004(1)
C(6)	0.019(1)	0.036(1)	0.041(1)	-0.011(1)	0.008(1)	0.003(1)
C(7)	0.029(1)	0.025(1)	0.030(1)	-0.003(1)	-0.001(1)	0.008(1)
C(8)	0.016(1)	0.021(1)	0.015(1)	0.000(1)	0.001(1)	0.002(1)
C(9)	0.020(1)	0.022(1)	0.017(1)	-0.002(1)	-0.004(1)	0.002(1)
C(10)	0.022(1)	0.024(1)	0.019(1)	0.001(1)	-0.004(1)	0.004(1)
C(11)	0.022(1)	0.020(1)	0.018(1)	0.002(1)	0.001(1)	0.003(1)
C(12)	0.023(1)	0.022(1)	0.021(1)	-0.002(1)	-0.002(1)	0.000(1)
C(13)	0.019(1)	0.024(1)	0.019(1)	-0.001(1)	-0.003(1)	0.002(1)
Br(1)	0.037(1)	0.021(1)	0.029(1)	0.004(1)	-0.001(1)	0.007(1)
O(1)	0.015(1)	0.020(1)	0.027(1)	0.002(1)	0.003(1)	0.002(1)

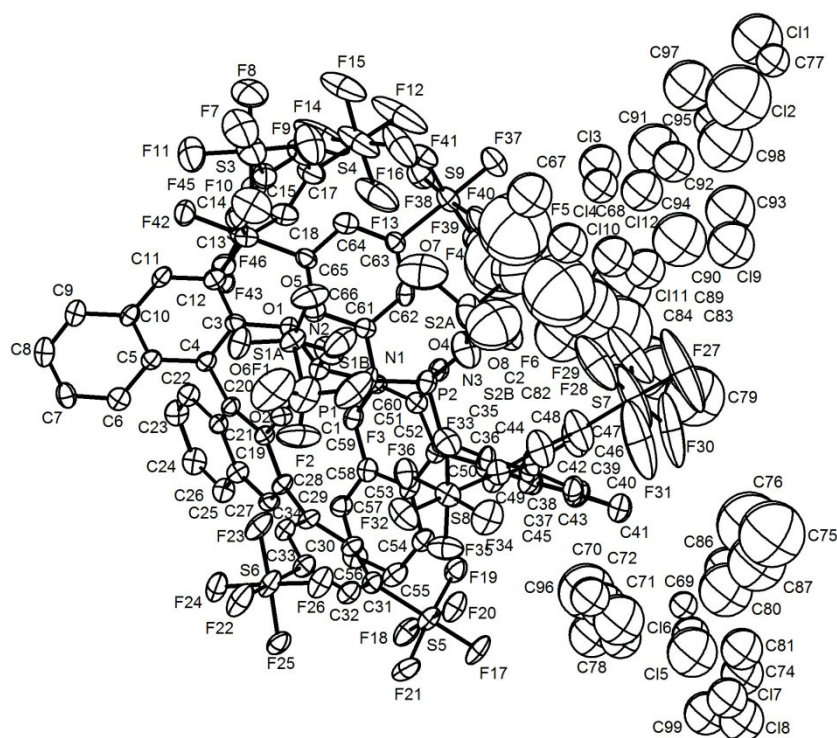
7 EXPERIMENTAL PART

Hydrogen coordinates and isotropic displacement parameters (\AA^2).

	x	y	z	U_{eq}
H(1)	0.2141	0.3330	0.5281	0.021
H(2A)	-0.0170	0.2890	0.6333	0.024
H(2B)	0.1388	0.2996	0.7108	0.024
H(5A)	0.3372	0.5309	0.5309	0.028
H(5B)	0.4484	0.5707	0.6177	0.028
H(6A)	-0.1378	0.4383	0.7738	0.048
H(6B)	-0.2553	0.4399	0.6834	0.048
H(6C)	-0.1722	0.5580	0.7235	0.048
H(7A)	-0.0276	0.6816	0.6568	0.042
H(7B)	0.1386	0.7068	0.5857	0.042
H(7C)	0.1924	0.7061	0.6874	0.042
H(9)	0.5614	0.2382	0.6845	0.024
H(10)	0.6922	0.0506	0.6959	0.026
H(12)	0.3031	-0.0630	0.5142	0.026
H(13)	0.1743	0.1246	0.5029	0.025

7 EXPERIMENTAL PART

X-ray structural analysis parameter for 22c:



Identification code	10698
Empirical formula	$C_{83.20} H_{33} Cl_{3.80} F_{44.80} N_3 O_{7.20} P_2 S_{10}$
Color	colourless
Formula weight	2558.17 $g \cdot mol^{-1}$
Temperature	100(2) K
Wavelength	1.54178 Å
Crystal system	orthorhombic
Space group	$P 2_1 2_1 2$, (no. 18)
Unit cell dimensions	$a = 18.7656(13) \text{ \AA}$ $\alpha = 90^\circ$. $b = 41.726(3) \text{ \AA}$ $\beta = 90^\circ$. $c = 14.4668(10) \text{ \AA}$ $\gamma = 90^\circ$.
Volume	11327.8(14) Å ³
Z	4
Density (calculated)	1.500 $Mg \cdot m^{-3}$
Absorption coefficient	4.015 mm^{-1}
F(000)	5074 e
Crystal size	0.300 x 0.189 x 0.030 mm^3
θ range for data collection	4.831 to 63.596°.
Index ranges	-21 ≤ h ≤ 21, -47 ≤ k ≤ 48, -14 ≤ l ≤ 16
Reflections collected	165258
Independent reflections	18356 [$R_{int} = 0.0717$]
Reflections with $I > 2\sigma(I)$	16034

7 EXPERIMENTAL PART

Completeness to $\theta = 63.596^\circ$	99.1 %	
Absorption correction	Gaussian	
Max. and min. transmission	0.90830 and 0.51138	
Refinement method	Full-matrix least-squares on F^2	
Data / restraints / parameters	18356 / 46 / 1405	
Goodness-of-fit on F^2	1.513	
Final R indices [$I > 2\sigma(I)$]	$R_1 = 0.0674$	$wR^2 = 0.1847$
R indices (all data)	$R_1 = 0.0785$	$wR^2 = 0.1920$
Absolute structure parameter	0.031(4)	
Extinction coefficient	0	
Largest diff. peak and hole	0.905 and -0.805 $e \cdot \text{\AA}^{-3}$	

The structure of the asymmetric unit in the crystal of **22c** was obtained with crystal solvent (hexane and dichloromethane). The structure of **22c** was solved by direct methods and refined by full-matrix least-squares against F^2 to $R_1 = 0.0674$ [$I > 2\sigma(I)$], $wR_2 = 0.1920$, 1405 parameters. The trifluoromethyl-sulfonyl-amino group is disordered over the two positions. In addition, the trifluoromethyl-sulfonyl-amino and trifluoromethyl-sulfonyl-phosphazene groups are slightly disordered. The major components (80% occupation) could be located and refined. Only the S atoms of the minor triflate components could be located and refined. All non-H atoms of one of the two trifluoromethyl-sulfonyl-amino/phosphazene groups were refined with anisotropic atomic displacement parameters. The atomic displacement parameters of the F, C and O atoms of the second trifluoromethyl-sulfonyl-amino/phosphazene group were restrained to be isotropic with an effective standard deviation of 0.005, whereby the atomic displacement parameters of the three F atoms were constrained to be equal. For this tri-fluoromethyl-sulfonyl-amino/phosphazene group the respective S...F, C-F and F...F distances were restrained to be equal with an effective standard deviation of 0.02, as were the S-C distances of both trifluoromethyl-sulfonyl-amino/phosphazene groups (total 46 restraints). The solvate (dichloromethane/hexane) region of the crystal was modeled by C and Cl atoms of various occupancies and refined isotropic atomic displacement parameters. A void of 43.95 %A, close to symmetry elements, remained (0.4 % of the unit cell volume, probe radius 1.2 %A, grid spacing 0.7 %A). The H atom attached to the trifluoromethyl-sulfonyl-amino group could not be located and was refined using a riding model, as were the other H atoms in the imidodiphosphorimidate (IDPI). The riding model used C-H distances of 0.95 Å and $U_H = 1.2 \times U_C(\text{CH}_{\text{aromatic}})$ and 0.88 Å and $U_H = 1.5 \times U_N(\text{NH})$. $S = 1.522$, residual electron density 0.90 (0.82 Å from F6)/ -0.80 (0.95 from F29) $e \text{\AA}^{-3}$. The Flack parameter (Parsons' method: Parsons, Flack and Wagner, *Acta Cryst.* B69 (2013) 249-259) is 0.031(4) [6454 quotients].

7 EXPERIMENTAL PART

Atomic coordinates and equivalent isotropic displacement parameters (\AA^2).

U_{eq} is defined as one third of the trace of the orthogonalized U_{ij} tensor.

	x	y	z	U_{eq}
C(1)	-0.0927(7)	0.3431(4)	0.5747(8)	0.068(4)
C(2)	0.1322(13)	0.4636(6)	0.3201(18)	0.203(16)
C(3)	-0.1190(4)	0.3272(2)	0.2149(5)	0.027(2)
C(4)	-0.1132(4)	0.2951(2)	0.1997(4)	0.025(1)
C(5)	-0.1765(3)	0.2761(2)	0.1881(5)	0.026(2)
C(6)	-0.1755(4)	0.2426(2)	0.1802(5)	0.031(2)
C(7)	-0.2386(4)	0.2255(2)	0.1698(5)	0.033(2)
C(8)	-0.3053(4)	0.2416(2)	0.1692(5)	0.037(2)
C(9)	-0.3075(4)	0.2742(2)	0.1772(5)	0.030(2)
C(10)	-0.2437(3)	0.2927(2)	0.1873(5)	0.027(2)
C(11)	-0.2458(3)	0.3257(2)	0.1999(5)	0.028(2)
C(12)	-0.1853(4)	0.3440(2)	0.2145(5)	0.030(2)
C(13)	-0.1913(4)	0.3790(2)	0.2275(5)	0.031(2)
C(14)	-0.2424(4)	0.3916(2)	0.2894(6)	0.039(2)
C(15)	-0.2506(4)	0.4242(2)	0.2958(6)	0.043(2)
C(16)	-0.2105(5)	0.4456(2)	0.2446(7)	0.052(2)
C(17)	-0.1597(5)	0.4330(2)	0.1841(7)	0.048(2)
C(18)	-0.1497(4)	0.4002(2)	0.1766(6)	0.041(2)
C(19)	-0.0018(3)	0.2821(2)	0.2825(4)	0.024(1)
C(20)	-0.0423(3)	0.2793(2)	0.2040(5)	0.026(2)
C(21)	-0.0156(4)	0.2594(2)	0.1311(5)	0.027(2)
C(22)	-0.0490(4)	0.2573(2)	0.0444(5)	0.030(2)
C(23)	-0.0231(4)	0.2377(2)	-0.0240(5)	0.037(2)
C(24)	0.0378(4)	0.2190(2)	-0.0065(5)	0.037(2)
C(25)	0.0720(4)	0.2203(2)	0.0755(5)	0.032(2)
C(26)	0.0476(4)	0.2411(2)	0.1460(5)	0.028(2)
C(27)	0.0834(4)	0.2433(2)	0.2328(5)	0.028(2)
C(28)	0.0595(3)	0.2632(2)	0.3005(4)	0.025(1)
C(29)	0.0913(4)	0.2616(2)	0.3962(5)	0.029(2)
C(30)	0.1641(4)	0.2630(2)	0.4099(5)	0.029(2)
C(31)	0.1922(4)	0.2579(2)	0.4975(5)	0.029(2)
C(32)	0.1477(4)	0.2506(2)	0.5721(5)	0.033(2)
C(33)	0.0748(4)	0.2482(2)	0.5559(5)	0.031(2)

7 EXPERIMENTAL PART

C(34)	0.0474(4)	0.2539(2)	0.4701(5)	0.028(2)
C(35)	0.2607(4)	0.3532(2)	0.3578(5)	0.030(2)
C(36)	0.2917(4)	0.3416(2)	0.2776(5)	0.030(2)
C(37)	0.3657(4)	0.3473(2)	0.2622(5)	0.036(2)
C(38)	0.3991(4)	0.3406(2)	0.1758(5)	0.036(2)
C(39)	0.4693(4)	0.3488(2)	0.1631(6)	0.043(2)
C(40)	0.5094(5)	0.3617(2)	0.2346(7)	0.050(2)
C(41)	0.4793(4)	0.3686(2)	0.3167(6)	0.043(2)
C(42)	0.4060(4)	0.3623(2)	0.3334(6)	0.036(2)
C(43)	0.3726(4)	0.3715(2)	0.4160(6)	0.039(2)
C(44)	0.2996(4)	0.3677(2)	0.4293(5)	0.034(2)
C(45)	0.2668(4)	0.3808(2)	0.5138(5)	0.036(2)
C(46)	0.2838(6)	0.4109(3)	0.5440(7)	0.063(3)
C(47)	0.2534(6)	0.4231(3)	0.6257(7)	0.068(3)
C(48)	0.2061(6)	0.4044(2)	0.6782(7)	0.061(3)
C(49)	0.1888(4)	0.3742(2)	0.6464(5)	0.038(2)
C(50)	0.2180(4)	0.3615(2)	0.5661(5)	0.034(2)
C(51)	0.1884(4)	0.3429(2)	0.1702(5)	0.029(2)
C(52)	0.2461(4)	0.3263(2)	0.2059(5)	0.029(2)
C(53)	0.2586(3)	0.2949(2)	0.1730(5)	0.029(2)
C(54)	0.3097(4)	0.2745(2)	0.2155(5)	0.033(2)
C(55)	0.3197(4)	0.2431(2)	0.1826(5)	0.039(2)
C(56)	0.2816(4)	0.2325(2)	0.1048(5)	0.036(2)
C(57)	0.2323(4)	0.2515(2)	0.0623(5)	0.031(2)
C(58)	0.2180(4)	0.2830(2)	0.0962(5)	0.029(2)
C(59)	0.1651(4)	0.3033(2)	0.0572(5)	0.032(2)
C(60)	0.1499(4)	0.3326(2)	0.0912(5)	0.026(2)
C(61)	0.0998(4)	0.3548(2)	0.0421(5)	0.028(2)
C(62)	0.1227(4)	0.3859(2)	0.0221(5)	0.031(2)
C(63)	0.0815(4)	0.4055(2)	-0.0332(5)	0.028(2)
C(64)	0.0164(4)	0.3957(2)	-0.0689(5)	0.035(2)
C(65)	-0.0058(4)	0.3648(2)	-0.0458(5)	0.031(2)
C(66)	0.0349(4)	0.3439(2)	0.0092(5)	0.032(2)
C(67)	-0.026(4)	0.5337(17)	0.623(5)	0.14(2)
C(68)	0.036(2)	0.5669(11)	0.660(3)	0.083(12)
C(69)	0.444(2)	0.3890(11)	0.913(3)	0.051(11)
C(70)	0.3138(9)	0.3638(4)	0.9426(12)	0.107(5)
C(71)	0.3838(17)	0.3577(7)	0.902(2)	0.178(11)
C(72)	0.3852(12)	0.3514(5)	0.8029(16)	0.144(7)

7 EXPERIMENTAL PART

C(73)	0.4503(14)	0.3365(6)	0.7647(19)	0.117(7)
C(74)	0.6996(17)	0.3420(8)	0.559(2)	0.123(9)
C(75)	0.529(5)	0.447(2)	0.782(7)	0.31(4)
C(76)	0.534(5)	0.434(2)	0.662(6)	0.30(4)
C(77)	0.352(3)	0.6380(12)	0.000(3)	0.077(12)
C(78)	0.4494(12)	0.3193(5)	0.6588(16)	0.142(7)
C(79)	0.437(2)	0.4626(10)	0.398(3)	0.262(17)
C(80)	0.591(3)	0.3843(12)	0.596(4)	0.188(17)
C(81)	0.6619(17)	0.3586(8)	0.602(2)	0.121(9)
C(82)	0.3048(18)	0.4290(8)	0.151(2)	0.211(12)
C(83)	0.348(5)	0.4560(17)	0.217(5)	0.33(3)
C(84)	0.400(3)	0.4567(13)	0.322(5)	0.20(2)
C(85)	0.380(3)	0.4419(14)	0.161(4)	0.108(16)
C(86)	0.600(5)	0.389(3)	0.507(8)	0.13(3)
C(87)	0.566(8)	0.419(4)	0.691(10)	0.25(6)
C(88)	0.404(3)	0.4524(11)	0.234(4)	0.160(15)
C(89)	0.281(5)	0.4597(18)	0.243(6)	0.28(3)
C(90)	0.361(4)	0.4683(16)	0.056(5)	0.26(3)
C(91)	0.326(5)	0.541(2)	-0.091(7)	0.19(3)
C(92)	0.320(3)	0.5505(16)	0.019(4)	0.118(18)
C(93)	0.413(5)	0.549(2)	0.080(6)	0.18(3)
C(94)	0.324(3)	0.5206(16)	-0.022(5)	0.121(18)
C(95)	0.342(2)	0.5822(11)	-0.025(3)	0.079(11)
C(96)	0.399(3)	0.3417(14)	0.669(4)	0.21(2)
C(97)	0.308(5)	0.588(2)	-0.102(7)	0.18(3)
C(98)	0.359(7)	0.580(3)	0.044(9)	0.22(4)
C(99)	0.701(5)	0.306(3)	0.537(7)	0.13(3)
N(1)	0.0636(3)	0.3502(2)	0.3053(4)	0.036(2)
N(2A)	-0.0478(4)	0.3613(2)	0.4081(5)	0.048(2)
N(2B)	-0.0478(4)	0.3613(2)	0.4081(5)	0.048(2)
N(3A)	0.1359(5)	0.4043(2)	0.3498(6)	0.066(2)
N(3B)	0.1359(5)	0.4043(2)	0.3498(6)	0.066(2)
O(1)	-0.0571(2)	0.3453(1)	0.2326(4)	0.032(1)
O(2)	-0.0232(2)	0.3040(1)	0.3516(3)	0.028(1)
O(3)	0.1863(2)	0.3488(1)	0.3700(3)	0.035(1)
O(4)	0.1696(3)	0.3722(1)	0.2120(3)	0.031(1)
O(5)	-0.1466(5)	0.3905(2)	0.4826(6)	0.063(2)
O(6)	-0.1675(4)	0.3358(2)	0.4240(5)	0.048(2)
O(7)	0.0153(8)	0.4304(3)	0.3361(9)	0.119(4)

7 EXPERIMENTAL PART

O(8)	0.1010(12)	0.4386(5)	0.4791(13)	0.186(7)
F(1)	-0.1516(5)	0.3389(3)	0.6237(5)	0.107(4)
F(2)	-0.0569(5)	0.3175(2)	0.5644(6)	0.090(3)
F(3)	-0.0526(4)	0.3662(2)	0.6167(5)	0.083(3)
F(4)	0.1332(19)	0.4545(8)	0.2377(19)	0.364(11)
F(5)	0.0871(19)	0.4855(6)	0.332(2)	0.364(11)
F(6)	0.1901(16)	0.4691(8)	0.353(2)	0.364(11)
F(7)	-0.3746(4)	0.4542(2)	0.4431(5)	0.084(2)
F(8)	-0.3467(3)	0.4643(1)	0.2980(5)	0.074(2)
F(9)	-0.2647(4)	0.4668(2)	0.4098(5)	0.080(2)
F(10)	-0.2924(4)	0.4173(2)	0.4545(4)	0.079(2)
F(11)	-0.3743(3)	0.4148(1)	0.3427(5)	0.069(2)
F(12)	-0.0636(5)	0.4838(2)	0.0563(7)	0.141(4)
F(13)	-0.0395(4)	0.4385(2)	0.1259(7)	0.112(3)
F(14)	-0.1259(6)	0.4420(2)	0.0260(5)	0.122(4)
F(15)	-0.1731(4)	0.4836(1)	0.1025(5)	0.093(2)
F(16)	-0.0849(4)	0.4798(2)	0.2040(6)	0.104(3)
F(17)	0.3697(2)	0.2610(1)	0.5347(3)	0.045(1)
F(18)	0.3022(2)	0.2373(1)	0.4315(3)	0.044(1)
F(19)	0.2957(2)	0.2900(1)	0.4535(3)	0.040(1)
F(20)	0.2773(2)	0.2823(1)	0.6041(3)	0.043(1)
F(21)	0.2848(2)	0.2296(1)	0.5828(3)	0.046(1)
F(22)	-0.0297(2)	0.2222(2)	0.7298(3)	0.058(2)
F(23)	-0.0408(2)	0.2600(1)	0.6255(3)	0.047(1)
F(24)	-0.0201(2)	0.2088(1)	0.5841(3)	0.047(1)
F(25)	0.0747(2)	0.2079(1)	0.6785(3)	0.041(1)
F(26)	0.0535(2)	0.2588(1)	0.7194(3)	0.045(1)
F(27)	0.2966(9)	0.4976(3)	0.6963(8)	0.234(9)
F(28)	0.1908(6)	0.4710(2)	0.6838(7)	0.133(4)
F(29)	0.2658(7)	0.4768(2)	0.5627(7)	0.144(5)
F(30)	0.3572(7)	0.4570(3)	0.6434(7)	0.170(6)
F(31)	0.2857(8)	0.4506(3)	0.7654(7)	0.193(7)
F(32)	0.0732(3)	0.3289(1)	0.7669(4)	0.059(1)
F(33)	0.0735(3)	0.3790(1)	0.7210(4)	0.050(1)
F(34)	0.1630(3)	0.3595(2)	0.8062(3)	0.064(2)
F(35)	0.1766(3)	0.3195(1)	0.7041(4)	0.058(1)
F(36)	0.0881(2)	0.3390(1)	0.6195(3)	0.047(1)
F(37)	0.1457(3)	0.4783(1)	-0.0944(4)	0.056(1)
F(38)	0.0959(3)	0.4390(1)	-0.1701(3)	0.047(1)

7 EXPERIMENTAL PART

F(39)	0.1926(2)	0.4305(1)	-0.0841(4)	0.049(1)
F(40)	0.1370(3)	0.4524(1)	0.0370(3)	0.047(1)
F(41)	0.0406(3)	0.4607(1)	-0.0502(4)	0.047(1)
F(42)	-0.1634(2)	0.3399(1)	-0.1351(3)	0.049(1)
F(43)	-0.0573(2)	0.3176(1)	-0.1228(3)	0.043(1)
F(44)	-0.0710(3)	0.3654(1)	-0.1918(3)	0.049(1)
F(45)	-0.1280(2)	0.3835(1)	-0.0675(3)	0.047(1)
F(46)	-0.1138(2)	0.3362(1)	0.0016(3)	0.041(1)
P(1)	-0.0144(1)	0.3413(1)	0.3268(1)	0.029(1)
P(2)	0.1328(1)	0.3696(1)	0.3114(1)	0.032(1)
S(1A)	-0.1190(1)	0.3589(1)	0.4613(2)	0.036(1)
S(1B)	-0.0649(7)	0.3753(4)	0.4756(10)	0.069(4)
S(3)	-0.3172(1)	0.4402(1)	0.3746(2)	0.058(1)
S(2A)	0.0916(2)	0.4294(1)	0.3878(3)	0.068(1)
S(2B)	0.1563(11)	0.4310(4)	0.3799(12)	0.082(5)
S(4)	-0.1079(2)	0.4601(1)	0.1158(3)	0.087(1)
S(5)	0.2868(1)	0.2595(1)	0.5178(1)	0.033(1)
S(6)	0.0186(1)	0.2345(1)	0.6485(1)	0.039(1)
S(7)	0.2751(3)	0.4630(1)	0.6628(3)	0.145(2)
S(8)	0.1270(1)	0.3501(1)	0.7103(1)	0.040(1)
S(9)	0.1155(1)	0.4446(1)	-0.0650(1)	0.040(1)
S(10)	-0.0899(1)	0.3512(1)	-0.0941(1)	0.037(1)
Cl(1)	0.3225(15)	0.6421(7)	-0.026(2)	0.180(10)
Cl(2)	0.336(3)	0.6082(14)	0.027(3)	0.304(19)
Cl(3)	0.1011(8)	0.5567(4)	0.4146(11)	0.122(4)
Cl(4)	0.0986(12)	0.5123(5)	0.5210(15)	0.113(6)
Cl(5)	0.6299(6)	0.3380(3)	0.4771(8)	0.095(3)
Cl(6)	0.6318(11)	0.3333(5)	0.5244(15)	0.175(7)
Cl(7)	0.6658(7)	0.3332(3)	0.6724(9)	0.113(4)
Cl(8)	0.6984(12)	0.3277(5)	0.6874(14)	0.137(6)
Cl(9)	0.2268(11)	0.5852(5)	0.7243(15)	0.152(6)
Cl(10)	0.0796(9)	0.5422(4)	0.7731(12)	0.117(4)
Cl(11)	0.1244(9)	0.5479(4)	0.7886(11)	0.111(4)
Cl(12)	0.1749(16)	0.5665(7)	0.680(2)	0.202(10)

7 EXPERIMENTAL PART

Bond lengths [Å] and angles [°].

C(1)-F(2)	1.273(17)	C(1)-F(1)	1.325(15)
C(1)-F(3)	1.365(17)	C(1)-S(1A)	1.836(13)
C(1)-S(1B)	2.03(2)	C(2)-F(6)	1.21(3)
C(2)-F(4)	1.25(3)	C(2)-F(5)	1.26(3)
C(2)-S(2B)	1.68(3)	C(2)-S(2A)	1.89(3)
C(3)-C(4)	1.359(10)	C(3)-O(1)	1.410(8)
C(3)-C(12)	1.430(10)	C(4)-C(5)	1.439(10)
C(4)-C(20)	1.488(10)	C(5)-C(6)	1.405(10)
C(5)-C(10)	1.437(10)	C(6)-C(7)	1.389(10)
C(7)-C(8)	1.422(11)	C(8)-C(9)	1.365(11)
C(9)-C(10)	1.433(10)	C(10)-C(11)	1.388(10)
C(11)-C(12)	1.386(10)	C(12)-C(13)	1.474(10)
C(13)-C(18)	1.390(11)	C(13)-C(14)	1.415(11)
C(14)-C(15)	1.370(12)	C(15)-C(16)	1.382(12)
C(15)-S(3)	1.817(8)	C(16)-C(17)	1.396(13)
C(17)-C(18)	1.387(12)	C(17)-S(4)	1.788(9)
C(19)-C(20)	1.372(9)	C(19)-O(2)	1.413(8)
C(19)-C(28)	1.418(9)	C(20)-C(21)	1.432(10)
C(21)-C(22)	1.405(10)	C(21)-C(26)	1.427(10)
C(22)-C(23)	1.372(10)	C(23)-C(24)	1.410(11)
C(24)-C(25)	1.350(11)	C(25)-C(26)	1.414(10)
C(26)-C(27)	1.427(10)	C(27)-C(28)	1.361(10)
C(28)-C(29)	1.509(9)	C(29)-C(30)	1.383(10)
C(29)-C(34)	1.388(10)	C(30)-C(31)	1.389(10)
C(31)-C(32)	1.397(10)	C(31)-S(5)	1.801(7)
C(32)-C(33)	1.390(10)	C(33)-C(34)	1.365(10)
C(33)-S(6)	1.798(7)	C(35)-C(36)	1.385(10)
C(35)-C(44)	1.403(10)	C(35)-O(3)	1.420(8)
C(36)-C(37)	1.425(10)	C(36)-C(52)	1.488(10)
C(37)-C(42)	1.424(11)	C(37)-C(38)	1.425(11)
C(38)-C(39)	1.375(11)	C(39)-C(40)	1.388(12)
C(40)-C(41)	1.348(12)	C(41)-C(42)	1.420(11)
C(42)-C(43)	1.404(12)	C(43)-C(44)	1.392(11)
C(44)-C(45)	1.473(11)	C(45)-C(46)	1.368(12)
C(45)-C(50)	1.432(11)	C(46)-C(47)	1.409(13)
C(47)-C(48)	1.406(14)	C(47)-S(7)	1.795(10)
C(48)-C(49)	1.377(12)	C(49)-C(50)	1.390(11)

7 EXPERIMENTAL PART

C(49)-S(8)	1.793(8)	C(51)-C(52)	1.385(10)
C(51)-O(4)	1.408(9)	C(51)-C(60)	1.420(10)
C(52)-C(53)	1.414(11)	C(53)-C(54)	1.425(10)
C(53)-C(58)	1.435(10)	C(54)-C(55)	1.406(12)
C(55)-C(56)	1.404(11)	C(56)-C(57)	1.363(11)
C(57)-C(58)	1.431(10)	C(58)-C(59)	1.420(10)
C(59)-C(60)	1.350(10)	C(60)-C(61)	1.500(10)
C(61)-C(66)	1.385(10)	C(61)-C(62)	1.394(10)
C(62)-C(63)	1.381(10)	C(63)-C(64)	1.386(11)
C(63)-S(9)	1.813(7)	C(64)-C(65)	1.398(10)
C(65)-C(66)	1.406(10)	C(65)-S(10)	1.817(7)
C(67)-C(68)	1.89(8)	C(68)-Cl(10)	2.10(5)
C(69)-C(71)	1.74(5)	C(70)-C(71)	1.46(3)
C(71)-C(72)	1.46(3)	C(72)-C(73)	1.48(3)
C(72)-C(96)	2.00(6)	C(73)-C(78)	1.69(3)
C(73)-C(96)	1.70(6)	C(74)-C(81)	1.17(4)
C(74)-Cl(6)	1.42(3)	C(74)-C(99)	1.54(11)
C(74)-Cl(5)	1.78(3)	C(74)-Cl(7)	1.79(4)
C(74)-Cl(8)	1.95(4)	C(75)-C(76)	1.82(12)
C(75)-C(87)	1.89(16)	C(76)-C(87)	0.96(16)
C(77)-Cl(1)	0.68(5)	C(77)-Cl(2)	1.34(6)
C(78)-C(96)	1.34(5)	C(79)-C(84)	1.32(6)
C(80)-C(86)	1.32(10)	C(80)-C(81)	1.72(5)
C(81)-Cl(7)	1.47(3)	C(81)-Cl(6)	1.64(4)
C(81)-Cl(8)	1.91(4)	C(81)-Cl(5)	2.09(3)
C(82)-C(85)	1.52(7)	C(82)-C(83)	1.68(7)
C(82)-C(89)	1.90(9)	C(83)-C(88)	1.09(8)
C(83)-C(85)	1.17(9)	C(83)-C(89)	1.32(9)
C(83)-C(84)	1.81(9)	C(84)-C(88)	1.29(6)
C(85)-C(88)	1.23(7)	C(85)-C(90)	1.91(9)
C(86)-Cl(5)	2.26(10)	C(91)-C(94)	1.32(10)
C(91)-C(92)	1.64(11)	C(91)-C(97)	1.97(13)
C(91)-C(95)	1.97(11)	C(92)-C(94)	1.38(8)
C(92)-C(98)	1.47(13)	C(92)-C(95)	1.52(8)
C(92)-C(93)	1.95(11)	C(93)-C(98)	1.70(14)
C(95)-C(98)	1.06(12)	C(95)-C(97)	1.30(9)
C(95)-Cl(2)	1.33(6)	C(97)-Cl(2)	2.12(10)
C(98)-Cl(2)	1.28(13)	C(99)-Cl(6)	1.74(10)
C(99)-Cl(5)	2.08(10)	N(1)-P(2)	1.531(6)

7 EXPERIMENTAL PART

N(1)-P(1)	1.543(6)	N(2A)-S(1A)	1.545(7)
N(2A)-P(1)	1.573(6)	N(2B)-S(1B)	1.183(15)
N(2B)-P(1)	1.573(6)	N(3A)-S(2A)	1.445(9)
N(3A)-P(2)	1.553(8)	N(3B)-S(2B)	1.256(17)
N(3B)-P(2)	1.553(8)	O(1)-P(1)	1.589(5)
O(2)-P(1)	1.604(5)	O(3)-P(2)	1.575(5)
O(4)-P(2)	1.600(5)	O(5)-S(1A)	1.447(8)
O(6)-S(1A)	1.434(7)	O(7)-S(2A)	1.615(16)
O(8)-S(2A)	1.386(18)	F(7)-S(3)	1.576(6)
F(8)-S(3)	1.596(7)	F(9)-S(3)	1.570(7)
F(10)-S(3)	1.568(7)	F(11)-S(3)	1.577(6)
F(12)-S(4)	1.553(7)	F(13)-S(4)	1.575(8)
F(14)-S(4)	1.539(10)	F(15)-S(4)	1.580(7)
F(16)-S(4)	1.578(9)	F(17)-S(5)	1.577(4)
F(18)-S(5)	1.583(5)	F(19)-S(5)	1.584(5)
F(20)-S(5)	1.579(5)	F(21)-S(5)	1.564(5)
F(22)-S(6)	1.570(5)	F(23)-S(6)	1.576(5)
F(24)-S(6)	1.596(5)	F(25)-S(6)	1.590(5)
F(26)-S(6)	1.583(5)	F(27)-S(7)	1.578(8)
F(28)-S(7)	1.645(12)	F(29)-S(7)	1.570(12)
F(30)-S(7)	1.587(14)	F(31)-S(7)	1.583(14)
F(32)-S(8)	1.571(5)	F(33)-S(8)	1.577(5)
F(34)-S(8)	1.592(5)	F(35)-S(8)	1.583(5)
F(36)-S(8)	1.573(5)	F(37)-S(9)	1.575(5)
F(38)-S(9)	1.581(5)	F(39)-S(9)	1.587(5)
F(40)-S(9)	1.565(5)	F(41)-S(9)	1.573(5)
F(42)-S(10)	1.574(5)	F(43)-S(10)	1.583(5)
F(44)-S(10)	1.573(5)	F(45)-S(10)	1.576(5)
F(46)-S(10)	1.584(5)	Cl(1)-Cl(2)	1.63(6)
Cl(3)-Cl(4)	2.41(3)	Cl(5)-Cl(6)	0.71(2)
Cl(6)-Cl(7)	2.24(3)	Cl(7)-Cl(8)	0.69(2)
Cl(9)-Cl(12)	1.41(3)	Cl(10)-Cl(11)	0.901(18)
Cl(10)-Cl(12)	2.46(3)	Cl(11)-Cl(12)	2.00(3)
F(2)-C(1)-F(1)	113.0(14)	F(2)-C(1)-F(3)	110.8(12)
F(1)-C(1)-F(3)	108.4(11)	F(2)-C(1)-S(1A)	109.9(9)
F(1)-C(1)-S(1A)	107.5(9)	F(3)-C(1)-S(1A)	107.0(10)
F(6)-C(2)-F(4)	115(2)	F(6)-C(2)-F(5)	114(2)
F(4)-C(2)-F(5)	111(2)	F(6)-C(2)-S(2A)	107(2)

7 EXPERIMENTAL PART

F(4)-C(2)-S(2A)	106(2)	F(5)-C(2)-S(2A)	102(2)
C(4)-C(3)-O(1)	119.5(6)	C(4)-C(3)-C(12)	123.6(7)
O(1)-C(3)-C(12)	117.0(6)	C(3)-C(4)-C(5)	119.7(6)
C(3)-C(4)-C(20)	120.2(6)	C(5)-C(4)-C(20)	119.9(6)
C(6)-C(5)-C(10)	119.4(6)	C(6)-C(5)-C(4)	123.2(6)
C(10)-C(5)-C(4)	117.3(6)	C(7)-C(6)-C(5)	120.6(7)
C(6)-C(7)-C(8)	120.6(7)	C(9)-C(8)-C(7)	119.8(7)
C(8)-C(9)-C(10)	121.4(7)	C(11)-C(10)-C(9)	121.6(6)
C(11)-C(10)-C(5)	120.1(6)	C(9)-C(10)-C(5)	118.2(6)
C(12)-C(11)-C(10)	123.0(6)	C(11)-C(12)-C(3)	116.2(7)
C(11)-C(12)-C(13)	120.3(7)	C(3)-C(12)-C(13)	123.5(6)
C(18)-C(13)-C(14)	118.5(7)	C(18)-C(13)-C(12)	121.3(7)
C(14)-C(13)-C(12)	120.1(7)	C(15)-C(14)-C(13)	119.3(8)
C(14)-C(15)-C(16)	122.8(8)	C(14)-C(15)-S(3)	118.9(7)
C(16)-C(15)-S(3)	118.3(6)	C(15)-C(16)-C(17)	117.7(8)
C(18)-C(17)-C(16)	120.9(8)	C(18)-C(17)-S(4)	120.4(7)
C(16)-C(17)-S(4)	118.7(7)	C(17)-C(18)-C(13)	120.7(8)
C(20)-C(19)-O(2)	119.0(6)	C(20)-C(19)-C(28)	123.6(6)
O(2)-C(19)-C(28)	117.4(5)	C(19)-C(20)-C(21)	117.8(6)
C(19)-C(20)-C(4)	119.4(6)	C(21)-C(20)-C(4)	122.7(6)
C(22)-C(21)-C(26)	118.2(6)	C(22)-C(21)-C(20)	122.5(6)
C(26)-C(21)-C(20)	119.3(6)	C(23)-C(22)-C(21)	121.5(7)
C(22)-C(23)-C(24)	119.3(7)	C(25)-C(24)-C(23)	121.3(7)
C(24)-C(25)-C(26)	120.4(7)	C(25)-C(26)-C(27)	121.5(6)
C(25)-C(26)-C(21)	119.2(6)	C(27)-C(26)-C(21)	119.3(6)
C(28)-C(27)-C(26)	121.2(6)	C(27)-C(28)-C(19)	118.3(6)
C(27)-C(28)-C(29)	120.2(6)	C(19)-C(28)-C(29)	120.9(6)
C(30)-C(29)-C(34)	119.1(6)	C(30)-C(29)-C(28)	121.4(6)
C(34)-C(29)-C(28)	118.9(6)	C(29)-C(30)-C(31)	120.0(6)
C(30)-C(31)-C(32)	120.8(6)	C(30)-C(31)-S(5)	121.1(5)
C(32)-C(31)-S(5)	118.1(5)	C(33)-C(32)-C(31)	118.3(7)
C(34)-C(33)-C(32)	120.8(7)	C(34)-C(33)-S(6)	120.7(5)
C(32)-C(33)-S(6)	118.4(6)	C(33)-C(34)-C(29)	121.2(6)
C(36)-C(35)-C(44)	123.3(6)	C(36)-C(35)-O(3)	118.2(6)
C(44)-C(35)-O(3)	118.4(6)	C(35)-C(36)-C(37)	118.8(7)
C(35)-C(36)-C(52)	119.4(6)	C(37)-C(36)-C(52)	121.5(7)
C(42)-C(37)-C(38)	119.1(7)	C(42)-C(37)-C(36)	118.5(7)
C(38)-C(37)-C(36)	122.2(7)	C(39)-C(38)-C(37)	119.3(8)
C(38)-C(39)-C(40)	121.2(8)	C(41)-C(40)-C(39)	120.8(8)

7 EXPERIMENTAL PART

C(40)-C(41)-C(42)	121.1(8)	C(43)-C(42)-C(41)	121.8(7)
C(43)-C(42)-C(37)	119.9(7)	C(41)-C(42)-C(37)	118.3(7)
C(44)-C(43)-C(42)	121.8(7)	C(43)-C(44)-C(35)	117.3(7)
C(43)-C(44)-C(45)	119.0(7)	C(35)-C(44)-C(45)	123.6(7)
C(46)-C(45)-C(50)	119.7(8)	C(46)-C(45)-C(44)	120.4(7)
C(50)-C(45)-C(44)	119.9(7)	C(45)-C(46)-C(47)	120.4(9)
C(48)-C(47)-C(46)	120.5(9)	C(48)-C(47)-S(7)	119.8(7)
C(46)-C(47)-S(7)	119.7(8)	C(49)-C(48)-C(47)	118.4(8)
C(48)-C(49)-C(50)	122.3(8)	C(48)-C(49)-S(8)	119.5(6)
C(50)-C(49)-S(8)	118.2(6)	C(49)-C(50)-C(45)	118.7(7)
C(52)-C(51)-O(4)	118.0(6)	C(52)-C(51)-C(60)	123.1(7)
O(4)-C(51)-C(60)	118.8(6)	C(51)-C(52)-C(53)	117.9(6)
C(51)-C(52)-C(36)	119.7(7)	C(53)-C(52)-C(36)	122.4(6)
C(52)-C(53)-C(54)	121.5(7)	C(52)-C(53)-C(58)	119.5(6)
C(54)-C(53)-C(58)	118.9(7)	C(55)-C(54)-C(53)	120.1(7)
C(56)-C(55)-C(54)	119.7(7)	C(57)-C(56)-C(55)	121.6(7)
C(56)-C(57)-C(58)	120.5(7)	C(59)-C(58)-C(57)	122.8(6)
C(59)-C(58)-C(53)	118.2(6)	C(57)-C(58)-C(53)	119.0(7)
C(60)-C(59)-C(58)	122.9(7)	C(59)-C(60)-C(51)	117.4(6)
C(59)-C(60)-C(61)	121.5(6)	C(51)-C(60)-C(61)	120.8(6)
C(66)-C(61)-C(62)	120.3(7)	C(66)-C(61)-C(60)	120.7(6)
C(62)-C(61)-C(60)	118.7(6)	C(63)-C(62)-C(61)	119.9(6)
C(62)-C(63)-C(64)	122.3(6)	C(62)-C(63)-S(9)	118.9(5)
C(64)-C(63)-S(9)	118.7(5)	C(63)-C(64)-C(65)	116.5(7)
C(64)-C(65)-C(66)	123.0(7)	C(64)-C(65)-S(10)	117.2(5)
C(66)-C(65)-S(10)	119.7(5)	C(61)-C(66)-C(65)	117.9(7)
C(67)-C(68)-Cl(10)	96(3)	C(70)-C(71)-C(72)	116(3)
C(70)-C(71)-C(69)	115(3)	C(72)-C(71)-C(69)	102(3)
C(71)-C(72)-C(73)	117(2)	C(71)-C(72)-C(96)	173(3)
C(73)-C(72)-C(96)	56(2)	C(72)-C(73)-C(78)	121(2)
C(72)-C(73)-C(96)	78(2)	C(78)-C(73)-C(96)	46(2)
C(81)-C(74)-Cl(6)	78(3)	C(81)-C(74)-C(99)	135(5)
Cl(6)-C(74)-C(99)	72(4)	C(81)-C(74)-Cl(5)	88(3)
C(99)-C(74)-Cl(5)	77(4)	C(81)-C(74)-Cl(7)	55(2)
Cl(6)-C(74)-Cl(7)	87(2)	C(99)-C(74)-Cl(7)	90(4)
Cl(5)-C(74)-Cl(7)	109.3(19)	C(81)-C(74)-Cl(8)	71(2)
Cl(6)-C(74)-Cl(8)	105(2)	C(99)-C(74)-Cl(8)	84(4)
Cl(5)-C(74)-Cl(8)	127(2)	C(87)-C(76)-C(75)	79(10)
Cl(1)-C(77)-Cl(2)	102(6)	C(96)-C(78)-C(73)	67(3)

7 EXPERIMENTAL PART

C(86)-C(80)-C(81)	93(6)	C(74)-C(81)-Cl(7)	85(3)
C(74)-C(81)-Cl(6)	58(2)	Cl(7)-C(81)-Cl(6)	91(2)
C(74)-C(81)-C(80)	145(4)	Cl(7)-C(81)-C(80)	121(3)
Cl(6)-C(81)-C(80)	96(2)	C(74)-C(81)-Cl(8)	74(2)
Cl(6)-C(81)-Cl(8)	97.5(19)	C(80)-C(81)-Cl(8)	137(3)
C(74)-C(81)-Cl(5)	58(2)	Cl(7)-C(81)-Cl(5)	108.4(19)
C(80)-C(81)-Cl(5)	90(2)	Cl(8)-C(81)-Cl(5)	112.5(17)
C(85)-C(82)-C(89)	85(4)	C(88)-C(83)-C(85)	66(7)
C(88)-C(83)-C(89)	150(10)	C(85)-C(83)-C(89)	139(10)
C(88)-C(83)-C(82)	120(8)	C(85)-C(83)-C(82)	62(5)
C(89)-C(83)-C(82)	78(6)	C(88)-C(83)-C(84)	45(4)
C(85)-C(83)-C(84)	108(7)	C(89)-C(83)-C(84)	105(7)
C(82)-C(83)-C(84)	138(5)	C(88)-C(84)-C(79)	144(6)
C(79)-C(84)-C(83)	170(6)	C(83)-C(85)-C(88)	54(5)
C(83)-C(85)-C(82)	76(6)	C(88)-C(85)-C(82)	123(5)
C(83)-C(85)-C(90)	99(6)	C(88)-C(85)-C(90)	123(5)
C(82)-C(85)-C(90)	87(4)	C(80)-C(86)-Cl(5)	94(6)
C(76)-C(87)-C(75)	71(10)	C(83)-C(88)-C(85)	60(5)
C(83)-C(88)-C(84)	99(7)	C(85)-C(88)-C(84)	152(6)
C(83)-C(89)-C(82)	60(5)	C(94)-C(91)-C(92)	54(5)
C(94)-C(91)-C(97)	135(8)	C(92)-C(91)-C(97)	81(6)
C(94)-C(91)-C(95)	102(7)	C(92)-C(91)-C(95)	49(4)
C(94)-C(92)-C(98)	146(8)	C(94)-C(92)-C(95)	126(6)
C(94)-C(92)-C(91)	51(5)	C(98)-C(92)-C(91)	114(7)
C(95)-C(92)-C(91)	77(5)	C(94)-C(92)-C(93)	98(5)
C(98)-C(92)-C(93)	58(6)	C(95)-C(92)-C(93)	89(4)
C(91)-C(92)-C(93)	113(6)	C(98)-C(93)-C(92)	47(5)
C(91)-C(94)-C(92)	75(6)	C(98)-C(95)-C(97)	167(10)
C(98)-C(95)-Cl(2)	64(8)	C(97)-C(95)-Cl(2)	108(6)
C(98)-C(95)-C(92)	67(8)	C(97)-C(95)-C(92)	113(6)
Cl(2)-C(95)-C(92)	117(5)	C(98)-C(95)-C(91)	115(9)
C(97)-C(95)-C(91)	70(5)	Cl(2)-C(95)-C(91)	165(5)
C(92)-C(95)-C(91)	54(4)	C(78)-C(96)-C(73)	66(3)
C(78)-C(96)-C(72)	110(4)	C(73)-C(96)-C(72)	46.1(17)
C(95)-C(97)-C(91)	71(6)	C(91)-C(97)-Cl(2)	106(6)
C(95)-C(98)-Cl(2)	68(9)	C(95)-C(98)-C(92)	72(8)
Cl(2)-C(98)-C(92)	123(10)	C(95)-C(98)-C(93)	123(10)
Cl(2)-C(98)-C(93)	161(10)	C(92)-C(98)-C(93)	75(8)
C(74)-C(99)-Cl(6)	51(3)	C(74)-C(99)-Cl(5)	57(4)

7 EXPERIMENTAL PART

P(2)-N(1)-P(1)	157.1(5)	S(1A)-N(2A)-P(1)	133.1(5)
S(1B)-N(2B)-P(1)	171.2(9)	S(2A)-N(3A)-P(2)	142.2(7)
S(2B)-N(3B)-P(2)	164.4(12)	C(3)-O(1)-P(1)	120.9(4)
C(19)-O(2)-P(1)	116.1(4)	C(35)-O(3)-P(2)	119.2(5)
C(51)-O(4)-P(2)	115.8(4)	N(1)-P(1)-N(2B)	113.6(4)
N(1)-P(1)-N(2A)	113.6(4)	N(1)-P(1)-O(1)	106.3(3)
N(2B)-P(1)-O(1)	112.5(4)	N(2A)-P(1)-O(1)	112.5(4)
N(1)-P(1)-O(2)	112.2(3)	N(2B)-P(1)-O(2)	107.9(3)
N(2A)-P(1)-O(2)	107.9(3)	O(1)-P(1)-O(2)	104.1(3)
N(1)-P(2)-N(3B)	123.0(4)	N(1)-P(2)-N(3A)	123.0(4)
N(1)-P(2)-O(3)	106.3(3)	N(3B)-P(2)-O(3)	107.3(4)
N(3A)-P(2)-O(3)	107.3(4)	N(1)-P(2)-O(4)	110.6(3)
N(3B)-P(2)-O(4)	104.0(4)	N(3A)-P(2)-O(4)	104.0(4)
O(3)-P(2)-O(4)	104.3(3)	O(6)-S(1A)-O(5)	117.8(5)
O(6)-S(1A)-N(2A)	113.8(4)	O(5)-S(1A)-N(2A)	110.9(5)
O(6)-S(1A)-C(1)	105.4(6)	O(5)-S(1A)-C(1)	103.4(6)
N(2A)-S(1A)-C(1)	103.6(5)	N(2B)-S(1B)-C(1)	109.1(12)
F(10)-S(3)-F(9)	90.3(4)	F(10)-S(3)-F(7)	87.9(4)
F(9)-S(3)-F(7)	87.8(3)	F(10)-S(3)-F(11)	90.5(4)
F(9)-S(3)-F(11)	175.9(3)	F(7)-S(3)-F(11)	88.2(3)
F(10)-S(3)-F(8)	176.0(3)	F(9)-S(3)-F(8)	89.8(4)
F(7)-S(3)-F(8)	88.0(4)	F(11)-S(3)-F(8)	89.1(4)
F(10)-S(3)-C(15)	92.1(4)	F(9)-S(3)-C(15)	91.9(4)
F(7)-S(3)-C(15)	179.7(4)	F(11)-S(3)-C(15)	92.1(3)
F(8)-S(3)-C(15)	91.9(4)	O(8)-S(2A)-N(3A)	119.4(9)
O(8)-S(2A)-O(7)	123.2(10)	N(3A)-S(2A)-O(7)	110.7(6)
O(8)-S(2A)-C(2)	103.3(13)	N(3A)-S(2A)-C(2)	96.7(8)
O(7)-S(2A)-C(2)	95.5(9)	N(3B)-S(2B)-C(2)	117.3(16)
F(14)-S(4)-F(12)	87.7(5)	F(14)-S(4)-F(13)	88.7(5)
F(12)-S(4)-F(13)	88.8(4)	F(14)-S(4)-F(16)	175.8(5)
F(12)-S(4)-F(16)	88.3(5)	F(13)-S(4)-F(16)	90.0(5)
F(14)-S(4)-F(15)	91.8(5)	F(12)-S(4)-F(15)	87.2(4)
F(13)-S(4)-F(15)	176.0(4)	F(16)-S(4)-F(15)	89.2(4)
F(14)-S(4)-C(17)	92.2(4)	F(12)-S(4)-C(17)	179.4(5)
F(13)-S(4)-C(17)	91.7(4)	F(16)-S(4)-C(17)	91.8(4)
F(15)-S(4)-C(17)	92.2(4)	F(21)-S(5)-F(17)	87.9(3)
F(21)-S(5)-F(20)	90.2(3)	F(17)-S(5)-F(20)	88.0(2)
F(21)-S(5)-F(18)	90.6(3)	F(17)-S(5)-F(18)	88.0(2)
F(20)-S(5)-F(18)	175.8(3)	F(21)-S(5)-F(19)	175.2(2)

7 EXPERIMENTAL PART

F(17)-S(5)-F(19)	87.3(3)	F(20)-S(5)-F(19)	89.5(3)
F(18)-S(5)-F(19)	89.3(3)	F(21)-S(5)-C(31)	92.5(3)
F(17)-S(5)-C(31)	179.5(3)	F(20)-S(5)-C(31)	92.4(3)
F(18)-S(5)-C(31)	91.7(3)	F(19)-S(5)-C(31)	92.3(3)
F(22)-S(6)-F(23)	88.3(3)	F(22)-S(6)-F(26)	87.8(3)
F(23)-S(6)-F(26)	89.9(3)	F(22)-S(6)-F(25)	87.1(3)
F(23)-S(6)-F(25)	175.4(3)	F(26)-S(6)-F(25)	89.7(3)
F(22)-S(6)-F(24)	87.4(3)	F(23)-S(6)-F(24)	90.5(3)
F(26)-S(6)-F(24)	175.2(3)	F(25)-S(6)-F(24)	89.6(3)
F(22)-S(6)-C(33)	179.2(4)	F(23)-S(6)-C(33)	92.5(3)
F(26)-S(6)-C(33)	92.1(3)	F(25)-S(6)-C(33)	92.0(3)
F(24)-S(6)-C(33)	92.6(3)	F(29)-S(7)-F(27)	88.5(6)
F(29)-S(7)-F(31)	177.2(5)	F(27)-S(7)-F(31)	88.7(7)
F(29)-S(7)-F(30)	90.1(6)	F(27)-S(7)-F(30)	87.0(7)
F(31)-S(7)-F(30)	89.6(8)	F(29)-S(7)-F(28)	89.4(7)
F(27)-S(7)-F(28)	90.3(7)	F(31)-S(7)-F(28)	90.8(6)
F(30)-S(7)-F(28)	177.2(5)	F(29)-S(7)-C(47)	92.3(5)
F(27)-S(7)-C(47)	178.1(10)	F(31)-S(7)-C(47)	90.5(5)
F(30)-S(7)-C(47)	91.3(5)	F(28)-S(7)-C(47)	91.4(5)
F(32)-S(8)-F(36)	88.3(3)	F(32)-S(8)-F(33)	88.3(3)
F(36)-S(8)-F(33)	90.7(3)	F(32)-S(8)-F(35)	87.4(3)
F(36)-S(8)-F(35)	89.3(3)	F(33)-S(8)-F(35)	175.7(3)
F(32)-S(8)-F(34)	87.6(3)	F(36)-S(8)-F(34)	175.9(3)
F(33)-S(8)-F(34)	89.8(3)	F(35)-S(8)-F(34)	89.9(3)
F(32)-S(8)-C(49)	179.6(4)	F(36)-S(8)-C(49)	92.0(3)
F(33)-S(8)-C(49)	91.8(3)	F(35)-S(8)-C(49)	92.5(3)
F(34)-S(8)-C(49)	92.1(3)	F(40)-S(9)-F(41)	90.7(3)
F(40)-S(9)-F(37)	88.6(3)	F(41)-S(9)-F(37)	88.7(3)
F(40)-S(9)-F(38)	176.2(3)	F(41)-S(9)-F(38)	89.2(3)
F(37)-S(9)-F(38)	87.6(3)	F(40)-S(9)-F(39)	90.4(3)
F(41)-S(9)-F(39)	176.1(3)	F(37)-S(9)-F(39)	87.6(3)
F(38)-S(9)-F(39)	89.4(3)	F(40)-S(9)-C(63)	92.2(3)
F(41)-S(9)-C(63)	92.0(3)	F(37)-S(9)-C(63)	178.9(3)
F(38)-S(9)-C(63)	91.6(3)	F(39)-S(9)-C(63)	91.7(3)
F(44)-S(10)-F(42)	88.4(3)	F(44)-S(10)-F(45)	89.9(3)
F(42)-S(10)-F(45)	87.2(3)	F(44)-S(10)-F(43)	90.7(3)
F(42)-S(10)-F(43)	88.6(3)	F(45)-S(10)-F(43)	175.8(3)
F(44)-S(10)-F(46)	176.3(3)	F(42)-S(10)-F(46)	87.9(3)
F(45)-S(10)-F(46)	89.8(3)	F(43)-S(10)-F(46)	89.4(3)

7 EXPERIMENTAL PART

F(44)-S(10)-C(65)	91.8(3)	F(42)-S(10)-C(65)	179.0(4)
F(45)-S(10)-C(65)	91.8(3)	F(43)-S(10)-C(65)	92.4(3)
F(46)-S(10)-C(65)	91.9(3)	C(77)-Cl(1)-Cl(2)	53(5)
C(98)-Cl(2)-C(95)	48(6)	C(98)-Cl(2)-C(77)	147(8)
C(95)-Cl(2)-C(77)	125(5)	C(98)-Cl(2)-Cl(1)	161(8)
C(95)-Cl(2)-Cl(1)	117(4)	C(98)-Cl(2)-C(97)	83(7)
C(77)-Cl(2)-C(97)	100(4)	Cl(1)-Cl(2)-C(97)	84(4)
Cl(6)-Cl(5)-C(74)	49(2)	Cl(6)-Cl(5)-C(99)	53(3)
C(74)-Cl(5)-C(99)	46(3)	C(99)-Cl(5)-C(81)	74(3)
Cl(6)-Cl(5)-C(86)	95(4)	C(74)-Cl(5)-C(86)	88(3)
C(99)-Cl(5)-C(86)	134(4)	C(81)-Cl(5)-C(86)	61(3)
Cl(5)-Cl(6)-C(74)	109(3)	Cl(5)-Cl(6)-C(81)	120(3)
Cl(5)-Cl(6)-C(99)	108(4)	C(74)-Cl(6)-C(99)	57(4)
C(81)-Cl(6)-C(99)	95(4)	Cl(5)-Cl(6)-Cl(7)	159(3)
C(74)-Cl(6)-Cl(7)	53.2(16)	C(99)-Cl(6)-Cl(7)	72(4)
Cl(8)-Cl(7)-C(81)	120(3)	Cl(8)-Cl(7)-C(74)	92(3)
Cl(8)-Cl(7)-Cl(6)	124(3)	C(81)-Cl(7)-Cl(6)	47.3(14)
Cl(7)-Cl(8)-C(74)	67(2)	Cl(11)-Cl(10)-C(68)	115(2)
Cl(11)-Cl(10)-Cl(12)	49.7(16)	C(68)-Cl(10)-Cl(12)	69.6(15)
Cl(10)-Cl(11)-Cl(12)	110(2)	Cl(9)-Cl(12)-Cl(11)	100.4(19)
Cl(9)-Cl(12)-Cl(10)	118.6(19)		

7 EXPERIMENTAL PART

Anisotropic displacement parameters (\AA^2).

The anisotropic displacement factor exponent takes the form:

$$-2\pi^2 [h^2 a^{*2} U_{11} + \dots + 2 h k a^* b^* U_{12}].$$

	U ₁₁	U ₂₂	U ₃₃	U ₂₃	U ₁₃	U ₁₂
C(1)	0.064(8)	0.109(12)	0.031(7)	0.001(7)	0.005(6)	-0.009(8)
C(2)	0.204(17)	0.197(17)	0.209(17)	-0.002(7)	-0.011(7)	0.015(7)
C(3)	0.031(4)	0.026(4)	0.024(4)	0.004(3)	-0.002(3)	0.000(3)
C(4)	0.025(3)	0.032(4)	0.019(4)	0.003(3)	-0.002(3)	0.000(3)
C(5)	0.025(3)	0.034(4)	0.020(4)	0.006(3)	0.001(3)	-0.001(3)
C(6)	0.034(4)	0.039(4)	0.019(4)	0.002(3)	0.003(3)	-0.001(3)
C(7)	0.038(4)	0.035(4)	0.027(4)	0.000(3)	0.006(3)	-0.011(3)
C(8)	0.034(4)	0.051(5)	0.026(4)	-0.007(3)	0.007(3)	-0.015(4)
C(9)	0.026(4)	0.047(5)	0.019(4)	-0.004(3)	0.006(3)	-0.006(3)
C(10)	0.022(3)	0.038(4)	0.020(4)	0.000(3)	-0.002(3)	-0.001(3)
C(11)	0.019(3)	0.039(4)	0.025(4)	0.004(3)	-0.003(3)	-0.002(3)
C(12)	0.030(4)	0.036(4)	0.024(4)	0.000(3)	0.000(3)	0.002(3)
C(13)	0.035(4)	0.030(4)	0.029(4)	0.002(3)	0.001(3)	0.005(3)
C(14)	0.034(4)	0.041(5)	0.042(5)	-0.003(3)	0.001(3)	0.000(3)
C(15)	0.039(4)	0.038(5)	0.052(6)	-0.006(4)	0.003(4)	0.002(4)
C(16)	0.060(6)	0.032(4)	0.062(6)	0.003(4)	0.017(5)	0.003(4)
C(17)	0.052(5)	0.035(5)	0.059(6)	0.006(4)	0.009(4)	0.005(4)
C(18)	0.047(5)	0.036(4)	0.040(5)	0.003(3)	0.006(4)	0.009(4)
C(19)	0.025(3)	0.028(4)	0.018(3)	-0.001(3)	-0.002(3)	0.001(3)
C(20)	0.024(3)	0.030(4)	0.024(4)	0.003(3)	-0.005(3)	-0.001(3)
C(21)	0.026(3)	0.027(4)	0.028(4)	0.004(3)	-0.004(3)	-0.003(3)
C(22)	0.033(4)	0.039(4)	0.018(4)	0.004(3)	0.002(3)	-0.002(3)
C(23)	0.045(4)	0.047(5)	0.018(4)	-0.002(3)	-0.001(3)	-0.005(4)
C(24)	0.034(4)	0.046(5)	0.030(4)	-0.008(3)	0.010(3)	0.000(4)
C(25)	0.029(4)	0.037(4)	0.031(4)	-0.008(3)	0.005(3)	0.001(3)
C(26)	0.027(3)	0.033(4)	0.023(4)	-0.002(3)	0.004(3)	0.003(3)
C(27)	0.032(4)	0.028(4)	0.025(4)	0.003(3)	-0.007(3)	0.002(3)
C(28)	0.021(3)	0.038(4)	0.016(4)	0.002(3)	0.000(2)	0.003(3)
C(29)	0.023(3)	0.037(4)	0.027(4)	0.002(3)	-0.004(3)	0.005(3)
C(30)	0.026(4)	0.036(4)	0.024(4)	0.003(3)	-0.002(3)	0.003(3)
C(31)	0.022(3)	0.035(4)	0.029(4)	0.001(3)	0.005(3)	0.000(3)
C(32)	0.028(4)	0.047(4)	0.024(4)	0.004(3)	0.000(3)	0.001(3)
C(33)	0.024(4)	0.041(4)	0.028(4)	0.000(3)	0.003(3)	0.003(3)

7 EXPERIMENTAL PART

C(34)	0.023(3)	0.036(4)	0.026(4)	-0.001(3)	-0.002(3)	0.000(3)
C(35)	0.023(3)	0.039(4)	0.027(4)	-0.001(3)	0.003(3)	-0.009(3)
C(36)	0.026(4)	0.034(4)	0.030(4)	0.001(3)	0.000(3)	-0.009(3)
C(37)	0.028(4)	0.046(5)	0.035(4)	-0.001(3)	0.000(3)	-0.002(3)
C(38)	0.034(4)	0.039(4)	0.035(4)	-0.002(3)	0.008(3)	-0.005(3)
C(39)	0.026(4)	0.059(5)	0.045(5)	0.005(4)	0.008(3)	0.000(4)
C(40)	0.037(4)	0.053(5)	0.060(6)	-0.001(4)	0.000(4)	-0.007(4)
C(41)	0.033(4)	0.053(5)	0.042(5)	-0.004(4)	-0.002(4)	-0.008(4)
C(42)	0.028(4)	0.044(5)	0.036(5)	0.000(3)	-0.001(3)	-0.009(3)
C(43)	0.036(4)	0.043(4)	0.038(5)	-0.002(3)	-0.007(3)	-0.008(4)
C(44)	0.035(4)	0.043(4)	0.026(4)	0.002(3)	-0.004(3)	-0.004(3)
C(45)	0.043(4)	0.041(4)	0.025(4)	-0.008(3)	0.001(3)	-0.011(4)
C(46)	0.082(7)	0.065(6)	0.042(6)	-0.015(5)	0.017(5)	-0.025(6)
C(47)	0.095(8)	0.060(6)	0.049(6)	-0.028(5)	0.037(6)	-0.027(6)
C(48)	0.078(7)	0.059(6)	0.046(6)	-0.022(5)	0.020(5)	-0.019(5)
C(49)	0.042(4)	0.041(5)	0.030(4)	-0.001(3)	0.004(3)	-0.003(4)
C(50)	0.031(4)	0.045(4)	0.024(4)	-0.002(3)	0.001(3)	-0.003(3)
C(51)	0.032(4)	0.031(4)	0.023(4)	0.000(3)	0.003(3)	0.000(3)
C(52)	0.030(4)	0.039(4)	0.019(4)	0.002(3)	0.000(3)	-0.003(3)
C(53)	0.023(3)	0.046(4)	0.017(4)	0.002(3)	0.001(3)	-0.004(3)
C(54)	0.027(4)	0.044(4)	0.027(4)	0.003(3)	0.000(3)	0.000(3)
C(55)	0.030(4)	0.056(5)	0.031(4)	0.005(4)	-0.001(3)	0.004(4)
C(56)	0.037(4)	0.039(4)	0.032(4)	-0.001(3)	0.009(3)	0.004(3)
C(57)	0.034(4)	0.035(4)	0.024(4)	0.000(3)	-0.005(3)	0.000(3)
C(58)	0.027(3)	0.035(4)	0.024(4)	-0.002(3)	0.007(3)	-0.004(3)
C(59)	0.031(4)	0.039(4)	0.025(4)	-0.006(3)	-0.004(3)	-0.005(3)
C(60)	0.031(4)	0.028(4)	0.021(4)	0.001(3)	-0.003(3)	0.000(3)
C(61)	0.035(4)	0.026(4)	0.022(4)	-0.002(3)	-0.001(3)	0.002(3)
C(62)	0.032(4)	0.035(4)	0.026(4)	-0.007(3)	-0.003(3)	-0.008(3)
C(63)	0.034(4)	0.024(4)	0.024(4)	-0.004(3)	0.000(3)	-0.001(3)
C(64)	0.045(4)	0.034(4)	0.025(4)	0.000(3)	0.000(3)	0.005(3)
C(65)	0.042(4)	0.024(4)	0.026(4)	0.003(3)	-0.005(3)	-0.004(3)
C(66)	0.034(4)	0.036(4)	0.026(4)	0.002(3)	-0.004(3)	-0.001(3)
N(1)	0.019(3)	0.050(4)	0.040(4)	-0.010(3)	-0.005(3)	-0.007(3)
N(2A)	0.058(4)	0.039(4)	0.047(5)	-0.016(3)	0.018(3)	0.008(3)
N(2B)	0.058(4)	0.039(4)	0.047(5)	-0.016(3)	0.018(3)	0.008(3)
N(3A)	0.083(6)	0.054(5)	0.062(6)	-0.033(4)	0.011(5)	-0.010(4)
N(3B)	0.083(6)	0.054(5)	0.062(6)	-0.033(4)	0.011(5)	-0.010(4)
O(1)	0.026(2)	0.030(3)	0.041(3)	0.007(2)	-0.007(2)	-0.005(2)

7 EXPERIMENTAL PART

O(2)	0.031(3)	0.028(3)	0.025(3)	-0.001(2)	-0.002(2)	0.006(2)
O(3)	0.023(2)	0.056(3)	0.025(3)	0.005(2)	0.000(2)	-0.005(2)
O(4)	0.031(3)	0.035(3)	0.027(3)	-0.003(2)	-0.002(2)	-0.002(2)
O(5)	0.073(5)	0.062(5)	0.054(5)	-0.023(4)	-0.010(4)	0.044(4)
O(6)	0.031(4)	0.069(5)	0.045(4)	-0.012(4)	0.004(3)	-0.008(3)
O(7)	0.138(9)	0.119(8)	0.100(8)	0.020(7)	0.035(7)	0.046(8)
O(8)	0.197(12)	0.218(13)	0.143(11)	-0.064(10)	-0.025(10)	0.089(10)
F(1)	0.095(6)	0.198(11)	0.028(4)	0.025(5)	0.008(4)	-0.002(7)
F(2)	0.126(7)	0.077(5)	0.065(5)	0.025(4)	-0.020(5)	0.036(5)
F(3)	0.068(5)	0.139(8)	0.040(4)	-0.031(4)	-0.017(3)	0.024(5)
F(4)	0.371(13)	0.350(13)	0.372(13)	-0.008(8)	0.023(8)	0.006(8)
F(5)	0.371(13)	0.350(13)	0.372(13)	-0.008(8)	0.023(8)	0.006(8)
F(6)	0.371(13)	0.350(13)	0.372(13)	-0.008(8)	0.023(8)	0.006(8)
F(7)	0.082(4)	0.070(4)	0.099(5)	-0.030(4)	0.041(4)	0.009(3)
F(8)	0.063(3)	0.058(4)	0.103(5)	0.001(3)	0.024(3)	0.027(3)
F(9)	0.086(4)	0.059(4)	0.095(5)	-0.038(3)	0.029(4)	-0.011(3)
F(10)	0.101(5)	0.080(4)	0.055(4)	-0.012(3)	0.036(3)	0.014(4)
F(11)	0.043(3)	0.062(3)	0.101(5)	-0.021(3)	0.019(3)	-0.002(3)
F(12)	0.172(8)	0.047(4)	0.203(9)	0.051(5)	0.139(8)	0.040(4)
F(13)	0.090(5)	0.053(4)	0.193(9)	0.040(5)	0.083(5)	0.018(3)
F(14)	0.231(10)	0.051(4)	0.085(5)	0.031(4)	0.079(6)	0.031(5)
F(15)	0.128(6)	0.043(3)	0.107(5)	0.024(3)	0.054(5)	0.031(4)
F(16)	0.106(5)	0.048(4)	0.158(7)	-0.015(4)	0.062(5)	-0.020(4)
F(17)	0.015(2)	0.084(3)	0.034(3)	0.000(2)	-0.001(2)	0.001(2)
F(18)	0.027(2)	0.070(3)	0.036(3)	-0.011(2)	0.002(2)	0.009(2)
F(19)	0.029(2)	0.055(3)	0.037(3)	0.013(2)	0.000(2)	-0.007(2)
F(20)	0.029(2)	0.072(3)	0.028(2)	-0.013(2)	0.000(2)	-0.002(2)
F(21)	0.030(2)	0.069(3)	0.040(3)	0.020(2)	-0.002(2)	0.008(2)
F(22)	0.030(2)	0.111(5)	0.032(3)	0.022(3)	0.000(2)	-0.015(3)
F(23)	0.023(2)	0.082(3)	0.034(3)	0.005(2)	0.003(2)	0.006(2)
F(24)	0.036(2)	0.070(3)	0.035(3)	0.010(2)	-0.007(2)	-0.018(2)
F(25)	0.030(2)	0.061(3)	0.034(2)	0.020(2)	-0.007(2)	-0.004(2)
F(26)	0.032(2)	0.080(3)	0.024(2)	-0.004(2)	0.004(2)	-0.006(2)
F(27)	0.372(19)	0.140(8)	0.192(10)	-0.132(8)	0.193(12)	-0.181(11)
F(28)	0.205(10)	0.064(4)	0.130(7)	-0.041(5)	0.103(8)	-0.043(5)
F(29)	0.244(12)	0.059(4)	0.130(7)	-0.031(4)	0.117(8)	-0.058(6)
F(30)	0.208(11)	0.188(10)	0.113(7)	-0.096(7)	0.084(7)	-0.162(9)
F(31)	0.295(15)	0.192(10)	0.093(7)	-0.100(7)	0.092(8)	-0.179(11)
F(32)	0.068(3)	0.047(3)	0.061(3)	-0.002(2)	0.029(3)	-0.005(3)

7 EXPERIMENTAL PART

F(33)	0.053(3)	0.041(3)	0.057(3)	-0.011(2)	0.018(2)	0.005(2)
F(34)	0.072(4)	0.094(4)	0.026(3)	-0.004(3)	0.002(2)	-0.005(3)
F(35)	0.067(3)	0.058(3)	0.050(3)	0.017(2)	0.018(3)	0.024(3)
F(36)	0.047(3)	0.048(3)	0.047(3)	-0.014(2)	0.007(2)	-0.009(2)
F(37)	0.069(3)	0.038(3)	0.061(3)	0.005(2)	0.005(3)	-0.014(2)
F(38)	0.066(3)	0.043(3)	0.032(3)	0.006(2)	0.002(2)	-0.008(2)
F(39)	0.044(3)	0.042(3)	0.059(3)	0.005(2)	0.010(2)	-0.005(2)
F(40)	0.068(3)	0.031(2)	0.043(3)	-0.010(2)	-0.003(2)	-0.012(2)
F(41)	0.061(3)	0.026(2)	0.055(3)	0.000(2)	0.007(2)	0.005(2)
F(42)	0.046(3)	0.050(3)	0.051(3)	0.012(2)	-0.018(2)	-0.016(2)
F(43)	0.050(3)	0.034(2)	0.045(3)	-0.001(2)	-0.011(2)	-0.008(2)
F(44)	0.063(3)	0.056(3)	0.029(3)	0.017(2)	-0.015(2)	-0.019(2)
F(45)	0.042(3)	0.040(3)	0.059(3)	0.006(2)	-0.011(2)	0.003(2)
F(46)	0.038(2)	0.049(3)	0.038(3)	0.013(2)	-0.004(2)	-0.006(2)
P(1)	0.026(1)	0.033(1)	0.029(1)	-0.005(1)	0.002(1)	0.001(1)
P(2)	0.031(1)	0.037(1)	0.029(1)	-0.008(1)	0.000(1)	-0.003(1)
S(1A)	0.034(1)	0.050(1)	0.025(1)	-0.005(1)	-0.002(1)	0.008(1)
S(1B)	0.056(8)	0.088(10)	0.063(9)	-0.022(7)	-0.019(6)	0.020(7)
S(3)	0.057(1)	0.048(1)	0.069(2)	-0.012(1)	0.021(1)	0.004(1)
S(2A)	0.054(2)	0.055(2)	0.093(3)	-0.038(2)	0.008(2)	-0.003(2)
S(2B)	0.114(14)	0.055(8)	0.077(10)	-0.010(7)	0.023(9)	-0.014(8)
S(4)	0.109(2)	0.034(1)	0.117(3)	0.021(2)	0.068(2)	0.016(1)
S(5)	0.022(1)	0.051(1)	0.025(1)	0.001(1)	-0.001(1)	0.002(1)
S(6)	0.023(1)	0.069(1)	0.025(1)	0.007(1)	-0.002(1)	-0.006(1)
S(7)	0.228(5)	0.097(3)	0.110(3)	-0.071(2)	0.107(3)	-0.104(3)
S(8)	0.046(1)	0.038(1)	0.035(1)	0.000(1)	0.007(1)	0.002(1)
S(9)	0.052(1)	0.028(1)	0.039(1)	-0.002(1)	0.003(1)	-0.005(1)
S(10)	0.042(1)	0.036(1)	0.034(1)	0.009(1)	-0.010(1)	-0.005(1)

Hydrogen coordinates and isotropic displacement parameters (\AA^2).

	x	y	z	U_{eq}
H(6)	-0.1313	0.2314	0.1820	0.037
H(7)	-0.2371	0.2028	0.1630	0.040

7 EXPERIMENTAL PART

H(8)	-0.3483	0.2297	0.1631	0.044
H(9)	-0.3523	0.2848	0.1762	0.036
H(11)	-0.2908	0.3361	0.1986	0.033
H(14)	-0.2707	0.3777	0.3261	0.047
H(16)	-0.2173	0.4680	0.2504	0.062
H(18)	-0.1140	0.3921	0.1363	0.049
H(22)	-0.0905	0.2697	0.0329	0.036
H(23)	-0.0460	0.2369	-0.0826	0.044
H(24)	0.0552	0.2051	-0.0534	0.044
H(25)	0.1126	0.2072	0.0860	0.039
H(27)	0.1246	0.2306	0.2435	0.034
H(30)	0.1950	0.2676	0.3595	0.035
H(32)	0.1667	0.2474	0.6322	0.039
H(34)	-0.0026	0.2526	0.4609	0.034
H(38)	0.3730	0.3305	0.1275	0.043
H(39)	0.4907	0.3456	0.1043	0.052
H(40)	0.5588	0.3658	0.2254	0.060
H(41)	0.5075	0.3778	0.3643	0.051
H(43)	0.4005	0.3805	0.4642	0.047
H(46)	0.3164	0.4236	0.5097	0.076
H(48)	0.1865	0.4123	0.7343	0.073
H(50)	0.2059	0.3405	0.5463	0.040
H(54)	0.3372	0.2820	0.2662	0.039
H(55)	0.3520	0.2290	0.2129	0.047
H(56)	0.2904	0.2116	0.0811	0.043
H(57)	0.2073	0.2437	0.0099	0.038
H(59)	0.1393	0.2958	0.0050	0.038
H(62)	0.1665	0.3935	0.0465	0.037
H(64)	-0.0115	0.4094	-0.1069	0.042
H(66)	0.0184	0.3229	0.0233	0.038
H(2A)	-0.0204	0.3771	0.4271	0.057
H(2B)	-0.0865	0.3665	0.3770	0.057
H(3A)	0.1802	0.4111	0.3476	0.080
H(3B)	0.0897	0.4079	0.3521	0.080

7 EXPERIMENTAL PART

7.4.4 Mechanistic Studies

Excess Diene Reaction:

In a flame-dried Schlenk tube under argon, catalyst **22c** (27 mg, 12 μ mol, 0.05 equiv), 5 Å molecular sieves (210 mg), MeCy (3.0 mL) were added. Subsequently, benzaldehyde (250 mg, 2.36 mmol, 1.0 equiv), followed by 2,3-dimethyl-1,3-butadiene (**20a**) (800 mg, 9.74 mmol, 4.1 equiv) were added in at -78 °C. The reaction mixture was then stirred at -20 °C for 30 min and quenched by the addition of trimethylamine (1 drop). The solution was warmed to room temperature and 1,2,4,5-tetramethylbenzene (134 mg, 1.0 mmol) was added as an internal standard. Analysis of the crude reaction mixture by ^1H NMR showed that the reaction was quenched at $15 \pm 0.6\%$ completion of **20a** (relative to starting diene **20a**). Purification of **21a** was performed by column chromatography on silica gel using diethyl 2–6% ether/pentane as the eluent (198 mg, 1.05 mmol). Under argon, the obtained **21a** was transferred to a NMR tube (50 mg of **21a** in 0.5 mL CD_2Cl_2), and the NMR tube was then sealed by melting. Two samples were identically prepared for the following NMR analysis.

The reaction was carefully repeated and **21a** (210 mg, 1.12 mmol) was obtained at $16 \pm 0.8\%$ completion of **20a** (relative to starting diene **20a**). Another two identical NMR samples were prepared.

^{13}C Spectra Measurement:

The ^{13}C spectra were measured at 150.93 MHz on an Avance 600MHz NMR spectrometer equipped with a cryogenically-cooled TXI ($^1\text{H}/^{13}\text{C}/^{15}\text{N}$) probehead, using a single pulse calibrated at 40° followed by inverse-gated decoupling. A 40-s delay was used between pulses, the longest T_1 for the ^{13}C of interest being about 6s (C3). To obtain digital resolution of at least 5 points at the peak linewidth at half-height, an instrumental maximum of 128K points were collected over a sweep-width of 155 ppm centered at 46 ppm, followed by zero-filling to 256K points before Fourier transformation. Integrations were determined numerically using a ± 7.5 Hz region for each peak. In general, an automatic polynomial baseline correction of order of at least 3 was applied. Integrals were simply calculated by summing the signal intensities over the peak regions.

7 EXPERIMENTAL PART

The relative ^{13}C compositions at C3 and C4 were assigned to be 1.000 in this intramolecular KIE measurement. The relative ^{13}C composition at C1 was calculated from the integration at C1 versus C4. The intramolecular KIE of C1 was the reciprocal of the average of relative ^{13}C compositions at C1. Similarly, the relative ^{13}C composition at C2 was calculated from the integration at C2 versus C3. The intramolecular KIE of C2 was the reciprocal of the average of relative ^{13}C compositions at C2. The standard deviations in the parentheses were calculated in a standard way.

Values shown are raw ^{13}C integrals of **21a** at $15 \pm 0.6\%$ completion of **20a**

Sample	C ₁	C ₂	C ₃	C ₄
1	85901	91898	91307	88351
1	85960	92516	91861	87659
1	86779	92491	92002	88020
1	86069	92518	93114	87888
1	95521	102349	101247	97308
1	95284	101747	101450	97669
1	95647	101314	101403	97199
1	86724	92809	93180	88907
2	350900	373893	373560	360129
2	355073	377562	376117	362694
2	354592	377015	377226	362330
2	355307	378537	378589	363559
2	356656	379971	379377	365966
2	358969	382854	381606	366213
2	357178	379629	380955	364419
2	357657	381297	380861	365602

7 EXPERIMENTAL PART

Values shown are raw ^{13}C integrals of **21a** at $16 \pm 0.8\%$ completion of **20a**

Sample	C ₁	C ₂	C ₃	C ₄
1	88077	93934	94519	89963
1	88941	93702	94374	90204
1	88368	94464	95318	91427
1	88895	94891	94633	91014
1	85510	91436	90853	88089
1	85932	92064	91378	88353
1	86267	91589	91263	88107
1	85986	91887	91145	87680
2	86474	91458	91995	87824
2	86153	91650	91278	88730
2	86674	91770	92088	89318
2	87694	92747	92224	89682
2	86601	93065	92773	89684
2	87276	93685	93009	89642
2	87239	93314	92793	88873
2	87527	93076	93567	89466

8 BIBLIOGRAPHY

1. J. B. Biot, *Bull. Soc. Philomath. Paris* **1815**, 190.
2. J. B. Biot, *Bull. Soc. Philomath. Paris* **1816**, 125.
3. J. A. Le Bel, *Soc. Chim. France* **1874**, 2, 337.
4. J. H. van't Hoff, *Bull. Soc. Chim. France* **1875**, 2, 295
5. K. Mislow, *Topics Stereochem.* **1999**, 22, 1.
6. H.-J. Federsel, *DRUG DISCOVERY* **2005**, 4, 685.
7. Rouhi, M. *Top pharmaceuticals: thalidomide. Chem. Eng. News* **2005**, 83, 122.
8. A. M. Thayer, *Chem. Eng. News* **2007**, 85, 11.
9. L. Pasteur, *Anal. Chim. Phys.* **1848**, 24, 442.
10. K. Gademann, *Asymmetric Synthesis II*, Wiley-VCH Verlag GmbH & Co. KGaA, **2012**, 317.
11. E. Fischer, *Berichte der deutschen chemischen Gesellschaft* **1894**, 27, 3189.
12. B. List, R. A. Lerner, C. F. Barbas, *J. Am. Chem. Soc.* **2000**, 122, 2395.
13. K. A. Ahrendt, C. J. Borths, D. W. C. MacMillan, *J. Am. Chem. Soc.* **2000**, 122, 4243.
14. D. Kampen, C. M. Reisinger, B. List, *Top. Curr. Chem.* **2009**, 291, 395.
15. a) W. S. Knowles, M. J. Sabacky, B. D. Vineyard, *J. Chem. Soc. Chem. Commun.* **1972**, 10; b) R. Noyori, *Science* **1990**, 248, 1194.
16. K. B. Sharpless, *Angew. Chem. Int. Ed.* **2002**, 41, 2024.
17. D. Seebach, *Angew. Chem. Int. Ed.* **1990**, 29, 1320.
18. J. von Liebig, *Justus Liebigs Ann. Chem.* **1860**, 113, 246.
19. H. Pracejus, *Justus Liebigs Ann. Chem.* **1960**, 634, 9.
20. Z. G. Hajos, D. R. Parrish, *J. Org. Chem.* **1974**, 39, 1615.
21. U. Eder, G. Sauer, R. Wiechert, *Angew. Chem. Int. Ed.* **1971**, 10, 496.
22. S. Bahmanyar, K. N. Houk, H. J. Martin, B. List, *J. Am. Chem. Soc.* **2003**, 125, 2475.
23. A. Berkessel, H. Gröger, *Asymmetric Organocatalysis*, Wiley-VCH: Weinheim, **2005**.
24. M. van Gemmeren, F. Lay, B. List, *Aldrichim Acta* **2014**, 47, 3.
25. R. J. Phipps, G. L. Hamilton, F. D. Toste, *Nature Chem.* **2012**, 4, 603.
26. J. Seayad, B. List, *Org. Biomol. Chem.* **2005**, 3, 719.

8 BIBLIOGRAPHY

27. J. Otera, *Modern Carbonyl Chemistry*, Wiley-VCH, Weinheim, **2000**.
28. M. S. Taylor, E. N. Jacobsen, *Angew. Chem. Int. Ed.* **2006**, *45*, 1520.
29. M. Sigman, E. N. Jacobsen, *J. Am. Chem. Soc.* **1998**, *120*, 4901.
30. J. Alemán, A. Parra, H. Jiang, K. A. Jørgensen, *Chem. Eur. J.* **2011**, *17*, 6890.
31. Y. Huang, A. K. Unni, A. N. Thadani, V. H. Rawal, *Nature* **2003**, *424*, 146.
32. A. G. Doyle, E. N. Jacobsen, *Chem. Rev.* **2007**, *107*, 5713.
33. T. Akiyama, *Chem. Rev.* **2007**, *107*, 5744.
34. T. Akiyama, J. Itoh, K. Yokota, K. Fuchibe, *Angew. Chem. Int. Ed.* **2004**, *43*, 1566.
35. D. Uraguchi, M. Terada, *J. Am. Chem. Soc.* **2004**, *126*, 5356.
36. M. Hatano, K. Moriyama, T. Maki, K. Ishihara, *Angew. Chem. Int. Ed.* **2010**, *49*, 3823.
37. M. Rueping, A. Kuenkel, I. Atodiresei, *Chem. Soc. Rev.*, **2011**, *40*, 4539.
38. S. Hoffmann, A. M. Seayad, B. List, *Angew. Chem. Int. Ed.* **2005**, *44*, 7424.
39. S. Mayer, B. List, *Angew. Chem. Int. Ed.* **2006**, *45*, 4193.
40. G. L. Hamilton, E. J. Kang, M. Mba, F. D. Toste, *Science* **2007**, *317*, 496.
41. G. B. Rowland, H. Zhang, E. B. Rowland, S. Chennamadhavuni, Y. Wang, J. C. Antilla, *J. Am. Chem. Soc.* **2005**, *127*, 15696.
42. X. H. Chen, X. Y. Xu, H. Liu, L. F. Cun, L.-Z. Gong, *J. Am. Chem. Soc.* **2006**, *128*, 14802.
43. Q.-S. Guo, D.-M. Du, J. Xu, *Angew. Chem. Int. Ed.* **2008**, *47*, 759.
44. F. Xu, D. Huang, C. Han, W. Shen, X. Lin, Y. Wang, *J. Org. Chem.* **2010**, *75*, 8677.
45. I. Čorić, S. Müller, B. List, *J. Am. Chem. Soc.* **2010**, *132*, 17370.
46. S. Li, J.-W. Zhang, X.-L. Li, D.-J. Cheng, B. Tan, *J. Am. Chem. Soc.* **2016**, *138*, 16561.
47. S. Harada, S. Kuwano, Y. Yamaoka, K. Yamada, K. Takasu, *Angew. Chem. Int. Ed.* **2013**, *52*, 10227.
48. X.-H. Chen, W.-Q. Zhang, L.-Z. Gong, *J. Am. Chem. Soc.* **2008**, *130*, 5652.
49. N. Momiyama, T. Konno, Y. Furiya, T. Iwamoto, M. Terada, *J. Am. Chem. Soc.* **2011**, *133*, 19294.
50. M. Terada, K. Sorimachi, D. Uraguchi, *Synlett* **2006**, *2006*, 133.
51. D. Nakashima, H. Yamamoto, *J. Am. Chem. Soc.* **2006**, *128*, 9626.
52. P. S. J. Kaib, B. List, *Synlett* **2016**, *27*, 156.

8 BIBLIOGRAPHY

53. T. Hashimoto, K. Maruoka, *J. Am. Chem. Soc.* **2007**, *129*, 10054.
54. a) D. Kampen, A. Ladépêche, G. Claßen, B. List, *Adv. Synth. Catal.* **2008**, *350*, 962; b) M. Hatano, T. Maki, K. Moriyama, M. Arinobe, K. Ishihara, *J. Am. Chem. Soc.* **2008**, *130*, 16858.
55. P. García-García, F. Lay, P. García-García, C. Rabalakos, B. List, *Angew. Chem. Int. Ed.* **2009**, *48*, 4363.
56. S. Gandi, B. List, *Angew. Chem. Int. Ed.* **2013**, *52*, 2573.
57. Z. Zhang, H. Y. Bae, J. Guin, C. Rabalakos, M. van Gemmeren, M. Leutzsch, M. Klusmann, B. List, *Nat. Commun.* **2016**, *7*, 12478.
58. S. Prévost, N. Dupré, M. Leutzsch, Q. Wang, V. Wakchaure, B. List, *Angew. Chem. Int. Ed.* **2014**, *55*, 8770.
59. I. Čorić, B. List, *Nature* **2012**, *483*, 315.
60. S. Liao, I. Čorić, Q. Wang, B. List *J. Am. Chem. Soc.* **2012**, *134*, 10765.
61. Y.-Y. Chen, Y.-J. Jiang, Y.-S. Fan, D. Sha, Q. Wang, G. Zhang, L. Zheng, S. Zhang, *Tetrahedron: Asymmetry* **2012**, *23*, 904.
62. M.-H. Zhuo, Y.-J. Jiang, Y.-S. Fan, Y. Gao, S. Liu, S. Zhang, *Org. Lett.* **2014**, *16*, 1096.
63. K. Wu, M.-H. Zhuo, D. Sha, Y.-S. Fan, D. An, Y.-J. Jiang, S. Zhang, *Chem. Commun.* **2015**, *51*, 8054.
64. K. Alder, F. Pascher, Schmitz, A. *Ber. Dtsch. Chem. Ges.* **1943**, *76*, 27.
65. K. Mikami, M. Shimizu, *Chem. Rev.* **1992**, *92*, 1021.
66. M. L. Clarke, M. B. France, *Tetrahedron* **2008**, *64*, 9003.
67. A. F. Trasarti, A. J. Marchi, C. R. J. Apesteguia, *Catal.* **2007**, *247*, 155.
68. W. D. Huntsman, V. C. Solomon and D. Eros, *J. Am. Chem. Soc.*, **1958**, *80*, 5455.
69. R. T. Ruck, E. N. Jacobsen, *J. Am. Chem. Soc.*, **2002**, *124*, 2882.
70. R. T. Ruck, E. N. Jacobsen, *Angew. Chem., Int. Ed.* **2003**, *42*, 4771.
71. S. Sakane, K. Maruoka, H. Yamamoto, *Tetrahedron* **1986**, *42*, 2203.
72. K. Mikami, E. Sawa, M. Terada, *Tetrahedron: Asymmetry* **1991**, *2*, 1403.
73. H. Itoh, H. Maeda, S. Yamada, Y. Hori, T. Mino, M. Sakamoto, *Org. Biomol. Chem.* **2015**, *13*, 5817.
74. C. Zhao, Q.-F. Sun, W. M. HartCooper, A. G. DiPasquale, F. D. Toste, R. G. Bergman, K. N. Raymond, *J. Am. Chem. Soc.* **2013**, *135*, 18802.

8 BIBLIOGRAPHY

75. D. Yang, M. Yang, N.-Y. Zhu, *Org. Lett.* **2003**, *5*, 3749.
76. Y.-J. Zhao, B. Li, L.-J. S. Tan, Z.-L. Shen, T.-P. Loh, *J. Am. Chem. Soc.* **2010**, *132*, 10242.
77. N. S. Rajapaksa, E. N. Jacobsen, *Org. Lett.* **2013**, *15*, 4238.
78. M. L. Grachan, M. T. Tudge, E. N. Jacobsen, *Angew. Chem., Int. Ed.* **2008**, *47*, 1469.
79. R. M. Beesley, C. K. Ingold, J. F. Thorpe, *J. Chem. Soc.* **1915**, *107*, 1080.
80. C. K. Ingold, *J. Chem. Soc.* **1921**, *119*, 305.
81. C. K. Ingold, S. Sako, J. F. Thorpe, *J. Chem. Soc.* **1922**, *120*, 1117.
82. M. E. Jung, *Synlett* **1990**, 186.
83. M. E. Jung, G. Piizzi, *Chem. Rev.* **2005**, *105*, 1735.
84. J. T. Williams, P. S. Bahia, J. S. Snaith, *Org. Lett.* **2002**, *4*, 3727.
85. J. T. Williams, P. S. Bahia, B. M. Kariuki, N. Spencer, D. Philp, J. S. Snaith, *J. Org. Chem.* **2006**, *71*, 2460.
86. J. Sauer, *Angew. Chem., Int. Ed.* **1966**, *5*, 211.
87. J. Sauer, *Angew. Chem., Int. Ed.* **1967**, *6*, 16.
88. H. B. Kagan, O. Riant, *Chem. Rev.* **1992**, *92*, 1007.
89. U. Pindur, L. Gundula, C. Otto, *Chem. Rev.* **1993**, *93*, 741.
90. P. Wessig, G. Müller, *Chem. Rev.* **2008**, *108*, 2051.
91. O. Diels, K. Alder, *Justus Liebigs Ann. Chem.* **1928**, *460*, 98.
92. K.C. Nicolaou, S. A. Snyder, T. Montagnon, G. Vassilikogiannakis, *Angew. Chem., Int. Ed.* **2002**, *41*, 1668.
93. J. A. Funel, S. Abele, *Angew. Chem. Int. Ed.* **2013**, *52*, 3822.
94. R. B. Woodward, R.Z. Hoffmann, *The Conservation of Orbital Symmetry* (Verlag Chemie, Weinheim, Germany) **1970**.
95. L. Fleming, *Frontier Orbitals and Organic Chemical Reactions* (Wiley, London) **1977**.
96. K. A. Jørgensen, *Angew. Chem. Int. Ed.* **2000**, *39*, 3558.
97. T. L. Gresham, T. R. Steadman, *J. Am. Chem. Soc.* **1949**, *71*, 737.
98. H. Du, K. Ding, *Handbook of Cyclization Reactions*, Ed. Wiley-VCH: Weinheim, **2009**, 1.
99. K. Maruoka, T. Itoh, T. Shirasaka, H. Yamamoto, *J. Am. Chem. Soc.* **1988**, *110*, 310.
100. N. Bednarski, C. Maring, S. Danishefsky, *Tetrahedron Lett.* **1983**, *24*, 3451.

8 BIBLIOGRAPHY

101. L. Lin, Y. Kuang, X. Liu, X. Feng, *Org. Lett.* **2011**, *13*, 3868.
102. Y. Huang, A. K. Unni, A. N. Thadani, V. H. Rawal, *Nature* **2003**, *424*, 146.
103. J. Guin, C. Rabalakos, B. List, *Angew. Chem. Int. Ed.* **2012**, *51*, 8859.
104. M. Terada, K. Mikami, T. Nakai, *Tetrahedron Lett.* **1991**, *32*, 935.
105. M. Johannsen, K. A. Jørgensen, *J. Org. Chem.* **1995**, *60*, 5757.
106. H. Griengl, K. P. Geppert, *Monatsh. Chem.* **1976**, *107*, 675.
107. V. K. Aggarwal, G. P. Vennall, P. N. Davey, C. Newman, *Tetrahedron Lett.* **1997**, *38*, 2569.
108. G. Odian, *Principles of Polymerization*, 4th Ed. Wiley-Interscience, Hoboken, NJ, **2004**.
109. K. Fujiwara, T. Kurahashi, S. Matsubara, *J. Am. Chem. Soc.* **2012**, *134*, 5512.
110. X. Zou, L. Yang, X. Liu, H. Sun, H. Lu, *Adv. Synth. Catal.* **2015**, *357*, 3040.
111. M. A. E. A. A. E. Remaily, V. R. Naidu, S. Ni, J. Franzén, *Eur. J. Org. Chem.* **2015**, 6610.
112. J. H. Kim, I. Čorić, S. Vallalath, B. List, *Angew. Chem. Int. Ed.* **2013**, *52*, 4474.
113. J. H. Kim, I. Čorić, C. Palumbo, B. List, *J. Am. Chem. Soc.* **2015**, *137*, 1778.
114. W. Oppolzer, *Angew. Chem., Int. Ed.* **1984**, *23*, 876.
115. M. Terada, *Synthesis* **2010**, *2010*, 1929.
116. D. Parmar, E. Sugiono, S. Raja, M. Rueping, *Chem. Rev.* **2014**, *114*, 9047.
117. M. Rueping, W. Ieawsuwan, A. P. Antonchick, B. J. Nachtsheim, *Angew. Chem., Int. Ed.* **2007**, *46*, 2097.
118. M. Sai, H. Yamamoto, *J. Am. Chem. Soc.* **2015**, *137*, 7091.
119. M. van Gemmeren, F. Lay, B. List, *Aldrichimica Acta* **2014**, *47*, 3.
120. J. H. Kim, I. Čorić, S. Vellalath, B. List, *Angew. Chem., Int. Ed.* **2013**, *52*, 4474.
121. R. J. Comito, F. G. Finelli, D. W. C. MacMillan, *J. Am. Chem. Soc.* **2013**, *135*, 9358.
122. M. Findeisen, S. Berger, *50 and More Essential NMR Experiments: A Detailed Guide*, Wiley-VCH, **2013**.
123. M. Findeisen, T. Brand, S. Berger, *Magn. Reson. Chem.*, **2007**, *45*, 175.
124. H. Eyring, *J. Chem. Phys.* **1935**, *3*, 107.
125. G. E. Briggs, J. B. S. Haldane, *Biochem. J.* **1925**, *19*, 338.
126. B. Li, Y. Shen, B. Li, *J. Phys. Chem. A* **2008**, *112*, 2311.
127. E. A. Crane, K. A. Scheidt, *Angew. Chem., Int. Ed.* **2010**, *49*, 8316.
128. C. Olier, M. Kaafarani, S. Gastaldi, M. P. Bertrand, *Tetrahedron* **2010**, *66*, 413.

8 BIBLIOGRAPHY

129. X. Han, G. Peh, P. E. Floreancig, *Eur. J. Org. Chem.* **2013**, 2013, 1193.
130. D. J. Kopecky, S. D. Rychnovsky, *J. Am. Chem. Soc.* **2001**, 123, 8420.
131. K.-P. Chan, Y. H. Ling, T.-P. Loh, *Chem. Commun.* **2007**, 939.
132. J. M. Tenenbaum, W. J. Morris, D. W. Custar, K. A. Scheidt, *Angew. Chem., Int. Ed.* **2011**, 50, 5892.
133. A. J. Bunt, C. D. Bailey, B. D. Cons, S. J. Edwards, J. D. Elsworth, T. Pheko, C. L. Willis, *Angew. Chem., Int. Ed.* **2012**, 51, 3901.
134. C. Lalli, P. van de Weghe, *Chem. Commun.* **2014**, 50, 7495.
135. J. Liu, L. Zhou, C. Wang, D. Liang, Z. Li, Y. Zou, Q. Wang, A. Goeke, *Chem. - Eur. J.* **2016**, 22, 6258.
136. C. S. Barry, N. Bushby, J. R. Harding, R. A. Hughes, G. D. Parker, R. Roe, C. L. Willis, *Chem. Commun.* **2005**, 3727.
137. R. Jasti, S. D. Rychnovsky, *J. Am. Chem. Soc.* **2006**, 128, 13640.
138. M. Breugst, R. Grée, K. N. Houk, *J. Org. Chem.* **2013**, 78, 9892.
139. A. Pictet, T. Spengler, *Ber. Dtsch. chem. Ges.* **1911**, 44, 2030.
140. M. S. Taylor, E. N. Jacobsen, *J. Am. Chem. Soc.* **2004**, 126, 10558.
141. J. Seayad, A. M. Seayad, B. List, *J. Am. Chem. Soc.* **2006**, 128, 1086.
142. Y. B. Zhou, J.-H. Wang, X. M. Li, X. C. Fu, Z. Yan, Y. M. Zeng, X. Li, *J. Asian Nat. Prod. Res.* **2008**, 10, 827.
143. K. Trisuwan, V. Rukachaisirikul, Y. Sukpondma, S. Phongpaichit, S. Preedanon, J. Sakayaroj, *Tetrahedron* **2010**, 66, 4484.
144. Y.-M. Yan, H.-Q. Dai, Y. Du, B. Schneider, H. Guo, D.-P. Li, L.-X. Zhang, H. Fu, X.-P. Dong, Y.-X. Cheng, *Bioorg. Med. Chem. Lett.* **2012**, 22, 4179.
145. L. Zhang, X. Zhu, B. Zhao, J. Zhao, Y. Zhang, S. Zhang, J. Miao, *Vasc. Pharmacol.* **2008**, 48, 63.
146. V. M. Lombardo, C. D. Thomas, K. A. Scheidt, *Angew. Chem. Int. Ed.* **2013**, 52, 12910.
147. E. Ascic, R. G. Ohm, R. Petersen, M. R. Hansen, C. L. Hansen, D. Madsen, D. Tanner, T. E. Nielsen, *Chem. Eur. J.* **2014**, 20, 3297.
148. P. S. Steyn, C. W. Holzapfel, *Tetrahedron* **1967**, 23, 4449.
149. P. R. R. Costa, L. M. Cabral, K. G. Alencar, L. L. Schmidt, M. L. A. A. Vasconcellos, *Tetrahedron Lett.* **1997**, 38, 7021.
150. A. Chimirri, G. De Sarro, A. De Sarro, R. Gitto, S. Grasso, S. Quartarone, P. Giusti, V. Libri, A. Constanti, A. G. Chapman, *J. Med. Chem.* **1997**, 40, 1258.

8 BIBLIOGRAPHY

151. D. O. A. Bianchi, F. Rúa, T. S. Kaufman, *Tetrahedron Lett.* **2004**, *45*, 411.
152. J. A. Funel, S. Abele, *Angew. Chem. Int. Ed.* **2013**, *52*, 3822.
153. K. A. Jørgensen, *Angew. Chem. Int. Ed.* **2000**, *39*, 3558.
154. L. Fleming, *Frontier Orbitals and Organic Chemical Reactions* (Wiley, London) **1977**.
155. P. S. J. Kaib, L. Schreyer, S. Lee, R. Properzi, B. List, *Angew. Chem. Int. Ed.* **2016**, *55*, 13200.
156. Y. Xie, G. J. Cheng, S. Lee, P. S. J. Kaib, W. Thiel, B. List, *J. Am. Chem. Soc.* **2016**, *138*, 14538.
157. Y. Yue, M. Turlington, X. Q. Yu, L. Pu, *J. Org. Chem.* **2009**, *74*, 8681.
158. A. Abate, M. Allievi, E. Brenna, C. Fuganti, F. G. Gatti, S. Serra, *Helv. Chim. Acta* **2006**, *89*, 177.
159. H. W. Thompson, D. G. Melillo, *J. Am. Chem. Soc.* **1970**, *92*, 3218.
160. K. N. Houk, Y.-T. Lin, F. K. Brown, *J. Am. Chem. Soc.* **1986**, *108*, 554.
161. N. Sogani, P. Sinha, R. K. Bansal, *Tetrahedron* **2014**, *70*, 735.
162. M. Wolfsberg, W. A. Van Hook, P. Paneth, L. P. N. Rebelo, *Isotope Effects in the Chemical, Geological, and Bio Sciences*, Springer: Dordrecht, **2010**.
163. D. A. Singleton, A. A. Thomas, *J. Am. Chem. Soc.* **1995**, *117*, 9357.
164. D. A. Singleton, M. J. Szymanski, *J. Am. Chem. Soc.* **1999**, *121*, 9455.
165. D. A. Singleton, S. R. Merrigan, B. R. Beno, K. N. Houk, *Tetrahedron Lett.* **1999**, *40*, 5817.
166. S. Xiang, M. P. Meyer, *J. Am. Chem. Soc.* **2014**, *136*, 5832.
167. E. E. Kwan, Y. Park, H. A. Besser, T. L. Anderson, E. N. Jacobsen, *J. Am. Chem. Soc.* **2017**, *139*, 43.

9 ACKNOWLEDGEMENTS

The PhD study in Max-Planck-Institut für Kohlenforschung is quite challenging, yet exciting for me. I am certainly grateful to Prof. Dr. Benjamin List for giving me a *second* chance to work in this amazing institute as a PhD candidate. As an advisor, Ben is always supportive and attentive, who is incredibly patient to train my skills in presentation and writing. In light of Ben's professional guidance and scientific experience, I am able to conduct and present my research results briefly and effectively, which definitely has a profound influence on my career.

I am grateful to Prof. Dr. Hans-Günther Schmalz for reviewing this thesis and to Prof. Dr. Uwe Ruschewitz and Dr. Martin Klußman for serving on my defence committee. I also thank Jennifer L. Kennemur, Dr. Chandra Kanta De and Dr. Youwei Xie for kind suggestions for this work.

The results presented in this doctoral work wouldn't have been possible without collaborations with a lot of colleagues. I would specially like to thank Dr. Markus Leutsch, Dr. Yiyang Zheng, Dr. M. Wasim Alachraf for collaborating on the carbonyl-ene cyclization reaction. Sincerely, thanks my colleague Dr. Philip S. J. Kaib, Dr. Gavin Chit Tsui for collaborating on the Prins cyclization and Dr. Sayantani Das, Dr. Chandra Kanta De for collaborating on oxa-Pictet-Spengler Reaction. I am extremely grateful to Dr. Heyjin Kim and Dr. Youwei Xie for their dedication in the [4+2]-cycloaddition. Arno Döring and Natascha Wippich were helpful during my whole PhD study. I am grateful to other technicians Stefanie Dehn, Hendrik van Thienen, Alexander Zwerschke. Dr. Chandra Kanta De and Dr. Martin Klußman are appreciated for teaching in Ph.D. seminars. Services of the GC, NMR, HPLC, and MS departments at the Max-Planck-Institut für Kohlenforschung are highly acknowledged for their collaborations. Finally, I am grateful to all my colleagues, especially Mattia, Liao, Hanyong, Tim, Sunggi, Lucas, Grischa for sharing their chemicals, ideas, as well as their happy experience in chemistry.

I am indebted to my great parents Jinwen Liu and Qine Zhang. Their insistence, kindness, and bravery always inspire me to carry on a wonderful and unique life.

10 APPENDIX

10.1 Erklärung

“Ich versichere, dass ich die von mir vorgelegte Dissertation selbständig angefertigt, die benutzten Quellen und Hilfsmittel vollständig angegeben und die Stellen der Arbeit – einschließlich Tabellen, Karten und Abbildungen –, die anderen Werken im Wortlaut oder dem Sinn nach entnommen sind, in jedem Einzelfall als Entlehnung kenntlich gemacht habe; dass diese Dissertation noch keiner anderen Fakultät oder Universität zur Prüfung vorgelegen hat; dass sie – abgesehen von unten angegebenen Teilpublikationen – noch nicht veröffentlicht worden ist sowie, dass ich eine solche Veröffentlichung vor Abschluss des Promotionsverfahrens nicht vornehmen werde. Die Bestimmungen der Promotionsordnung sind mir bekannt. Die von mir vorgelegte Dissertation ist von Herrn Professor Dr. Benjamin List betreut worden. ”

Ort, Datum

Unterschrift

10.2 Teilpublikationen

Bisher sind folgende Teilpublikationen veröffentlicht worden:

1. “Confined Acid-Catalyzed Asymmetric Carbonyl–Ene Cyclization”, L. Liu, M. Leutsch, Y. Zheng, W. M. Alachraf, W. Thiel, B. List, *J. Am. Chem. Soc.* **2015**, *137*, 13268–13271.
2. “The Organocatalytic Asymmetric Prins Cyclization”, T. G. Chit, L. Liu, B. List, *Angew. Chem. Int. Ed.* **2015**, *54*, 7703–7706.
3. “A General Catalytic Asymmetric Prins Cyclization”, L. Liu,⁺ P. S. J. Kaib,⁺ A. Tap, B. List, *J. Am. Chem. Soc.* **2016**, *138*, 10822–10825. (⁺equal contribution)
4. “Nitrated Confined Imidodiphosphates Enable a Catalytic Asymmetric Oxa-Pictet–Spengler Reaction”, S. Das,⁺ L. Liu,⁺ Y. Zheng, W. M. Alachraf, W. Thiel, C. K. De, and B. List, *J. Am. Chem. Soc.* **2016**, *138*, 9429–9432. (⁺equal contribution)
5. “Catalytic Asymmetric [4+2]-Cycloaddition of Dienes with Aldehydes”, L. Liu, H. Kim, Y. Xie, C. Farès, P. S. J. Kaib, R. Goddard, B. List, *J. Am. Chem. Soc.* **2017**, *139*, 13656–13659.